



**The Potential of Plant Polyphenols as Natural Photostable
Sunscreen Active Ingredients**

by

Serina Pooja Sowman

(B.Sc. Hons. University of KwaZulu-Natal, South Africa)

Submitted in fulfilment of the academic requirements for the degree of Master
of Science in the School of Chemistry and Physics,

University of KwaZulu-Natal,

Durban, South Africa

July 2022

Abstract

Protection from the sun dates to prehistoric times as a measure against the deleterious effects of solar ultraviolet (UV) radiation. Overexposure to this harmful UV radiation is a leading cause of pathological changes of the skin, such as erythema and the worst being skin cancer. Commercial sunscreen products contain UV filter substances that are designed to protect human skin from erythema. These sunscreen products incorporate chemical UV-absorbing compounds and physical blockers that allow UV radiation to be reflected, scattered, or absorbed. This research discusses the use of certain organic UV absorbers and their importance in protection against the effects of UV radiation.

The issues faced with certain UV absorbers are that they are susceptible to photodegradation over time, their degradation products can be phototoxic, and they provide protection only over a limited wavelength region. This causes a significant problem in sunscreen products as their efficacy is reduced. This has led to research on finding an alternative solution that can provide beneficial protection and maintain photostability. Interest was drawn to the plant kingdom for a more natural source of sunscreen absorbers since plants have developed various photoprotection mechanisms to counter enhanced levels of UV radiation. Polyphenols in plants have strong UV-absorbing properties that cover a broad spectrum, and they also possess excellent antioxidant activity. Therefore, they can play a dual role by acting as both natural absorbers of harmful radiation and quenchers of free radical damage also caused by sunlight.

This project highlights the limitations in photostability of four commonly used chemical UV filters found in commercial sunscreen products, namely, avobenzone, benzophenone-9, 2-ethylhexyl-*p*-methoxycinnamate and 4-methylbenzylidene camphor, and involves testing a South African based plant extract to increase the current efficacy of sunscreens due to its photochemoprotective properties. Attempts at photostabilising the selected UV filters were made by incorporating extracts from *Sutherlandia frutescens*, also known as the Cancer Bush plant. Photostability studies were conducted on the extracts alone and when mixed with each of the sunscreen filters by means of UV-visible spectrophotometry. Phenolic compounds, namely, flavonoids and phenolic acids, were extracted, identified and quantified.

From an industrial perspective, a cheaper alternative to the Cancer Bush plant is extracting polyphenols from commercial tea. Phenolic acids were extracted from Rooibos and green teas by means of a simple ethanol-water extraction technique. For comparison, the tea extracts were

compared with the Cancer Bush extract. Green tea was found to provide excellent photostability.

The phenolic acids that were extracted from the Cancer Bush plant and teas were analysed by high-performance liquid chromatography (HPLC). The identification and quantitation of six phenolic acids was achieved by reversed-phased HPLC. Identification of phenolic acids was achieved by matching the retention times and spectra of the extract components with those of phenolic acid standards. The identified phenolic acids were gallic acid, *p*-hydroxybenzoic acid, vanillic acid, caffeic acid, syringic acid and *p*-coumaric acid. The six phenolic acids were identified in the Cancer Bush ethanol-water extract and *p*-coumaric acid showed the highest concentration. Only three phenolic acids were successfully identified in the green tea extract and four in the Rooibos tea extract with the highest concentration being *p*-coumaric acid.

A general sunscreen formulation was employed to assess the possible inclusion of polyphenols in sunscreens. Sunscreens were made with and without UV filters and photostability tests were conducted. A small amount of sunscreen was smeared onto a quartz plate and exposed to sunlight for a total of six hours. UV-visible spectrophotometric analysis was conducted at 30-minute intervals before and after exposure to determine their photostability. Sunscreen formulations containing plant extracts showed noteworthy photostability when compared with products without plant extracts by increasing the absorbance values. This shows that plant extracts may contribute synergistically to improve the efficacy of sunscreen formulations. The stability of the sunscreens was tested to determine formulation stability and safety. Furthermore, *in vitro* testing was applied to test sunscreen formulation parameters, such as, sun protection factor (SPF) and occlusion factor. Results show that the addition of the Cancer Bush plant improved the SPF of the sunscreen preparation.

Therefore, this research has shown that the addition of the Cancer Bush extract can improve photostability and provide additional UV protection.

Preface

The experimental work described in this thesis was carried out in the School of Chemistry and Physics, University of KwaZulu-Natal, Durban from July 2018 to July 2022, under the supervision of Professor B.S. Martincigh.

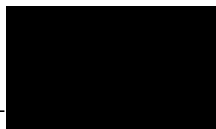
These studies represent original work by the author and have not otherwise been submitted in any form for any degree or diploma to any tertiary institution. Where use has been made of the work of others it is duly acknowledged in the text.

Declaration 1: Plagiarism

I, **Serina Pooja Sowman**, declare that

1. The research reported in the dissertation, except where otherwise indicated, is my original research.
2. This dissertation has not been submitted for any degree or examination at any other University.
3. This dissertation does not contain other person's data, pictures, graphs or other information, unless specifically acknowledged as being sourced from other persons.
4. This dissertation does not contain other persons' writing, unless specifically acknowledged as being sourced from other researchers. Where other written sources have been quoted, then:
 - a. Their words have been re-written but the general information attributed to them has been referenced.
 - b. Where their exact words have been used, then their writing has been placed in italics and inside quotation marks, and referenced.
5. This thesis does not contain text, graphics or tables copied and pasted from the Internet, unless specifically acknowledged, and the source being detailed in the dissertation and in the References sections.

Signed: _____



Declaration 2: Presentations and publications

Poster presentations

1. Postgraduate research and innovation symposium (PRIS) 2017

Title: The Potential of Plant Polyphenols as Natural Photostable Sunscreens

University of KwaZulu-Natal, Westville Campus, September 2017

2. 30th IFSCC Congress, Munich, Germany 2018

Title: The Potential of Plant Polyphenols as Notable Photostable Sunscreen Actives

Munich, Germany, 18 – 21 September 2018

3. Postgraduate research and innovation symposium (PRIS) 2019

Title: The Potential of Plant Polyphenols as Natural Photostable Sunscreen Actives

University of KwaZulu-Natal, Westville Campus, 6-7 September 2019

4. International Chemistry Conference in Botswana 2019

Title: The Potential of Plant Polyphenols as Natural Photostable Sunscreen Actives

UB Conference Centre, Gaborone, Botswana, 25-27th September 2019

Signed



Date: 20 July 2022

Acknowledgements

My postgraduate years at the University of KwaZulu-Natal have had influences from numerous individuals, both from within the university and externally. I am sincerely grateful to all these individuals, for without them this project would have not been possible.

I would like to thank:

- My supervisor, Professor B. S. Martincigh, for her invaluable guidance, knowledge and support through my M.Sc. research. Your mentorship has moulded me into the scientist I am today.
- Members of my research group for their encouragement and support in the laboratory, as well as the technical staff including; Raj Somaru, Unathi Bongaza, Thiloshini Naidoo and Malini Padaychee.
- My current employer, Union Swiss, for the support, encouragement and, allowing me the time to complete my studies.
- I would like to thank my family for their encouragement and support. I am especially grateful to my parents, Suran and Reena Sowman, my brothers, Silesh and Sovay Sowman, my aunt Meena Dayal, uncle Anil Somaroo, and finally my partner, Shimano Chetty. I am truly grateful for the sacrifices that you have made to help me achieve my ambitions..

Table of Contents

Abstract	i
Preface	iii
Declaration 1: Plagiarism.....	iv
Declaration 2: Presentations and publications.....	v
Acknowledgements	vi
Table of Contents.....	vii
Abbreviations	x
List of Figures	xii
List of Schemes.....	xxi
List of Tables.....	xxii
Chapter 1: Introduction	1
1.1 UV radiation	1
1.2 <i>Sutherlandia frutescens</i> (Cancer Bush plant)	2
1.3 Motivation for study	4
1.4 Aim and objectives	4
1.5 Synopsis of study and structure of dissertation	4
Chapter 2: Literature Review.....	6
2.1 Historical perspective of sun protection	6
2.2 The effects of UV radiation on human skin.....	7
2.2.1 Structure of the skin	7
2.2.2 Harmful effects of UV radiation on the skin.....	9
2.3 Sunscreens	14
2.3.1 Chemistry and mechanism of sunscreens	15
2.3.2 Sun Protection Factor.....	17
2.3.3 UVA measurement.....	18
2.4 Photostability of sunscreens	20
2.4.1 The photostability of organic UV filters	22
2.4.2 Broad spectrum filters.....	31
2.5 Plants with photostabilisation potential	32
Chapter 3: Experimental Procedures	49
3.1 Chemicals	49

3.2 Cancer Bush extraction methods	51
3.2.1 Boiling water extraction	51
3.2.2 Ethanol-water extraction	52
3.2.3 Flavonoid extraction.....	52
3.2.4 Phenolic acid extraction	53
3.3 Phenolic acid extraction for commercial teas	54
3.4 Qualitative tests	54
3.4.1 Test for flavonoids	54
3.4.2 Test for phenols.....	54
3.5 UV/Vis absorption spectroscopy	55
3.5.1 An introduction to UV/Vis absorption spectroscopy	55
3.5.2 UV/Vis spectrophotometer.....	56
3.6 Photostability experiments	58
3.6.1 Irradiation source	58
3.6.2 Commonly used UV absorbers	61
3.6.3 UV absorbers mixed with Cancer Bush extracts.....	62
3.6.4 Extracts from commercial teas.....	62
3.7 High performance liquid chromatography analysis.....	62
3.7.1 Introduction and instrumentation	62
3.7.2 HPLC parameters	64
3.7.3 Experimental procedure	65
3.8 Sunscreen formulation	66
3.8.1 Example sunscreen formulation.....	66
3.8.2 Adjusted sunscreen formulation.....	67
3.8.3 Experimental procedure	70
3.9 Sunscreen Assessment	71
3.9.1 Photostability studies for sunscreen products	71
3.9.2 Preliminary stability tests	71
3.9.3 In vitro tests.....	72
Chapter 4: Results and Discussion	75
4.1 Photostability assessment	76
4.1.1 Commonly used UV filters in different solvents	76
4.1.2 Cancer Bush plant extracts.....	88
4.1.3 Mixtures of UV chemical absorbers and Cancer Bush extracts.....	91
4.1.4 Flavonoid extracts from the Cancer Bush plant.....	106
4.1.5 Phenolic acids extracted from the Cancer Bush plant.....	114
4.1.6 Phenolic acids extracted from tea leaves	128
4.2 HPLC analysis	133
4.2.1 Phenolic acids.....	134
4.2.2 Cancer Bush plant	147
4.2.3 Tea extracts	150
4.2.4 Concentrations of phenolic acids in plant extracts.....	152

4.3 Sunscreens	154
4.3.1 UV analysis of sunscreen formulations.....	155
4.3.2 Stability studies	162
4.3.3 In vitro tests.....	166
Chapter 5: Conclusion and Recommendations for Future Work.....	169
References.....	172
Appendix A.....	191
Appendix B.....	193
Appendix C.....	199

Abbreviations

A – absorbance

b – path length

BCC – basal cell carcinoma

BMDBM – 4-*tert*-butyl-4'-methoxydibenzoylmethane (avobenzone)

c – concentration

COLIPA – European Cosmetic, Toiletry and Perfumery Association

DNA – deoxyribonucleic acid

ϵ – molar absorption coefficient

EHMC – 2-ethylhexyl-*p*-methoxy cinnamate

FDA – Food and Drug Administration

g – gram

GABA – γ -aminobutyric acid

GC – guanine-cytosine

GC/MS – gas chromatography/mass spectrometry

HPLC – high performance liquid chromatography

INCI – International Nomenclature of Cosmetic Ingredients

IPD – immediate pigment darkening

IR – infrared radiation

L – litre

LC/MS – liquid chromatography/mass spectrometry

LLE – liquid-liquid extraction

LOD – limit of detection

LOQ – limit of quantification

LSE – liquid-solid extraction

MBC – 4-methylbenzylidene camphor

MED – minimal erythematol dose

min – minute

ml – millilitre

MM – malignant melanoma

MMP – matrix metalloproteinase

NA – not applicable

ND – Not determined

nm – nanometer

NS – Not soluble

PABA – *para*-aminobenzoic acid

PBSA – 2-phenylbenzimidazole-5-sulfonic acid

PDA – photodiode array

PFA – ultraviolet A protection factor

PPD – persistent-pigment darkening

ROS – reactive oxygen species

RNA – ribonucleic acid

RNS – reactive nitrogen species

RP – reversed phase

S – soluble

SCC – squamous cell carcinoma

SCCS – Scientific Committee for Consumer Safety

SPF – sun protection factor

TMBP – 3-(3,4,5-trimethoxybenzylidene-2-4-pentanedione)

US – United States

UV – ultraviolet

List of Figures

Figure 1.1: The electromagnetic spectrum. ³	2
Figure 1.2: (A) <i>Sutherlandia frutescens</i> (Cancer Bush plant) planted at the Agricultural Research Council-Vegetable and Ornamental Plants Research Station, Roodeplaat, Gauteng, and (B) flowers. ¹³	3
Figure 2.1: Three-dimensional view of the skin structure. ³⁸	8
Figure 2.2: Skin cell layers. ³⁸	9
Figure 2.3 The absorption of UV radiation and the various energy releasing pathways. ⁷⁰	16
Figure 2.4 Structures of phenolic acids: (A) benzoic acid derivatives, and (B) cinnamic acid derivatives.	34
Figure 2.5: Chemical structure of aloesin.	38
Figure 2.6: Chemical structure of polyprenol.	42
Figure 3.1: A diagram showing the basic components of a double-beam UV/Vis spectrophotometer. ²⁵⁸	56
Figure 3.2: A typical UV spectrum. ²⁵⁹	58
Figure 3.3: A diagram of the Osram 500 W/2 high pressure mercury lamp (Osram and schematic drawing). ²⁶⁰	59
Figure 3.4: Output of the Osram HBO 500 W/2 high pressure mercury lamp. ²⁶¹	59
Figure 3.5: A photograph of the irradiation equipment showing the insulated steel box (A), containing the lamp, connected to an extractor (B) and the external bracket (C) which holds the filter, shutter and sample cuvette. The photograph also shows the fan (D) and the igniter (E).	60
Figure 3.6: Transmission spectrum of the 10 mm thick Pyrex filter.	60
Figure 3.7: Close-up of the external bracket holding the shutter gate, filter and cuvette.	61
Figure 3.8: Components of a HPLC. ²⁶²	63
Figure 4.1: Photostability of benzophenone-9 dissolved in methanol. The spectra were recorded every 30 minutes for a total period of six hours, and were acquired in a 1 cm pathlength quartz cuvette against air as the reference.	78

- Figure 4.2: Photostability of avobenzene dissolved in methanol. The spectra were recorded every 30 minutes for a total period of six hours, and were acquired in a 1 cm pathlength quartz cuvette against air as the reference.79
- Figure 4.3 Absorbance of avobenzene dissolved in methanol at 245 and 358 nm after 30-minute irradiation intervals indicating the loss of the *enol*-form (at 358 nm) and the formation of the *keto*-form (at 245 nm).80
- Figure 4.4: Photostability of avobenzene in ethyl acetate. The spectra were recorded every 30 minutes for a total period of six hours, and were acquired in a 1 cm pathlength quartz cuvette against air as the reference.81
- Figure 4.5: Photostability of avobenzene in cyclohexane. The spectra were recorded every 30 minutes for a total period of six hours, and were acquired in a 1 cm pathlength quartz cuvette against air as the reference.82
- Figure 4.6: Absorbance of avobenzene dissolved in cyclohexane monitored at 351 nm and at 261 nm after 30-minute irradiation intervals indicating the loss of the *enol*-form (at 351 nm) and the formation of the *keto*-form (at 263 nm).82
- Figure 4.7: Photostability of MBC dissolved in methanol. The spectra were recorded every 30 minutes for a total period of six hours, and were acquired in a 1 cm pathlength quartz cuvette against air as the reference.83
- Figure 4.8: Photostability of MBC dissolved in ethyl acetate. The spectra were recorded every 30 minutes for a total period of six hours, and were acquired in a 1 cm pathlength quartz cuvette against air as the reference.84
- Figure 4.9: Photostability of MBC dissolved in cyclohexane. The spectra were recorded every 30 minutes for a total period of six hours, and were acquired in a 1 cm pathlength quartz cuvette against air as the reference.85
- Figure 4.10: Photostability of EHMC dissolved in methanol. The spectra were recorded every 30 minutes for a total period of six hours, and were acquired in a 1 cm pathlength quartz cuvette against air as the reference.86
- Figure 4.11: Photostability of EHMC dissolved in ethyl acetate. The spectra were recorded every 30 minutes for a total period of six hours, and were acquired in a 1 cm pathlength quartz cuvette against air as the reference.87

- Figure 4.12: Photostability of EHMC dissolved in cyclohexane. The spectra were recorded every 30 minutes for a total period of six hours, and were acquired in a 1 cm pathlength quartz cuvette against air as the reference.88
- Figure 4.13: Photostability of the boiling water Cancer Bush extract dissolved in methanol. The spectra were recorded every 30 minutes for a total period of six hours, and were acquired in a 1 cm pathlength quartz cuvette against air as the reference.....90
- Figure 4.14: Photostability of the Cancer Bush ethanol-water extract dissolved in methanol. The spectra were recorded every 30 minutes for a total period of six hours, and were acquired in a 1 cm pathlength quartz cuvette against air as the reference.....91
- Figure 4.15: Photostability of benzophenone-9 mixed with the boiling water Cancer Bush extract and dissolved in methanol. The spectra were recorded every 30 minutes for a total period of six hours, and were acquired in a 1 cm pathlength quartz cuvette against air as the reference.....92
- Figure 4.16: Photostability of benzophenone-9 mixed with the Cancer Bush ethanol-water extract and dissolved in methanol. The spectra were recorded every 30 minutes for a total period of six hours, and were acquired in a 1 cm pathlength quartz cuvette against air as the reference.....93
- Figure 4.17: Photostability of avobenzone mixed with the boiling water Cancer Bush extract dissolved in methanol. The spectra were recorded every 30 minutes for a total period of six hours, and were acquired in a 1 cm pathlength quartz cuvette against air as the reference.....95
- Figure 4.18: Absorbance of avobenzone mixed with the boiling water Cancer Bush extract dissolved in methanol at 245 nm and 356 nm after 30-minute irradiation intervals indicating the loss of the *enol*-form and the formation of the *keto*-form.....95
- Figure 4.19: Photostability of avobenzone mixed with the Cancer Bush ethanol-water extract dissolved in methanol. The spectra were recorded every 30 minutes for a total period of six hours, and were acquired in a 1 cm pathlength quartz cuvette against air as the reference.....96
- Figure 4.20: Absorbance of avobenzone mixed with the Cancer Bush ethanol-water extract dissolved in methanol at 245 and 356 nm after 30 minute irradiation intervals confirming that phototautomerization was prevented.97

Figure 4.21: Photostability of avobenzone mixed with the Cancer Bush ethanol-water extract dissolved in ethyl acetate. The spectra were recorded every 30 minutes for a total period of six hours, and were acquired in a 1 cm pathlength quartz cuvette against air as the reference.....98

Figure 4.22: Photostability of avobenzone mixed with the Cancer Bush ethanol-water extract dissolved in cyclohexane. The spectra were recorded every 30 minutes for a total period of six hours, and were acquired in a 1 cm pathlength quartz cuvette against air as the reference.....99

Figure 4.23: Absorbance of avobenzone mixed with the Cancer Bush ethanol-water extract and dissolved in cyclohexane monitored at 351 nm and at 261 nm after 30-minute irradiation intervals indicating the loss of the *enol*-form (at 351 nm) and the formation of the *keto*-form (at 263 nm)..... 100

Figure 4.24: Photostability of MBC mixed with the Cancer Bush ethanol-water extract dissolved in methanol. The spectra were recorded every 30 minutes for a total period of six hours, and were acquired in a 1 cm pathlength quartz cuvette against air as the reference...101

Figure 4.25: Photostability of MBC mixed with the Cancer Bush ethanol-water extract dissolved in ethyl acetate. The spectra were recorded every 30 minutes for a total period of six hours, and were acquired in a 1 cm pathlength quartz cuvette against air as the reference...102

Figure 4.26: Photostability of MBC mixed with the Cancer Bush ethanol-water extract dissolved in cyclohexane. The spectra were recorded every 30 minutes for a total period of six hours, and were acquired in a 1 cm pathlength quartz cuvette against air as the reference...103

Figure 4.27: Photostability of EHMC mixed with the Cancer Bush ethanol-water extract dissolved in methanol. The spectra were recorded every 30 minutes for a total period of six hours, and were acquired in a 1 cm pathlength quartz cuvette against air as the reference...104

Figure 4.28: Photostability of EHMC mixed with the Cancer Bush ethanol-water extract dissolved in ethyl acetate. The spectra were recorded every 30 minutes for a total period of six hours, and were acquired in a 1 cm pathlength quartz cuvette against air as the reference...105

Figure 4.29: Photostability of EHMC mixed with the Cancer Bush ethanol-water extract dissolved in cyclohexane. The spectra were recorded every 30 minutes for a total period of six hours, and were acquired in a 1 cm pathlength quartz cuvette against air as the reference...106

Figure 4.30: Photostability of water-ethanol flavonoid extract from the Cancer Bush dissolved in methanol. The spectra were recorded every 30 minutes for a total period of six hours, and were acquired in a 1 cm pathlength quartz cuvette against air as the reference. 108

- Figure 4.31: Photostability of Cancer Bush water-ethanol extract mixed with benzophenone-9 and dissolved in methanol. The spectra were recorded every 30 minutes for a total period of six hours, and were acquired in a 1 cm pathlength quartz cuvette against air as the reference. 109
- Figure 4.32: Photostability of Cancer Bush water-ethanol flavonoid extract mixed with avobenzene and dissolved in methanol. The spectra were recorded every 30 minutes for a total period of six hours, and were acquired in a 1 cm pathlength quartz cuvette against air as the reference..... 110
- Figure 4.33: Absorbance of avobenzene mixed with the Cancer Bush water-ethanol flavonoid extract dissolved in methanol at 245 nm and 356 nm after 30-minute irradiation intervals indicating the loss of the *enol*-form and the formation of the *keto*-form..... 110
- Figure 4.34: Photostability of the Cancer Bush water-ethanol extract mixed with MBC dissolved in methanol. The spectra were recorded every 30 minutes for a total period of six hours, and were acquired in a 1 cm pathlength quartz cuvette against air as the reference... 111
- Figure 4.35: Photostability of the Cancer Bush water-ethanol flavonoid extract mixed with EHMC and dissolved in methanol. The spectra were recorded every 30 minutes for a total period of six hours, and were acquired in a 1 cm pathlength quartz cuvette against air as the reference..... 112
- Figure 4.36: Photostability of Cancer Bush ethyl acetate-ethanol flavonoid extract dissolved in methanol. The spectra were recorded every 30 minutes for a total period of six hours, and were acquired in a 1 cm pathlength quartz cuvette against air as the reference. 113
- Figure 4.37: Photostability of the Cancer Bush ethyl acetate-ethanol flavonoid extract mixed with avobenzene and dissolved in methanol. The spectra were recorded every 30 minutes for a total period of six hours, and were acquired in a 1 cm pathlength quartz cuvette against air as the reference..... 114
- Figure 4.38: Comparison of the diethyl ether and ethyl acetate layers obtained after Soxhlet and ultrasonic-assisted extraction of phenolic acids from the Cancer Bush. The spectra were acquired in a 1 cm pathlength quartz cuvette against air as the reference. 117
- Figure 4.39: Photostability of the diethyl ethyl layer from the ultrasonic-assisted phenolic acid extraction of the Cancer Bush dissolved in methanol. The spectra were recorded every 30

minutes for a total period of six hours, and were acquired in a 1 cm pathlength quartz cuvette against air as the reference.	118
Figure 4.40: Photostability of the ethyl acetate layer from the ultrasonic-assisted phenolic acid extraction of the Cancer Bush dissolved in methanol. The spectra were recorded every 30 minutes for a total period of six hours, and were acquired in a 1 cm pathlength quartz cuvette against air as the reference.	118
Figure 4.41: Photostability of the diethyl ether phenolic acid layer from ultrasonic-assisted extraction of the Cancer Bush mixed with benzophenone-9 and dissolved in methanol. The spectra were recorded every 30 minutes for a total period of six hours, and were acquired in a 1 cm pathlength quartz cuvette against air as the reference.	119
Figure 4.42: Photostability of the ethyl acetate phenolic acid layer from ultrasonic-assisted extraction of the Cancer Bush mixed with benzophenone-9 and dissolved in methanol. The spectra were recorded every 30 minutes for a total period of six hours, and were acquired in a 1 cm pathlength quartz cuvette against air as the reference.	120
Figure 4.43: Photostability of the diethyl ether phenolic acid layer from ultrasonic-assisted extraction of the Cancer Bush mixed with avobenzone and dissolved in methanol. The spectra were recorded every 30 minutes for a total period of six hours, and were acquired in a 1 cm pathlength quartz cuvette against air as the reference.	121
Figure 4.44: Absorbance of the diethyl ether phenolic acid layer from ultrasonic-assisted extraction of the Cancer Bush mixed with avobenzone dissolved in methanol at 245 and 358 nm after 30-minute irradiation intervals indicating little change in the <i>enol</i> - and <i>keto</i> -forms of avobenzone.	122
Figure 4.45: Photostability of the ethyl acetate phenolic acid extract from ultrasonic-assisted extraction of the Cancer Bush mixed with avobenzone and dissolved in methanol. The spectra were recorded every 30 minutes for a total period of six hours, and were acquired in a 1 cm pathlength quartz cuvette against air as the reference.	123
Figure 4.46: Absorbance of the ethyl acetate phenolic acid extract from ultrasonic-assisted extraction of the Cancer Bush mixed with avobenzone dissolved in methanol at 245 and 358 nm after 30-minute irradiation intervals indicating little change in the <i>enol</i> - and <i>keto</i> -forms of avobenzone	123

- Figure 4.47: Photostability of MBC mixed with the diethyl ether extract from ultrasonic-assisted extraction of the Cancer Bush and dissolved in methanol. The spectra were recorded every 30 minutes for a total period of six hours, and were acquired in a 1 cm pathlength quartz cuvette against air as the reference. 125
- Figure 4.48: Photostability of MBC mixed with the ethyl acetate phenolic acid extract from ultrasonic-assisted extraction of the Cancer Bush and dissolved in methanol. The spectra were recorded every 30 minutes for a total period of six hours, and were acquired in a 1 cm pathlength quartz cuvette against air as the reference. 126
- Figure 4.49: Photostability of EHMC the mixed with diethyl ether phenolic acid extract from ultrasonic-assisted extraction of the Cancer Bush and dissolved in methanol. The spectra were recorded every 30 minutes for a total period of six hours, and were acquired in a 1 cm pathlength quartz cuvette against air as the reference. 127
- Figure 4.50: Photostability of EHMC mixed with the ethyl acetate phenolic acid extract from ultrasonic-assisted extraction of the Cancer Bush and dissolved in methanol. The spectra were recorded every 30 minutes for a total period of six hours, and were acquired in a 1 cm pathlength quartz cuvette against air as the reference. 127
- Figure 4.51: Photostability of an ethanol-water green tea extract dissolved in methanol. The spectra were recorded every 30 minutes for a total period of six hours, and were acquired in a 1 cm pathlength quartz cuvette against air as the reference..... 130
- Figure 4.52: Photostability of an ethanol-water Rooibos tea extract dissolved in methanol. The spectra were recorded every 30 minutes for a total period of six hours, and were acquired in a 1 cm pathlength quartz cuvette against air as the reference..... 131
- Figure 4.53: Photostability of an ethanol-water Cancer Bush extract dissolved in methanol. The spectra were recorded every 30 minutes for a total period of six hours, and were acquired in a 1 cm pathlength quartz cuvette against air as the reference..... 132
- Figure 4.54: Photostability of green and Rooibos tea extracts, with the Cancer Bush plant extract dissolved in methanol. The spectra were recorded every 30 minutes for a total period of six hours, and were acquired in a 1 cm pathlength quartz cuvette against air as the reference. 133
- Figure 4.55: UV spectra of the six phenolic acid standards recorded by the PDA detector.. 137

- Figure 4.56: HPLC chromatogram of the 10 mg ml⁻¹ multi-standard phenolic acid solution obtained at 254 nm with the mobile phase composition of 12% MeOH and 1% acetic acid in Millipore water. The column was a Zorbax Eclipse XDB C18, the flow rate was 1.00 ml min⁻¹, and the injection volume was 10 µl. 139
- Figure 4.57: Calibration curves and residual plots for the determination of (A) gallic acid, (B) *p*-hydroxybenzoic acid, (C) vanillic acid, (D) caffeic acid, (E) syringic acid and (F) *p*-coumaric acid obtained at 254 nm. 145
- Figure 4.58: HPLC chromatograms of the Cancer Bush ethanol-water extract obtained at 254 and 309 nm with the mobile phase composition of 12% MeOH and 1% acetic acid in Millipore water. The column was a Zorbax Eclipse XDB C18, and the flow rate was 1.00 ml min⁻¹. The injected volume was 10 µl. 148
- Figure 4.59: UV spectra observed for vanillic acid and *p*-hydroxybenzoic acid respectively. 149
- Figure 4.60: HPLC chromatograms of the Cancer Bush extract (tea extraction method) obtained at 254 and 309 nm with the mobile phase composition of 12% MeOH and 1% acetic acid in Millipore water. The column was a Zorbax Eclipse XDB C18, the flow rate was 1.00 ml min⁻¹. The injected volume was 10 µl. 150
- Figure 4.61: HPLC chromatograms of the green tea extract obtained at 254 and 309 nm with the mobile phase composition of 12% MeOH and 1% acetic acid in Millipore water. The column was a Zorbax Eclipse XDB C18, the flow rate was 1.00 ml min⁻¹. The injected volume was 10 µl. 151
- Figure 4.62: HPLC chromatograms of the Rooibos tea extract obtained at 254 and 309 nm with mobile phase composition of 12% MeOH and 1% acetic acid in Millipore water. The column was a Zorbax Eclipse XDB C18, the flow rate was 1.00 ml min⁻¹. The injected volume was 10 µl. 152
- Figure 4.63: SPF 1.2 – Example formulation with reduced concentrations of UV filters. The spectra were recorded every 30 minutes for a total period of six hours, and were acquired on a quartz plate against air as the reference. 157
- Figure 4.64: SPF 1.3 – Example formulation with reduced concentrations of UV filters and the addition of the Cancer Bush ethanol-water extract. The spectra were recorded every 30 minutes

for a total period of six hours, and were acquired on a quartz plate against air as the reference.	158
Figure 4.65: SPF 2.1 – Adjusted formulation with avobenzone, benzophenone-9, MBC and EHMC. The spectra were recorded every 30 minutes for a total period of six hours, and were acquired on a quartz plate against air as the reference.....	159
Figure 4.66: SPF 2.2 – Adjusted formulation with avobenzone, benzophenone-9, MBC and EHMC with the addition of the Cancer Bush ethanol-water extract. The spectra were recorded every 30 minutes for a total period of six hours, and were acquired on a quartz plate against air as the reference.	161
Figure 4.67: SPF 2.3 – Adjusted formulation with avobenzone, benzophenone-9, MBC and EHMC with the addition of green tea extract. The spectra were recorded every 30 minutes for a total period of six hours, and were acquired on a quartz plate against air as the reference.	161
Figure 4.68: Images shown in order of left to right respectively, example formulation SPF 1.1 – Elementis Maui Milk SPF 15 – Attempt 1 (standard concentrations), SPF 1.2 – Elementis Maui Milk SPF 15 – Attempt 2 (reduced UV filter concentrations), and SPF 1.3 – Elementis Maui Milk SPF 15 – Attempt 3 (reduced UV filter concentrations with the Cancer Bush extract).	162
Figure 4.69: Images shown in order of left to right respectively, adjusted formulation SPF 2.1 – Elementis Maui Milk SPF 15 – Attempt 3 (the four UV filters used in this study), SPF 2.2 – Elementis Maui Milk SPF 15 – Attempt 2 (the four UV filters used in this study with Cancer Bush extract), and SPF 2.3 – Elementis Maui Milk SPF 15 – Attempt 3 (the four UV filters used in this study with green tea extract).....	163
Figure 4.70: Centrifugation before (A) and after (B) three consecutive runs.....	165

List of Schemes

Scheme 2.1: Formation of thymine cyclobutane dimers ⁵²	11
Scheme 2.2 : Formation of pyrimidine (6-4) pyrimidone photoproduct ⁵²	11
Scheme 2.3: The mechanisms leading to the formation of 8-oxo-7,8-dihydroguanine ⁵⁰	12
Scheme 2.4: Cinnamates undergo a <i>trans-cis</i> isomerisation when exposed to UV radiation ⁵⁴	20
Scheme 2.5: <i>Keto-enol</i> tautomerism of BMDBM ⁵⁴	21
Scheme 2.6: Photo-fragmentation of BMDBM into a phenyl radical and a benzoyl radical ..	21
Scheme 2.7: Dimerisation of EHMC ¹⁰²	21

List of Tables

Table 2.1: Chemical structures of organic UV filters approved by the FDA ⁶⁸	23
Table 2.2: List of botanical compounds with photoprotection properties that are used in sunscreen formulations	35
Table 3.1: Chemical UV absorbers	49
Table 3.2: Phenolic acids	50
Table 3.3: Other raw materials.....	50
Table 3.4: Plant materials	51
Table 3.5: Solvents.....	51
Table 3.6: Example formulation guideline	68
Table 3.7: Adjusted formulation guideline	69
Table 3.8: Normalised product function used in the calculation of SPF	73
Table 4.1: Solubility of UV filters in solvents of different polarity.	76
Table 4.2: The wavelengths of maximum absorption of avobenzone in different solvents	78
Table 4.3: Solubility of UV filters mixed with Cancer Bush extracts in solvents of different polarity	89
Table 4.4: Solubility of flavonoid extracts and UV filters in solvents of different polarity ..	107
Table 4.5: Yield of crude extract and purified extract obtained for each phenolic acid extraction method.....	116
Table 4.6: Amounts of materials used to extract phenolic acids from teas and the Cancer Bush, and the yields of extracts obtained.....	129
Table 4.7: Preparation of standard phenolic acid solutions made up to a total volume of 100 ml in MeOH	135
Table 4.8: Retention times and λ_{\max} values for each phenolic acid standard.....	136
Table 4.9: Concentration of each phenolic acid used for calibration	138
Table 4.10: Quality control parameters for the determination of phenolic acids	146
Table 4.11: Concentration (mg l^{-1}) of phenolic acids found in plant extracts	153

Table 4.12: Masses obtained for photostability analysis of sunscreen formulations.....	156
Table 4.13: Physiochemical parameters of SPF formulations before and after preliminary stability studies.....	164
Table 4.14: SPF values determined for the sunscreen preparations	167
Table 4.15: Occlusion factors obtained for the six sunscreen formulations prepared.	168

Chapter 1: Introduction

Protection from the sun dates to prehistoric times as a measure against the deleterious effects of solar ultraviolet (UV) radiation. Overexposure to this harmful UV radiation is a leading cause of pathological changes of the skin, such as erythema and the worst being skin cancer. Commercial sunscreen products available on the market are used for daily protection from UV radiation. Sunscreen products contain UV filter substances that are designed to protect human skin from erythema. These sunscreen products incorporate chemical UV-absorbing compounds and physical blockers that allow UV light to be reflected, scattered, or absorbed. Most sunscreens available require frequent re-application due to the product being rubbed off through wear or the product photodegrading on exposure to UV radiation. Re-application is undesirable to the consumer for various reasons. It is, therefore, necessary to improve the photostability of these products by increasing the efficacy of the UV filters.

Sun protection is a major concern in the cosmetic industry due to its limitations. The issues faced with certain UV absorbers are that they are susceptible to photodegradation over time, their degradation products can be phototoxic, and they provide protection only over a limited wavelength region. As a cosmetic scientist, it is necessary to ensure that these products maintain a certain level of protection from the sun throughout the day. This will add an appeal to the product, thereby promoting sales. Therefore, it is essential that sunscreens act as intended and should not photodegrade on use. Consequently, it is necessary to find means to improve the efficacy of current UV absorbers, and thereby improve the efficacy of a sunscreen formulation.

This has led to research on finding an alternative solution that can provide beneficial protection and maintain photostability. Interest was drawn to the plant kingdom for a more natural source of sunscreen absorbers since plants have developed various photoprotection mechanisms to counter enhanced levels of UV radiation. In this research polyphenols extracted from the plant *Sutherlandia frutescens*, as well as those from green tea and Rooibos tea, were investigated. These extracts were studied for their ability to photostabilise photolabile UV filters.

1.1 UV radiation

The sun emits electromagnetic radiation that is transmitted by vibratory motion in the form of electromagnetic waves.¹ These waves differ from one another in frequency (cycles per second) and in wavelength (the linear length of one cycle).² The electromagnetic spectrum arranges

the radiation in order of frequency or wavelength as seen in Figure 1.1. A portion of the spectrum consists of ultraviolet (100 to 400 nm), visible (400 to 780 nm) and infrared (780 to 10^6 nm) radiation.

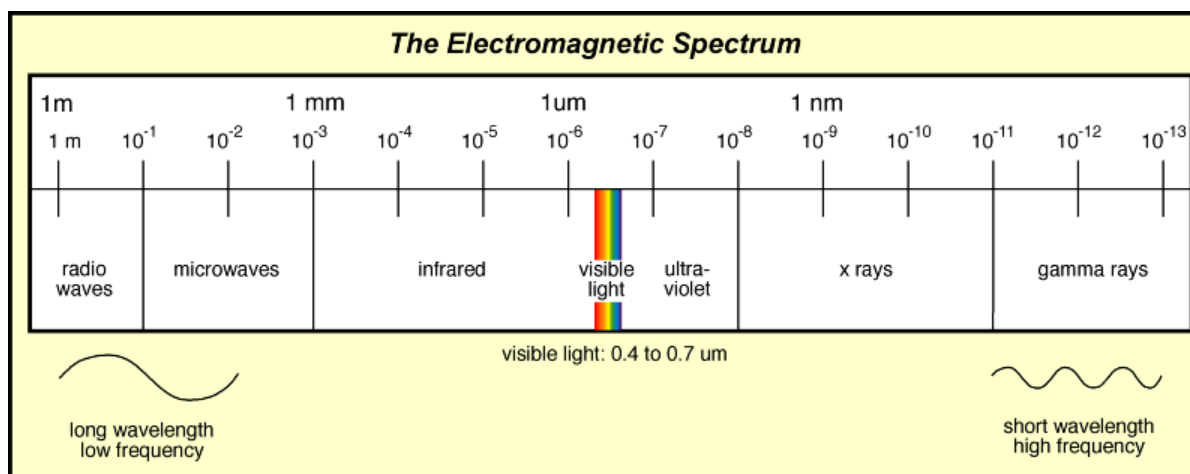


Figure 1.1: The electromagnetic spectrum.³

Human beings sense infrared radiation (IR) as heat and visible radiation is seen optically.⁴ UV radiation is not directly sensed but has the largest tendency to damage skin.⁵ For biological effects, UV radiation is divided into three components: UVC (100 to 280 nm), UVB (280 to 315 nm) and UVA (315 to 400 nm).⁶ Only a part of the UV radiation reaches the earth's surface, and this depends on the location, the season, cloud cover, air pollution and humidity.⁷ When UV radiation strikes the skin, some of it is reflected, some is absorbed, and some is transmitted. UVC radiation is the most energetic. Although it is the most harmful of the three, it is filtered out by the ozone layer and does not reach the earth's surface. UVB radiation is biologically active and is partially absorbed by the ozone layer.⁸ Only UVB radiation of wavelengths greater than 290 nm falls on the earth's surface and this contributes 5% of the solar UV radiation incident on the earth's surface. Most of the UV radiation that reaches the earth's surface is UVA. UVA is less energetic than UVB but penetrates deeper into the skin than UVB. UVA is chiefly responsible for many types of severe skin damage.^{9, 10} UVA can be further divided into UVA₁ (340 to 400 nm) and UVA₂ (320 to 340 nm). Individuals respond differently to UV radiation depending on their sensitivity and habits of sun exposure.¹¹

1.2 *Sutherlandia frutescens* (Cancer Bush plant)

Sutherlandia frutescens, shown in Figure 1.2A, a flowering shrub belongs to the family Fabaceae (legume, pea or bean family). Commonly used names refer to the plant's medicinal properties, such as Kankerbos (Afrikaans), Ummwele – Spear of light (Zulu and Xhosa), and

Cancer Bush (English).¹² The Cancer Bush has been used for hundreds of years by the indigenous people of South Africa and is believed to be the most commonly used healing plant. It grows in the dry parts of southern Africa and neighbouring countries. It is a perennial short-lived shrub reaching up to 2 m in height. The plant produces orange-red flowers, shown in Figure 1.2B, during the second half of the year and is adaptable to summer and winter rainfall areas.¹³ The plant was named after the botanist James Sutherland (1639-1719).^{12, 14} Traditional applications include the treatment of external wounds, internal fevers, stomach problems, diabetes, depression, and cancer.^{15, 16}

It is believed that the polyphenolic compounds present in the plant hold radical scavenging properties.¹⁷ Phytochemical investigations detected levels of L-canavanine, L-arginine, pinitol, γ -aminobutyric acid (GABA), asparagine and secondary plant metabolites such as saponins (triterpene glycosides).¹² Smith and Myburgh¹⁸ proposed that the active ingredients strengthen the immune system and activate physiological resources. *In vitro* studies reported the Cancer Bush plant's anti-oxidant, anti-inflammatory, anti-carcinogenic and antibacterial effects.^{16, 18}

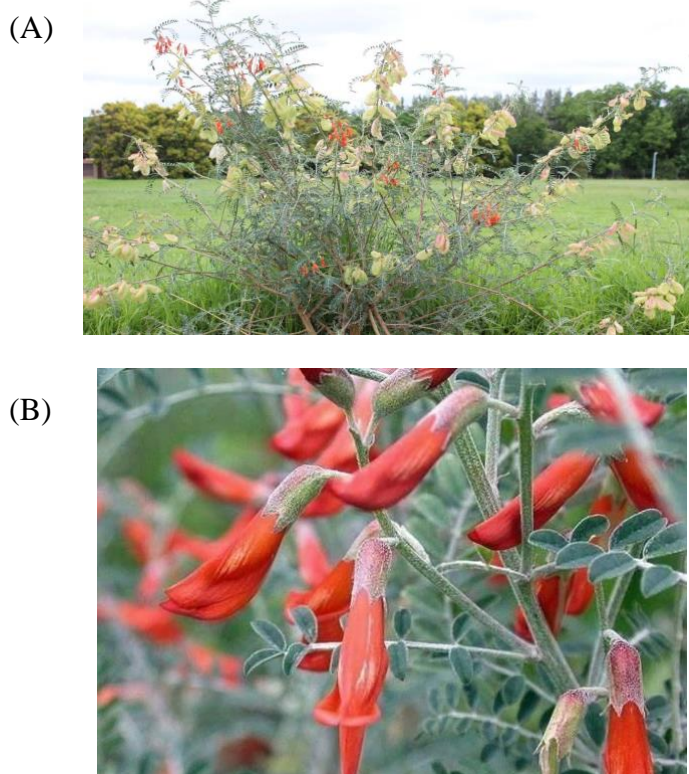


Figure 1.2: (A) *Sutherlandia frutescens* (Cancer Bush plant) planted at the Agricultural Research Council-Vegetable and Ornamental Plants Research Station, Roodeplaat, Gauteng, and (B) flowers.¹³

1.3 Motivation for study

Skin cancer and other skin diseases are attributed to excessive exposure to sunlight. Commercial sunscreen products contain organic UV filters. This research discusses the use of four commonly used organic UV absorbers and their importance in protection against the effects of UV radiation. Organic UV filters are limited by photodegradation and possible induction of photoallergic responses. This causes a significant problem in sunscreen products as their efficacy is reduced. This has led to research on finding an alternative solution that can provide beneficial protection and maintain photostability. Interest was drawn to the plant kingdom for a more natural source of sunscreen absorbers since plants have developed various photoprotection mechanisms to counter enhanced levels of UV radiation.

The potential use of Cancer Bush plant extracts in sunscreen formulations is under consideration and must be investigated further. Polyphenols in plant extracts have excellent antioxidant activity and have strong UV absorbing properties that cover a broad spectrum. Therefore, they can play a dual role by acting as both natural absorbers of harmful radiation and quenchers of free radical damage also caused by sunlight.

1.4 Aim and objectives

The aim of the study was to determine whether polyphenols from natural sources could serve as sunscreen active ingredients either on their own or when used correctly with approved UV filters.

The aim was achieved by undertaking the following objectives:

- To determine the photostability of commonly used UV filters.
- To extract, identify and quantify polyphenols from the leaves of the Cancer Bush and different teas and to determine their photoprotective capacity.
- To determine the photostability of green and Rooibos tea extracts and compare them with those derived from the Cancer Bush.
- To investigate if polyphenols could improve the photostability of photolabile UV filters.
- To investigate the effect of polyphenols in sunscreen formulations.

1.5 Synopsis of study and structure of dissertation

Attempts at photostabilising the selected UV filters were made by using polyphenols, specifically phenolic acids and flavonoids, obtained from plant extracts. The extracts were

derived from the Cancer Bush plant and Rooibos and green teas. The photostabilisation potential of these plant extracts on sunscreen absorbers was investigated. Photostability studies were conducted on the extracts alone and when mixed with each of the UV filters. A general sunscreen formulation was employed to assess the possible inclusion of polyphenols in sunscreens. Sunscreens were made with and without UV filters and photostability tests were conducted.

Chapter 1 provides a general introduction of sunscreens and the Cancer Bush plant, a motivation for the study, the aim and objectives, and a general outline of the content of this dissertation.

A detailed literature review is provided in Chapter 2 and covers the skin structure and damages to the skin by UV radiation, the chemistry and photostability of organic and inorganic sunscreen UV filters, the mechanism of sunscreens, as well as the photostability of plant extracts.

Chapter 3 presents the experimental methodology. This chapter includes materials and methods of the techniques used for the extractions of polyphenols, and photostability and high performance liquid chromatography (HPLC) investigations.

Chapter 4 discusses the results obtained for the experiments carried out.

Chapter 5 summarizes and concludes the dissertation and provides recommendations for future research.

Chapter 2: Literature Review

2.1 Historical perspective of sun protection

It is unknown when exactly individuals started protecting themselves from the sun. During prehistoric times to the early 20th century, members of the higher society believed it was crucial to protect themselves from exposure to sunlight to keep a fair complexion.¹⁹ This allowed for separation of the wealthy from the lower-class people who appeared to have a darker skin. A dark skin appearance signified those who were compelled to do manual labour to gain an income. This concept was nullified at the turn of the 20th century due to industrialization.²⁰ The change forced migration of underprivileged people into metropolitan areas to work. This affected both the rich and the poor similarly.²¹ Cities were reinforced with walls, houses were built closer to each other and streets were narrow.² The erection of factories forced people to work long hours, and narrow sunless towns created a desire for people to go outdoors more often. Henceforth, the allure of sunlight became apparent.

Around the 1890's, Niels Finsen also ignited the need for outdoor activities when he discovered the benefits of sunlight for certain skin problems such as *lupus vulgaris*.²²⁻²⁴ But it was fashion icon Coco Chanel who ignited the need for obtaining a proper suntan in the 1920s.²⁵ She transformed the elite to appreciate the 'tanned look' thereby setting a social trend that reformed people's perspective. During this time, it also became necessary in residential areas to build lavish homes with bigger lawns, fancy gardens and large swimming pools. All these factors contributed to excessive sun exposure.

However, this appeal declined when Norman Paul of Sydney published his book, entitled *The Influence of Sunlight in the Production of Cancer of the Skin*²⁶ creating awareness worldwide. In 1922, Karl Eilham Hausser and Wilhelm Vahle²⁷ discovered that UV radiation between 280 and 315 nm was in fact responsible for erythema, the familiar skin reddening known as sunburn. Thus, the benefits of the sun and obtaining a suntan were moderated. The need for protection against the sun became vital, leading to the development of photoprotective products such as sunscreens.

Sunscreens were introduced to the market in the 1920's to prevent sunburn. The first commercial chemical sunscreen was introduced in the United States (US) in 1928 and contained benzyl salicylate and benzyl cinnamate.²⁸ The development of photoprotective products grew in interest during World War II when there was a need to protect US soldiers from sunburn in tropical countries.^{19, 29} Experiments done during the war provided a number

of ingredients that contained protective significance. Benjamin Green invented the Red Veterinary Petroleum (Red Vet Pet) in 1944.^{19, 30} It was a sticky, red jelly substance that had limited efficiency.³⁰ The first effective sunscreen was developed by Franz Grieter in 1946 called *Gletscher Crème*.^{19, 31}

By 1967, sunscreen formulations included the infamous *para*-aminobenzoic acid (PABA) and its ester derivatives, such as 2-ethylhexyl-*o*-dimethylaminobenzoate (Padimate O) and amyl *p*-dimethylaminobenzoate (Padimate A).^{5, 19, 32} PABA, after being patented in 1943, became the primary organic sunscreen active ingredient for many years due to its ability to absorb UV rays very well and its insolubility to water.¹¹ Its use multiplied when dermatologists prescribed it to their patients and instructed them to massage it into their skin well to last longer. Over time, with multiple studies providing substantial evidence, it was discovered that PABA resulted in phototoxicity³³ and photoallergic contact dermatitis³⁴ reactions in patients. Hodges *et al.*³³ discovered that UV exposure to PABA enhanced bacterial cytotoxicity. Sutherland *et al.*³⁴ showed that PABA can penetrate into cells and cause the formation of cyclobutane pyrimidine dimers in deoxyribonucleic (DNA) of bacterial and mammalian cells. Subsequently, it was found that PABA was able to form adducts with thymine and thymidine when exposed to UV radiation.^{11, 35} Such dimer and adduct formation results in severe structural mutations in the DNA molecule and subsequent cancer development. Mayer and Baer^{29, 36} provided evidence of PABA reacting with other chemical components in treatment drugs that triggered an allergy. These sensitization reactions were a leading precursor to skin cancer. Consumers also disliked the yellow colouration of the agent that stained clothing.³⁷ Collectively, after much debate and research studies, sunscreens containing PABA represented a human hazard on exposure to UV radiation and were banned.²⁰ In 1999, 14 other chemical sunscreen agents were approved by the US Food and Drug Administration (FDA) for over-the-counter use in sun care products.²⁸

2.2 The effects of UV radiation on human skin

2.2.1 Structure of the skin

The human skin covers the entire body and accounts for about 7% of total body weight in an average adult.³⁸ Without the skin, human beings will be attacked by bacteria and decrease from water and heat loss. The skin consists of three layers: epidermis, dermis and a fatty layer (also called the subcutaneous) (see Figure 2.1).

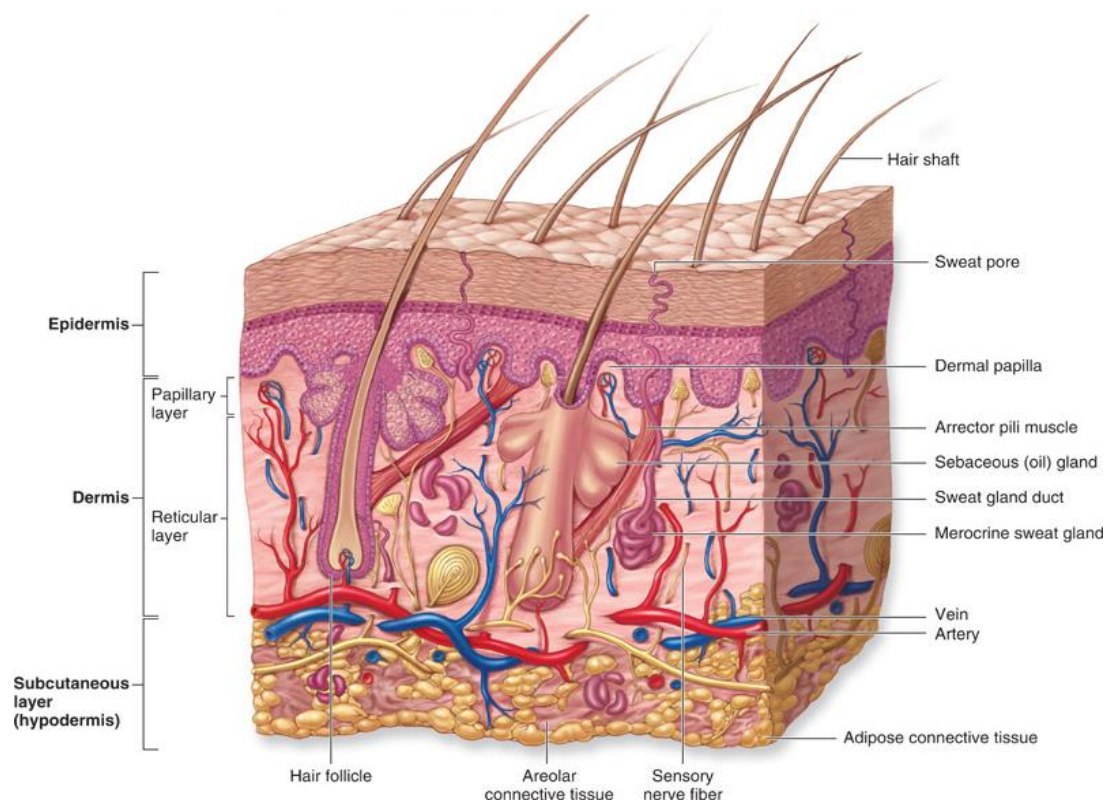


Figure 2.1: Three-dimensional view of the skin structure.³⁸

The epidermis is the outer and toughest layer of the skin. The toughness of the skin comes from a fibrous protein called keratin, which is a major structural component of the skin and gives the epidermis its protective properties. The epidermis contains five sublayers (see Figure 2.2): (i) to (v) as detailed below.³⁹⁻⁴¹

- (i) The stratum corneum contains dead, mature skin cells called keratinocytes. Keratinocytes are rich in reactive oxygen species (ROS) detoxifying enzymes and thus provide natural protection against ROS.⁴² This outer layer contains three quarters of the epidermal thickness and constantly sheds to be replaced by new cells pushed up from below.
- (ii) The stratum lucidum is a thin and translucent layer found between the stratum corneum and the stratum granulosum. It is made up of dead, flattened cells and helps reduce friction between the two adjacent layers.
- (iii) The stratum granulosum layer produces keratin and materials that prevent evaporation from the skin.
- (iv) The stratum spinosum contains the keratin-producing cells that are formed in the stratum basale.
- (v) The stratum basale forms the deepest epidermal layer and is attached to the underlying dermis. The cells of this layer continuously divide and form new keratinocytes to replace

the ones that are constantly shed. This layer also contains melanocytes, which are the cells that produce the pigment melanin.

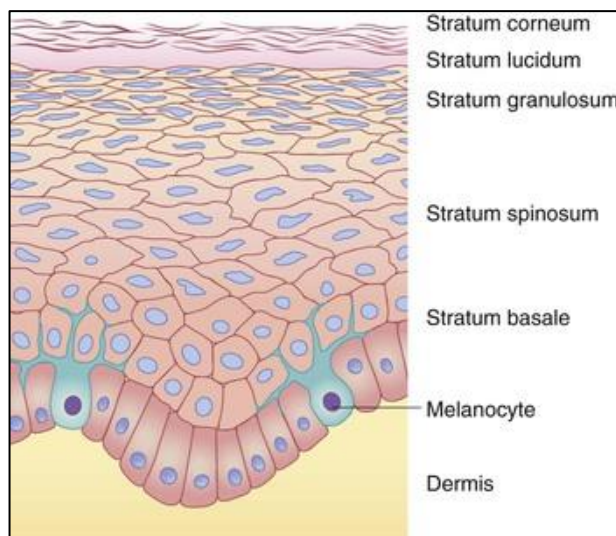


Figure 2.2: Skin cell layers.³⁸

The dermis is the lower layer of the skin that contains two sublayers: the papillary layer and the reticular layer as described below.³⁸

- (i) The papillary layer contains collagen and elastic fibres that give strength to the skin. The collagen and elastic fibres form a loosely woven mat with small blood vessels that allow phagocytes and other defensive cells to wander freely to patrol for bacteria.
- (ii) The reticular layer consists of coarse, irregularly arranged, dense fibrous connective tissue and holds 80% of the dermis. It is the network of the blood vessels.

Together the epidermis and dermis form the cutaneous layer. The subcutaneous layer (area below the skin) lies underneath the cutaneous layer.³⁹ It holds most of the body's fat, so it varies in thickness from one person to another.

2.2.2 Harmful effects of UV radiation on the skin

There are three pigments that contribute to the colouring of human skin: melanin, carotene and haemoglobin.³⁸ Only melanin, found in the stratum basale (Figure 2.2), is made in the skin. Melanin is produced by the body as a photoprotective measure. The photoprotective action of melanin is mediated via absorption of UV radiation, accompanied by dissipation as heat, multiple scattering of UV rays with subsequent absorption, quenching of excited states and free-radical scavenging (efficient neutralization of free radicals by eumelanin).⁴³ All humans have the same comparative number of melanocytes, but differentiation in skin colouring originates from geographical habitation. For example, darker skinned people are found near

the equator and lighter skinned people are found at the poles. Skin colouring can also be differentiated by race and the amount of melanin made and retained in the skin.³⁸ For example, darker skinned people produce much more melanosomes than fair skinned people.

Melanocytes are important in forming a pigment shield that protects the skin from the damaging effects of UV radiation.³⁸ Too much sun exposure causes a considerable build-up of melanin, that helps protect DNA in cells from UV radiation. The accumulation helps by absorbing the rays and releasing the energy as heat. However, the rate at which melanin is produced during this time is much faster than the repair of photo-damaged DNA, resulting in a visible darkening of the skin (known as a suntan).³⁸

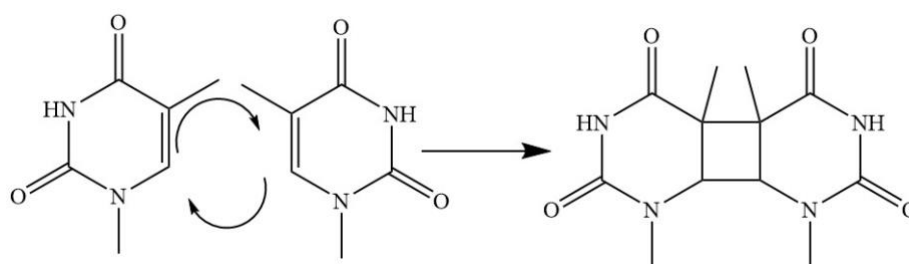
Even though the human body creates melanin as a protective shield, prolonged sun exposure will ultimately damage the skin causing acute or chronic problems for the skin. Acute effects include erythema, sunburn, inflammation, pigmentation, hyperplasia, immunosuppression and vitamin D synthesis.^{21, 44} Chronic effects include mutations, photocarcinogenesis, photoaging, premature aging of the of the skin, rough texture, mottled pigmentation, basalomas and skin cancer.^{21, 45}

The adverse effects are caused by clumping of the elastic fibres causing leathery skin. This temporarily depresses the immune system and can lead to alterations of the DNA in skin cells and in due course can result in skin cancer which is the worst of the chronic effects. Another disadvantage of UV radiation is destruction of the body's folic acid that is necessary for DNA synthesis.³⁸ This can also impair the development of an unborn baby's nervous system.³⁸

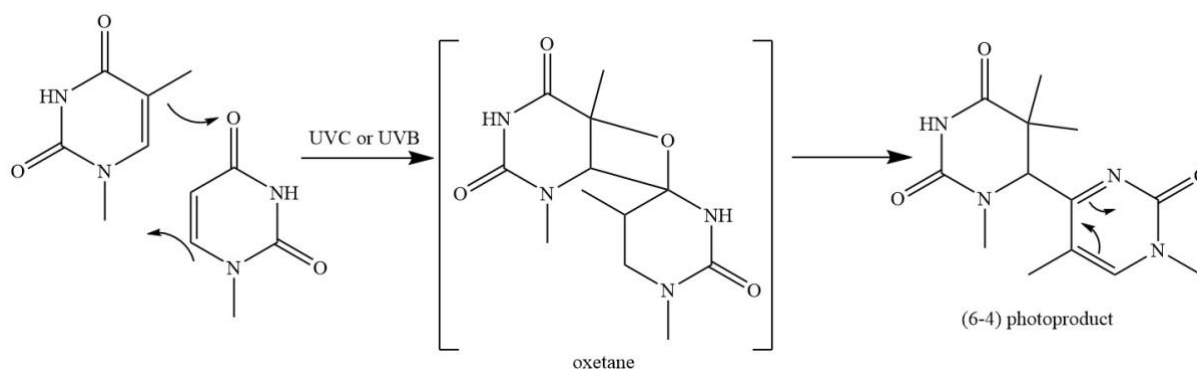
Chromophores in the skin, which includes melanin, DNA, ribonucleic acid (RNA), proteins, lipids, water, aromatic amino acids, etc., are responsible for absorbing UV energy.⁴⁶ Absorption of various UV photons results in different photochemical reactions and secondary interactions. In the absence of the ozone layer, exposure to UVC has the potential to kill unicellular organisms in a short amount of time, including skin cells, and cause mutations in DNA such as pyrimidine dimers.⁸

The way in which absorbed UVB and UVA energy damages the skin can be differentiated by their unique mechanisms. UVB has a short wavelength with slightly more energy than UVA and only penetrates the epidermis. Low doses of UVB are beneficial to the skin as it triggers the synthesis of vitamin D and supports the immune system.^{47, 48} However, higher doses of UVB on the skin can be lethal and mutagenic to skin cells.⁴⁹ DNA bases absorb at about 260 nm, in the UVC range, with the tail end of the spectrum absorbing in the UVB range. DNA

exposure to UVB can lead to the mutagenicity and lethality action of dimeric pyrimidine photoproducts. This includes the formation of cyclobutane pyrimidine dimers and pyrimidine (6-4) pyrimidone photoproducts.^{50,51} The formation of thymine cyclobutane, shown in Scheme 2.1, can form various diastereoisomers including: *cis-syn*, *cis-anti*, *trans-anti* and *trans-syn*.⁵² These photoproducts form when two adjacent pyrimidines (thymines, TT, or cytosines, CC) form a covalent bond creating a chemical intermediate that is not found in DNA. The formation of pyrimidine (6-4) pyrimidone photoproducts is shown in Scheme 2.2. This process leads to the formation oxetane which is unstable. This is a result from a [2+2] cycloaddition of the C5-C6 double bond of the 5'-end pyrimidine and the C4 carbonyl group of the 3'-end thymine.⁵² When the 3'-end base is a cytosine, an azetidine intermediate is formed. Spontaneous rearrangement of the oxetane or azetidine causes the formation of the pyrimidine (6-4) pyrimidone photoproducts.^{52, 53} The structural DNA lesion causes damage to DNA, RNA and proteins.⁵ This prevents pyrimidines from base pairing and DNA from replicating. This leads to inflammation, sunburn, skin cancer and aging of the skin.⁸



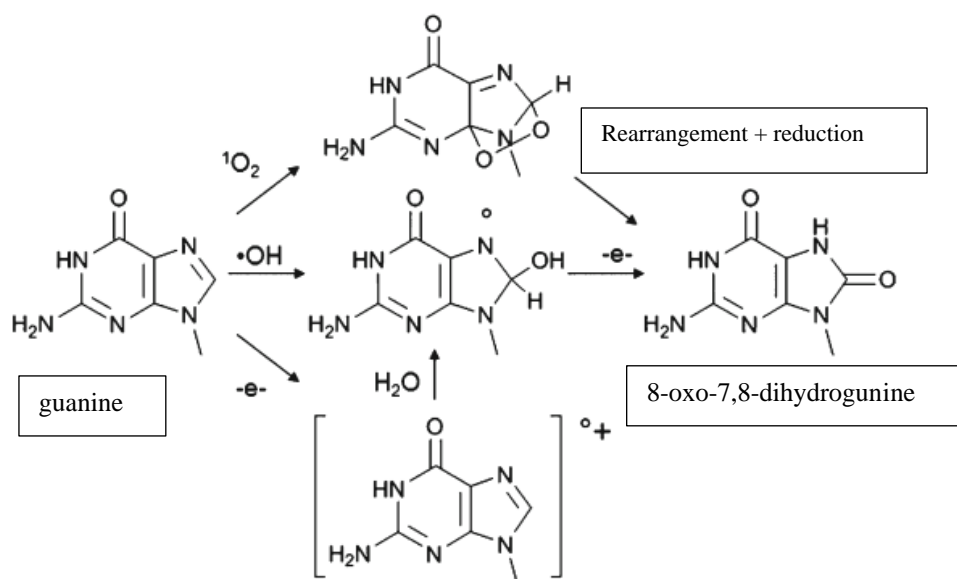
Scheme 2.1: Formation of thymine cyclobutane dimers⁵²



Scheme 2.2 : Formation of pyrimidine (6-4) pyrimidone photoproduct⁵²

UVA is able to penetrate deeper into the skin, reaching the dermis. DNA does not significantly absorb UVA to cause direct damage. Damage is caused through photosensitized oxidation.⁵⁴ Photosensitisers generate harmful ROS and reactive nitrogen species (RNS) that alter proteins, lipids and DNA. ROS damage leads to premature skin aging, wrinkle formation,

photoimmunosuppression and a higher risk of skin cancers due to alteration of DNA bases.¹¹ UVA radiation also stimulates the formation of cyclobutane pyrimidine dimers and a variety of oxidative lesions such as single strand breaks and oxidized bases. The most frequent damage produced by several mechanisms is 8-oxo-7,8-dihydroguanine, shown in Scheme 2.3.⁵⁰ The oxidation of guanine into 8-oxoguanine can base pair with adenine via two hydrogen bonds. When the second strand is synthesized, the base position originally occupied by a guanine is then replaced with a thymine causing mutations during replication of DNA.⁴⁹



Scheme 2.3: The mechanisms leading to the formation of 8-oxo-7,8-dihydroguanine⁵⁰

2.2.2.1 Skin cancer

As mentioned before, the leading factor in developing skin cancer is prolonged contact with UV radiation that damages DNA bases.³⁸ The incidence of skin cancer has grown drastically over the last two decades.²⁸ It is important to note that the human body develops a guard against the generation of skin cancer. This takes place when the skin gets tanned by the sun, or more severely, burned by the sun, it speeds up its process of creating a protein called Fas.⁵⁵ Fas causes damaged skin cells to perish and peel off the skin thereby decreasing the risk of the cells mutating into skin cancer.³⁸ However, the damage caused to the skin occurs faster than Fas can be produced.

The mechanism in which sunlight can cause skin cancers occurs in two ways. The first mechanism is direct alteration of DNA keratinocytes, causing keratinocytes to grow abnormally.⁵⁶ This leads to formation of abnormal structures within the epidermal layer causing mutations and photochemical modifications.⁴⁷ The second mechanism is suppression

of the immune response thereby, allowing for enhanced growth of tumours.⁵⁷ Although the skin contains Langerhans cells to identify and destroy malignant cells, UV radiation also impairs these cells and hence reduces the body's natural defence.⁵⁸

The three major types of skin cancer are the following.^{38, 59, 60}

- (1) Basal cell carcinoma (BCC) is the least harmful but accounts for 80% of the skin cancer occurrences. BCC commonly occurs on sun-exposed areas of the head, neck and upper torso. These cancers occur in the stratum basale layer. They grow slowly forming a lump or dry, scaly area. As the BCC grows, it appears as a sore and is unable to heal. It is unlikely for basal cell cancer to spread to other parts of the body. But if left untreated, it can grow into nearby areas and invade the bone or other tissues causing damage and disfigurement.⁶⁰
- (2) Squamous cell carcinoma (SCC) is the second most common skin cancer. It results from the keratinocytes of the stratum spinosum. It appears as a scaly reddened papule that occurs on the head and hands. It can also develop into chronic skin sores or scars. It grows rapidly in deeper layers of the skin and can spread to other areas of the body if not treated. When caught early, there is a high chance of a complete cure. This type of skin cancer is commonly found in albinos who have a defect in one of several genes that produce or distribute melanin.
- (3) Malignant melanoma (MM) is the most dangerous type of skin cancer. It is cancer of melanocytes and is highly metastatic and resistant to chemotherapy. Melanoma can arise whenever there is a pigment or pre-existing mole. This cancer can become life threatening if not treated within six weeks. The American Cancer Society suggests that people who stay outdoors more often should follow the ABCDE rule found on their website for examining this type of skin cancer.⁶⁰ The A stands for asymmetry where one part of a mole or birthmark does not match the other. The B stands for border. Melanoma borders are usually uneven and may have edges that are irregular, ragged, notched or blurred. The C stands for colour. Multiple colours are a warning sign and notes when the colour is not the same all over. This may include different shades of brown, black or sometimes with patches of pink, red, white or blue. The D stands for diameter and notes if the spot is larger than six millimetres, although melanomas can sometimes be smaller than this. The E stands for evolving and notes if the mole changes size, shape, colour or any new symptom such as bleeding, itching or crusting occurs. It is important to note that causes of melanoma are complex and not only related to exposure to solar radiation.

Therefore, sun protection measures have been advocated to decrease the risk of skin cancer and other skin problems such as erythema. This incorporates staying out of the sun during peak hours between 10h00 to 16h00, the use of sunscreens and wearing protective clothing including long sleeves, hats and sunglasses, among other measures. Today, individuals benefit from sunscreen products that are high in sun protection factor (SPF) with a broad UV protection to cover both UVA and UVB radiation.¹⁹ The application of high SPF products should not be used as an excuse to stay out in the sun for prolonged periods of time. Some skin lotions have also been formulated to repair damaged DNA cells before they can develop into cancer cells.³⁸

2.3 Sunscreens

Sunscreen products come in various forms ranging from powders, creams, sprays and lotions. The primary use of sunscreens is to protect the skin from short-term and long-term effects of UV radiation.⁶¹ While sunscreens have been proven to reduce the amount of UV radiation absorbed by the skin, these products are still under a lot of scrutiny. Researchers such as Garland and Gorham have reported that the use of sunscreens can increase the chances of skin cancer.^{62, 63} Gallagher⁶⁴ reported that sunscreens can reduce the risk of SCC, however, there is no convincing evidence to support that it reduces the risk of BCC and MM. Literature, however, provides enough evidence to prove the benefits of using sunscreens provided that it is to be used as the last step in sun protection and comes after the use of shade during peak hours and protective clothing.^{19, 31, 61}

An ideal sunscreen would contain a combination of physical and chemical agents, provide protection against a broad spectrum (i.e.: UVA and UVB), must be stable to heat, have cosmetic appeal, must be non-toxic and non-irritant, hypoallergenic and economical.^{61, 65} Sunscreens must be created to prevent sunburn, freckling, discolouration, photoaging, skin cancer, phototoxic and photo-allergic reactions, photosensitivity diseases, and inflammatory hyperpigmentation.^{61, 66}

Initially, sunscreens were developed to prevent sunburn by mostly focussing on UVB radiation, which contains more erythemogenic wavelengths. This was because UVA radiation was considered harmless due to its low energy wavelengths.⁶⁷ It was only until the last decade that scientists discovered the damage caused by UVA radiation. UVA can penetrate deeper into the skin, causing photoaging and DNA damage through photosensitizing oxidation.⁵⁴ This caused a change in sunscreen development and cosmetic industries moved towards the

manufacturing of broad-spectrum sunscreens. Broad spectrum sunscreen products are much more effective as they provide protection against the entire UV range.

2.3.1 Chemistry and mechanism of sunscreens

Sunscreens are photochemical systems containing UV-absorbing filters.⁵⁴ All UV chemical absorbers found in sunscreens contain aromatic functional groups that are conjugated with a carbonyl electron-donating group. The electron-donating group is either *para*- or *ortho*- to an amine or methoxy electron-accepting group.²⁰ The conjugation is responsible for absorbing UV radiation.⁶⁸ The substitution orientation is important. A *para*-orientation favours electron delocalization and transfers an electron.²⁰ The electron delocalization energy corresponds to the UVA and UVB radiation energy. Therefore, when an electron found in the chemical filter absorbs UV radiation, the electron is excited and moves from the ground state to a higher energy state.

Three processes can occur in this excited state:⁶¹

- (i) Photostable filter – dissipates its absorbed energy to the environment as thermal energy or a photon of lower energy and returns to the ground state. It is fully capable of absorbing UV radiation again.
- (ii) Photo-unstable filter – undergoes a change in its chemical structure or is degraded. It is not capable of absorbing UV radiation again.
- (iii) Photo-reactive filter – reacts with surrounding ingredients of the sunscreen, oxygen, skin proteins and lipids. This leads to the production of unwanted reactive species or photo-adducts.

An ideal sunscreen would only contain photostable filters as it is the harmless way to proceed. The excited electron from the singlet ground state can move to a higher energy singlet state and maintain its electronic spin state. From the higher energy state, the electron returns to the ground state by losing its excess energy in various photophysical and photochemical pathways as seen in Figure 2.3.¹⁷ The harmless ways of doing so is releasing thermal energy through vibrational relaxation transitions (non-radiative decay) or through release of a photon of energy of longer wavelength called fluorescence (radiative decay).⁶⁹

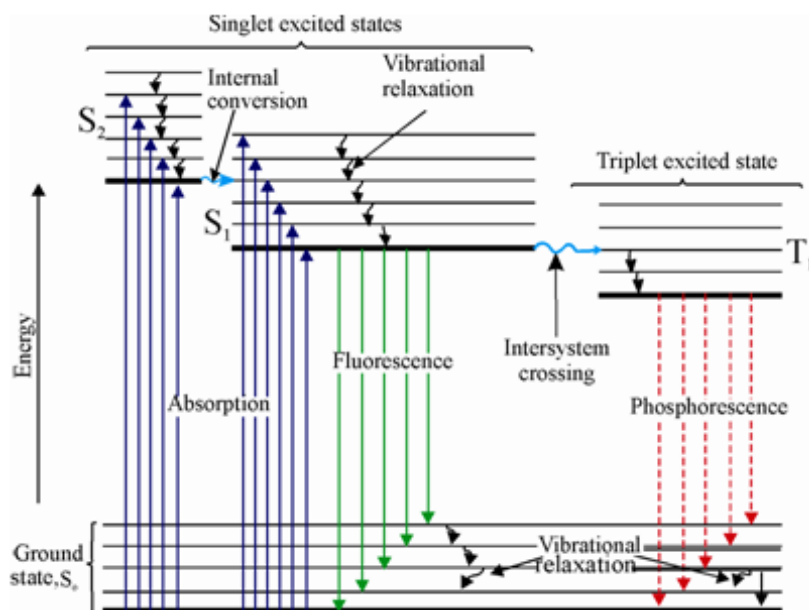


Figure 2.3 The absorption of UV radiation and the various energy releasing pathways.⁷⁰

However, the excited electron could also intersystem cross to a triplet state. This can result in harmful dissipation of radiation. In the triplet state, it can move back to the ground state with phosphorescence by emitting a photon.⁵⁴ However, further photochemical reactions can occur from the triplet state resulting in photolabile UV filters. Photochemical dissipation pathways are unwelcome as they reduce the efficacy of sunscreens and can be detrimental if they occur within the body.¹⁷

Conversely, when UV filters are combined as in a broad-spectrum sunscreen, some tend to be stabilised in the presence of others. This is due to the filters behaving as singlet or triplet quenchers.⁵⁴ Quenching is a process whereby an excited molecule undergoes intermolecular deactivation by another excited molecule. Combined filters form an overlap of electron clouds. The filter in an electronically excited state condition (the donor) can interact with a ground-state molecule of the other UV filter (the acceptor) and transfer its energy. The electron movement from the excited molecule is sensed and the energy is transferred to the ground state molecule. No photon is emitted or exchanged. The acceptor is known as a quencher and the donor is known as a sensitiser.⁷¹ A better quenching capacity is experienced when the overlap is greater.⁷² The advantage of an energy transfer is that it eliminates the chances of other photochemical reactions from occurring and offers photoprotection.

To protect against both UVB and UVA, the sunscreen must contain a combination of UV filters whose absorption profiles cover the entire UV region. UV protection is dependent on sunscreens to contain chemical filters that either absorb, scatter or reflect UV radiation. These

chemicals are generally divided into two types of filters: inorganic (physical blockers) and organic (chemical absorbers). Inorganic agents work by scattering, reflecting or absorbing UV radiation. The latter is dependent on their particle size. These filters include titanium dioxide and zinc oxide. These filters are not the focus of this research and are not discussed further. Organic agents are chemical absorbers (UV filters) and are subdivided into UVA filters (which absorb predominantly UVA radiation), UVB filters (absorb mainly UVB radiation), and broad spectrum filters (which absorb both UVA and UVB radiation).⁵⁴

The chemical structure of the filter influences its absorption.⁷³ When the number of resonance structures increases, it becomes easier to stabilize the excited state.¹⁹ This leads to a stronger absorption at longer wavelengths. To be an effective filter, the molecule chosen needs to protect against the entire UV range, be photo-chemically stable in sunlight, dissolve or disperse easily and permanently in the product, remain in place after perspiration or swimming, must be non-toxic, and must not cause irritation or an allergy.⁷³ Due to these requirements, there are strict guidelines that state the maximum concentration for each filter in the final product. The concentration of each filter determines the degree of protection of the final sunscreen product.⁷³ Particle size is also important. A decrease in particle size improves the cosmetic acceptability. Both concentration and particle size are critical for the final protection provided.⁷⁴

Sunscreens that can dissolve and disperse the UV filters uniformly can enhance the overall UV protection.⁷⁵ A good UV filter must dissipate the absorbed energy in a safe manner. For it not to be harmful to the consumer, it must disperse of the energy faster than the time for any side-reaction to occur. It is important to note that a surplus of UV filters in a poorly formulated product tend to accumulate in the valleys of the skin, leaving an uneven coverage.⁷⁶ This leads to a lower SPF protection. On the other hand, UV filters in a well-formulated product provide an even coverage of the skin, and hence provide better protection from the sun.

2.3.2 Sun Protection Factor

Commercial sunscreen products display a mandatory numeric label called the sun protection factor (SPF). This can come in various strengths ranging from 5 to 50+. The SPF is a measure of the effectiveness of a sunscreen formulation, a concept originally proposed by Rudolf Schulze.⁷⁷ SPF is defined as the ratio of UV energy needed to produce a minimal erythema dose (MED) on protected to unprotected skin. More simply, it is the ratio of sun exposure that the skin can tolerate before burning or erythema is apparent with and without sunscreen protection.⁵ This is expressed mathematically in Equation 1:

$$\text{SPF} = \frac{\text{minimal erythema dose in sunscreen-protected skin}}{\text{minimal erythema dose in non-sunscreen-protected skin}} \quad (1)$$

The SPF follows the following grading system: low (SPF 2-15), medium (SPF 15-30), high (SPF 30-50), highest (SPF 50+).⁶¹ It is suggested that application of a product with SPF 5 provides sunburn protection for five times longer than for unprotected skin. A sunscreen with an SPF of 15, has the ability to filter out about 94% of UVB rays, but an SPF 30 blocks about 97%.⁷⁸ This 3% difference is the distinction between an aesthetically pleasing sunscreen and an undesirable one.⁶¹ Products with a higher SPF tend to be uncomfortable due to the higher concentrations of active ingredients.⁷⁹

The definition of SPF is only a measure of UVB protection. It is not a measure for the less erythemogenic but still deleterious longer wavelengths of UVA radiation.^{11, 67} Determination of the SPF of a product includes an accurately detailed protocol on the number of test subjects, skin types, the sites of testing (e.g. lower back), the source of light, the method of reading the results and calculating the final SPF by mathematical equations.⁸⁰

The SPF value of a sunscreen formulation is determined by an *in vivo* method. This requires a group of volunteers to measure the least amount of UV energy required to produce minimal erythema on sunscreen protected skin to the amount of energy required to produce the same erythema on unprotected skin.⁸¹ These methods allow for testing of photostability and substantivity simultaneously. Substantivity is defined as the ability of a sunscreen to maintain efficacy and withstand adverse conditions such as exposure to water and sweat.⁸² Such methods are widely used by the European Cosmetic, Toiletry and Perfumery Association (COLIPA) and FDA.⁸⁰ Nevertheless, these methods are limited in terms of costing, time and require high doses of UV exposure to the volunteers.

2.3.3 UVA measurement

Once the detrimental aspects of UVA radiation were realised, methods had to be developed to evaluate the efficacy of UVA protection. This can be measured by *in vivo* and *in vitro* methods. The *in vivo* method is called the Persistent-Pigment Darkening (PPD) method.⁸³ This method measures the minimal darkening effect of UVA radiation on the skin before and after exposure to UVA energy.⁸⁴ The equation for UVA-PF is defined as the minimal pigmenting dose (MPD = UVA dose when darkening of the skin is visible) on protected skin over the MPD on unprotected skin (Equation 2).^{85, 86}

$$\text{UVA - PF} = \frac{\text{minimal pigment dose in protected skin}}{\text{minimal pigment dose in unprotected skin}} \quad (2) \quad 87, 88$$

Other *in vivo* techniques that can be used to measure the efficacy of UVA protection include immediate pigment darkening (IPD)⁸⁹ and the erythema protection factor (PFA) test method.⁹⁰

⁹¹ Although SPF is the most reliable indicator of the efficacy of sunscreen filters for UVB radiation, the erythema protection factor is more accurate. This is because the erythema protection factor considers the erythematous response after 24 hours.^{46, 89-91}

In vitro testing methods are currently being developed to prevent the involvement of human volunteers.⁹¹ They are also much faster, reproducible and economical. These methods involve a variety of UV spectrometers to conduct measurements of spectral transmittance.^{91, 92} Tests involve combining UV filters into a cream emulsion and applying this onto a synthetic support, or in spectrometric analysis of dilute solutions of sunscreen products.^{85, 86} However, without human volunteers, the results are questionable. Bunhu *et al.*⁴⁷ studied the *in vitro* critical wavelength method to evaluate broad spectrum protection. The study compared the photostabilities of commercial sunscreens dispersed in solution versus the smearing the sunscreen emulsion on quartz plates. Their results showed that the behaviour of sunscreens in solution are extremely diverse when compared with the same emulsion smeared on a quartz plate. They found that sunscreen products displayed higher photostabilities in solution than on a quartz plate.⁴⁷ This could be attributed to the different vehicles' influence on the photochemical behaviour of active ingredients. This implied that *in vitro* testing by spectrometric analysis of dilute solutions is not an effective way of measuring UVA as results are not relevant to practical conditions.

According to a study conducted by Robinson and Rademaker in 1998, sunscreens are recommended to be applied at least 30 minutes before exposure to allow for adequate diffusion into the stratum corneum.⁹³ The FDA suggests an application of 2 mg cm⁻² to all exposed areas in order to protect the skin. The sunscreen must be reapplied every two hours, after swimming, vigorous activity, excessive perspiration, or towelling.⁹⁴ However, these guidelines are not obeyed by consumers and, hence, consumers do not receive the optimal benefits a sunscreen can provide.⁹⁵

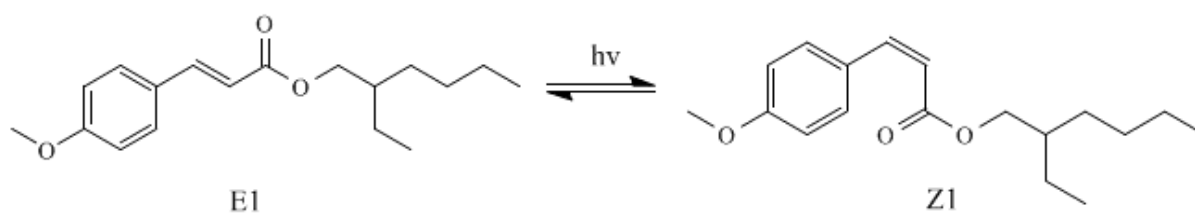
Presently, there is a high selection of sunscreen products that cover the broad spectrum with a high SPF. These sunscreens, as well as cosmetic and hair products, contain a variety of organic and inorganic UV filters that are combined to reach a balanced UVA/UVB protection.⁶⁵ The combination of UV filters allowed in sunscreens, cosmetics and hair products not only protects against sunburn, but also shields against other sun-induced adverse effects such as

photosensitivity, skin aging and as mentioned before, some types of skin cancer such as SCC and actinic keratoses.^{64, 65, 96}

2.4 Photostability of sunscreens

The photostability of chemical absorbers used in sunscreens is an important consideration in the manufacturing process. One of the challenges of making an effective sunscreen is that some UV filters tend to photodegrade after exposure to UV irradiation. This decreases the product's efficiency, reduces its photoprotective power, and promotes phototoxicity and photoallergic contact dermatitis.⁹⁷ If these chemical agents remain photolabile, their efficacy becomes limited and all health risks are still viable. Due to this, as well as the rise in sunscreen usage, photostability testing is vital and has grown in interest over the years. These filters must be critically studied before they are marketed in order to increase their efficiency, prevent the release of organic UV filters into the environment, and to consider possible ecological impacts and their behaviour on the skin.^{96, 98, 99}

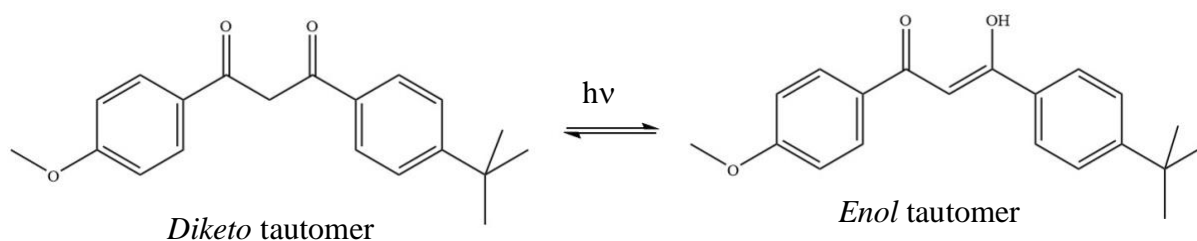
On exposure to UV energy, some of the original UV filter molecules can undergo photochemical reactions such as photoisomerisation, phototautomerisation, photofragmentation and photodimerisation. These filters then convert to isomers, tautomers, fragments or dimers, which are less effective or completely ineffective in providing UV protection. This results in alteration or destruction of the filter capacity and causes a decrease in the SPF of the sunscreen product. Isomerisation of UV filters include *cis-trans* isomers. For example, cinnamates undergo *trans-cis* isomerisation as shown in Scheme 2.4, and the *trans*-form has a higher absorption coefficient than the *cis*-form. Hence, transformation to the *cis*-form results in a decrease of SPF.



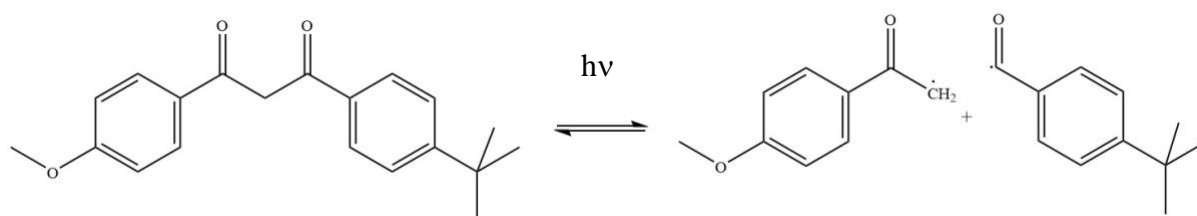
Scheme 2.4: Cinnamates undergo a *trans-cis* isomerisation when exposed to UV radiation⁵⁴

Keto-enol tautomerism is shown in Scheme 2.5 by using avobenzene (4-*tert*-butyl-4'-methoxydibenzoylmethane (BMDBM)) as an example. Here, the *enol* form absorbs in the UVA range. After irradiation, it converts to the *diketo*-form which absorbs in the UVC range which is not relevant for a sunscreen. Scheme 2.6 shows UV filters that can fragment and

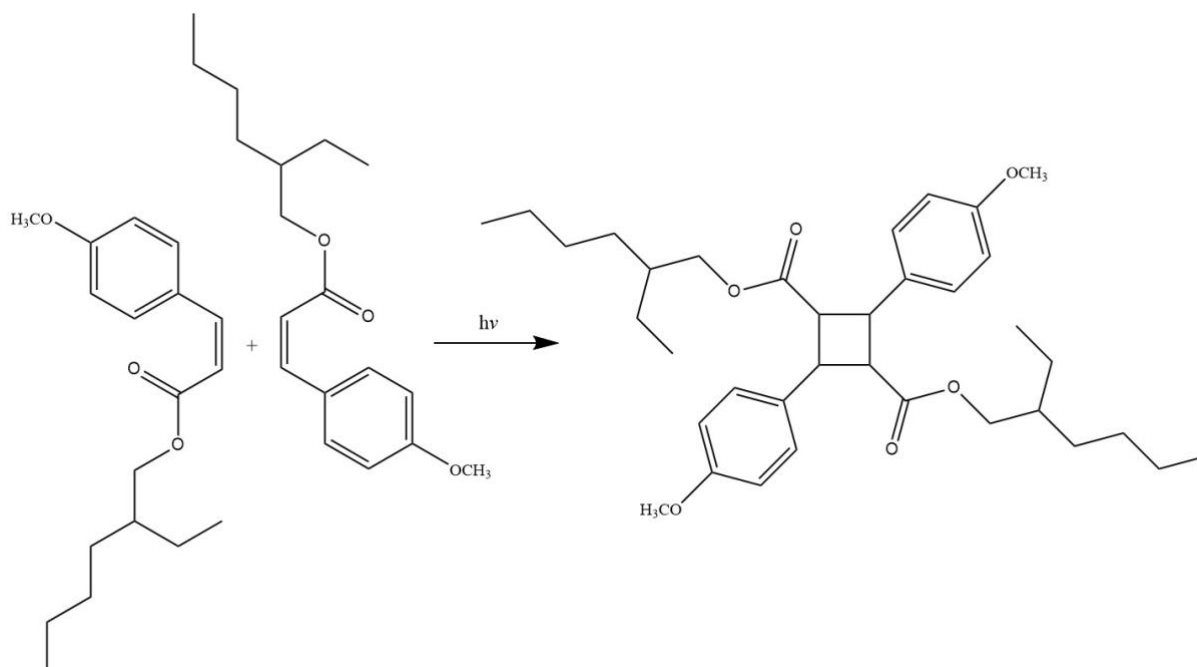
produce by-products after irradiation or by reacting with other UV filters.^{100, 101} Photodimerisation results in loss of protective capacity in the photoadduct as a result of loss of conjugation in the molecule 2-ethylhexyl-*para*-methoxycinnamate (EHMC) as shown in Scheme 2.7.



Scheme 2.5: *Keto-enol* tautomerism of BMDBM⁵⁴



Scheme 2.6: Photo-fragmentation of BMDBM into a phenyl radical and a benzoyl radical



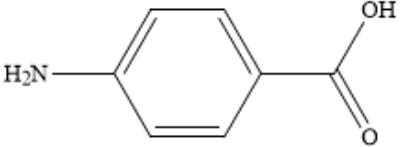
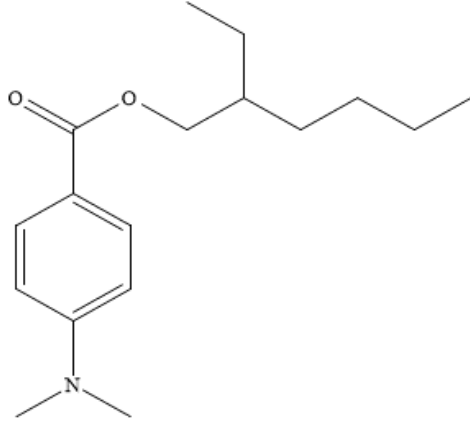
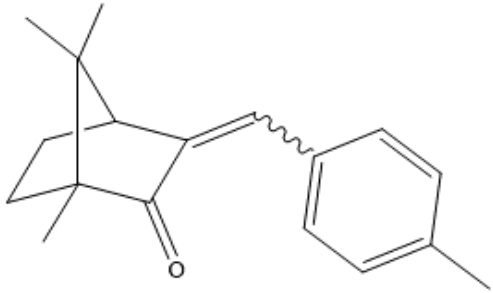
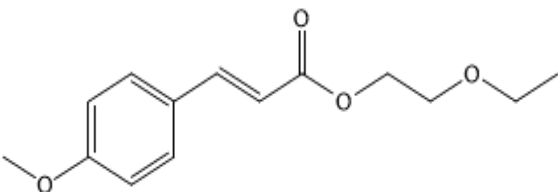
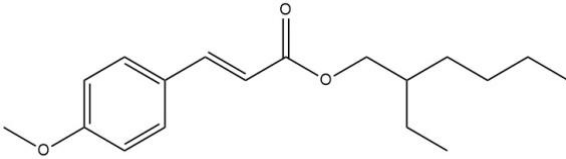
Scheme 2.7: Dimerisation of EHMC¹⁰²

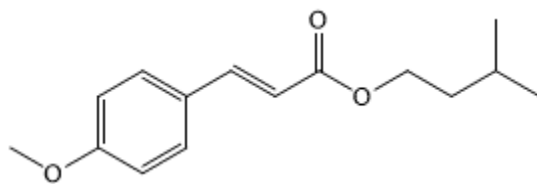
Because of these reactions and degradation, sunscreens must be developed to be photostable to maintain their UV protection efficiency. This can be achieved by combining different filters or by making use of SPF boosters.

2.4.1 The photostability of organic UV filters

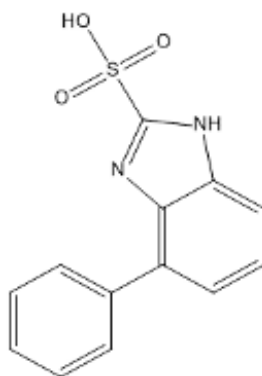
The focal point of designing organic sunscreen products is to choose a combination of UV filters (chemical absorbers) to provide broad-spectrum protection. The efficacy of the sunscreen products are dependent on the photostabilisation of the combination of these chemical absorbers. Chemical absorbers are active ingredients that absorb UV radiation to a variable extent within a specific range of wavelength depending on their chemical structure.¹⁰³ The combination of UV filters are two-fold. The combination of two or more UV filters can offer synergistic capabilities with regard to the overall efficacy and photostabilisation of the active principles. However, the combination can also result in degradation if a photoreaction occurs between filters. Therefore, in order to develop an ideal sunscreen product, photostable UV filter combinations are imperative. Care should be taken to select a UV filter that can act as a photostabiliser to stabilise the photolabile filters and act as a photoprotector itself.¹⁷ Table 2.1 provides some of the popular chemical absorbers used in sunscreen formulations. Attempts to improve the photostability of some of the chemical absorbers are briefly discussed.^{17, 103}

Table 2.1: Chemical structures of organic UV filters approved by the FDA⁶⁸

UVB FILTERS	
Aminobenzoate (PABA derivatives)	
 <p>PABA (<i>para</i>-aminobenzoic acid)</p>	 <p>Padimate-O (2-ethylhexyl-4-(dimethylamino)benzoate)</p>
Camphors	
 <p>Enzacamene (4-methylbenzylidene camphor (MBC))</p>	
Cinnamates	
 <p>Cinoxate (2-ethoxyethyl <i>p</i>-methoxycinnamate)</p>	 <p>Octinoxate (2-ethylhexyl-<i>p</i>-methoxycinnamate (EHMC))</p>



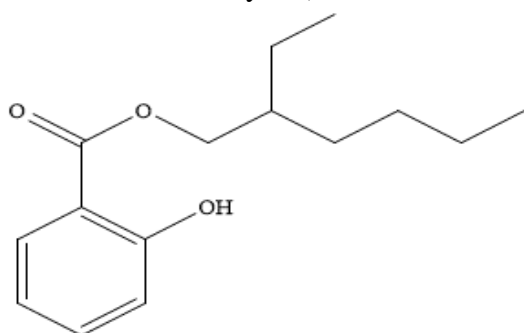
Isoamyl methoxycinnamate

Ensulizole

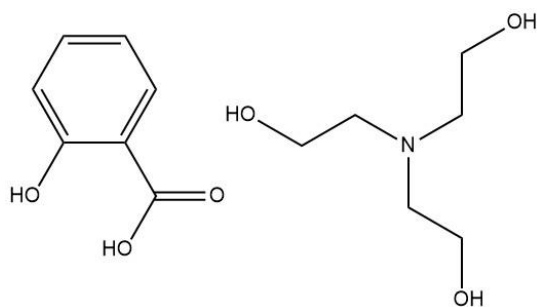
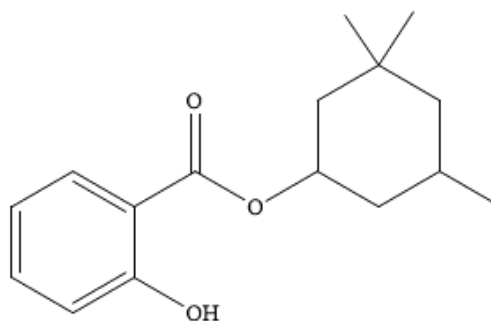
(2-phenylbenzimidazole-5-sulfonic acid)

Salicylates

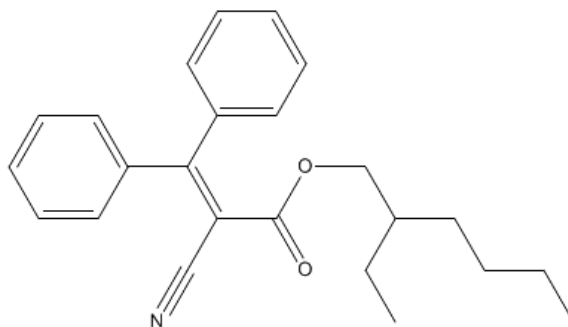
Octisalate (octyl salicylate or 2-ethylhexyl salicylate)



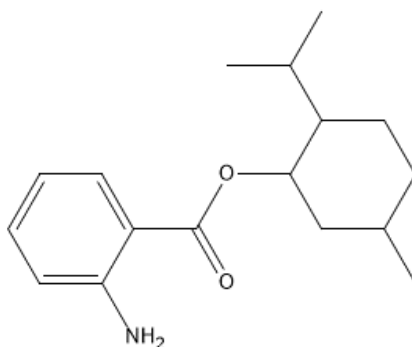
Homosalate (homomenthyl salicylate)



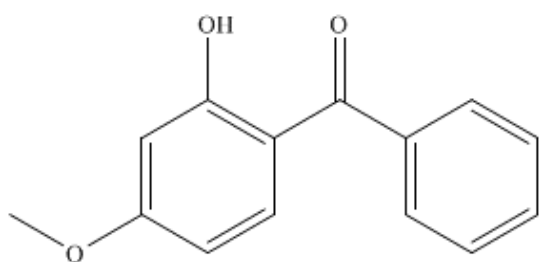
Trolamine salicylate (triethanolamine salicylate)

Octocrylene

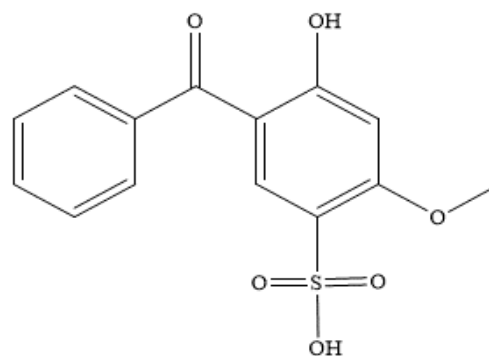
2-ethylhexyl-2-cyano-3,3-diphenylacrylate

UVA FILTERS**Anthranilates**

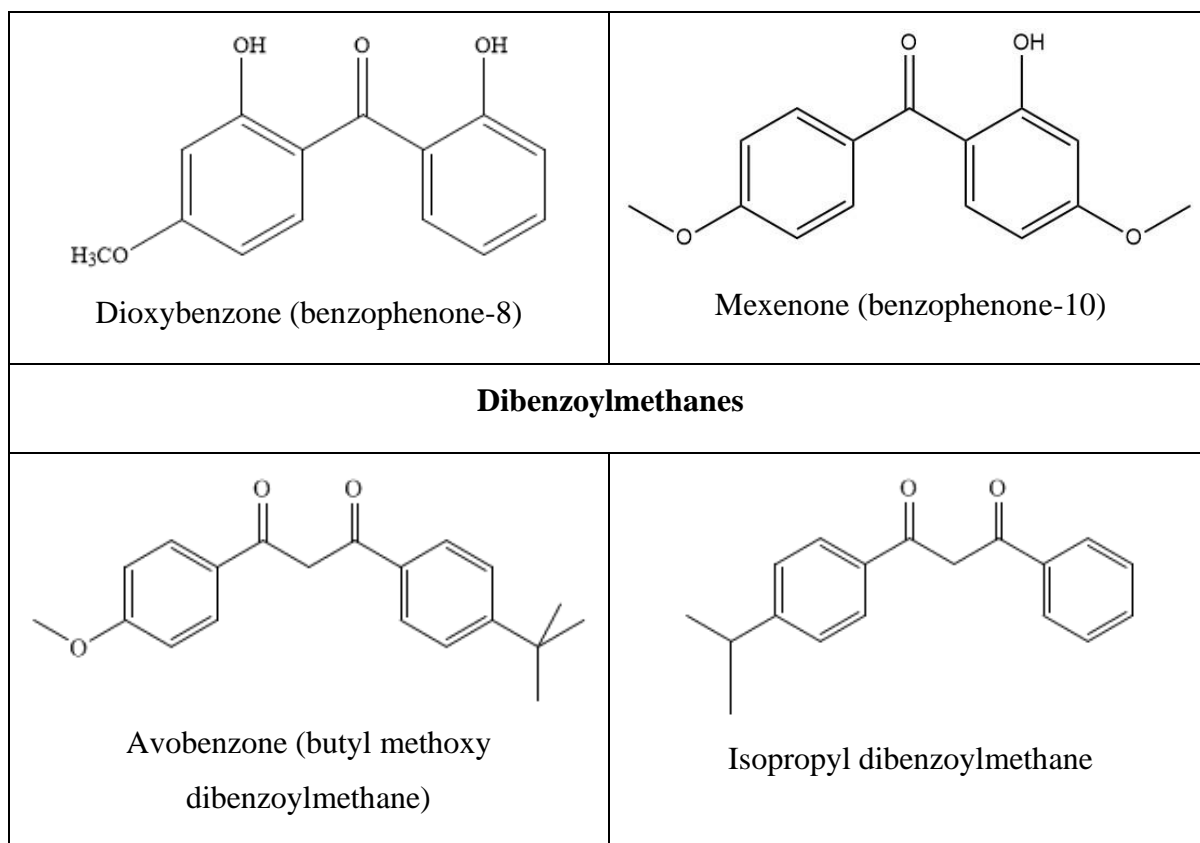
Meradimate (menthyl anthranilate)

Benzophenones

Oxybenzone (benzophenone-3)



Sulisobenzene (benzophenone-4)



2.4.1.1 Organic UVB agents:

- (i) **Aminobenzoates** include PABA (*para*-aminobenzoic acid) and its derivative, Padimate-O (2-ethylhexyl-4-(dimethylamino)benzoate). PABA was the first widely used UV filter due to its high substantivity. The chemical composition of PABA is a benzene ring substituted with an amino group and a carboxylic acid. PABA is a white crystalline powder that is insoluble in water.¹⁰⁴ Its peak absorption wavelength is 283 nm.⁶⁸ Reasons for the discontinuation of PABA included photoallergic reactions in humans as well as cross-reaction with other *para*-molecules. Many consumers also expressed their displeasure with the yellow discoloration.¹⁰⁴ Padimate-O was developed as an alternative as it has a better safety profile and does not stain the skin.^{29, 78} In Padimate-O, the carboxyl group of PABA has been converted into a branched chain ester, and the amino-group has been converted into a dimethylamino group.¹⁰⁵ The peak absorption wavelength of Padimate-O occurs at 311 nm. Padimate-O is not as effective as PABA and needs to be combined with other UV filters to increase the overall SPF. Padimate-O offers easy incorporation into cosmetic products and is often used in hair products. Pathak and Robins reported that studies conducted on hairless mice showed sunscreens containing Padimate-O protected mice from development of

UV-induced skin cancer upon repeated UV exposure.¹⁰⁶ However, Knowland *et al.*^{105, 107} warned of the possible toxicity of Padimate-O since they found that it is mutagenic in sunlight. Sunscreens containing Padimate-O could generate mutations and rapidly divide cells that are deficient in DNA repair. It caused direct strand breaks and oxidative lesions mainly at guanine-cytosine (GC) base pairs.¹⁰⁸ This was detected via various tests.^{29, 68, 78, 104, 106}

- (ii) **Camphor derivatives** are reasonably effective UVB filters with good photostability. They include enzacamene (4-methylbenzylidene camphor (MBC)) which has a maximum peak absorption at 300 nm.⁷⁸ Camphor-based absorbers are said to be more stable than cinnamates, but also undergo *cis-trans* photoisomerisation.¹⁰¹ Deflandre and Lang¹⁰⁹ reported that the photoisomerisation can occur insignificantly and reaches a photostable equilibrium rapidly. They also showed that photoisomerisation and photodegradation of camphor derivatives is not dependent on oxygen nor concentration.¹⁰⁹ Photoisomerisation is generally solvent-dependent.^{78, 101, 109}
- (iii) **Cinnamates** include cinoxate (2-ethoxyethyl-*p*-methoxycinnamate) and octinoxate (2-ethylhexyl-*p*-methoxycinnamate (EHMC)). They are the most popular UVB filters as they do not stain or cause irritation to the skin.^{73, 104} Cinnamates are very effective, have a good safety profile and are readily compatible with other UV filters. A disadvantage of cinnamates is that they undergo photoisomerisation. They exist in both the *cis*- and *trans*-isomer forms. They hold the *trans*-form in sunscreens and convert to the *cis*-form when irradiated with UV radiation. This conversion results in loss of protective capacity. Cinoxate has a peak absorption at 289 nm and is rarely used.⁷⁸

EHMC has an absorption profile from 270 to 328 nm.⁶⁸ Its peak absorption is at 310 nm. Sunscreen products containing EHMC are known to be photolabile due to its photoisomerisation.^{110, 111} The degradation causes formation of the *cis*-isomer which has a peak absorption at shorter wavelength and a smaller molar absorption coefficient. Christensen *et al.*¹¹² studied the phototoxicity of EHMC and BMDDBM in mice cells at concentrations lower than typical levels in sunscreens and reported that sun-exposed EHMC is more toxic than the unexposed filter due to the breakdown products at shorter wavelengths when exposed to light. EHMC also has poor substantivity and requires stabilisation with other UV filters to achieve a high SPF. However, various combinations result in these filters becoming photolabile and reduce its UV protection.^{68, 113} Another drawback of EHMC is its incompatibility with avobenzone

(BMDBM), which is a widely used UVA filter. Avobenzone (BMDBM) destabilises the cinnamate molecule due to the triplet excited state of the cinnamic chromophore being lower than the excited state of BMDBM.^{114, 115} Hence, it may undergo photosensitised isomerisation in the presence of BMDBM. Chatelain *et al.*⁹⁷ and Perugini *et al.*¹¹⁶ discussed some of the attempts made to stabilise EHMC. The efficacy of EHMC is increased when encapsulated in polymethylmethacrylate microspheres.^{68, 117} Encapsulating techniques have shown to improve the photostability, but their efficacy is reduced when exposed to sunlight.¹¹⁶

- (iv) **Ensulizole** (2-phenylbenzimidazole sulfonic acid (PBSA)) is a water-soluble UVB filter with an absorption profile ranging from 290-320 nm. Its maximum absorption peak is at 310 nm.⁷⁸ Its aesthetically pleasing formulation provides a lighter, less oily consistency than other sunscreen ingredients. It is used to enhance the SPF of the final product by combination with other organic and inorganic agents.^{47, 78} It is common in daily moisturisers. Skin reactions seldom occur with PBSA. However, Stevenson and Davies confirmed that PBSA functions as an efficient photosensitiser of guanine base damage in DNA when exposed to UVB radiation.¹¹⁸ They showed that PBSA is active at sub-millimolar concentrations and induce the formation of piperidine-labile cleavage sites to the positions of guanine residues.¹¹⁸
- (v) **Salicylate** derivatives are the weakest organic UVB filters. These include octisalate (octyl salicylate or 2-ethylhexyl salicylate), homosalate (homomenthyl salicylate) and trolamine salicylate (triethanolamine salicylate). They have an absorption profile from 290 – 315 nm.⁶⁸ Octisalate and homosalate are weak UVB filters. Octisalate has a maximum absorption at 307 nm and homosalate at 306 nm.⁶⁸ The two are exceptionally stable, non-sensitising and water-insoluble. They also hold favourable safety and toxicological profiles as they do not penetrate the stratum corneum.⁴⁶ They are highly photostable agents used to reduce photodegradation of other active sunscreen ingredients, such as benzophenones and avobenzone, but must be used in high concentrations in order to meet SPF requirements.⁷³ Their hydrophobic ability serves as solvents for other sunscreen chemicals.¹⁰⁴ Trolamine salicylate is hydrophilic and is used in hair products as a photoprotective agent.⁷⁸
- (vi) **Octocrylene** (2-ethylhexyl-2-cyano-3,3-diphenylarylate) is another weak UVB absorber. It has an absorption profile from 290 to 360 nm with its peak absorption at 307 nm.⁶⁸ Octocrylene has an excellent safety profile with low chances of irritation on

the skin, phototoxicity and photoallergic potential.¹¹⁹ Octocrylene can offer improved photostability of the final product when combined with other ingredients and is regarded as the best photostabiliser for avobenzone. However, in the past it was costly and difficult to integrate into sunscreen products.¹⁰⁴ This filter also has a low substantivity and loses its efficacy when exposed to sweat and water.^{68, 104, 119} The Scientific Committee for Consumer Safety (SCCS) has recently reviewed the use of octocrylene in cosmetic products and has restricted its use as a UV filter at a maximum concentration of 10%.¹²⁰ This restriction will be implemented from August 2022 in the Official Journal of the European Union.

2.4.1.2 Organic UVA agents

- (i) **Anthranilate** derivatives include Meradimate (menthyl anthranilate) and homomenthyl-*N*-acetyl anthranilate. Anthranilates absorb mainly in the UVA range up to about 350 nm. Anthranilates are commonly used in Neutrogena cosmetics. Meradimate is a weaker filter used to enhance UVA₂ protection (320 to 340 nm) and was developed as an alternate to oxybenzone.¹²¹ Advantages include its liquid state, miscibility with cosmetic oils, easy emulsification within aqueous formulations, and that it is colourless and odourless.¹²¹
- (ii) **Benzophenones** are aromatic ketones that provide broad spectrum UV protection. The FDA has approved three benzophenones: oxybenzone, sulisobenzene and dioxybenzone.⁶⁷ The most common is oxybenzone (benzophenone-3) which has an absorption profile from 270 to 350 nm. Its maximum absorption peaks are found at 288 and 325 nm.⁶⁸ Oxybenzone is commonly used with a favourable toxicological profile based on repeated exposure in rodents.⁴⁶ Oxybenzone is highly stable but has weak UV absorbing capabilities. The filter is commonly used as a photostabiliser rather than a proper sunscreen agent. However, it has the highest incidence of photoallergic contact dermatitis and is very sensitive to oxidation.^{104, 122} The oxidation creates oxygen radicals upon UV exposure and can interrupt the antioxidant system which is harmful to the homeostasis of the epidermis.^{46, 123} Sundaram *et al.*¹²⁴ showed that topical application of oxybenzone caused UVA-induced photo-inactivation of thioredoxin reductase, a vital antioxidant enzyme, in skin biopsies. Oxybenzone has systemic absorption after dermal application and can therefore be detected in urine and the blood stream in significant concentrations.^{46, 125}

Another disadvantage of oxybenzone include its link to coral bleaching. Studies were released by Danovaro *et al.*¹²⁶ and Downs *et al.*¹²⁷ linking coral damage to oxybenzone

exposure. However, this link is being widely investigated among the environmental community as the studies were only conducted on a laboratory scale. In 2019, the University of Maryland Centre for Environmental Science conducted research looking at UV filter concentrations in coral tissue. The results showed that the concentrations of oxybenzone were significantly lower than the known lethal thresholds.¹²⁸ Consumers have an overall positive experience with benzophenones, although skin reactions are the highest among general filters.⁴⁶ The Scientific Committee for Consumer Safety (SCCS) has recently reviewed the use of oxybenzone in cosmetic products and has stated that its use as a UV filter in sunscreen products at a maximum concentration of 6% is not safe.¹²⁰ This restriction will be implemented from August 2022 in the Official Journal of the European Union.

(iii) **Dibenzoylmethanes** include avobenzene (4-tert-butyl-4'-methoxydibenzoylmethane (BMDBM)). Avobenzene is the most common and was the first FDA accepted organic filter to protect against UVA radiation. It is the only long-range UVA filter that is approved by the FDA as it has an absorption profile ranging from 310 to 400 nm with its peak absorption at 360 nm.⁶⁸ However, avobenzene is photolabile and loses its efficiency just one hour after UV exposure.^{109, 129} Avobenzene exists in two tautomeric forms: the *enol*-tautomer and the *keto*-tautomer. The *keto*-tautomer occurs in one symmetrical geometric form while the *enol*-tautomer is unsymmetrical and can occur in many geometric forms that absorb in the UVA range.^{130, 131} *Keto-enol* tautomerism was shown in Scheme 2.5. The *enol* form absorbs in the UVA range. After irradiation, it converts to the *diketo*-form which absorbs in the UVC range which is not relevant for a sunscreen. The *enol*-tautomer can also undergo photoisomerisation to inert, non-photoprotective compounds.¹³² The photostability of avobenzene is solvent-dependent and has been shown to be stable in protic solvents and photolabile in aprotic organic solvents.^{129, 133}

Avobenzene affects the stability of other active sunscreen ingredients. For example, addition of a common UVB filter octinoxate (EHMC) with avobenzene accelerates the degradation of both compounds.¹³⁴ Here, when avobenzene is in its excited state after absorption of UV radiation, it can cause EHMC to undergo photoisomerisation.¹³⁵ This alters both filters resulting in a loss of UV protection.

Carrier modifications to sunscreen formulations have improved the photostability issues, this includes the addition of stabilisers such as octocrylene and Tinosorb S.¹³⁶ Addition of octyltriazone also increases avobenzene's stability.¹⁹ Avobenzene has also shown an 80

percent increase in photostabilisation on addition of the combination between octocrylene, oxybenzone and diethylhexyl 2,6-naphthalate (patented by Neutrogena, known as Helioplex™).¹³⁷ Chaudhuri *et al.*¹³⁸ showed the ability of 3-(3,4,5-trimethoxybenzylidene-2-4-pentanedione (TMBP) to effectively stabilise avobenzone in both solution and formulated products boosting *in vivo* SPF by >50% whereby the main chromophores of TMBP are preserved through light-induced reactions and triplet-state energy transfer from avobenzone and TMBP. In Europe and Asia, bemotrizinol, 4-methylbenzylidene camphor and polysilicone are used to stabilise avobenzone.^{19, 121, 136, 137}

2.4.2 Broad spectrum filters

Most sunscreens these days contain a combination of UV filters to protect against the broad spectrum of UV radiation. Damian *et al.*¹³⁹ were able to show that broad spectrum sunscreens provide greater immune protection than narrow-spectrum sunscreens. Broad spectrum filters absorb both UVB and UVA radiation. It is necessary to evaluate the photostability of these combinations to ensure proper protection from UV radiation, as well as the subsequent effect on sunscreen performance. For example, as previously mentioned the most common combination to offer broad spectrum protection of EHMC and avobenzone is photolabile.¹⁴⁰

(i) **Tinosorb derivatives** include Tinosorb S (bisethylhexyloxyphenol methoxyphenyl triazene) and Tinosorb M (methylene-bis-benzotriazolyl tetramethylbutylphenol). They are extremely photostable because of their molecular structure that enables them to dissipate the excitation energy by heat transfer and vibrational relaxation.⁷⁸ Tinosorb S is an oil soluble filter with an absorption profile ranging from 280-380 nm. This compound also does not penetrate the skin. Tinosorb S can act in two ways: it can absorb photons or it can reflect them. Chatelain *et al.*⁹⁷ have reported that Tinosorb S can be used to stabilise avobenzone and EHMC.

Tinosorb M is also a broad-spectrum sunscreen that shares similar properties to Tinosorb S. It has absorption peaks at 303 and 358 nm.⁷⁸ It is made of microfine organic particles dispersed in the aqueous phase of sunscreen emulsions.⁷⁸ However, Tinosorb M is insoluble in cosmetic oils. Tinosorb derivatives are excellent in preventing photoaging as they reduce the penetration of UV, have good photostability and are non-allergic.⁴⁶

(iv) **Mexoryl filters** include drometrizole trisiloxane (Mexoryl XL) and ecamsule (terephthalydene dicamphor sulfonic acid or Mexoryl SX). They are registered trademarks developed by L'Oréal (Clichy, France). Mexoryl XL is a photostable hydroxybenzotriazole

derivative with its peak absorption at 303 and 344 nm. Mexoryl XL can absorb in both UVB and UVA ranges because of its two chemical groups. The first is 12-hydroxyphenylbenzotriazole which is photostable.⁷⁸ The second is its siloxane chain which is liposoluble.⁷⁸

Ecamsule is a broadband filter with an absorption profile from 290 to 390 nm with its peak absorption at 345 nm.⁶⁸ It possesses durable photostability and is water resistant with a favourable safety profile. Ecamsule can be combined with avobenzone and other UVB acceptors to provide a broad-spectrum sunscreen.⁴⁶ Ecamsule was shown to reduce UV-induced pigmentation, epidermal hyperplasia, decrease skin hydration and wrinkling.^{141, 142} Ecamsule is combined with avobenzone and octocrylene and used in Anthelios products in the United States.⁶⁷ This combination was also studied by Seite *et al.*¹⁴³ using a daily cream. They found that the combination reduced UV-induced skin damage and prevented biological changes associated with photoaging.

It must be mentioned that Mexoryl and Tinosorb are not listed by the FDA but are used in many parts of the world due to their photostability.

2.5 Plants with photostabilisation potential

Organic UV filters are limited in terms of providing broad spectrum protection, because of their photodegradation and phototoxicity. This has led scientists to look for alternatives that can provide beneficial protection and remain photostable. Scientists have turned to the plant kingdom for a more natural source of sunscreen active ingredients and this has been of great interest in the last few years. The reason for this is that plants have various photoprotection mechanisms against enhanced levels of UV radiation. This includes the production of high levels of antioxidants^{144, 145} and the synthesis of UV-absorbing compounds.^{105, 146} These photoprotective mechanisms are discussed in a review article by Hollosy.¹⁴⁴ Bonina *et al.*¹⁴⁵ discuss the potential use of flavonoids to prevent photooxidative stress in the skin. The determination of the antioxidant activity of plant extracts is well documented and is believed to be the future of prevention of skin cancer and erythema.

The plant domain offers a variety of substances that can be potential sunscreen resources for use in skin care products as safer alternatives. Plant extracts that can be added to skincare products are called botanicals.¹⁴⁷ Botanicals that are transferrable into skincare products are referred to as cosmeceuticals. The name cosmeceuticals was given by Albert Kligman.¹⁴⁸

Cosmeceuticals are defined as intermediary substances between drugs and cosmetics.¹⁴⁹ They do not require FDA approval before being marketed.¹⁴⁹

Several botanical agents have been investigated in animal models and culture systems. Only a few of them have been tested for their efficacy in humans.¹⁵⁰ Results from these studies show that these botanical agents are antimutagenic, anticarcinogenic and non-toxic. These botanicals belong to several chemical classes that include polyphenols, monoterpenes, flavonoids, organosulfides and indoles.¹⁵⁰ The use of botanical agents, however, is not an exclusive approach in decreasing UV effects. They can be used to provide additional benefits to the existing tactics.

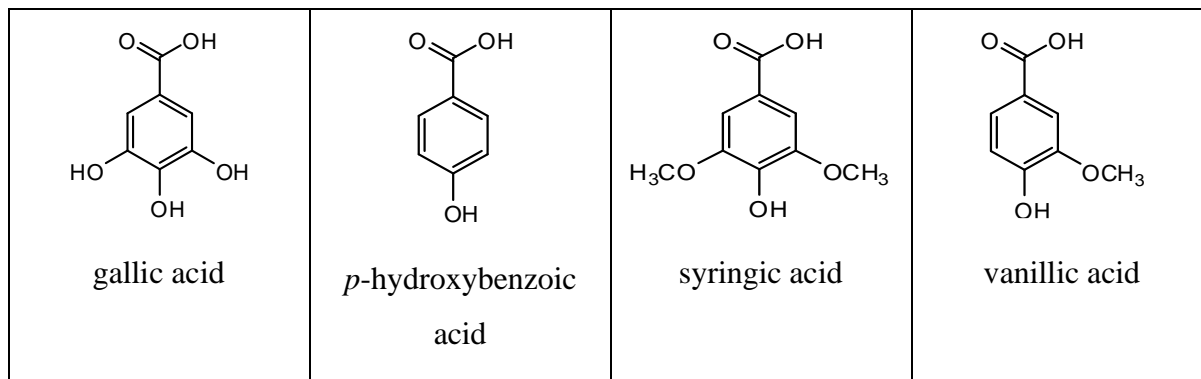
From the realm of plants, polyphenols appear promising to be used in sunscreens as potential stabilisers of photolabile chemical absorbers. Polyphenols include phenolic acids, flavonoids and polymeric polyphenols and are found in various plants, teas, seaweeds and wines.¹³³ Polyphenols contain phenolic rings that act as natural pigments and sunscreens in plants.¹³³ Phenolic acids are a subcategory of polyphenols that possess a carboxylic acid function. They contain a single benzene ring bearing hydroxyl and/or methoxy substituents. Phenolic acids are divided into two groups depending on their structure: benzoic acid derivatives and cinnamic acid derivatives (Figure 2.4).¹⁵¹ Common benzoic acids are gallic acid, *p*-hydroxybenzoic acid, salicylic acid, syringic acid and vanillic acid. They are conjugated with sugars or organic acids and may be present in a soluble form.¹⁵² Cinnamic acid derivatives include caffeic acid, chlorogenic acid (5-caffeoylquinic acid) and *p*-coumaric acid. These are found in several conjugated forms that contain mainly esters of hydroxyl acids such as tartaric acid and sugar derivatives.^{133, 151-153}

Phenolic acids offer natural protection as they can absorb a broad spectrum of UV radiation, have high photostability and outstanding antioxidant properties.^{154, 155} As antioxidants they are beneficial in delaying skin aging. They are also able to reduce the penetration of UV into the skin, decrease inflammation, oxidative stress and DNA damaging effects.¹⁵⁶

Plant extracts are commonly used in certain cosmetic formulations to delay skin aging because of their antioxidant properties.¹⁵⁷ The antioxidant agents are able to minimise free radical activity. Ollengo¹⁵⁸ investigated the photostabilisation potential of polyphenols, namely: grape seed, mulberry and liquorice root extract, on common sunscreen preparations. He demonstrated various photoprotective potentials. However, in that work he showed that the use of lavender negatively impacted the sunscreen preparations and formed a number of

photoproducts. Therefore, it can be said that not all plant polyphenols will be effective in photostabilisation of sunscreen active ingredients.

(A)



(B)

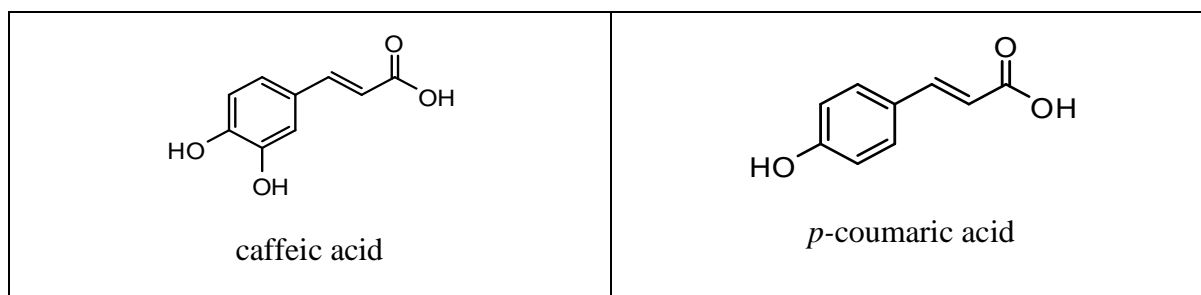


Figure 2.4 Structures of phenolic acids: (A) benzoic acid derivatives, and (B) cinnamic acid derivatives.

Considerations that need to be taken when evaluating the efficacy of a botanical extract include:




- (i) The source of the plant material – The botanical extract can be found in different areas of the plant with varying chemical constituents.¹⁴⁹ This can include leaves, fruits, roots, barks, flowers, stems and berries.^{147, 149} The biological activity of the individual plant extract is dependent on where the active chemical compound is found.¹⁴⁷ The season in which the plant is gathered and the climate conditions also influence the chemical composition and the quality of an extracted herbal substance.^{147, 149}
- (ii) The processing required before the plant extract is added to a skin care product – adding a botanical as raw, crushed leaves to a skin care product is not aesthetically pleasing.¹⁴⁷ To obtain a botanical that can easily be incorporated into a cosmetic formulation is a highly complex process. The extract requires processes such as heating or a way to obtain an oil or aqueous liquid form that can easily be added to the cosmetic

formulation.¹⁴⁷ It must be determined whether this particular process will concentrate or destroy the active chemical that provides the skin benefit.


- (iii) The amount of active ingredient found in the extract - plays an important role in determining its efficacy. A single plant and its different components can contain hundreds of different chemicals and the active compounds become difficult to characterise chemically.¹⁴⁹ However, a botanical can be added in low concentrations to achieve the desirable effects and the additions of small amounts will be an additional marketing benefit.^{147, 149}

Table 2.2 contains a list of a few of the most popular compounds with the potential to absorb UV radiation that are currently used in dermatological sunscreen formulations. The table includes the International Nomenclature of Cosmetic Ingredients (INCI) which are systematic names recognized to identify cosmetic ingredients.

Table 2.2: List of botanical compounds with photoprotection properties that are used in sunscreen formulations

Botanical compound	Plant name	Family name	INCI name	Formulation example
<i>Aloe ferox</i> Mill.	Cape aloe	Asphodelaceae	Aloe Ferox Leaf Extract	
Lycopene	Carotenoids		Lycopene	
<i>Beta-carotenoids</i>			<i>Beta-carotene</i>	
Curcumin	<i>Curcuma longa</i> Linn	Zingiberaceae	Curcuma longa root extract	

Genistein			Genistein	
Ginkgo biloba	Maidenhair tree	Ginkgoaceae	Ginkgo Biloba Leaf Extract	
Lignin				
<i>Polypodium leucatomos</i>	<i>Phlebodium aureum</i>	Polypodiaceae	Polypodium leucatomos root extract	
Resveratrol			Resveratrol	
Rosa flower	<i>Rosa damascena</i>	Rosaceae	Rosa Damascena Flower Extract	
Silymarin	<i>Silybum marianum</i> L. Gaertn	Asteraceae	Silybum Marian Extract/ Milk Thistle	

Tea polyphenols	<i>Camellia sinensis</i>	Theaceae	Camellia Sinensis Leaf Extract	
Cancer Bush	<i>Sutherlandia frutescens</i>	Microphylla	Sutherlandia frutescens	-

INCI – International Nomenclature of Cosmetic Ingredients

(i) *Aloe ferox*

The *Aloe ferox* (bitter aloe or Cape aloe) has been a part of the traditional use by indigenous people of South Africa for centuries.¹⁵⁹ The plant contains phenols, flavonoids, flavanols, proanthocyanidins, tannins, alkaloids and saponins.¹⁶⁰ It was primarily used for healing burns and alleviating pain. Traditionally, it was used to treat dermatitis, acne and skin diseases such as skin cancer by either being applied topically or taken internally.¹⁶¹ This plant is exclusively found in the Cape province of South Africa.¹⁶²

Aloe ferox is able to restore the activity of epidermal cells that are reduced by exposure to UV radiation.¹⁶¹ This results in the reduction of photoaging. Wintola¹⁶⁰ reported that the plant possesses strong antioxidant activity due to its ability to absorb UV radiation, quench free radicals (a generator of ROS), and decompose peroxides generated in the system.

Aloe ferox has gained widespread popularity in the cosmetic industry and is used as a vital ingredient in cosmetic formulations and food supplements.¹⁶³ The first aloe factory was established in Albertina, Western Cape, in the early 1990s.¹⁶⁴ This factory started the industrial processing of *Aloe ferox* gel. The South African *Aloe ferox* industry was estimated to be worth R4 million annually, in 1996. Since then it has grown to approximately R12 to 15 million.¹⁶⁵

Aloesin, in the form of a gel, is a chromone derive isolated from Cape aloes leaves.¹⁶³ The structure of aloesin is show in Figure 2.5. The leaves can be collected without harming the plant. Haynes *et al.*¹⁶⁶ were the first to describe that aloesin is the parent compound of the aloe chromones stating that aloesin was found throughout the genus. Yagi and Takeo¹⁶⁷ and Jones *et al.*¹⁶⁸ were able to show that the plant extract provided pigmentation-altering agents for cosmetic and therapeutic applications. Aleosin was found to inhibit hyperpigmentation in human skin after exposure to UV radiation and the results were dependent on the

concentrations used.¹⁶⁹ The first patent was filed in 2008 by Steenkamp *et al.*¹⁷⁰ The patent describes the hydrolytic conversion of aloeresin A to aloesin, thereby increasing the amount of aloesin available for extraction from the sap.

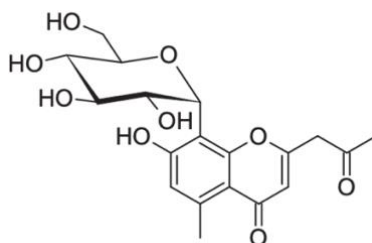


Figure 2.5: Chemical structure of aloesin.

The *Aloe* gel is added to various cosmetic products such as moisturisers, suntan lotions, sunscreens, shampoos and cleansers.^{159, 163} Aloesin can absorb UVB radiation with an absorption peak at 296 nm.¹⁷¹ Therefore, the chromone derivative can be used in sunscreen formulations in the concentrated form or diluted to at least 40%, under patent.¹⁶³ A higher dosage is recommended for sunscreens or anti-pigmentation formulations.

The aloe gel offers prevention of death of burn tissue and wrinkling, promotion of skin regeneration, immune stimulation, and protection from skin drying.¹⁶⁷ It also possesses anti-tumour activity and anti-inflammation. The sunscreen market currently contains a number of sunscreen formulations which include *Aloe ferox* as a key ingredient due to its benefits, as well as its sustainability. Sunscreen products currently on the market include: Aloe Ferox Sun Care Lotion SPF 50, Sunumbra Family Natural Sunscreen Lotion, SPF 30+, and Alcare Aloe Sun SPF 50 Sunscreen Spray, among others.

(ii) Carotenoids

Carotenoid pigments are found in all green plants, carrots, and tomatoes, among others. They are believed to be suitable compounds for use in photoprotection as they are able to protect plants against excess light, photosensitisation and photooxidative stress.¹⁷² The carotenoid pigments in plants are responsible for protection from its own chlorophyll.¹⁵⁰ Chlorophyll can absorb in the UVA range, which can be harmful to the plant.¹⁵⁰ Carotenoids contain a long central chain of conjugated double bonds with acyclic or cyclic substituents. Their conjugation is responsible for their antioxidant properties and their ability to protect against cellular damage and aging of the skin.¹⁷³ They are very effective singlet oxygen quenchers and are excellent scavengers of oxygen radicals.^{172, 173}

Carotene supplements have been thoroughly investigated for their potential in preventing sunburn.^{173, 174} These include *beta*-carotene and lycopene. *Beta*-carotene is an endogenous photoprotector found in carrots, spinach, sweet potato and pumpkins. Studies conducted by Stahl *et al.*¹⁷² show that oral supplementation with *beta*-carotene has the ability to prevent UV-induced erythema formation. But this requires a prolonged timeframe for treatment before exposure and during.¹⁷⁵⁻¹⁷⁷ *Beta*-carotene is an effective singlet oxygen quencher and inclusion in the diet can protect the skin from lipid peroxidation and reduction of matrix metalloproteinase (MMP)-9 activation caused by UVA induced photodamage.¹⁷⁸ There have been clinical studies confirming that *beta*-carotene promotes lung cancer.¹⁷⁹ These studies include the *alpha*-tocopherol, *beta*-carotene cancer prevention in Finland¹⁸⁰ and the *beta*-carotene and Retinol Efficacy Trial in US¹⁸¹. These studies imply that *beta*-carotene needs to be used with caution and at safe levels for human consumption.

Beta-carotene is able absorb to in the UV-visible regions with its peak absorption in the visible region.¹⁸² Darvin *et al.*¹⁸³ showed that topical application of *beta*-carotene can also protect the skin against exposure to infrared radiation by scavenging free radicals. Freita *et al.*¹⁸⁴ evaluated the influence of *beta*-carotene on the photostability of five UV filters, namely; EHMC, avobenzene, octocrylene, bemotrizinole and octyltriazone. Their work also involved identification of degradation products and the assessment of photoreactivity. Their results showed that improved photostability was achieved when the combination of antioxidants, *beta*-carotene and *trans*-resveratrol, were included with the UV filters in a sunscreen formulation.¹⁸⁴ No phototoxic risks were observed. In another study, Frietas and Gaspar,¹⁸² evaluated the photostability, photoreactivity, phototoxicity and UVA protection of apigenin, chrysin and *beta*-carotene and found that the compounds were photostable both, individually and in combination, with no phototoxic skin responses observed. The three antioxidants were deemed compatible for use in sunscreen formulations.

Lycopene is a red carotenoid found in apricots, papaya and guava, among others and is a major carotenoid of tomatoes. The content of lycopene found in tomatoes can vary, depending on the type of tomato and ripening.¹⁷² Lycopene has been reported to have many health benefits due to its ability to protect cells against oxidative damage.¹⁷² It is very effective in preventing singlet oxygen radicals, perhaps even the best. A 12-week indigestion study conducted by Stahl *et al.*¹⁷² also showed a decrease in sensitivity towards erythema. It must be noted that ingestion of dietary carotenoids allow for photoprotective properties within the body.¹⁷² Lycopene absorbs in the UVB region and has the potential to be used effectively in sunscreen

formulations.^{185, 186} Sjahjadi *et al.*¹⁸⁷ successfully incorporated lycopene-rich purified tomato extracts into a sunscreen cream and showed that protection against UV was achieved.

Beta-carotene and lycopene have been included as active ingredients or antioxidants in a number of sunscreen formulations including: Deborah Milano Formula Pura BB Cream SPF 20, Aptiva Bee Sun Safe Satin Touch Tan Perfecting Body Oil SPF 30, and Aptiva Suncare Tanning Body Oil SPF 30.

(iii) **Curcumin**

Curcumin (diferuloylmethane) is a yellow substance obtained from the root of the turmeric plant known as *Curcuma longa* Linn, which belongs to the Zingiberaceae family.^{149, 150} Curcumin is well known for its medicinal benefits and has been used in Indian cooking since ancient times. Curcuminoids are polyphenols that act as potent antioxidants and are scavengers of radicals such as ROS and RNS.¹⁸⁸ The medical benefits of curcumin include inhibiting carcinogenesis in several tumour model systems.¹⁸⁸⁻¹⁹¹ Other preliminary studies conducted show that curcumin possesses antioxidant and anti-inflammatory effects in mouse models by significantly inhibiting the number of tumours per mouse through dietary administration.^{189, 191, 192}

Curcumin in a gel form was found to rapidly heal burns when topically applied, as well as, repair photodamaged skin.¹⁹³ Adusumilli *et al.*¹⁹⁴ investigated the potential of curcumin nanoparticles as a photoprotective adjuvant for topical delivery in mice. Their results showed that treated mice showed less erythema, induration and scale compared with controls. They proposed that when a stable formulation is delivered effectively, curcumin can modify gene expression of inflammatory cytokines, limit acute DNA damage and reduce inflammation and apoptotic response to UVB radiation. They also stated that further investigation is required into applications alongside sunscreens.

Presently, an abundance of products contain turmeric in their ingredient list which include moisturisers, anti-aging, and night repair products. The compound is difficult to transfer into a cosmetic formulation because of its smell and colour. Current suncare products on the market using curcumin as an active ingredient include: Atomy Absolute Essence Sun UV Protector SPF 50 and Holika Holika Mild Sun Cushion SPF 45. The UV/Vis absorption spectrum performed by Rodrigues *et al.*¹⁹⁵ showed peak absorption at 261 and 417-480 nm. The use of sunscreen compositions containing an extract of *Curcuma longa* L. has been patented.¹⁹⁶

(iv) **Genistein**

Genistein (4',5,7-trihydroxyiso-flavone) is found in soy, ginkgo biloba extract, Greek oregano and Greek sage.^{197, 198} Preliminary studies conducted by Wei *et al.*^{199, 200} show that genistein possesses antioxidant and anticarcinogenic effects in the skin. Their work also provides evidence of genistein inhibiting UV-induced oxidative damage.²⁰¹ The isoflavone metabolites also showed anti-inflammatory and anti-immunosuppression when applied topically to hairless mice.

Topical application of genistein in humans has shown effective protection against UV-induced skin damage.¹⁴⁹ Kang *et al.*²⁰² were able to show that topical treatment of human skin with genistein prevented UV-induced erythema and growth factor receptor tyrosine kinase activity. However, their work stated that genistein cannot be used as a sunscreen active ingredient as λ_{max} is 262.5 nm which is in the UVC region.²⁰² Moore *et al.*²⁰³ evaluated the photoprotective efficacy of genistein within the context of full thickness human reconstructed skin to acute challenges with UVB irradiation. Their results showed that genistein is a potent chemoprotective agent against carcinogenesis and were also able to show that the compound did not provide a blocking effect when irradiated with UVB radiation.²⁰³ Presently, genistein is used in certain sunscreens and moisturisers for an antiaging effect, such as, VENEFFECT Anti-Aging Moisturiser SPF 15 and Dr Zenovia Vitamin C Brightening Moisturiser SPF 30.

(v) **Ginkgo biloba**

Ginkgo biloba is found in trees that belong to the Ginkgoaceae family.¹⁵⁰ The plant leaves of Ginkgo biloba contain unique polyphenols such as terpenoids, flavonoids (epicatechin, catechin, rutin, apigenin, luteolin and quercetin) and flavonol glycosides.²⁰⁴ The abundance of polyphenols enables strong anti-inflammatory and antioxidant effects that are able to prevent carcinogenesis.^{205, 206} They are also able to scavenge free radicals.¹⁵⁷

A study determined the photochemoprotective properties of ginkgo biloba extracts in mouse skin.²⁰⁶ Findings of this study showed a decrease in the number of sunburnt cells. It is believed that the extract may be a photoprotective and therapeutic agent and this contributes to the prevention of skin cancer.^{150, 206} Only fractions of ginkgo are added to antiaging moisturisers, but their antiaging benefits have not been confirmed.¹⁴⁷

Zhang *et al.*²⁰⁷ investigated the physicochemical and antibacterial activity of polyphenol (Figure 2.6), an active ingredient found in the Ginkgo biloba leaves, in formulation. Their work showed that polyphenol in a liposomal gel formulation is a promising strategy for the

development and application of cosmetic and medicinal products due to their outstanding antioxidant capabilities. Their extraction technique also provides a high purity extract achievable for industrial application with a small particle size, high homogeneity, good physiochemical stability, suitable plastic flow and high preservative activity.²⁰⁷ Mercurio *et al.*²⁰⁸ evaluated photoprotective effects of cosmetic formulations containing UV filters, vitamins, Ginkgo biloba and red algae extracts. The results showed that the formulations protected the skin from erythema when exposed to UV radiation and the combination of vitamins, ginkgo biloba and red algae extract can significantly improve the performance of sunscreens and prevent UV-induced DNA damage. This was confirmed by a substantial decrease in UV-induced apoptotic keratinocytes through the topical application of sunscreen in mice which suggest a reduction in skin damage by UV radiation.²⁰⁸

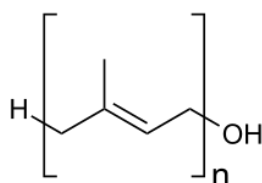


Figure 2.6: Chemical structure of polyphenol.

The Ginkgo Biloba leaf extract is used in a number of cosmetic products for its antioxidant activities including: Missha M Signature Real Complete B.B. Cream SPF 25, Nude Protector Solar Sunscreen Crema 70 SPF, and Consonant The Perfect Sunscreen SPF 30.

(vi) Lignin

The use of lignin in several commercial sunscreen products has been shown to offer a high broad spectrum sunscreen. This is due to the strong absorption ability of the functional groups (such as phenolics, ketones and other chromophores) in lignin to absorb UV radiation much better than typical organic UV filters.²⁰⁹⁻²¹¹ The phenolic hydroxyl groups hold high antioxidant properties.^{211, 212} Lignin offers a cheaper alternative to other botanical extracts as it can be found in abundance in nature and through industrial production. Lignin is generated by plants via carbon dioxide (CO₂) photosynthesis with no carbon footprint.²¹³

Qian *et al.*²¹² have reported that an addition of 2 wt.% of lignin increases a sunscreen product with SPF 15 to SPF 30. They were also able to show that the sunscreen's performance improves with UV-radiation time. These advantages could stem from lignin's antioxidant properties and the synergistic effects of lignin with other active ingredients.^{212, 213} Therefore,

lignin has potential to be used in sunscreen formulations as a much greener alternative to synthetic organic UV filters.

(vii) ***Polypodium leucotomos***

Polypodium leucotomos is an extract from a tropical fern known as *Phlebodium aureum*. It was used by the Native Americans to treat inflammatory disorders.²¹⁴ *Polypodium leucotomos* extracts, commercial name, Fernblock, have been given orally and/or applied topically and have been shown to have photoprotective ability against UV-induced phototoxic reaction, and pigmentary and histologic changes such as photoaging.^{215, 216}

Siscovick *et al.*²¹⁷ conducted a study by adding the extract to drinking water for mice. They found that this inhibited UVB radiation-induced skin cancer. Preliminary studies conducted on both human and animal models have shown that this extract reduces erythema and contains antioxidant, anti-inflammatory and photoprotective benefits.^{215, 218} Because of the ability of *polypodium leucotomos* to inhibit immunosuppression, it is also able to prevent UV-induced skin cancer.²¹⁷ In the USA, an oral supplement is taken one hour before sun exposure.¹⁴⁹ The supplement needs to be used in conjunction with a broad-spectrum sunscreen for optimal benefits.¹⁴⁹ Zamarron *et al.*²¹⁹ showed that Fernblock prevents cell damage and reduces the increase in MMP-1 and cathepsin K expression caused by visible and infrared A radiation

Fernblock, used as a sunscreen active ingredient, displays a wide range of benefits with no toxicity and allergenic potential. The extract is currently used under the name “Fernblock” in a few sunscreen and antiaging products including the popular brands Heliocare and Antioxidine.^{216, 220} Fernblock is used as the key ingredient in the Heliocare sunscreen range.

(viii) **Resveratrol**

Resveratrol (*trans*-3,4',5-trihydroxystilbene) is a polyphenolic phytoalexin found in the skin and seeds of grapes, nuts, fruits, and red wine.¹⁴⁹ When these plants are attacked by fungal pathogens, they react by synthesising resveratrol.²²¹ Resveratrol occurs in the *cis*- and *trans*-form, the *trans*-form being more stable. It is a potent antioxidant with strong anti-inflammatory and antiproliferative properties.^{222, 223} Preliminary studies showed that resveratrol inhibited skin cancer.²²⁴ Studies involving the topical application in hairless mice inhibited UVB skin damage.^{150, 225}

Bhattacharya *et al.*²²⁶ attempted to develop a novel herbal sunscreen formulation using resveratrol and green tea extracts in place of physical or chemical UV filters. Resveratrol

showed λ_{\max} at 310 nm and results confirmed that a sunscreen formulation with the combination of resveratrol and green tea extract provides good photoprotective ability with satisfactory antioxidant activity.²²⁶ Such a formulation can provide a viable alternative for conventional sunscreens that contain synthetic UV filters. Freita *et al.*¹⁸⁴ showed that improved photostability was achieved when the combination of antioxidants, *beta*-carotene and *trans*-resveratrol, were present with the UV filters in a sunscreen formulation. Resveratrol is used in many different skincare products such as sunscreens and eye creams. Current sun care products on the market include Paula's Choice Resist Super-Light Wrinkle Defense SPF 30, Platinum Skin Care Fade Bright Skin Lightening, and Dr Dennis Gross Sheer Mineral Sun Spray Broad Spectrum SPF 50.

(ix) *Rosa damascene* flower extracts

Rosa damascene belongs to the Rosaceae family. It is a small plant with aromatic pink flowers. Benefits of the extract include cooling, soothing, astringent and anti-inflammatory effects.²²⁷ Several preliminary studies confirm that the *Rosa* flower contains aromatic and flavonoid compounds such as kaempferol, quercetin and pectolinargenin.²²⁸ The flavonoids exist as the major component within the extracts.

Tabrizi *et al.*²²⁹ investigated the *Rosa damascene* flowers as an antisolar agent using three extracts. Extracts were shown to absorb UV radiation in the wavelength range of 200 – 400 nm depending on the solvents used.²²⁹ For example, a hydroalcoholic extract made with water: ethanol (50:50) is able to have maximum absorption throughout the range of 200 – 400 nm. The hydroalcoholic extract can do this because the solvent can extract numerous pigments and colouring agents from the plant. These extracts can absorb UV radiation because of their colour.

However, this is not as effective as an ether extract as the hydroalcoholic extract is low in flavonoid content. An ether extract was shown to effectively absorb in the range of 200 – 400 nm because of its high flavonoid content. Tabrizi *et al.*²²⁹ suggest that the ability of the ether extract to absorb UV radiation is solely based on the flavonoids and not pigments and colouring. Their work also showed that incorporating the extracts into a base cream increased its UVA and UVB absorption ability, making it a viable extract to add into sunscreen formulations.²²⁹

As mentioned above, these extracts cannot be solely responsible for UV protection, but they are capable of working well with other agents used in sunscreen formulations. However,

further studies are still required in order to safely use the *Rosa damascene* extracts in sunscreens.¹⁵⁰ Current sun care products which include *Rosa damascene* flower extracts in their ingredient list are Acorelle Sun Cream For Babies SPF 50+ Bio, Kypris Pot of Shade Helitropic SPF 30, and Circulove Day SPF 20 Probiotic Day Cream.

(x) **Silymarin**

Silymarin is derived from the milk thistle plant, *Silybum marianum*.⁶⁸ Silymarin is a polyphenolic flavonoid comprising of flavonoids such as silybin, silibinin, silydianin, isosilybin and silychristine.⁶⁸ Silybin is the major component with the highest biological potency proven to have antioxidant, anti-inflammatory and anticarcinogenic properties.²³⁰⁻²³² The flavonoids are responsible for the strong antioxidant properties. These are capable of scavenging ROS and preventing lipid and lipoprotein oxidation.^{68, 232} The mechanisms behind the anticarcinogenic properties are still under investigation. Silymarin displays chemoprotective activity against skin cancer and inhibits the promotion of tumours.²³³

The UV absorption maximum of silymarin occurs at 287 nm.²³⁴ Svobodova *et al.*²³⁵ investigated the effect of silymarin and its main constituent silybin on human dermal fibroblasts with UVA stimulated damage. Treatment resulted in the reduction of UVA stimulated ROS generation and single strand break production and a decrease in the activation of caspase-3 and protein level of MMP-1.²³⁵ Their results showed that both silymarin and silybin are non-phototoxic and have UVA photoprotective capability by preventing UVA damage in skin cells and, therefore, could be useful agents in UV protective dermatological preparations. Mpharm *et al.*'s²³⁶ work involved the development, characterisation and evaluation of solid lipid nanoparticles incorporated into a sunscreen cream. The results showed that sunscreen containing silymarin solid lipid nanoparticles displayed increased photoprotective capabilities and the efficiency of silymarin increased as the concentration of emulsifier increased.

Silymarin is used in several antiaging, moisturising, and sun protective products.¹⁴⁹ The use of silymarin in sunscreen formulations may offer favourable advantages with additional anti-carcinogenic protection. Existing sun care products include Go-To Zincredible SPF 15 (Untinted) and Jovees Sun Defence Natural Care SPF 50.

(xi) **Tea polyphenols**

Tea from the plant *Camellia sinensis* of the Theaceae family is the second most consumed beverage. Approximately 2.5 million metric tons of dried tea is produced annually.²³⁷ There are various types of tea around the world. These include green tea, black tea, hibiscus,

camomile and Rooibos tea. Tea contains powerful antioxidants as it is rich in catechins.¹⁵⁰ Tea polyphenolics have been shown to possess photoprotective properties and these tend to vary with the type of tea. They also act as potent antioxidants that can scavenge ROS.¹⁵⁰ The structure of the polyphenol determines the scavenging effect. Preliminary studies confirm the antimutagenic and anticarcinogenic properties of these compounds in animal models.²³⁸

Black tea comprises of polyphenolic polymers.²³⁸ Black tea absorbs UVB but is unable to absorb all of the UVA rays. Therefore, its main function is to reduce burning and skin damage from UVB. Zhao *et al.*²³⁹ showed that a black tea extract inhibits erythema in mice models. They were also able to show a decrease in erythema in humans. Sopyan *et al.*²⁴⁰ investigated the effect of black tea leaves against UV radiation in lotion preparations. Their work showed that the black tea extract provided effective photoprotection against UV radiation, with an increase in SPF when compared to the lotion without the black tea extract. The lotion preparation made with the black tea was shown to be safe for topical use and non-irritating on the skin. Turkoglu and Cigirgil²⁴¹ showed that an alcoholic extract of black tea absorbs between 250 to 300 nm. This extract was then formulated into a gel application and tested *in vivo* for evaluation of protection against UV radiation and they concluded that the black tea gel was effective in protecting the skin from broad range UV radiation. There were also no toxicological concerns associated with the black tea gel and it could be safely applied in large amounts.

Rooibos tea contains phenolic acids (ferulic and syringic acid) and flavonoids (quercetin, luteolin, aspalathin, and nothofagin) that are specific to Rooibos and contribute to its antioxidant activity.²⁴² Ferulic acids are hydroxycinnamic acids present in plants, vegetable foods and Rooibos tea. Studies conducted by Saija *et al.*²⁴³ showed by means of *in vivo* and *in vitro* methods that ferulic acid provided significant protection against UVB irradiation and can be successfully employed as a topical agent. Rooibos tea extracts are used in a wide range of products.²⁴⁴

Green tea polyphenols contain beneficial flavonoids that act as potent antioxidants.¹⁴⁷ Green tea contains catechin monomers that can inhibit erythema, carcinogenesis and immunosuppression.⁷⁸ Picard showed that green tea polyphenols are able to prevent skin cancer in mouse skin models.²⁴⁵ A study conducted by Elmets *et al.*²⁴⁶ showed that topically applied green tea polyphenols on humans displayed a decrease in erythema, a decline in number of sunburn cells, a decrease in DNA damage and protection of Langerhans cells. In another study by Camouse *et al.*²⁴⁷, they showed that the topical application of green and white tea was

found to offer UV protection. However, the protection was not because of direct UV absorption or sunscreen effects. Their work showed that both green tea and white tea partially prevented UV induced depletion of Langerhans cells and UV-induced generation of 8-oxo-7,8-dihydroguanine in healthy subjects irradiated *in vivo*. Belo *et al.*²⁴⁸ were the first to investigate the photoprotective effects of a topical formulation containing green tea and Ginkgo biloba extracts on the dorsal skin of hairless mice against UVA/UVB irradiation. Their results showed that both extracts did not absorb in the UVA or UVB regions, however, formulations containing the Ginkgo biloba were shown to be effective in the presence of erythema. This phenomena is explained by the antioxidant effect.²⁴⁹

Green Rooibos extracts are very popular in South Africa. They are rich in antioxidants and provide protection against anti-aging, blemishes and pigmentation.²⁴² Studies involving the topical application of green tea polyphenols remain limited. Yet, many skincare products such as shower gels, toothpastes, shampoos and perfumes contain them.¹⁴⁹ Current sun care products include Raw Elements Face + Body Sunscreen Tube SPF 30, Arugot Organic Facial Sun Cream SPF 30, and Seibella Luminous CC Cream SPF 30 Pa++.

(xii) *Sutherlandia frutescens* (Cancer Bush plant)

Sutherlandia frutescens, subspecies *micophylla*, is referred to as the Cancer Bush plant. It was popular amongst the indigenous people of South Africa as the extracts were used to treat HIV/AIDS and cancer. Research data shows that the beneficial effects of the Cancer Bush plant may be due to the synergistic effect of a number of phytochemicals in the herbal extract.²⁵⁰ It is believed that the polyphenolic compounds present in the plant hold radical scavenging properties.¹⁷ These properties could be responsible for the anti-HIV and anti-tumour behaviour.

Mturi's work with the plant displayed spectra showing high UV absorption in both UVA and UVB regions.¹⁷ He also discusses the attempts made to stabilise some organic chemical absorbers with and without the use of the extract. Mturi was successful in stabilising avobenzone with the Cancer Bush extract in ethyl acetate and dimethyl sulfoxide.¹⁷ Fernandes *et al.*²⁵¹ were able to show the antioxidant properties of the Cancer Bush plant. A study by the Medical Research Council of South Africa confirmed that no toxicity surfaced in vervet monkeys when using high concentrations of the leaf in powder form.²⁵² Therefore, with the lack of toxicity and high absorption of UV radiation, the Cancer Bush plant could be a potential photostabiliser for sunscreen chemical absorbers and is the focus of this work.

Shaik *et al.*²⁵³ reported that the Cancer Bush plant contains five known active ingredients, namely; L-arginine, L-canavanine, GABA, pinitol and triterpenoid glycoside. Their work found that the yields of phytochemicals were higher in *in-vitro*-grown leaf extracts than in field-grown leaf and wild leaf extracts. Tobwala *et al.*²⁵⁴ and Tai *et al.*²⁵⁵ studied Cancer Bush tablets using gas chromatography/mass spectrometry (GC/MS) and liquid chromatography/mass spectrometry (LC/MS). Both groups showed the presence of arginine, canavanine and GABA in the tablets.

The use of the botanical extracts discussed in the preceding sections as natural sunscreen actives and natural antioxidants are growing in interest in the cosmetic industry. However, they cannot be solely responsible for full UV protection. The focus is on multifunction cosmetic formulations that include antioxidants with a reduction of synthetic UV filters. Ollengo¹⁵⁸ showed that commercially available sunscreens that contain plant extracts use lower levels of UV filters with improved photostability. These sunscreen products contained plant extracts from grapeseed, cranberry, lyceum, and jojoba, among others. Therefore, these extracts must be blended with synthetic chemical UV filters to provide optimal benefits and photoprotection.²⁵⁶ Botanical compounds are continuously being discovered and researched for use in sunscreen products to protect against harmful UV radiation. Improved photostability is achieved with the use of antioxidants which in turn will result in an improved safety profile and efficacy.

Chapter 3: Experimental Procedures

This chapter details the experimental work carried out to investigate the photostability of commercially available organic chemical absorbers and whether their efficacy could be enhanced through the addition of plant polyphenols. This required the use of chromatographic and spectroscopic techniques to quantify the active ingredients and assess the photostability of chemical absorbers in sunscreen formulations.

3.1 Chemicals

The chemicals, materials and solvents utilised are listed in Tables 3.1 to 3.3 respectively.

Table 3.1: Chemical UV absorbers

Chemical UV absorber	Common name	INCI name	Manufacturer	% Purity
4- <i>tert</i> -butyl-4'-methoxydibenzoylmethane	Avobenzone	Butyl methoxydibenzoyl methane	Merck	>99%
2,2'-dihydroxy-4,4'-dimethoxybenzophenone-5,5'-disulfonic acid sodium salt	Benzophenone-9	Benzophenone-9	The British Drug Houses LTD.	>99%
3-(4-methylbenzylidene)camphor	MBC / Enzacamene	4-methylbenzylidene camphor	Alfa Aesar	>99%
2-ethylhexyl- <i>p</i> -methoxycinnamate	Octinoxate (EHMC)	2-ethylhexyl- <i>p</i> -methoxycinnamate	Sigma-Aldrich	>98%
Homomenthyl salicylate	Homosalate	Homosalate	Merck	>99%

2-ethyl salicylate	Octisalate/ octyl salicylate	Ethylhexyl salicylate	Merck	>99%
2-ethylhexyl-2-cyano-3,3-diphenylarylate	Octocrylene	Octocrylene	Merck	>99%

Table 3.2: Phenolic acids

Phenolic acid	Manufacturer	% Purity
Gallic acid	Fluka	>98%
<i>p</i> -hydroxybenzoic acid	Aldrich Chemicals	>99%
Vanillic acid	Merck kGaA	>99%
Caffeic acid	Sigma-Aldrich	>98%
Syringic acid	Sigma-Aldrich	>95%
<i>p</i> -coumaric acid	Sigma-Aldrich	>98%

Table 3.3: Other raw materials

Chemicals	Manufacturer	% Purity
Dicapryl carbonate	BASF	>99%
C12-15 alkyl benzoate (and) disteardimonium hectorite (and) alcohol	Elementis	>99%
Dimethicone	Wacker	>99%
Isoamyl laurate	Oleon	>99%
Cetyl PEG/PPG-10/1 dimethicone	Evonik	>99%

Dimethicone/vinyl dimethicone crosspolymer	Dow Corning	>99%
--	-------------	------

Table 3.4: Plant materials

Name	Botanical name	Form	Supplier
Dried Cancer Bush plant	<i>Sutherlandia frutescens</i>	Powder	Karoo Herbs
Green tea leaves	<i>Camellia sinensis</i>	Leaves	Tetley
Rooibos tea leaves	<i>Aspalathus linearis</i>	Leaves	Five Roses

Table 3.5: Solvents

Solvent	Manufacture	% Purity
Millipore water	Millipore Milli-Q water purification system	
Methanol	Sigma-Aldrich	99.8%
Ethanol	Sigma-Aldrich	99.9%
Diethyl ether	Sigma-Aldrich	98%
Ethyl acetate	SMM Instruments	97%
Cyclohexane	Merck	99.5%
Petroleum ether	Sigma-Aldrich	99.9%
1,2-propanediol	VWR	99%

3.2 Cancer Bush extraction methods

3.2.1 Boiling water extraction

A volume of 40 ml of boiling Millipore water was added to 5 g of desiccated Cancer Bush powder and left to stir overnight. The mixture was then filtered under vacuum through a

Whatman filter paper. A 0.2 ml (200 μ l) aliquot of the filtered extract was diluted with Millipore water to a final volume of 25 ml in a volumetric flask for UV absorption spectroscopy investigation and photostability assessment. The procedure followed for this extraction technique was as reported by Liang *et al.*²⁵⁷

3.2.2 Ethanol-water extraction

A mass of 5 g of the Cancer Bush powder was immersed in 40 ml of 75:25 (v/v) ethanol: Millipore water solution (30 ml ethanol: 10 ml Millipore water). The mixture was placed in an oil bath at 65 °C and stirred for 30 minutes, and then filtered through a Whatman filter paper. The filtrate was evaporated under reduced pressure with a rotary evaporator. The crude extract was redissolved in 25 ml Millipore water. The aqueous solution was extracted three times with an equal volume of ethyl acetate to extract the polyphenols. The ethyl acetate extracts were combined and filtered again through Whatman filter paper. The ethyl acetate was evaporated under reduced pressure with a rotary evaporator. A few drops of dichloromethane were added to remove excess organic compounds after evaporation and a dark green solid extract was obtained.

For the UV/Vis analysis, a 32 mg mass of the solid green extract was dissolved with 25 ml methanol and analysed by UV/Vis spectrophotometry to obtain a UV absorption spectrum of the extract. The sample was then irradiated as described in Section 3.6.3 to assess its photostability.

3.2.3 Flavonoid extraction

Flavonoid compounds such as kaempferol, quercetin and pectolinargenin can be extracted by using three solvent systems: water-ethanol (50:50), ethyl acetate:ethanol (80:20), and ether. The hydroalcoholic and ethyl acetate:ethanol solvent extractions were prepared by maceration, whilst the ether extract was prepared via Soxhlet extraction.

3.2.3.1 Maceration

Approximately 10 g of the Cancer Bush powder was dissolved in 50 ml of the respective solvents and stirred for 3 days. Thereafter, the sample was shaken for several hours using a mechanical shaker. The extract was filtered under vacuum and concentrated over a water bath.

3.2.3.2 Soxhlet extraction

The Soxhlet apparatus was set up and the thimble was extracted with ether for 3 hours. Subsequently, approximately 10 g of the Cancer Bush powder was added into the thimble. A

volume of 50 ml of ether was added to a 250 ml round-bottom flask ensuring that the solvent only filled one third of the round-bottom flask. Bumping granules were added to the flask and the extraction was carried out for 3 days. After extraction, the filtrate was filtered under gravity into a weighed round-bottom flask and concentrated over a water bath. For the ethyl acetate: ethanol systems, the quantities of Cancer Bush powder and solvent were halved.

3.2.4 Phenolic acid extraction

Phenolic acids were extracted from the Cancer Bush plant by means of the following extraction methods described in Sections 3.2.4.1, 3.2.4.2 and 3.2.4.3.

3.2.4.1 Soxhlet extraction

The Soxhlet apparatus was set up and the thimble was extracted with solvent only. Approximately 10 grams of Cancer Bush powder was added into the clean thimble. A volume of 80 ml of methanol was added to a 250 ml round-bottom flask ensuring that the solvent only filled one third of the round-bottom flask. Bumping granules were added to the flask and the extraction was carried out for 18 hours. After extraction, the crude methanolic extract was filtered under gravity into a weighed round-bottom flask. The solvent was evaporated with a rotary evaporator at 56 °C. After removal of the solvent, a dark green tar-like residue was obtained.

3.2.4.2 Ultrasonic-assisted extraction

A mass of 10 grams of Cancer Bush powder was added to 50 ml of methanol in a 100 ml conical flask and subjected to ultrasonication for 30 minutes. The crude methanolic extract was filtered through a Whatman filter paper by gravity into a weighed 250 ml round-bottom flask. The residue from the conical flask was extracted twice more with fresh aliquots of 50 ml methanol by ultrasonication and filtered into a round-bottom flask. The methanol was evaporated with a rotary evaporator at 56 °C to obtain a dark solid green extract.

3.2.4.3 Liquid-liquid extraction

After solvent removal from the two extraction methods described in Sections 3.2.4.1 and 3.2.4.2, 80 ml of boiling water was added to each of the round-bottom flasks and left to stand overnight. This was done to allow for some of the methanolic extracts in the flask to be dissolved leaving behind the residues at the bottom of the flasks. After approximately 16 hours, each extract was filtered through a Whatman filter paper by gravity into a 400 ml beaker. Each filtered extract was divided into two portions of ~60 ml each. Each of these portions was then

extracted six times with 30 ml petroleum ether to remove lipophilic components. Subsequently, the first portion (~60 ml) was extracted six times with 30 ml diethyl ether, whilst the second portion was extracted six times with ethyl acetate. The extracts were dried with the addition of anhydrous sodium sulphate and filtered through Whatman filter paper under gravity into weighed round-bottom flasks. The solvents were removed by rotary evaporation at 30 °C for diethyl ether and 45 °C for ethyl acetate.

3.3 Phenolic acid extraction for commercial teas

A mass of 5 g of green and Rooibos tea, respectively, was weighed and added to 100 ml of 75:25 (v/v) ethanol:ethyl acetate solution in a weighed round-bottom flask. The flask was heated to 65 °C for 30 minutes using a hot plate. The solution was filtered under vacuum and the filtrate was added to a weighed round-bottom flask. The solvent was removed with rotary evaporation. A 25 ml aliquot of water was used to dissolve the extract and this was sequentially extracted three times with an equal volume of ethyl acetate. The ethyl acetate extracts were concentrated by rotary evaporation.

For comparison purposes, this extraction process was repeated with 5 g of Cancer Bush powder. After heating to 65 °C, the flask was ultrasonicated for an additional 30 minutes, and then the solution was filtered, and extracted following the above procedure.

3.4 Qualitative tests

3.4.1 Test for flavonoids

The procedure followed for the flavonoid identification test was as reported by Tabrizi *et al.*²²⁹ The pigments were removed by washing one gram of each extract obtained either by maceration or Soxhlet extraction with 20 ml of petroleum ether several times until the wash solution became colourless. The sediment was dissolved in 30 ml of ethanol (80%, v/v). The solution was filtered into two tubes; one tube served as the control. A mass of 20 mg of magnesium powder was added to the second tube. A solution of 37% (v/v) HCl was added in a dropwise manner until the magnesium powder was completely dissolved. The colour was observed to determine the content of flavonoid extracted. An orange colouration represents the presence of a low content of flavonoids, light red signifies a medium content, and dark red indicates a high content.

3.4.2 Test for phenols

A mass of 15 mg of each extract was dissolved in water and a few drops of 1% ferric chloride solution were added. The expected colouration was red, blue, green or purple to indicate the presence of phenols.

3.5 UV/Vis absorption spectroscopy

3.5.1 An introduction to UV/Vis absorption spectroscopy

UV/Vis spectroscopy is a simple, fast and inexpensive method used to determine the concentration of an analyte in solution. It provides information on the electronic transitions that take place in molecules. The process in which a molecule absorbs UV or visible light at a certain wavelength and becomes excited is called UV/Vis absorption. When the electron becomes excited, it moves from the ground state to a higher energy state. The absorbed energy is equivalent to the energy separation between the two levels. UV/Vis spectroscopy allows for the measurement of this transition from the spectra obtained.

Beer's law is a mathematical relation that allows one to determine the concentration of a substance in a solution by measuring the UV absorption spectrum of a solution. This relationship is shown in Equation 3,

$$A = \epsilon bc \quad (3)$$

where A is the absorbance, ϵ is the molar absorption coefficient ($\text{L mol}^{-1} \text{cm}^{-1}$), b is the path length (cm), and c is the concentration (M).

A UV/Vis spectrophotometer measures the absorption of the substance at a particular wavelength. The amount of light absorbed by the sample depends on the concentration, path length and how well the analyte absorbs light at a certain wavelength. The path length is related to the sample container (also known as a cuvette) used in analysis. The cuvette is made of a material that does not absorb light in the UV/Vis range. This material could be glass, quartz or plastic. A quartz cuvette is used for measurement of UV light, as plastic and glass absorb UV radiation. The molar absorption coefficient, ϵ , is determined by measuring the absorption of a sample with a known concentration and known path length. The molar absorption coefficient units are dependent on the path length and concentration units. The absorbance is a measure of how strongly a molecule absorbs light at a particular wavelength.

Different molecules can absorb different wavelengths of light and in the visible region the different wavelengths correspond to different colours. For example, red corresponds to 700 nm and blue to 400 nm. Wavelengths shorter than 350 nm fall in the ultraviolet region of the

electromagnetic spectrum. It is important to note that shorter wavelengths have higher energy. Molecules that can absorb light in the UV/Vis range of wavelengths contain functional groups called chromophores. Compounds that absorb in the visible region are coloured. These include transition metal ions and organic dyes. Colourless compounds only absorb in the UV region. Compounds that display intense absorption capabilities must be examined in dilute solutions. This allows for significant light energy to reach the detector. Dilution can be achieved by using completely transparent and non-absorbing solvents, such as water, ethanol, hexane and cyclohexane.

3.5.2 UV/Vis spectrophotometer

The components of a typical spectrophotometer are shown in Figure 3.1. The instrument contains two light sources, one for visible light (such as a tungsten lamp) and the other for UV light (such as a deuterium lamp). A mirror directs the beam of light onto a monochromator or diffraction grating where the light is separated into its individual wavelengths. The instrument scans through the spectrum and sends different wavelengths of light through to the sample in sequence. This is done by the diffraction grating which is able to rotate.

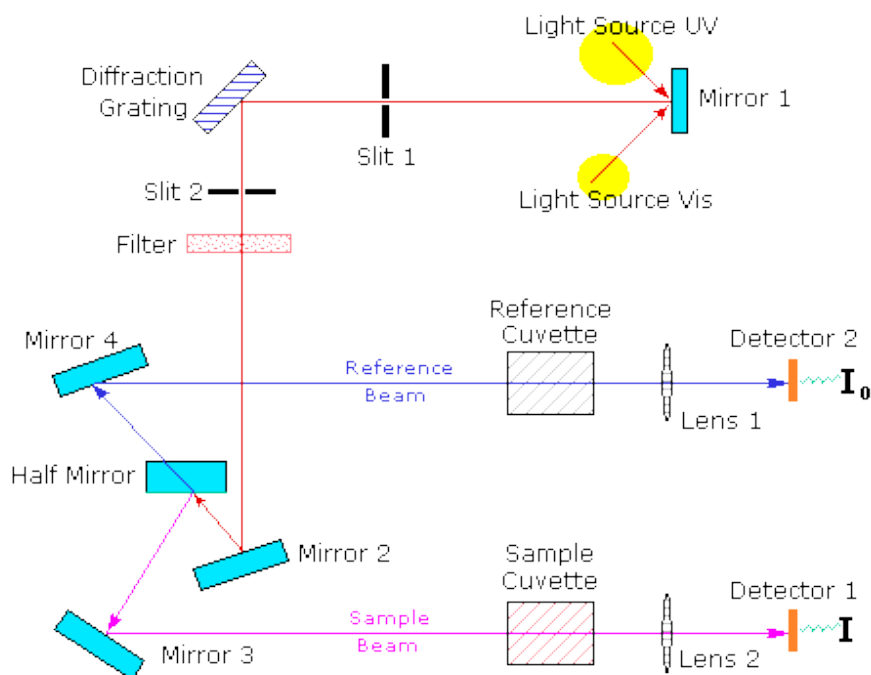


Figure 3.1: A diagram showing the basic components of a double-beam UV/Vis spectrophotometer.²⁵⁸

A single wavelength passes through a modulator. The modulator consists of a rotor with mirrors on it. Each monochromatic (single wavelength) beam in turn is split into two equal

intensity beams by a half mirror. One beam passes through a sample cell and the second passes through a reference cell. The first beam passes through the cuvette containing the sample which is a solution of the analyte in a transparent solvent. The second beam passes through the reference cell, which is an identical cuvette containing only the solvent, known as a blank. This type of instrument is referred to as a double-beam instrument. The intensities of both these light beams are directed by mirrors to a detector. The detector measures and compares the difference between the intensities. A signal proportional to the ratio of their intensities is sent to a computer that controls the instrument.

The absorbance of the sample, given by the logarithm of this ratio shown in Equation 4, gives a measure of how much light is being absorbed by the sample at a certain wavelength. The reference beam should not absorb any light and its intensity is defined as I_0 (incident light). The intensity of the sample beam is defined as I (transmitted light). If the sample does not absorb light, then $I = I_0$. If the sample absorbs light, I is less than I_0 . Absorption can also be represented as transmittance by Equation 5. Transmittance is the amount of light that passes through the sample and reaches the detector.

$$\text{Absorbance, } A = \log \frac{I_0}{I} \quad (4)$$

$$\text{Transmittance, } T = \frac{I}{I_0} \quad (5)$$

Following an analysis, a spectrum is obtained showing absorbance versus wavelength. A typical spectrum is shown in Figure 3.2. The peaks on the spectrum are the wavelengths of light that are absorbed by the sample. The troughs are where light passes through and is not absorbed. The wavelength of maximum absorbance is a characteristic value, λ_{max} . The spectrum allows for determination of the properties of the molecule and also for sample characterisation. However, UV/Vis absorption spectroscopy is most commonly used for quantitation by making use of Beer's Law.

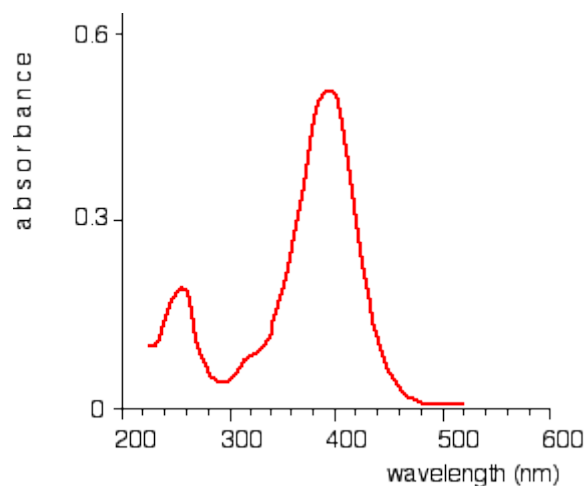


Figure 3.2: A typical UV spectrum.²⁵⁹

3.6 Photostability experiments

Chemical UV absorbers are incorporated into sunscreen products in order to absorb solar UV radiation. A UV radiation source is therefore required for determining the protective efficacy of chemical absorbers. The lamp is described in Section 3.6.1.

3.6.1 Irradiation source

An Osram HBO 500 W/2 high pressure mercury lamp (shown in Figure 3.3) was used as a source of UV radiation to determine the protective efficacy of the sample extracts. The lamp was suitable as it provided high radiant light in the UV and visible region, ranging from 260 to 610 nm (Figure 3.4).

Figure 3.5 shows the irradiation equipment and its individual components. The lamp is housed in an insulated steel box (A). The UV light emitted passes through an opening on one end of the steel box, through a 10 mm thick Pyrex filter to reach the sample contained in a cuvette to be irradiated. The Pyrex filter is used to mimic solar UV wavelengths. The filter only allows wavelengths greater than 300 nm to pass through (Figure 3.6). The steel box contains a shutter gate which must be opened to let the light through. The shutter gate, filter holder and cuvette holder form part of an external bracket attached in front of the steel box opening (Figure 3.7). The steel box is connected to an extractor (B). The system also includes a fan (D), power supply and igniter (E).

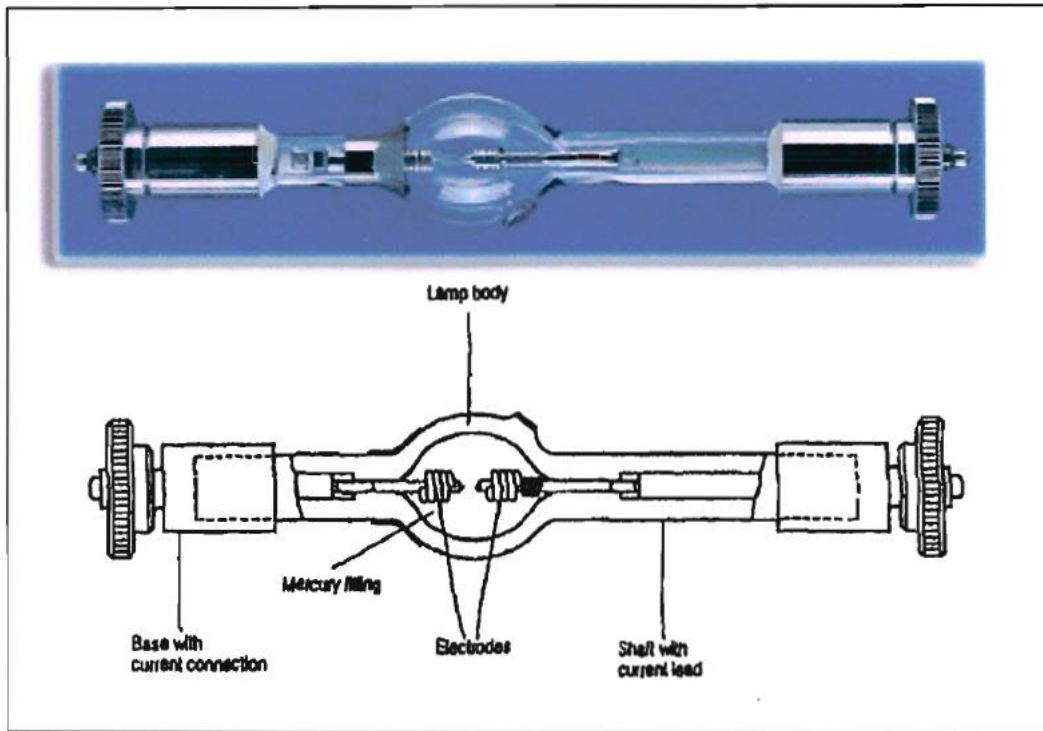


Figure 3.3: A diagram of the Osram 500 W/2 high pressure mercury lamp (Osram and schematic drawing).²⁶⁰

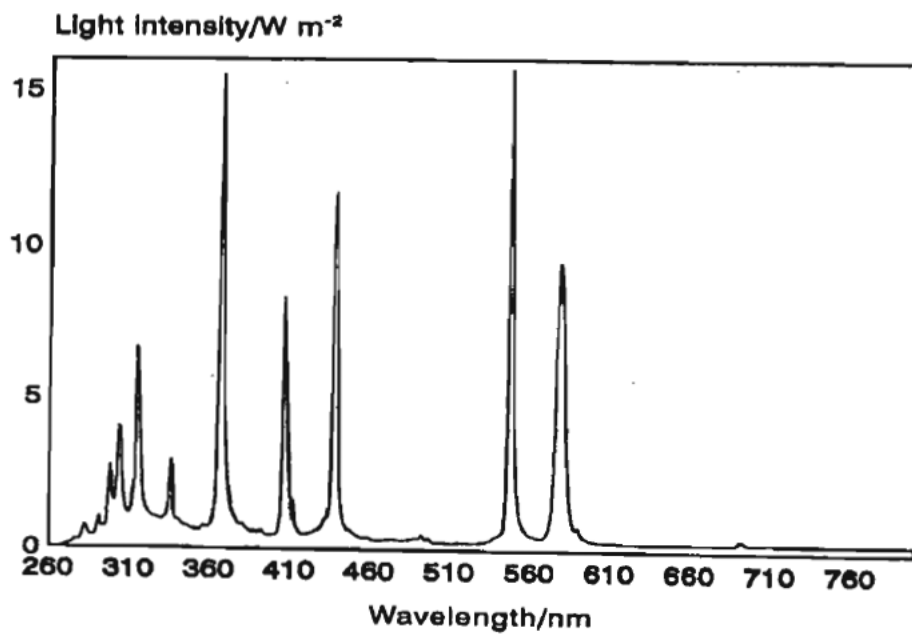


Figure 3.4: Output of the Osram HBO 500 W/2 high pressure mercury lamp.²⁶¹

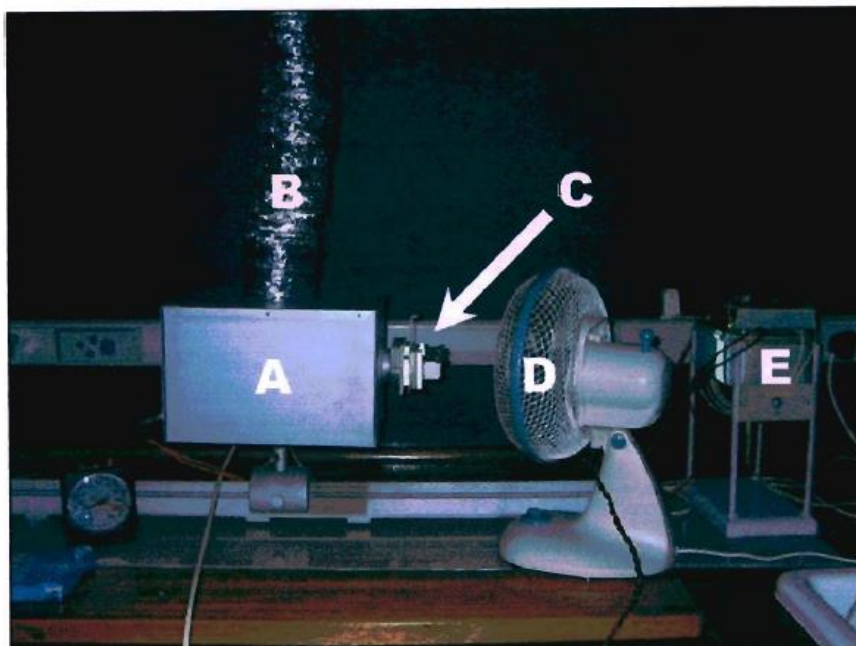


Figure 3.5: A photograph of the irradiation equipment showing the insulated steel box (A), containing the lamp, connected to an extractor (B) and the external bracket (C) which holds the filter, shutter and sample cuvette. The photograph also shows the fan (D) and the igniter (E).

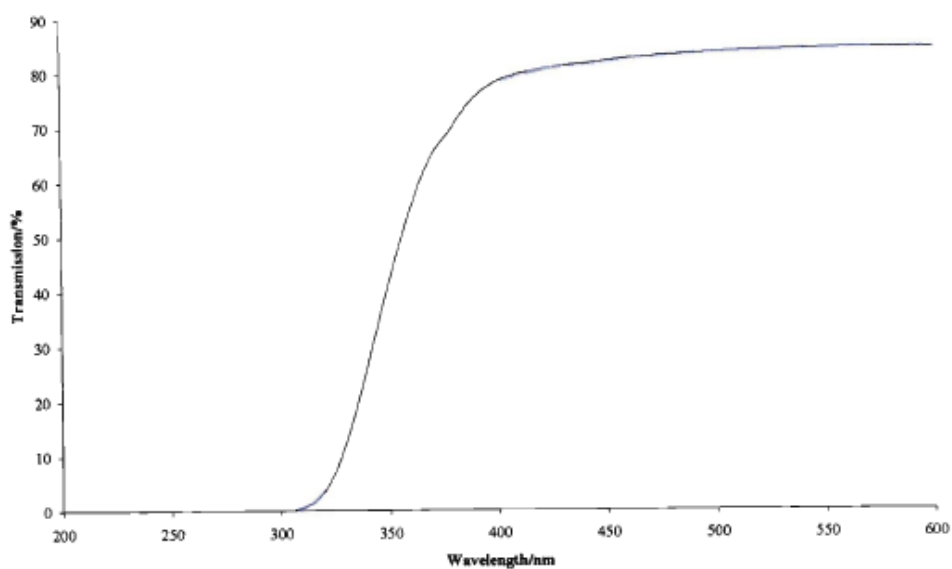


Figure 3.6: Transmission spectrum of the 10 mm thick Pyrex filter.

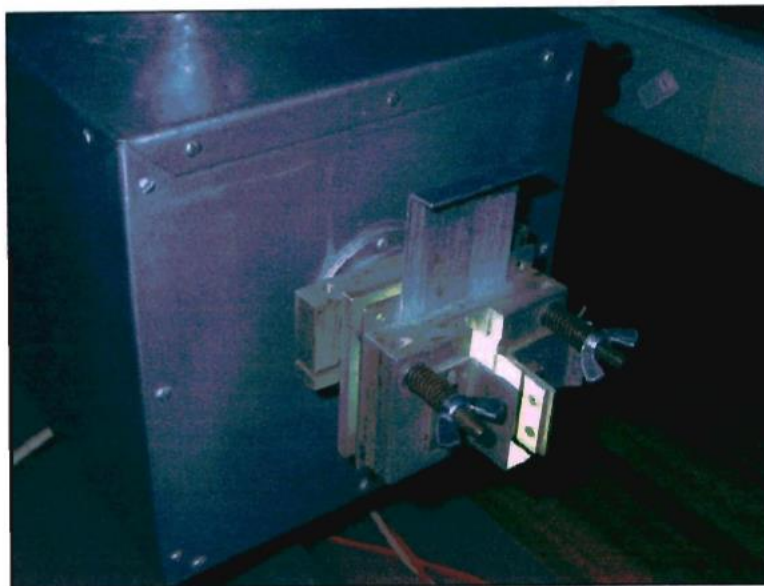


Figure 3.7: Close-up of the external bracket holding the shutter gate, filter and cuvette.

Samples need to be dissolved in a suitable solvent before irradiation can take place. Factors that need to be considered in the choice of solvent include the ability of the solvent to dissolve the chemical absorber and the antioxidant extract, the photostability of the solvent, and whether the absorbance of the absorber is not masked by the solvent, i.e., the solvent must be transparent over the wavelength range (UVB and UVA range) in which the chemical absorber absorbs.

For sample irradiation to take place, the Osram HBO 500 W/2 lamp required a 15-minute warm up period. A 10 mm thick Pyrex filter was placed between the lamp and the sample to be irradiated. The Pyrex filter allows for wavelengths greater than 300 nm to pass through. The samples to be irradiated were placed in a 1 mm pathlength quartz cuvette.

Samples must be irradiated at suitable time intervals for adequate degradation in different solvents and then examined by UV absorption spectroscopy with a Shimadzu UV-3600, UV/Vis-NIR double-beam spectrophotometer.

3.6.2 Commonly used UV absorbers

Commercial UV absorbers (avobenzene, benzophenone-9, 4-methylbenzylidene camphor and 2-ethylhexyl-*p*-methoxycinnamate) commonly used in sunscreen products were weighed to approximately 0.0100 g and dissolved in a total volume of 100 ml of solvent. The solvents used were based on polarity and included methanol, ethyl acetate and cyclohexane. Each sample was diluted to obtain an absorbance value below 1.2. The assessment of the photostability of the selected UV absorbers was carried out by measuring the UV spectrum of

each sample before and after irradiation for six hours at 30-minute intervals. The irradiations were conducted with the Osram HBO 500 W/2 lamp described in Section 3.6.1.

3.6.3 UV absorbers mixed with Cancer Bush extracts

Each UV absorber was weighed to approximately 0.0100 g and dissolved with 100 ml of solvent. Solvents used were based on polarity and included methanol, ethyl acetate and cyclohexane. Each sample was diluted to obtain an appropriate absorbance value around 1.2. A mass of 0.032 g of the Cancer Bush extract was then mixed with 100 ml of the solution. The mass was determined as the minimum amount of extract required to obey Beer's Law. The assessment of the photostability of the selected UV absorbers in the presence of the Cancer Bush extracts was carried out by measuring the UV spectrum of each sample before and after irradiation at 30-minute intervals for a total period of six hours. The Cancer Bush extracts tested included the boiling water extract and the ethanol-water extract.

3.6.4 Extracts from commercial teas

A small portion of each of the dried extracts was dissolved in 10 ml of HPLC-grade methanol and the UV spectrum of each extract solution was recorded in a quartz cuvette. Additionally, the three extracts of green tea, Rooibos tea and Cancer Bush solutions in methanol were mixed in equal volumes and the UV spectrum of the mixture was recorded. Irradiations of the same solution in a 1 cm pathlength cuvette were performed with the Osram HBO 500 W/2 lamp. The solution was not exposed to light apart from during the irradiation periods. The time intervals of irradiation were every 30 minutes for a total of six hours. The spectrum of the solution was recorded after each irradiation period.

3.7 High performance liquid chromatography analysis

The Cancer Bush and tea extracts contain a mixture of materials, including polyphenols. In order to be analysed, these products must be separated by a chromatographic method such as high performance liquid chromatography (HPLC). HPLC can be used to separate and identify the different substances in these mixtures.

3.7.1 Introduction and instrumentation

High performance liquid chromatography, HPLC (also referred to as high-pressure liquid chromatography) is a technique used in analytical chemistry to separate the components in a mixture and to identify and quantify each component. The separation occurs with two phases: the stationary phase and the mobile phase. This technique involves injecting a small volume

of a liquid sample into a column that is packed with tiny porous particles (called the stationary phase). Solvent (mobile phase) is then pumped at high pressure through the column to effect the separation. The compounds found in a sample are separated from each other by chemical and physical interactions that take place in the column between the stationary phase and the mobile phase. Figure 3.8 shows the typical components of a HPLC chromatograph.

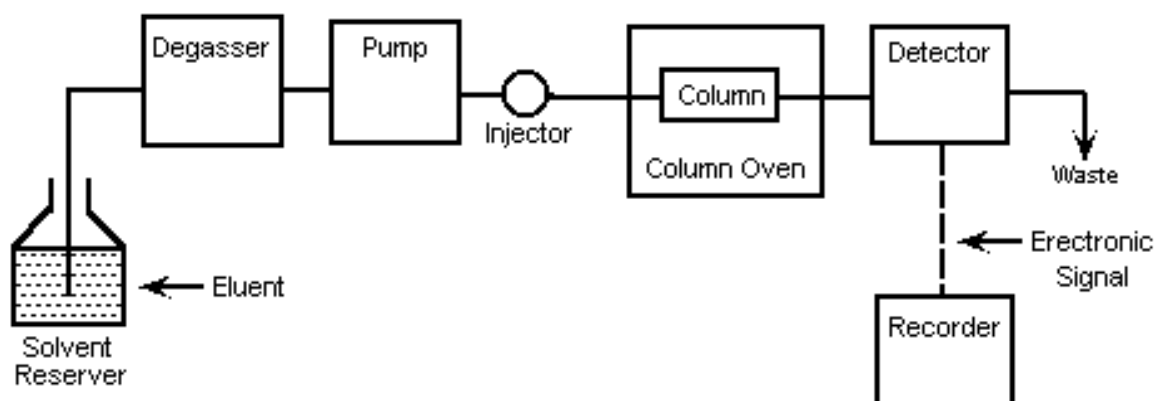


Figure 3.8: Components of a HPLC.²⁶²

A solvent housed in the solvent reservoir is needed to create the mobile phase. The mobile phase is typically made up of a mixture of water and an organic solvent (such as acetonitrile or methanol). The mobile phase is required to carry the sample through the HPLC system and to effect separation. This requires the use of a high-pressure pump to move the mobile phase continuously from the solvent container to a waste container. The role of the pump is to force the mobile phase through the column at a constant flow rate ($1\text{-}2\text{ ml min}^{-1}$). There are two types of pump operation: isocratic and gradient. An isocratic pump delivers a constant mobile phase composition, and a gradient pump delivers a variable mobile phase composition.

An injector system introduces the sample into the flow stream of the mobile phase. It must be able to withstand the high pressures of the mobile phase. The mobile phase, now carrying the sample, is passed through a column for separation, identification and quantification of the components to take place. The column is the pillar of the instrument. The analysis of the components depends on the choice of column. Columns are packed with the stationary phase in the form of very small spherical particles, typically between 1.5 to $10\text{ }\mu\text{m}$. The interaction between the stationary phase, the mobile phase and the sample components allows for separation to occur. The separated components are eluted from the column at different times and reach the detector. The detector is designed to recognise a characteristic of the sample components and convert this into useful data. There are many types of detectors, the most

common being a UV detector. The detector measures the amount of each component and sends signals to a computer that contains software that converts the data into a chromatogram.

HPLC can be performed in either normal or reversed phase modes. The most commonly used method is the reversed phase in which the HPLC separates compounds starting with the most polar and ending with non-polar compounds. In a gradient system, as the concentration of the organic solvent increases, the mobile phase becomes more non-polar. The solutes in the sample vary in polarity. As the mobile phase passes, the compounds bind to the column and are retained differently by the stationary phase. When the polarity of the compound matches the polarity of the mobile phase, the mobile phase will retain it more strongly than the stationary phase and it will be eluted. Subsequently, the solutes are detected separately depending on the time it takes for them to reach the detector. The weakly retained solutes reach the detector faster than the strongly retained solutes. The time taken for each compound to be eluted is referred to as the compound's retention time (R_f).

The HPLC system used in this study was a Shimadzu LC-20AD XR with a photodiode array (PDA) detector with the ability to monitor multiple wavelengths simultaneously.

3.7.2 HPLC parameters

In order to separate the components of the extracts use was made of HPLC with the following parameters:

Column: Zorbax Eclipse-XDB C18 reversed phase

Column temperature: 25 °C

Column dimensions: 4.6 × 150 mm

Column length: 100-250 nm

Column internal diameter: 3.9-4.6 mm

Particle size: 5 μm

Isocratic elution - Mobile phase: 12% MeOH and 87% Millipore water containing 1% acetic acid.

Flow rate: 1 mL min⁻¹

Injection volume: 10 μL

3.7.3 Experimental procedure

3.7.3.1 Column cleaning:

The column was cleaned once prior to use. The following gradient system was run through the column at a flow rate of 1 ml min⁻¹: Millipore water for 30 minutes, Millipore water to methanol changing linearly over 5 minutes, methanol for 30 minutes, methanol to acetonitrile changing linearly over 5 minutes, acetonitrile for 30 minutes, acetonitrile to tetrahydrofuran changing linearly over 5 minutes, and tetrahydrofuran for 30 minutes. The gradient system was repeated in reverse. The column was equilibrated by passing five times the column volume of mobile phase before analysis.

3.7.3.2 Performance check of C18 column

A solution containing uracil, phenol, 4-chlorobenzene and toluene in methanol with concentrations of 5, 200, 250 and 800 µg ml⁻¹ was injected. The retention times of the four compounds was matched with the performance report to see if the column performed optimally.

3.7.3.3 Preparation of mobile phase

The mobile phase was prepared by mixing 1% of acetic acid to 87% Millipore water with 12% methanol. The mobile phase was filtered through a 0.45 µm Durapore filters and degassed with helium.

3.7.3.4 Preparation of phenolic acid standards

Stock solutions of the six phenolic acids were prepared by dissolving 1 g of each phenolic acid in methanol in a 100 ml volumetric flask. A multi-standard solution was prepared by adding aliquots of 100, 200, 400, 800 and 1000 µl respectively, of each stock solution and making up to a total volume of 10 ml with the mobile phase. Therefore, five multi-standard solutions were prepared with approximate concentrations of 10, 20, 40, 80 and 100 mg ml⁻¹ respectively.

An injection of 20 µl of each standard solution separately was made to obtain the retention time and UV spectrum of each phenolic acid.

3.7.3.5 Preparation of the Cancer Bush extract

An aliquot of 500 µl of each Cancer Bush extract that were prepared in Section 3.2 was diluted with 500 µL of the 12% MeOH mobile phase and filtered into HPLC vials (initial concentration of extract was 12.50 mg ml⁻¹ and concentration injected into the chromatograph was 6.25 mg ml⁻¹).

3.7.3.6 Preparation of tea extracts

The tea extracts were prepared according to the method described in Section 3.3. Approximately 0.05 g of the extract was dissolved in 2 ml of 1% MeOH mobile phase and filtered into HPLC vials.

3.7.3.7 HPLC analysis method

All samples and standards were filtered through a Millipore 0.45 µm syringe filter into 1.5 ml HPLC vials before injection. The standards stock solutions and five multi-standard solutions were injected and run for 60 minutes each and this included blank injections between each run. The Cancer Bush and tea extracts were also run for 60 minutes.

3.8 Sunscreen formulation

Sunscreens are cosmetic formulations that are developed to attenuate UV radiation. The efficacy of a sunscreen product depends on the formulation. The formulations are often exposed to extreme conditions, yet must consistently deliver the active ingredient to provide uniform protection. Ingredients used in these products are usually dispersed in an emulsion (also called a vehicle).⁴⁷ Ingredients can include emulsifiers, emollients, rheology modifiers, film formers, stabilisers, preservatives, and active inorganic or organic components that solely interact with UV radiation, as well as, other components required for an aesthetic appeal. Emulsifiers promote the formation and physical stability of sunscreen emulsions; emollients act as vehicles for introducing oil-soluble sunscreen absorbers and also determine the consumer acceptance of the product; rheology modifiers control the viscosity/thickness of the formulation, film formers form films in the formulation, and stabilisers preserve and stabilise the emulsion. The vehicle formulation controls the absorption properties and the photostability of the active ingredients.⁴⁷ Plant extracts with an antioxidant function can be added to formulations. The formulation used generally depends on the market requirements and desired protection.

3.8.1 Example sunscreen formulation

Elementis is a global speciality chemical company that offers performance-driven additives that help create innovative formulations for consumer and industrial applications. In this experiment, an example sunscreen formulation, Maui Milk SPF 15 (S-2011-02), listed in an Elementis formulation guide was used, Formulation SPF 1.1. Table 3.6 lists the formulations that were prepared and analysed. Formulation SPF 1.2 is a repeat of Formulation SPF 1.1 with

a 50% reduction of each UV filter. This formulation was also used to compare the Cancer Bush ethanol-water extract and was labelled formulation SPF 1.3.

3.8.2 Adjusted sunscreen formulation

The formulation SPF 2.1 was an adjustment of formulation SPF 1.2 to include the four UV filters included in this work rather than the recommended UV filters listed in the formulation guideline. This formulation was remade to include the Cancer Bush ethanol-water extract (Formulation 2.2) and the green tea extract (Formulation 2.3). The formulations are shown in Table 3.7.

Table 3.6: Example formulation guideline

Phase	Trade name	INCI name	Supplier	Function	SPF 1.1	SPF 1.2	SPF 1.3
A	Cetiol CC	Dicaprylyl carbonate	BASF	Emollient	1.5%	1.5%	1.5%
	Eusolex HMS	Homosalate	Merck	UV filter	12.0%	6.0%	6.0%
	Eusolex OS	Ethylhexyl salicylate	Merck	UV filter	5.0%	2.5%	2.5%
	Eusolex OCR	Octocrylene	Merck	UV filter	2.0%	1.0%	1.0%
	Eusolex 9020	Butyl methoxydibenzoylmethane (Avobenzone)	Merck	UV filter	1.4%	0.7%	0.7%
B	Bentone Gel HS V	C12-15 alkyl benzoate (and) disteardimonium hectorite (and) alcohol	Elementis	Rheology modifier	7.5%	7.5%	7.5%
	Belsil DM5	Dimethicone	Wacker	Silicone	6.8%	6.8%	6.8%
	Jolee 7750	Isoamyl laurate	Oleon	Skin conditioning	2.5%	2.5%	2.5%
	ABIL EM 180	Cetyl PEG/ PPG-10/1 Dimethicone	Evonik	W/O emulsifier	2.0%	2.0%	2.0%
	Deionized water	Aqua		Solvent	48.8%	58.95%	58.95%
C	Dowasil EP 9801 Hydro Cosmetic Powder	Dimethicone/ vinyl dimethicone crosspolymer (and) silica (and) butylene glycol	Dow	Silicone	2.0%	2.0%	2.0%
	Propanediol	1,2-propanediol	VWR	Humectant	2.0%	2.0%	2.0%
	Sodium chloride	Sodium chloride	Merck	Rheology modifier	0.5%	0.5%	0.5%
D	Ethanol	Ethanol	Sigma-Aldrich	Alcohol	5.0%	5.0%	5.0%
	Euxyl PE 9010	Phenoxyethanol (and) ethylhexyl glycerine	Merck	Preservative	1.0%	1.0%	1.0%
	Cancer Bush ethanol-water extract			Antioxidant			0.05%

Table 3.7: Adjusted formulation guideline

Phase	Trade name	INCI name	Supplier	Function	SPF 2.1	SPF 2.2	SPF 2.3
A	Cetiol CC	Dicaprylyl carbonate	BASF	Emollient	1.5%	1.5%	1.5%
	Octinoxate	Ethylhexyl methoxycinnamate	Sigma-Aldrich	UV filter	6.0%	6.0%	6.0%
	Enzacamene	4-methylbenzylidene camphor (MBC)	Alfa Aesar	UV filter	2.5%	2.5%	2.5%
	Benzophenone	Benzophenone-9	The British Drug houses LTD.	UV filter	1.0%	1.0%	1.0%
	Eusolex 9020	Butyl methoxydibenzoylmethane (Avobenzone)	Merck	UV filter	0.1%	0.7%	0.7%
B	Bentone Gel HS V	C12-15 alkyl benzoate (and) disteardimonium hectorite (and) alcohol	Elementis	Rheology modifier	7.5%	7.5%	7.5%
	Belsil DM5	Dimethicone	Wacker	Silicone	6.8%	6.8%	6.8%
	Jolee 7750	Isoamyl laurate	Oleon	Skin conditioning	2.5%	2.5%	2.5%
	ABIL EM 180	Cetyl PEG/ PPG-10/1 Dimethicone	Evonik	W/O emulsifier	2.0%	2.0%	2.0%
C	Deionized water	Aqua		Solvent	59.0%	58.95%	58.95%
	Dowsil EP 9801 Hydro Cosmetic Powder	Dimethicone/ vinyl dimethicone crosspolymer (and) silica (and) butylene glycol	Dow	Silicone	2.0%	2.0%	2.0%
	Propanediol	1,2-propanediol	VWR	Humectant	2.0%	2.0%	2.0%
	Sodium chloride	Sodium chloride	Merck	Rheology modifier	0.5%	0.5%	0.5%
D	Ethanol	Ethanol	Sigma-Aldrich	Alcohol	5.0%	5.0%	5.0%
	Euxyl PE 9010	Phenoxyethanol (and) ethylhexyl glycerine	Merck	Preservative	1.0%	1.0%	1.0%

	Cancer Bush ethanol-water extract			Anti-oxidant		0.05%	
	Green tea extract		Tetley	Anti-oxidant			0.05%

3.8.3 Experimental procedure

The samples were prepared according to the instructions listed in the Elementis formulation guideline. Ingredients in Phase A were combined in a 150 ml beaker and heated to 75 °C with stirring until a clear solution was achieved. Phase B was combined and added to Phase A with a Silverson LM5 homogeniser and homogenised until uniform. Phase C was combined and stirred until uniform. Phase C was added to Phases A and B slowly with propeller mixing and homogenised shortly when completely combined. Phase D was added to Phase A, B, and C with propeller mixing and homogenised briefly.

Formulations that required the addition of the plant extracts were adjusted accordingly by reducing the amount of water proportionately. Each extract was added to ethanol and the preservative in Phase D and stirred until uniform and then added to Phases A, B, and C. The final mixture was homogenised briefly.

3.9 Sunscreen Assessment

3.9.1 Photostability studies for sunscreen products

The sunscreen formulations were applied on quartz plates by using a smear technique. A product surface application density of $\sim 1.0 \text{ mg cm}^{-2}$ was used. The quartz plate specifications were 4.5 cm in length, 2.5 cm width, and 0.2 cm thickness. The smearing technique was conducted as follows: the sample was spotted onto the plate, the spots were then smeared in a circular motion with a finger covered by a latex glove, the plates were left to dry in the dark for 30 minutes, and the masses of the plates were recorded before and after drying. The plates were left in sunlight for a total period of six hours and were subjected to UV/Vis spectrophotometry analysis every 30 minutes. The spectra were recorded against air as the blank.

3.9.2 Preliminary stability tests

Time is a vital parameter in the development of cosmetic products such as sunscreens. One of the key factors in formulation development is the stability of the product over time. To override time limitations, accelerated stability studies are performed. The objective of stability testing of cosmetic products is to verify if the product meets the intended physical, chemical and microbiological quality standards, as well as its functionality and aesthetics when stored under appropriate conditions.²⁶³

Stability studies must consider tests that will “accelerate” the effects of cosmetic product attributes which are susceptible to change under normal conditions of storage and use. By following protocol, stability testing will be able to “predict” the products’ quality, stability, safety and physical integrity under conditions designed to stress specific properties and variations in process conditions. Tests are conducted under controlled accelerated conditions and include appropriate conditions of storage, transport and use, chemical studies, microbiological studies and the compatibility between the formulation and packaging.²⁶³

Physical and chemical stability tests predict how well the product will resist common stresses such as temperature and light. These tests evaluate the products’ appearance, colour, odour, weight, pH value, viscosity, texture, flow and emulsion stability (signs of separation). Five stability parameters were selected for testing.

3.9.2.1 Organoleptic observation

Organoleptic observations were done visually including the physical form, colour, and the odour of the samples. These physical attributes were noted before and after centrifuging and temperature testing.

3.9.2.2 Centrifuge testing

Ultra-centrifugation determines the stability of the formulation. The testing is conducted by centrifuging the product between 3000 to 6000 rpm for three consecutive periods of 5 minutes. If the product remains stable without separation, it has a favourable chance of being commercially stable. Centrifugation was performed on the five formulations at 4000 rpm. Samples were subjected to five minutes of centrifugation for three consecutive runs and the appearance and homogeneity evaluated.

3.9.2.3 Determination of pH

pH measurements were made on each formulation with pH indicator sticks, ranging between pH of 0-14.

3.9.2.4 Rheological evaluation

The relative viscosity of each formulation was determined with a Brookfield Viscometer (Model RV-DVE), in a 250 ml beaker and read at 20 °C. The viscosity of samples was measured with a 05 spindle and the spindle speed was 10 and 12 revolutions per minute (rpm).

3.9.2.5 Physical stability test

Temperature testing is used as a predictor of long-term formulation stability. Temperature cycling and freeze/thaw tests can reveal some types of inadequacies more quickly than storage at constant temperature. A quick indication of formulation stability is the freeze/thaw test which is able to detect suspension problems and instability of emulsions. The samples are cycled from -10°C to 40°C for three to 14 cycles. The five formulations were subjected to three cycles and organoleptic characteristics, pH measurements and viscosity values were obtained to evaluate the formulations before and after the three cycles.

3.9.3 In vitro tests

3.9.3.1 SPF determination

The UV analysis obtained by methods described in Section 3.9.1 were utilised for the *in vitro* SPF value determination with and without UV radiation exposure. The absorbance of the

solution was determined in the wavelength range of 290 to 320 nm at 5 nm increments with air as the blank. The data obtained were processed using the Mansur²⁶⁴ equation as described in Equation 6.

$$\text{SPF} = \text{CF} \times \sum_{290}^{320} \text{EE} (\lambda) \times \text{I} (\lambda) \times \text{A} (\lambda) \quad (6)$$

where CF is the correction factor and has a value of 10, EE is the erythemal effect spectrum, I is the solar intensity spectrum, and A is the absorbance.^{264, 265}

The values of EE and I are constant. The values were determined by Sayre *et al.*²⁶⁵ and are shown in Table 3.6.

Table 3.8: Normalised product function used in the calculation of SPF

Wavelength/nm	EE × I (normalised)
290	0.015
295	0.0817
300	0.2874
305	0.32278
310	0.1864
315	0.0839
320	0.0180

3.9.3.2 Occlusion factor

The *in vitro* occlusion test was adapted from the method of Wissing *et al.*²⁶⁶ A weighed filter paper having a surface area of 18 cm² was placed over the mouth of a beaker containing 30 mL of distilled water and was used as the control. Approximately 250 mg of each sunscreen preparation was spread over a filter paper. Similar beakers with the same amount of water were covered with each of the filter papers containing the sunscreens. The beakers were placed in a hot air oven maintained at 37 °C for a time period of 24 hours. The volume of water lost from the beakers was measured. The occlusion factor was calculated using the formula shown

in Equation 7. An occlusion factor of zero indicated no occlusive effect compared with the reference, and 100 was the maximum occlusive factor.

$$F = 100 \times \frac{(A-B)}{A} \quad (7)$$

where A is the water loss without sunscreen, and B is the water loss with cream.

Chapter 4: Results and Discussion

Most sunscreen products on the market are accompanied by an instruction of reapplication every three to four hours to be optimally effective. The reason for this instruction is that the product can be rubbed off through wearing, and the UV filters used in these sunscreen products tend to degrade over time which is proportional to the amount of exposure received.

Sun protection is one of the major concerns in the cosmetic industry as sunscreen products are used by a vast majority globally. These sunscreens are added to everyday cosmetic products such as lipsticks and foundation. For modern day women on the go, reapplication is deemed unnecessary and time-consuming. As a cosmetic scientist, it is necessary to ensure that these products maintain a level of protection from the sun throughout the day. This will add an appeal to the product, thereby promoting sales. Therefore, it is essential that sunscreens act as intended and should not photodegrade on use.

As the cosmetic industry deems it urgent to photostabilise sunscreens in personal care products, there is a shift in interest to the use of plant antioxidants as possible photostabilisers. Plants contain polyphenols that are natural absorbers of sunlight. It is believed that polyphenols that absorb at similar wavelengths as photolabile chemical absorbers could act as potential photostabilisers by shielding the absorbers and scavenging any free radicals formed.

This chapter discusses the results of the experimental work described in Chapter 3. The chapter is divided into three sections. This first section reports on the photostability of four common organic chemical UV absorbers in different solvents upon irradiation. The polyphenolic extracts derived from the Cancer Bush plant and mixtures of these Cancer Bush extracts with the commonly used UV filters were also assessed for their photostability capabilities. In addition, green tea and rooibos tea, available commercially, were investigated as potential photostabilisers and are discussed. Tea extracts were used since they are known sources of polyphenols. The tea extracts were used to compare the polyphenolic extraction efficiency and photostabilising potential to that of the Cancer Bush plant extracts. The second section discusses the results of the HPLC analysis employed to identify and quantify phenolic acids obtained from the Cancer Bush plant extract, as well as the tea extracts. Phenolic acid standards were prepared and assessed in order to identify and quantify the phenolic acids in the extracts. The third section discusses the assessment of phenolic acid inclusion in sunscreen formulations. Sunscreen formulations were prepared with and without UV filters and photostability tests

were conducted. Stability tests were conducted to assess the stability and safety of the formulations.

4.1 Photostability assessment

4.1.1 Commonly used UV filters in different solvents

The classification of chemical absorbers in sunscreen preparations as UVA or UVB filters is dependent on their wavelength of maximum absorption: UVB filters absorb between 280 nm to 315 nm, and UVA filters absorb between 315 nm to 400 nm. The efficacy of the UV filter used as a chemical absorber can be determined by assessing how well it retains its absorption capacity upon irradiation with the respective wavelengths.

Four commonly used UV filters, namely, benzophenone-9, avobenzone (butyl methoxy dibenzoylmethane), 2-ethylhexyl-*p*-methoxycinnamate (EHMC) and 4-methylbenzylidene camphor (MBC) were investigated. Solutions of ca. 1×10^{-3} M of each absorber were prepared by dissolving them individually in either methanol, ethyl acetate or cyclohexane, to obtain an absorbance value within the boundaries of Beer's law (0.2 – 1.2). The solvents were selected based on their polarity and the solubilities of the UV filters are indicated in Table 4.1. UV absorbers were only studied in those solvents in which they were soluble. The solutions were analysed with a Shimadzu UV-3600, UV/Vis-NIR double-beam spectrophotometer before and after irradiation with light simulating solar radiation from an Osram HBO 500 W/2 lamp coupled with a 10 mm thick Pyrex filter. Irradiation was conducted for a total period of six hours, i.e.: from 09:00 a.m. to 15:00 p.m. The interval was based on when sun exposure is at its maximum and the solutions were monitored at 30-minute intervals.

Table 4.1: Solubility of UV filters in solvents of different polarity.

	Methanol	Cyclohexane	Ethyl acetate
Benzophenone-9	S	NS	NS
Avobenzone	S	S	S
4-methylbenzylidene camphor	S	S	S
2-ethylhexyl-<i>p</i>- methoxycinnamate	S	S	S

S – Soluble, NS – Not soluble

4.1.1.1 Benzophenone-9

Benzophenone-9 was selected as the benchmark as it has been reported for many years to be extremely photostable.^{97, 267} This is confirmed by the UV spectra shown in Figure 4.1. Although this filter is known to be completely stable, benzophenone-based filters are not a preferred choice in sunscreen products due to their recent scrutiny among consumers. Disadvantages of benzophenone-based filters include their persistence, bioaccumulation and toxicity linked with marine life and coral reefs. Another problem associated with benzophenone filters is their suspected irritancy to human skin. Studies by Sewlall²⁶⁸ showed that benzophenone-9 caused DNA strand breaks. Bolton *et al.*²⁶⁹ conducted *in vitro* studies and was able to show that benzophenone-9 photosensitises thymine dimer formation.

A major concern for the cosmetic industry is the yellow colour of the benzophenone-based filters. This becomes difficult for a company that works with beauty products such as foundations which need to be colour specific. The colour of the filter compromises the colour of the final product giving a yellow pigmentation. These disadvantages led to the investigation of other types of UV filters.

Figure 4.1 displays the UV spectra of benzophenone-9 dissolved in methanol. The spectrum confirms that benzophenone-9 is not susceptible to photodegradation over the six hour irradiation period. The spectrum exhibits two maxima at 281 and 332 nm. Thus, benzophenone-9 is classified as both a UVB and a short wavelength UVA filter. Benzophenone-9 was insoluble in ethyl acetate and cyclohexane and, hence, it was not studied in those solvents.

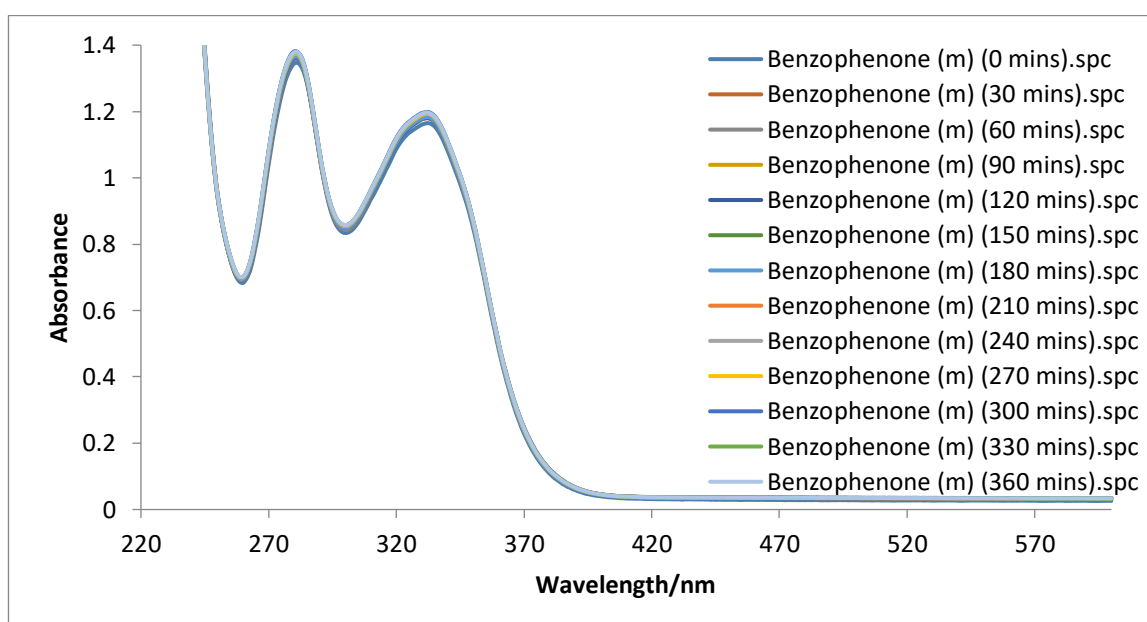


Figure 4.1: Photostability of benzophenone-9 dissolved in methanol. The spectra were recorded every 30 minutes for a total period of six hours, and were acquired in a 1 cm pathlength quartz cuvette against air as the reference.

4.1.1.2 Avobenzone

Avobenzone (BMDBM) belongs to the dibenzoylmethane group of filters that is used in sunscreen products. It is globally accepted and the most commonly used UVA chemical absorber. Avobenzone is known to show a decrease in absorbance over time. The filter exists in two tautomeric forms: the *enol*- and the *keto*-tautomer. Avobenzone exists in the *enol*-form in sunscreen formulations and this form absorbs in the UVA range between 340-360 nm. On exposure to UV radiation, the filter undergoes phototautomerization whereby the *enol*-form converts to the *diketo*-form which absorbs in the UVC range between 260-280 nm. This change is undesirable as human skin needs protection from UVA rather than UVC, which is not incident on the earth's surface. The filter can also undergo photofragmentation.^{100, 101} These alterations will cause a decrease in the SPF of a sunscreen product rendering the product ineffective.

The maximum absorption wavelength for avobenzone ranges from 350 to 365 nm, depending on the solvent used. The photostability of avobenzone is solvent-dependent. Andrae *et al.*¹³¹ and Dubois *et al.*¹³⁰ both reported avobenzone to be photolabile in acetonitrile. Panday²⁷⁰ and Roscher *et al.*²⁷¹ revealed its instability in cyclohexane. The wavelengths of maximum absorption (λ_{\max}) of avobenzone in each solvent are listed in Table 4.2, and increase with increasing polarity of the solvent. This trend is confirmed by Agrapidis-Paloympis *et al.*²⁷²

Table 4.2: The wavelengths of maximum absorption of avobenzone in different solvents

Solvent	Wavelength of maximum absorption of avobenzone, λ_{\max} /nm
Methanol	358
Ethyl acetate	356
Cyclohexane	351

These results confirm that avobenzone falls under a UVA filter with an absorption profile ranging between 310 nm to 400 nm. The efficacy of avobenzone as a UVA filter was

investigated by dissolving it in the respective solvents and irradiating the solutions with UV radiation of wavelengths greater than 300 nm.

Figure 4.2 shows the UV spectra of avobenzone dissolved in methanol and obtained at 30-minute intervals for a total irradiation period of six hours. The maximum absorbance of 1.16 is seen at a λ_{max} of 358 nm and this decreases slightly after each irradiation time interval. The spectrum showed that after each irradiation interval the solution showed a smaller loss in absorbance at the wavelength of maximum absorption than was observed for the other two solvents (see Figure 4.4 and 4.5). The spectra also show that a correlation exists between the loss of absorption at the λ_{max} of avobenzone in methanol, 358 nm, and the increase in absorbance at 245 nm. This correlation is shown in Figure 4.3. The *enol*-form of avobenzone absorbs at 358 nm and degrades upon irradiation, whereby the *keto*-form absorbs around 270 nm and increases in absorption upon irradiation. Thus, the correlation can be used to confirm phototautomerisation upon irradiation.

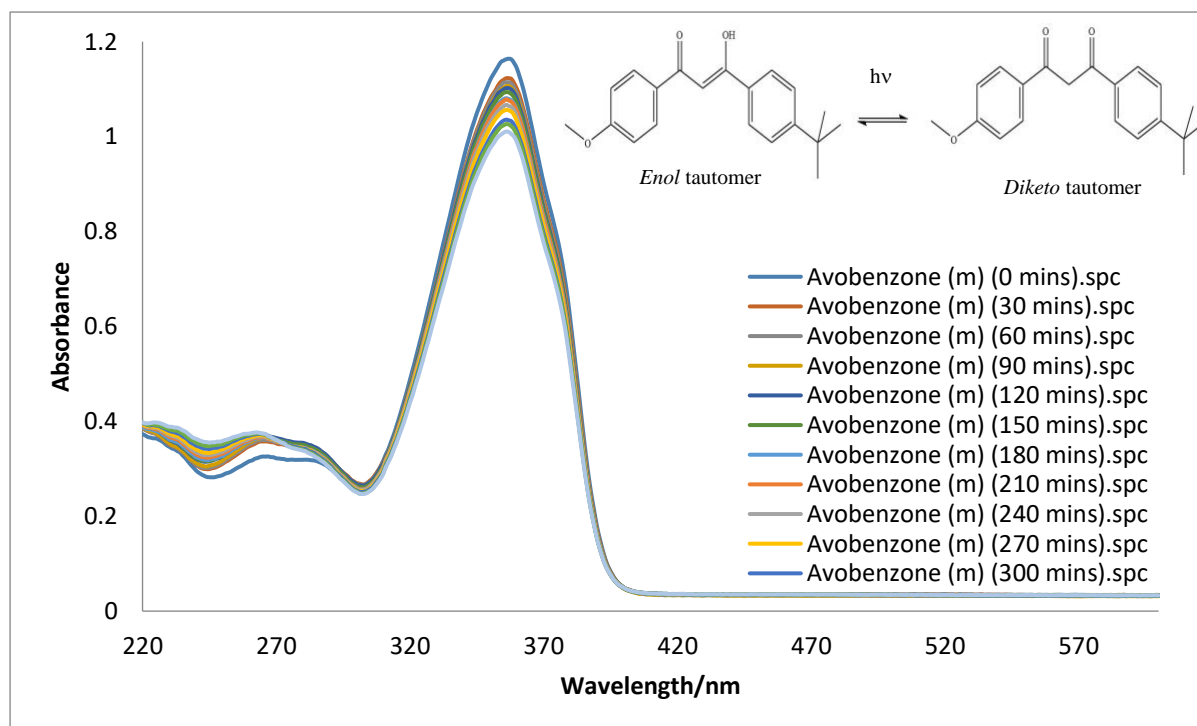


Figure 4.2: Photostability of avobenzone dissolved in methanol. The spectra were recorded every 30 minutes for a total period of six hours, and were acquired in a 1 cm pathlength quartz cuvette against air as the reference.

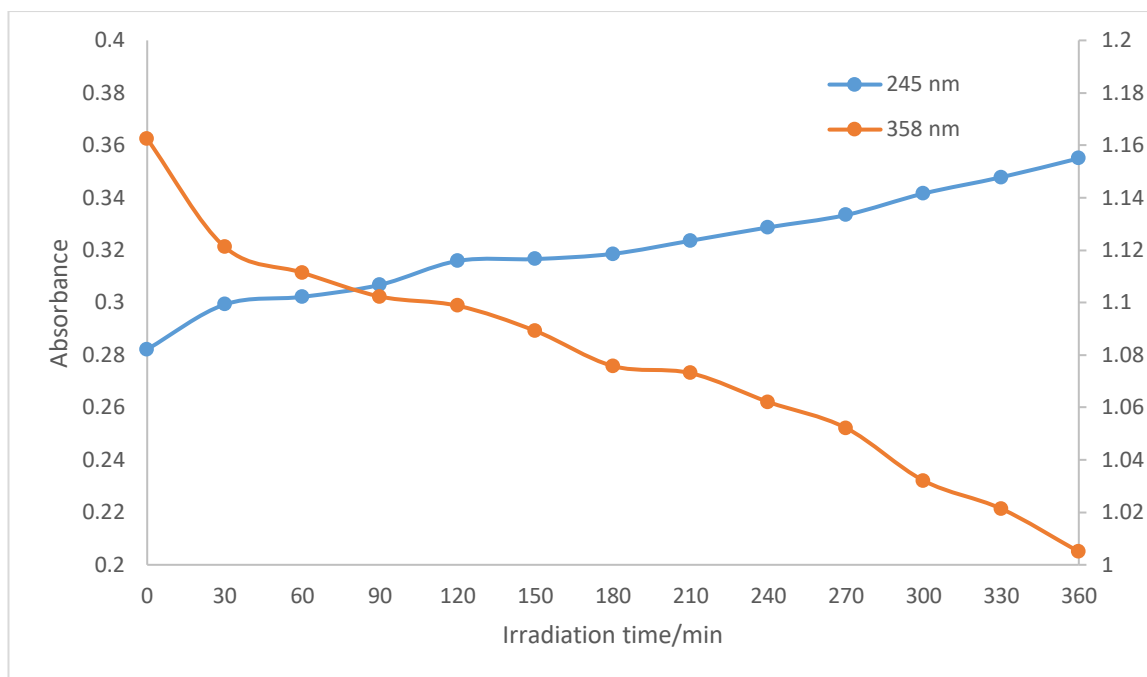


Figure 4.3 Absorbance of avobenzone dissolved in methanol at 245 and 358 nm after 30-minute irradiation intervals indicating the loss of the *enol*-form (at 358 nm) and the formation of the *keto*-form (at 245 nm).

The photostability of avobenzone dissolved in ethyl acetate shown in Figure 4.4 reveals that avobenzone showed more degradation than when dissolved in methanol with evidence of a conversion. The maximum absorbance of 1.23 is seen at wavelength 356 nm, and at 30-minute intervals, a decrease in absorbance is observed until 270 minutes is reached. Thereafter, absorbance is maintained. Between the wavelengths of 264 and 288 nm, an increase in absorbance was observed after each irradiation interval.

An isosbestic point was observed at 295 nm that separates the decrease in absorbance at 356 nm and the increase in absorbance at 264 nm. The presence of an isosbestic point indicates the presence of at least two species in equilibrium. In this case it would be the *enol*- and *keto*-forms. This can be used to confirm phototautomerisation upon irradiation.

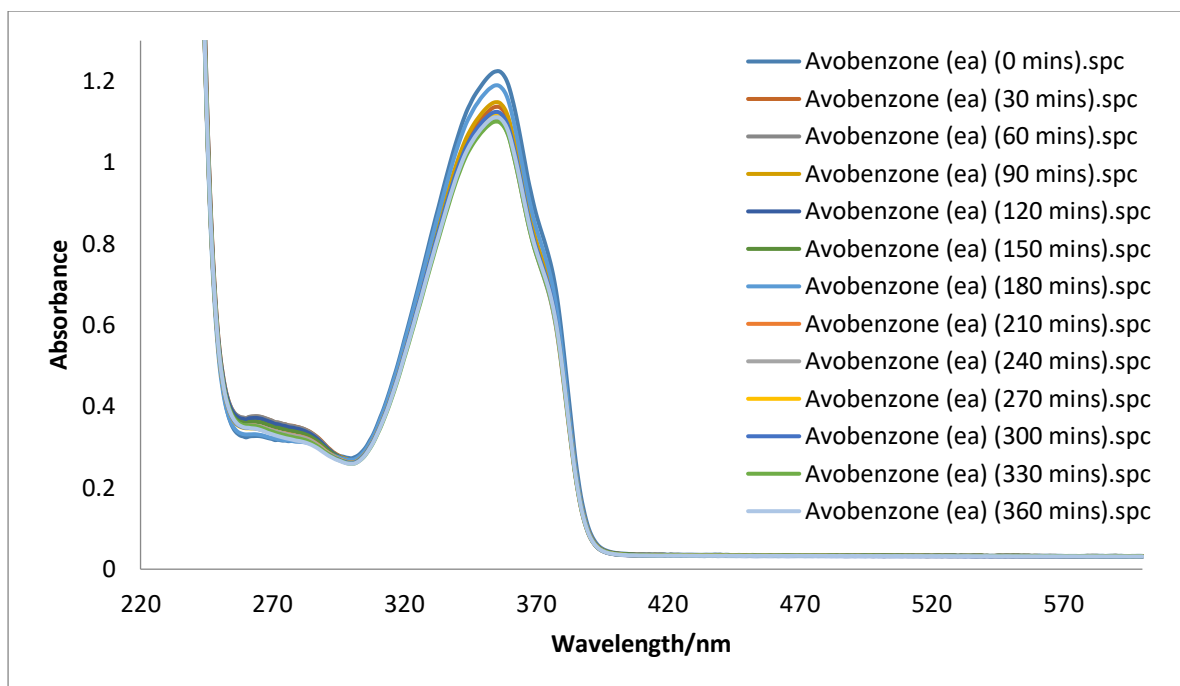


Figure 4.4: Photostability of avobenzone in ethyl acetate. The spectra were recorded every 30 minutes for a total period of six hours, and were acquired in a 1 cm pathlength quartz cuvette against air as the reference.

Figure 4.5 shows the UV spectra of avobenzone dissolved in cyclohexane obtained after 30-minute irradiation intervals. A significant amount of photodegradation is seen. This indicates that the type of solvent chosen plays an important role. The maximum absorbance of 1.16 is seen at a λ_{\max} of 351 nm and this decreased substantially after each irradiation time interval. An isosbestic point is again seen at approximately 263 nm and again indicates the presence of the phototautomerisation reaction. The correlation between the two forms of avobenzone is shown in Figure 4.6 and also confirmed the photodegradation upon irradiation. The *enol*-form of avobenzone absorbs at 351 nm, and the *keto*-form absorbs around 263 nm. Thus, the correlation can be used to confirm phototautomerisation upon irradiation.

Figures 4.2, 4.4 and 4.5 confirm that the polarity of the solvent is a major determinant in the photostability of a sunscreen absorber. Avobenzone was shown to photodegrade at a faster rate in the non-polar solvent cyclohexane than the polar solvent, methanol. The figures also revealed phototautomerisation in all three solvent categories, however, the extent of conversion was solvent dependent. Tobita *et al.*²⁷³ suggest that dibenzoylmethanes, such as avobenzone, exist predominantly in the chelated *enol* form in both polar and non-polar solvents, however, the *enol* content is higher in polar solvents due to strong intramolecular hydrogen bonds.

Hence, structural adjustments that will favour stabilization of the *enol*-form, along with polar solvents, will improve the photostability of avobenzone.

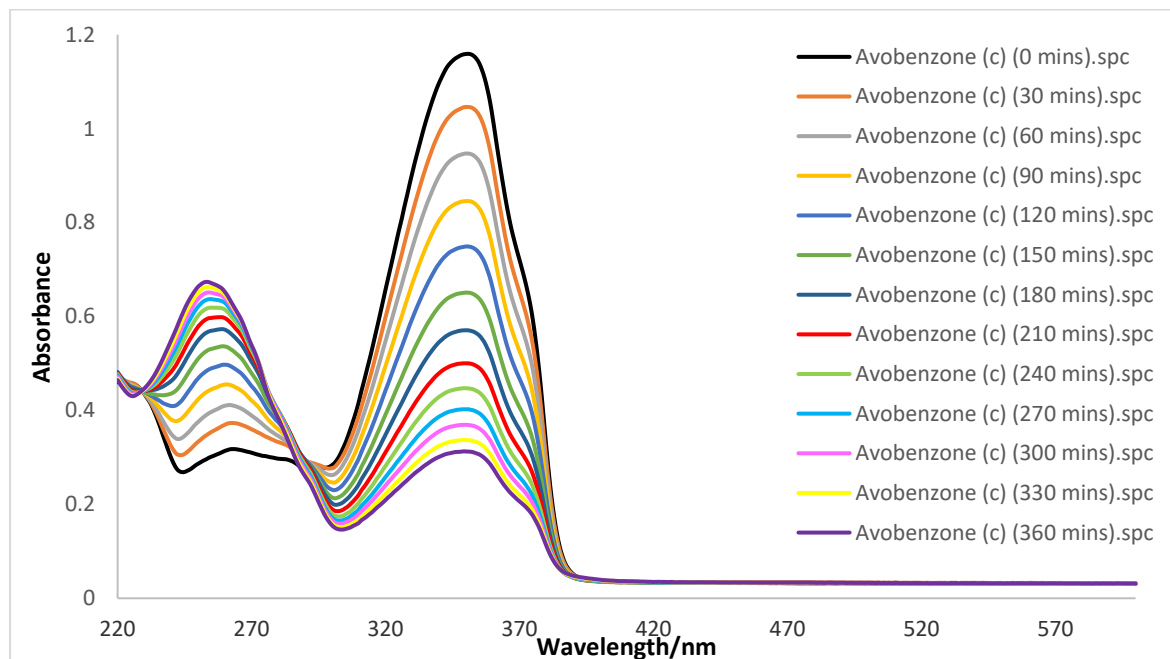


Figure 4.5: Photostability of avobenzone in cyclohexane. The spectra were recorded every 30 minutes for a total period of six hours, and were acquired in a 1 cm pathlength quartz cuvette against air as the reference.

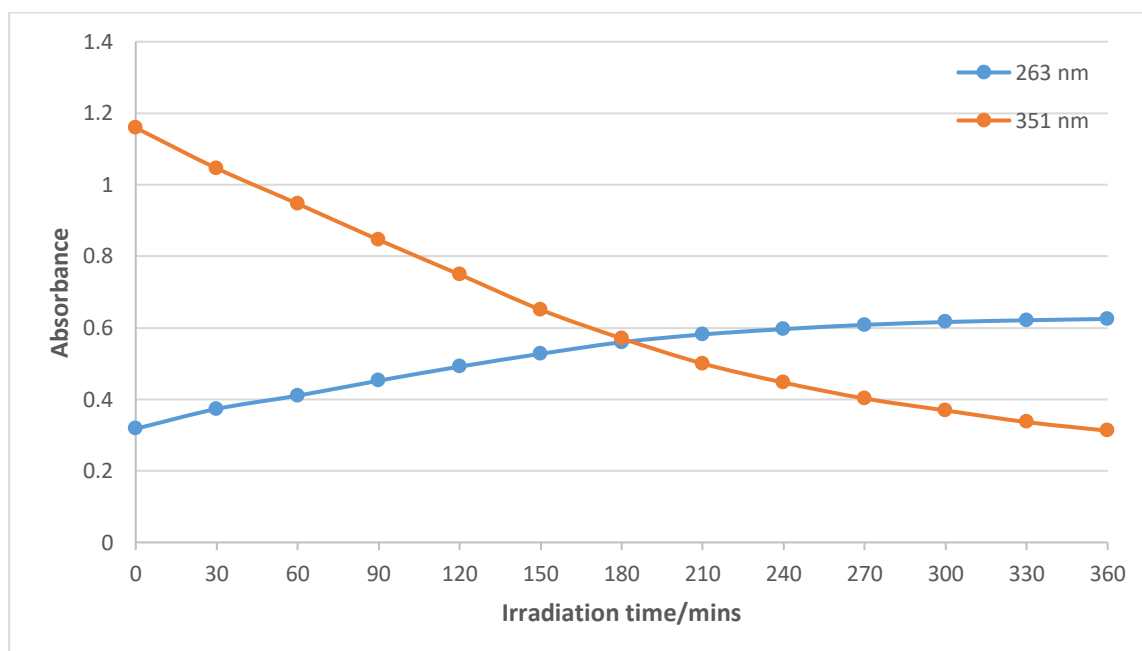


Figure 4.6: Absorbance of avobenzone dissolved in cyclohexane monitored at 351 nm and at 263 nm after 30-minute irradiation intervals indicating the loss of the *enol*-form (at 351 nm) and the formation of the *keto*-form (at 263 nm).

4.1.1.3 4-Methylbenzylidene camphor

Camphor derivatives display a maximum wavelength of absorption at 300 nm rendering them reasonably effective UVB absorbers. This group are known to undergo *cis-trans* transformation. Camphor derivatives are understood to be more stable than cinnamates, however, this was not evident in the results obtained here. The camphor derivative tested, 4-methylbenzylidene camphor (MBC), was observed to degrade more rapidly than the cinnamate, 2-ethylhexyl-*p*-methoxycinnamate, tested.

The UV spectra obtained for a 1×10^{-5} M solution of MBC that was prepared in methanol, and irradiated for six hours at 30-minute intervals, are shown in Figure 4.7.

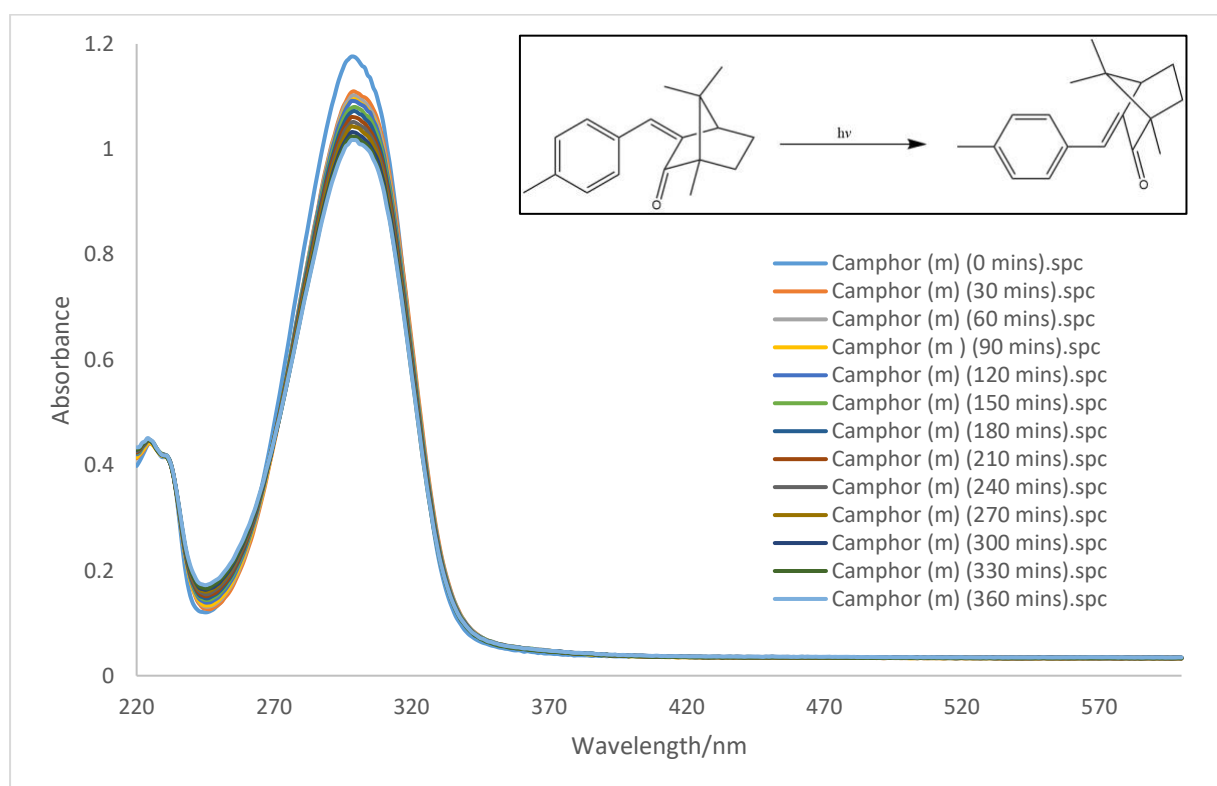


Figure 4.7: Photostability of MBC dissolved in methanol. The spectra were recorded every 30 minutes for a total period of six hours, and were acquired in a 1 cm pathlength quartz cuvette against air as the reference.

The spectra reveal a loss in absorbance of MBC with time at the maximum wavelength. The loss in absorbance was significant after the first 30 minutes, reducing from 1.18 to 1.11 at 300 nm. The total loss in absorbance after the six hour irradiation period was from 1.17 to 1.01 (0.16). The photo-instability of MBC observed is due to photoisomerisation. Photo-instability will occur until a photostationary state is reached.²⁷⁴ An isosbestic point is viewed at 265 nm

separating the loss of absorbance at λ_{\max} and the increase in absorbance at shorter wavelengths. An increase in absorbance is seen around wavelengths of 245 nm. This increase confirms photoisomerisation.

The photostability of MBC dissolved in ethyl acetate is shown in Figure 4.8. The wavelength of maximum absorption is seen at 295 nm, and again MBC photodegraded upon irradiation. The total loss of absorbance after six hours of irradiation was 0.13 (1.09 to 0.95). The spectra indicate that MBC shows less degradation than when dissolved in methanol. There is no evidence of a conversion. The solvent ethyl acetate absorbs in the wavelength range of 200 to 235 nm and a substantial increase in absorption is seen at these wavelengths. Therefore, photoisomerisation could not be determined in this region.

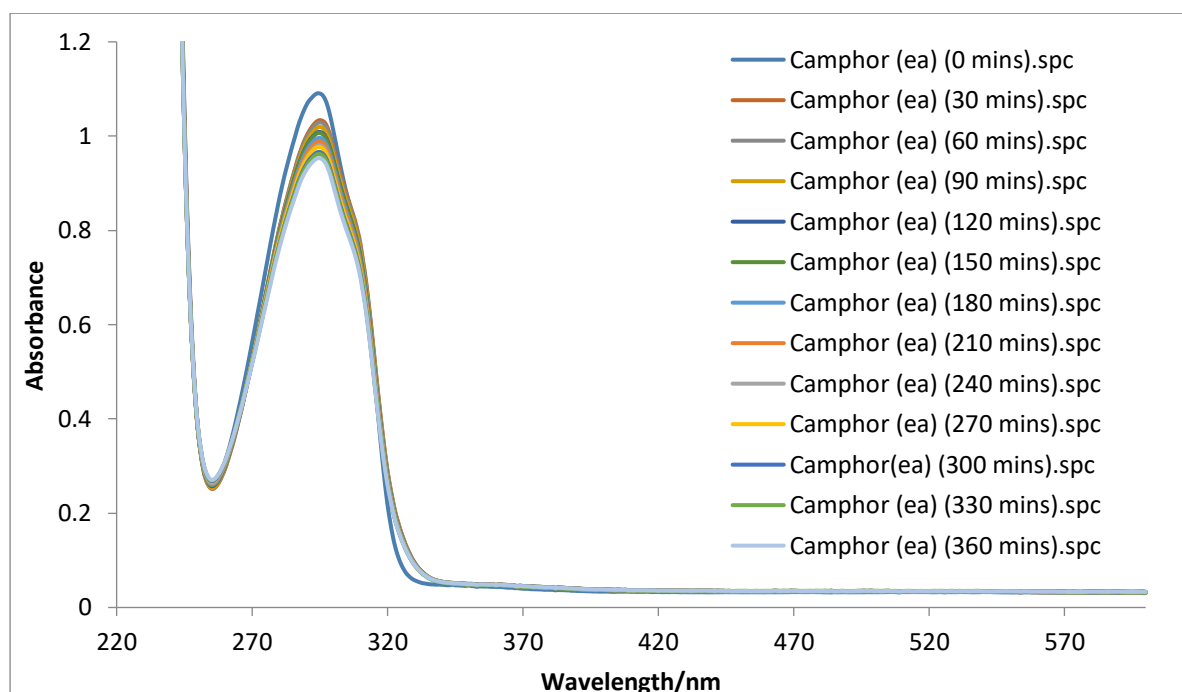


Figure 4.8: Photostability of MBC dissolved in ethyl acetate. The spectra were recorded every 30 minutes for a total period of six hours, and were acquired in a 1 cm pathlength quartz cuvette against air as the reference.

Figure 4.9 shows the UV spectra of MBC dissolved in cyclohexane obtained after 30-minute irradiation intervals. A maximum absorbance of 1.17 is seen at 293 nm with similar photodegradation observed as with the previous two solvents. The total absorption loss after six hours of irradiation was also 0.13 (1.17 to 1.04). The similarity of photodegradation seen for all three solvents indicates that the photoisomerisation of MBC is not solvent dependent.

An isosbestic point is observed at 246 nm that indicates there are two species in equilibrium. This is attributed to photoisomerisation.

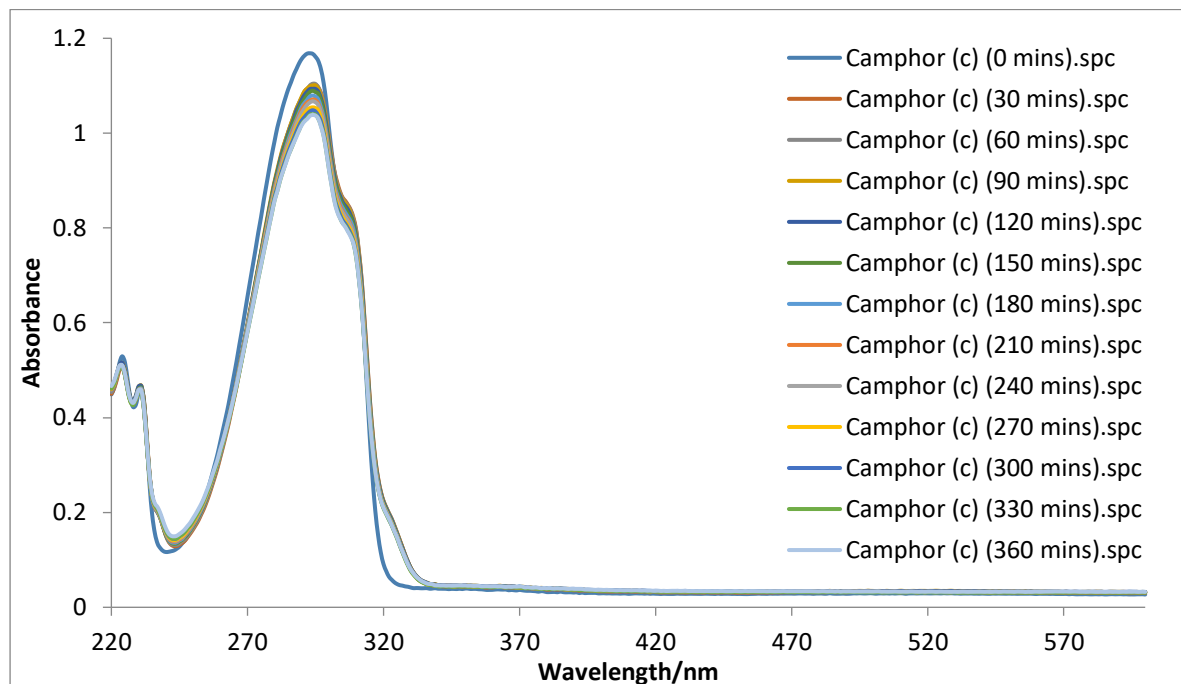


Figure 4.9: Photostability of MBC dissolved in cyclohexane. The spectra were recorded every 30 minutes for a total period of six hours, and were acquired in a 1 cm pathlength quartz cuvette against air as the reference.

4.1.1.4 2-Ethylhexyl-*p*-methoxycinnamate

The chemical, 2-ethylhexyl-*p*-methoxycinnamate (EHMC), is the most commonly used UVB absorber due to its absorption ability in the UVB region of the electromagnetic spectrum. Various studies by Tarras-Wahlberg *et al.*,¹⁰¹ Kowlaser¹¹⁰ and Broadbent¹⁰² showed that EHMC loses its absorbing capability through *trans-cis* photoisomerisation when exposed to sunlight. Pattanaargson *et al.*¹¹¹ and Lyambila⁶⁹ both confirm that the photoisomerisation reaction depends on two factors: the concentration of EHMC and the polarity of the solvent. The *cis*-isomer has a lower molar absorption coefficient, ϵ , which explains the loss in absorbance upon exposure to radiation. Broadbent¹⁰² and Lyambila⁶⁹ also showed that EHMC is able to photodimerise. This also causes a loss of absorption since some of the conjugation is lost in the photodimers.

Solutions of 1×10^{-5} M EHMC in the solvents methanol, ethyl acetate and cyclohexane were prepared separately and irradiated. The resulting UV spectra for EHMC dissolved in methanol, given in Figure 4.10, indicate a maximum absorption of 1.23 at 310 nm due to the *trans*-isomer,

with a shoulder at 300 nm due to the *cis*-isomer. After 30 minutes of irradiation, a rapid drop in absorbance at 310 nm of about 0.30 is observed. This is attributed to photoisomerisation. This loss was accompanied by an increase in absorbance between isosbestic points (points of intersection) at 240 nm and 270 nm. It is believed that the increase in absorbance at these points of intersection are due to self-dimerisation as the compound would lose conjugation and absorb at a much lower wavelength. The absorbance remained stable thereafter indicating that a photostationary state had been reached for this photoisomerisation.

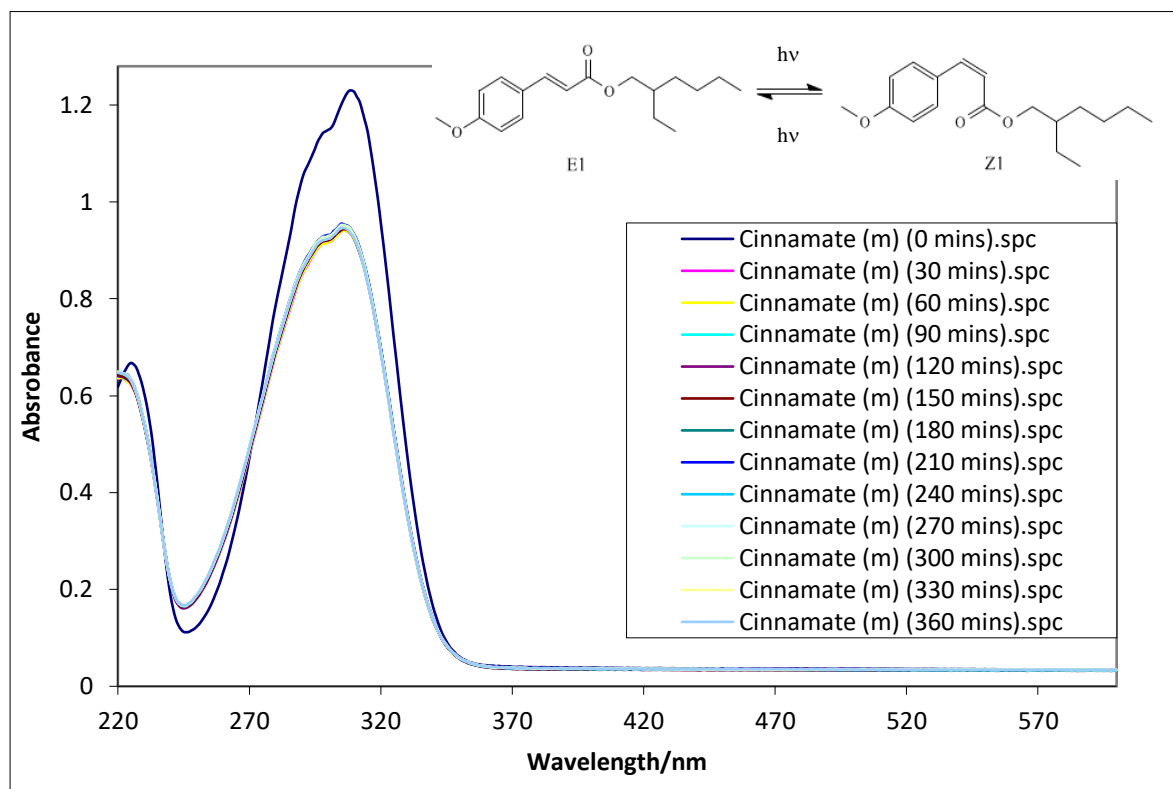


Figure 4.10: Photostability of EHMC dissolved in methanol. The spectra were recorded every 30 minutes for a total period of six hours, and were acquired in a 1 cm pathlength quartz cuvette against air as the reference.

Figure 4.11 shows the UV spectra of EHMC dissolved in ethyl acetate. An absorbance of 1.18 is seen at 308 nm with a similar shoulder at around 300 nm. A rapid drop in absorbance of 0.23 is also seen after 30 minutes of irradiation. This again confirms photoisomerisation. The loss in absorbance was complemented by an increase in absorbance at only one isosbestic point for 270 nm. The absorbance remained stable thereafter indicating that a photostationary state had been reached.

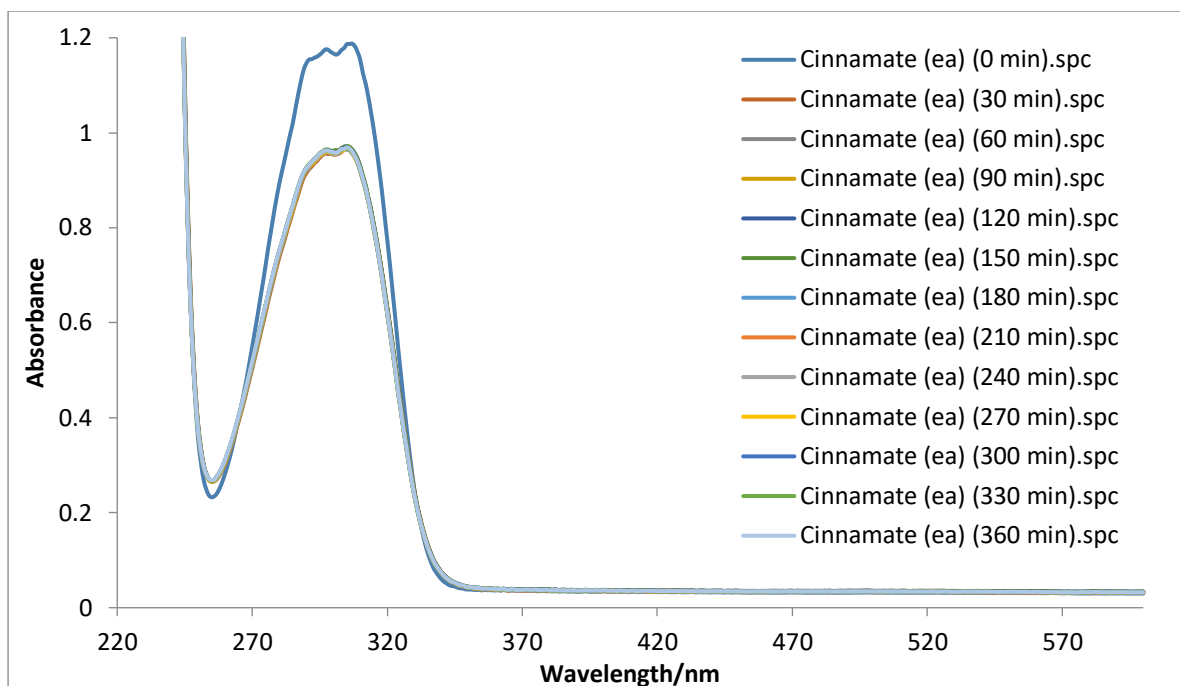


Figure 4.11: Photostability of EHMC dissolved in ethyl acetate. The spectra were recorded every 30 minutes for a total period of six hours, and were acquired in a 1 cm pathlength quartz cuvette against air as the reference.

The spectra obtained for EHMC dissolved in cyclohexane in Figure 4.12 gave a slightly different absorption profile whereby a right shoulder was shown at 300 nm with an absorbance of 1.26 now seen at 290 nm. After 30 minutes of irradiation, a rapid drop of 0.19 is observed, as in the case of the previous two solvents, and thereafter reaching a photostationary state. Broadbent¹⁰² and Lyambila⁶⁹ also showed that EHMC is able to photodimerise and concluded that when cyclohexane was used as a solvent, it allowed for more self-dimerisation to take place even before irradiation. The loss of absorption observed is due to conjugation being lost in the photodimers. This confirms that the photodegradation reaction depends on concentration and the polarity of the solvent. Therefore, non-polar solvents such as cyclohexane negatively affect photostability.

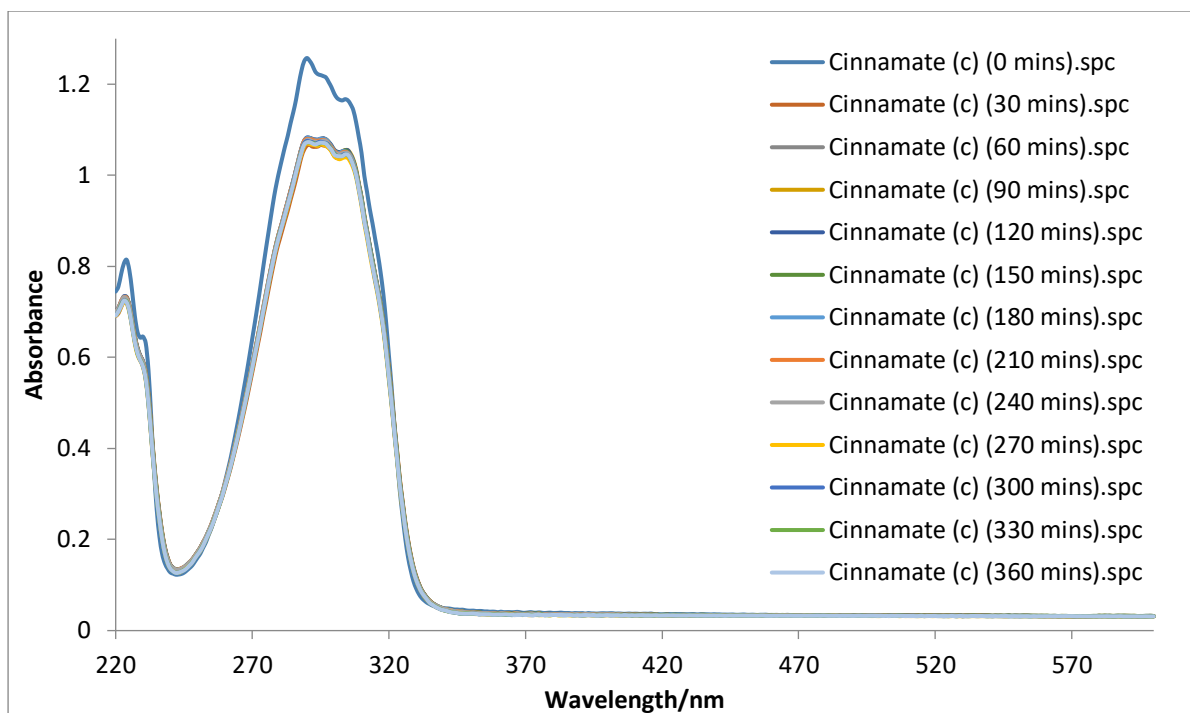


Figure 4.12: Photostability of EHMC dissolved in cyclohexane. The spectra were recorded every 30 minutes for a total period of six hours, and were acquired in a 1 cm pathlength quartz cuvette against air as the reference.

Both the camphor and cinnamate derivatives are known to undergo *cis-trans* transformation. Camphors are said to be more stable than cinnamates. However, this was not evident in the results obtained. We see that the MBC degraded more rapidly than EHMC. EHMC shows a drop in absorbance after 30 minutes, but remained stable thereafter. In both, benzylidene camphor derivatives and cinnamates, a photostationary state is reached shortly after exposure to UV radiation due to photoisomerisation.¹⁰¹ Again, the solvent also played a role.

4.1.2 Cancer Bush plant extracts

Plant extracts are extensively reported for their antioxidant activity. The potential photostabilising ability of plant extracts in cosmetics has not been widely reviewed. However, there is evidence to support the UV filtering ability of some of these natural phytochemicals. Rancan *et al.*²⁷⁵ conducted studies on lichen species and found that usnic acid, a dibenzofuran derivative, contained the best UVB filtering effect. The group found that the derivative provided an *in vivo* protection factor similar to Nivea Sun Spray LFS 5 and that the majority of the isolated compounds have good photo-absorption properties when compared to EHMC.²⁷⁵ Nevertheless, extreme caution must be applied with the use of plant extracts as photostabilisers as they could photodegrade.

Sutherlandia frutescens, subspecies *microphylla* (Cancer Bush) is a well-known multi-purpose medicinal plant used in Southern Africa.²⁵¹ The plant is widely used to treat a number of conditions, including inflammation and cancer.²⁷⁶ The Cancer Bush plant is rich in amino acids, pinitol and minuscule amounts of gamma aminobutyric acid.²⁷⁷ Southon²⁷⁸ conducted chemical studies to identify that the plant contained canavanine, a non-protein α -amino acid with anti-tumour properties. Fernandes *et al.*²⁵¹ showed that the Cancer Bush plant when extracted with hot water possesses significant reactive oxygen species scavenging properties in cell-free and in stimulated neutrophil systems.

The Cancer Bush plant contains polyphenolic compounds that display radical scavenging properties. The leaves of the plant were extracted according to the methods described in Sections 3.2.1 and 3.2.2. UV spectra of both the Cancer Bush extracts were obtained by diluting each extract in solvents of different polarity. Absorbance readings were obtained within the boundaries of Beer's law. The individual plant extracts were then mixed with each of the UV filters and tested for their photostabilising abilities. The solubility of the UV filters mixed in the respective extracts are shown in Table 4.3.

Table 4.3: Solubility of UV filters mixed with Cancer Bush extracts in solvents of different polarity

	Boiling water extract			Ethanol-water extract		
	M	EA	C	M	EA	C
Cancer Bush plant	S	NA	NA	S	NA	NA
Benzophenone-9	S	NS	NS	S	NS	NS
Avobenzone	S	NS	NS	S	S	S
4-methylbenzylidene camphor	NS	NS	NS	S	S	S
2-ethylhexyl-<i>p</i>-methoxycinnamate	NS	NS	NS	S	S	S

S – Soluble, NS – Not soluble, NA – Not applicable, M – methanol, EA – ethyl acetate, C – cyclohexane

The boiling water and ethanol-water extraction methods are believed to contain the most diverse yields of potential polyphenolic substances according to studies conducted by Mturi.¹⁷ A photostability assessment of these plant extracts was conducted in order to predict the mechanism involved in their photoprotective ability. Both the boiling water extract and ethanol-water extract were only soluble in methanol. Photostability tests of the ethanol-water extract mixed with UV filters were conducted in ethyl acetate and cyclohexane when the extract was soluble.

4.1.2.1 Boiling water extract

The UV spectra obtained for the boiling water extraction method are shown in Figure 4.13. The spectra show that the extract absorbs strongly in the UVB region and adequately in the UVA range. The spectrum exhibits a maximum at 265 nm giving an absorbance of 0.83. A decrease in absorption was seen after 30 minutes of irradiation. The maximum absorption decreased to 0.78 and after the six-hour irradiation period it decreased further to 0.74.

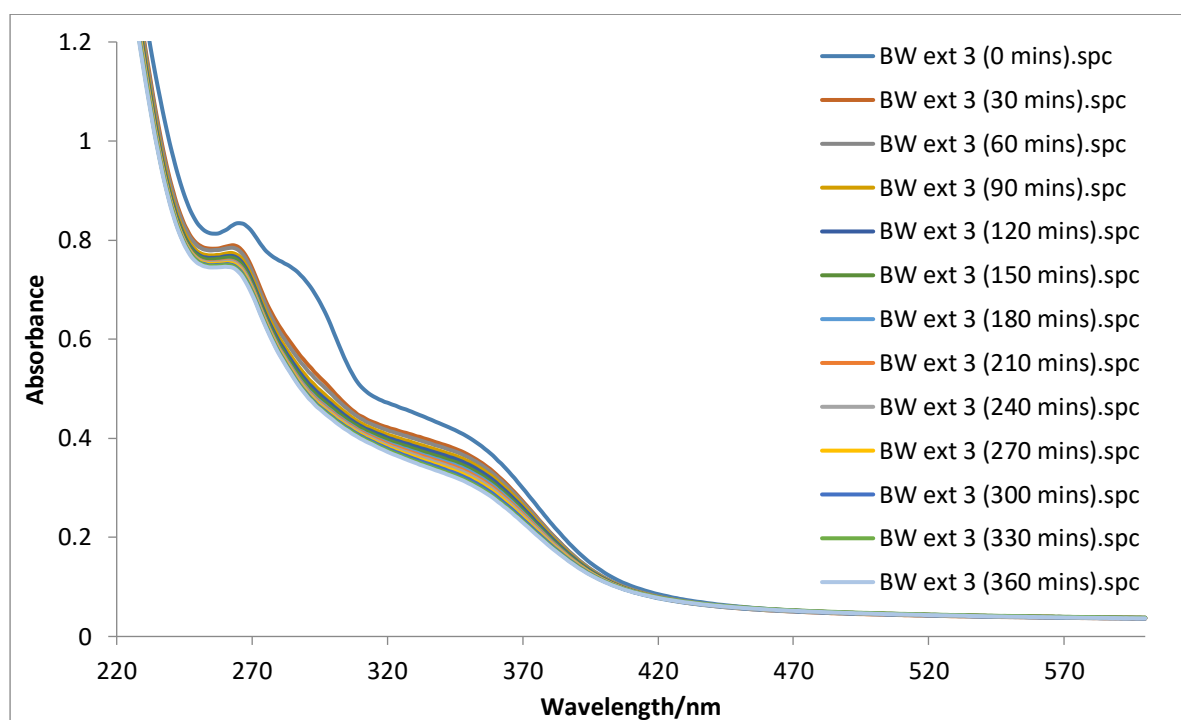


Figure 4.13: Photostability of the boiling water Cancer Bush extract dissolved in methanol. The spectra were recorded every 30 minutes for a total period of six hours, and were acquired in a 1 cm pathlength quartz cuvette against air as the reference.

4.1.2.2 Ethanol-water extract

The ethanol-water extract dissolved in methanol, shown in Figure 4.14, exhibited absorption in both the UVB and UVA regions. Arbitrary wavelengths were chosen at 295 nm for the UVB region and 350 nm in the UVA range in order to understand the data. An initial absorbance of 0.54 was seen at 295 nm and 0.40 at 350 nm. After the first 30 minutes of irradiation, the absorption decreased rapidly to 0.48 and 0.27, respectively. The absorbance continued to decrease after each irradiation period.

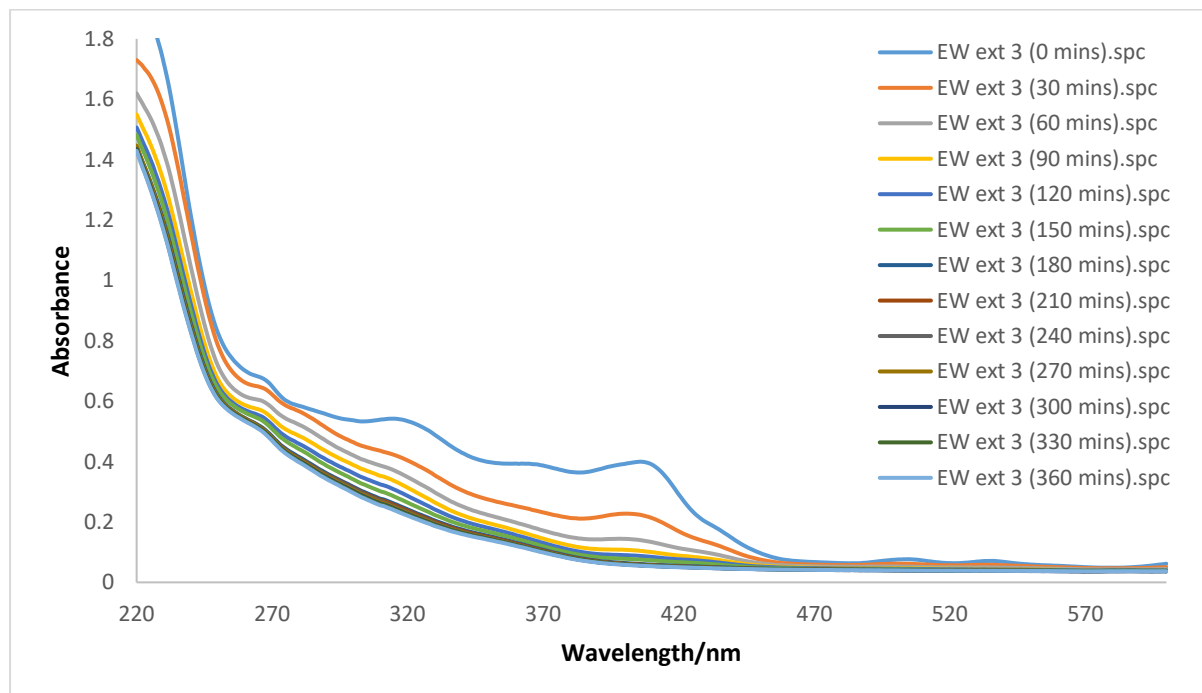


Figure 4.14: Photostability of the Cancer Bush ethanol-water extract dissolved in methanol. The spectra were recorded every 30 minutes for a total period of six hours, and were acquired in a 1 cm pathlength quartz cuvette against air as the reference.

Both extraction methods showed some absorption up to 400 nm and their photostability was tested in combination with the UV chemical absorbers.

4.1.3 Mixtures of UV chemical absorbers and Cancer Bush extracts

In order to optimise broad spectrum protection against the sun, it is common practice to combine two or more UV filters. However, certain combinations of UV filters result in a negative impact for sun protection. For example, the combination of avobenzone and EHMC results in photodegradation due to their unfavourable synergistic interactions.¹³⁴ Therefore, the addition of polyphenols, found in the Cancer Bush plant, to commonly used UV chemical

absorbers was investigated to determine if photostability could be achieved without other UV filter interactions.

The Cancer Bush extract was mixed with each individual chemical absorber in an attempt to photostabilise them. The chemical absorbers: benzophenone-9, avobenzone, MBC and EHMC, were investigated and discussed. The extracts prepared for these UV absorption studies were described in Section 3.6.3.

4.1.3.1 Benzophenone-9 and Cancer Bush extract

Figure 4.15 shows the UV spectra of benzophenone-9 mixed with the boiling water extract and dissolved in methanol. The spectrum shows that the UV filter with the Cancer Bush boiling water extract is not susceptible to photodegradation over the six-hour irradiation period and was able to achieve high absorbance values. The addition of the boiling water extract caused a shift at the two maxima from 281 and 332 nm to 282 and 333 nm, respectively. An exception is observed at the first maximum at 282 nm which is different from benzophenone-9 dissolved in methanol alone. At this point, a slight decrease in absorption after 30 minutes of irradiation, from 1.67 to 1.61, was observed.

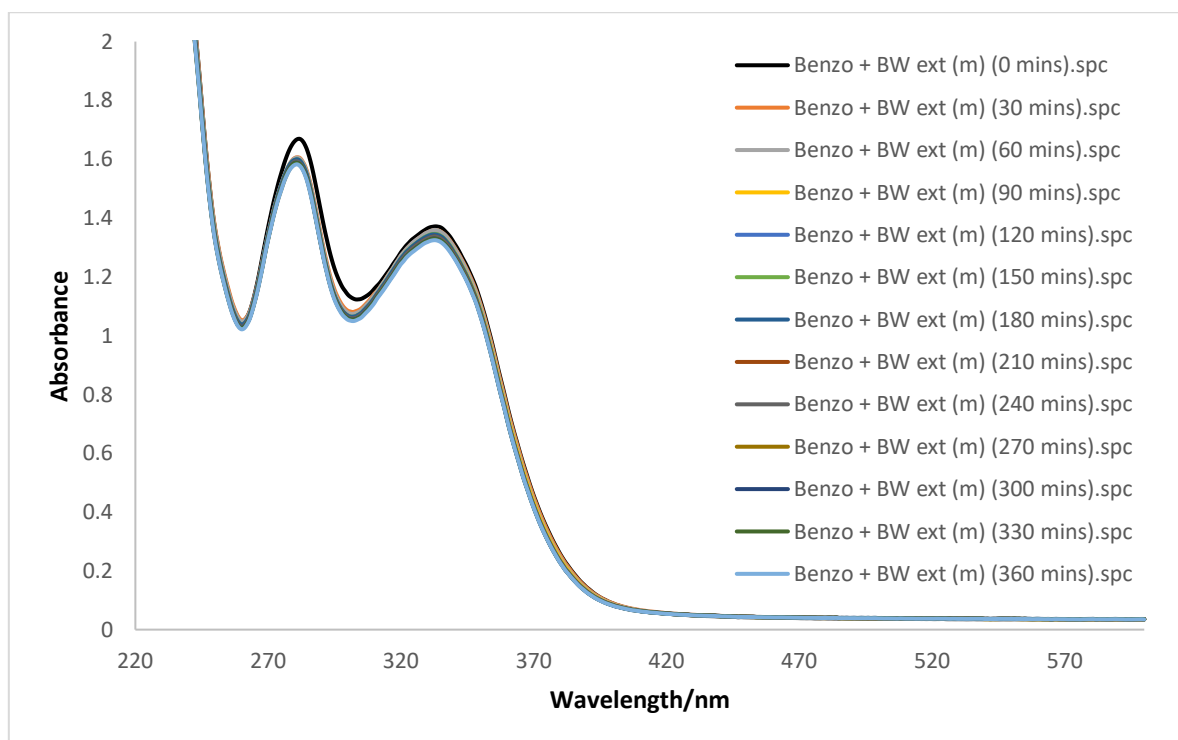


Figure 4.15: Photostability of benzophenone-9 mixed with the boiling water Cancer Bush extract and dissolved in methanol. The spectra were recorded every 30 minutes for a total

period of six hours, and were acquired in a 1 cm pathlength quartz cuvette against air as the reference.

Figure 4.16 shows the UV spectra of benzophenone-9 mixed with the ethanol-water extract dissolved in methanol. The spectrum shows that the UV filter mixed with the Cancer Bush ethanol-water extract was able to achieve a higher absorbance than for benzophenone-9 dissolved in methanol alone. It was not susceptible to photodegradation over the six-hour irradiation period, and it did not photodegrade after the first 30 minutes at the first maximum. The absorbance was shown to be photostable in the UVA range of 315 - 363 nm. After the six-hour irradiation period, an increase in absorbance was seen between wavelengths of 220 - 355 nm. This phenomenon indicates that the ethanol-water extract performs better than the boiling water extract and provides the UV filter with a positive effect.

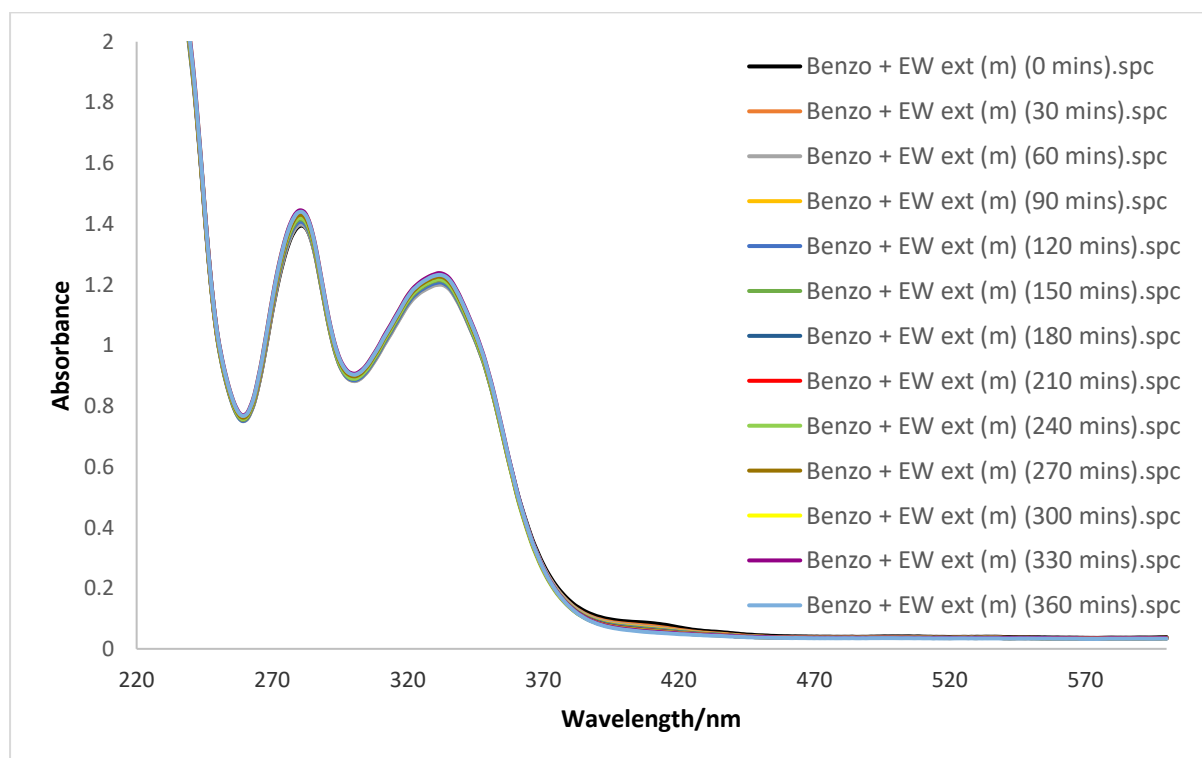


Figure 4.16: Photostability of benzophenone-9 mixed with the Cancer Bush ethanol-water extract and dissolved in methanol. The spectra were recorded every 30 minutes for a total period of six hours, and were acquired in a 1 cm pathlength quartz cuvette against air as the reference.

The benchmark, benzophenone-9, remained photostable when mixed with both of the Cancer Bush extracts. This can be used to indicate that the use of both Cancer Bush extracts will not

negatively impact the photostability of the remaining UV filters and could possibly only be beneficial.

4.1.3.2 Avobenzone and Cancer Bush extract

Avobenzone provides photoprotection in the long wavelength UVA range but undergoes phototautomerisation and photodegradation. The photostability of avobenzone dissolved in the three solvents: methanol, ethyl acetate, and cyclohexane, respectively in Section 4.1.1.2, was shown to be dependent on the polarity of the solvent. Schwack and Rudolph¹²⁹ illustrated that avobenzone tends to participate in phototautomerisation in a polar protic environment, whereby a carbonyl hydrogen abstraction reaction with the solvent or other hydrogen donors occurs. The *enol*-form has a maximum absorption at 358 nm in a polar environment. The *keto*-form has a maximum absorption at 260 nm in a polar aprotic environment. The conversion to the *keto*-form weakens the UV filter photoprotection. However, Schwack and Rudolph¹²⁹ also demonstrated that avobenzone undergoes reactive radical formation of benzoyl and phenacyl radicals in a non-polar environment resulting in its photodegradation. The photoproducts that are formed in this reaction are less absorbing in the UVA and UVB range. Mturi and Martincigh¹³³ were also able to show that the photostability of avobenzone was dependent on the polarity and proticity of the solvent.

The photostability of avobenzone mixed with the boiling water Cancer Bush extract and dissolved in methanol is shown in Figure 4.17. The maximum absorbance of 1.35 is seen at a λ_{max} of 358 nm and this decreases substantially after each irradiation time interval. As with avobenzone dissolved in methanol alone, the spectra also show that a correlation exists between the loss of absorption at the λ_{max} of avobenzone in methanol, 358 nm, and the increase in absorbance at 245 nm. This correlation is shown in Figure 4.18 and confirms phototautomerisation upon irradiation. The boiling water Cancer Bush extract was unsuccessful in photostabilising avobenzone and negatively impacted the polar protic environment.

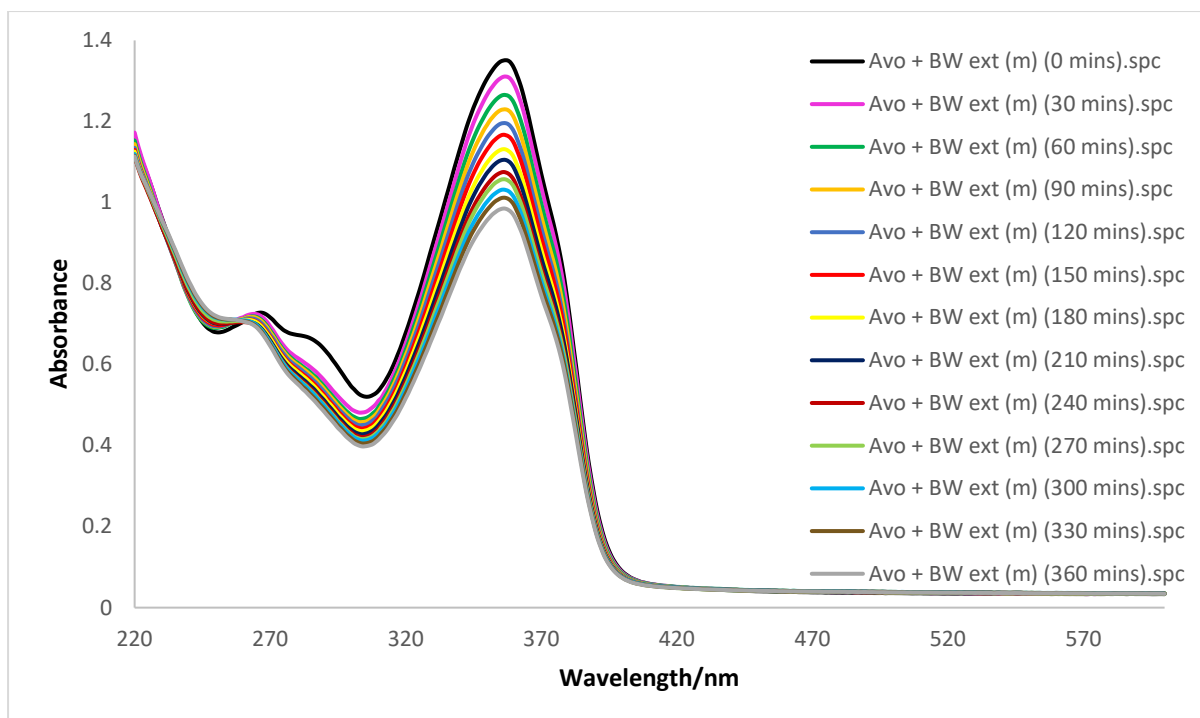


Figure 4.17: Photostability of avobenzone mixed with the boiling water Cancer Bush extract dissolved in methanol. The spectra were recorded every 30 minutes for a total period of six hours, and were acquired in a 1 cm pathlength quartz cuvette against air as the reference.

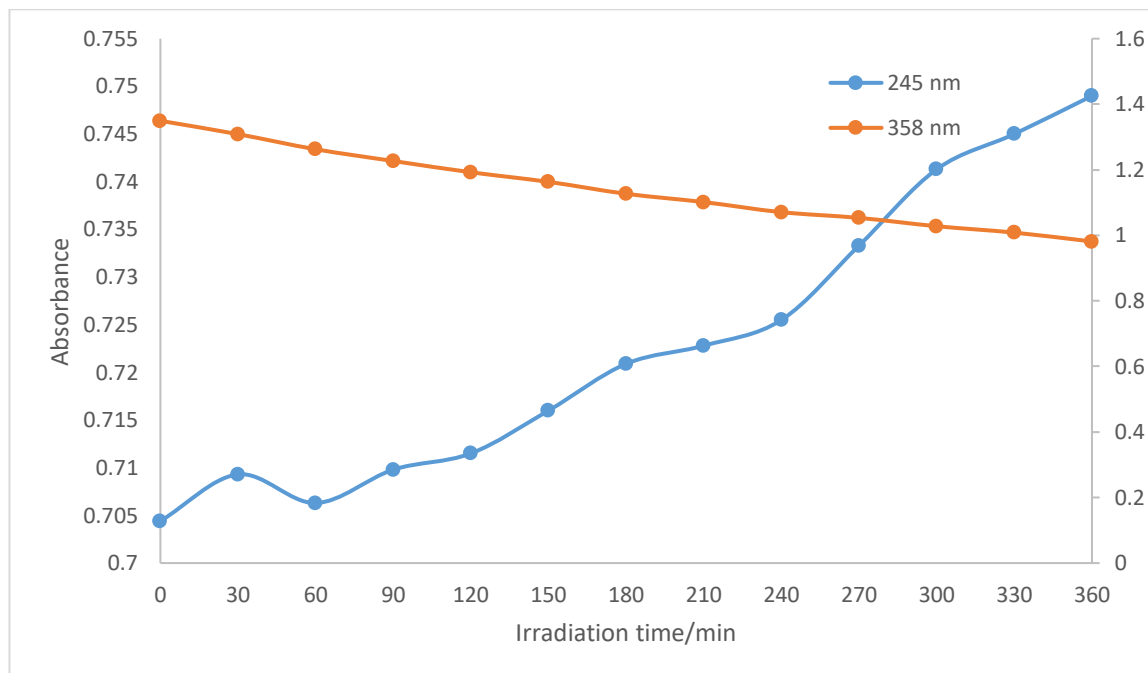


Figure 4.18: Absorbance of avobenzone mixed with the boiling water Cancer Bush extract dissolved in methanol at 245 nm and 356 nm after 30-minute irradiation intervals indicating the loss of the *enol*-form and the formation of the *keto*-form.

Avobenzone was immiscible in the boiling water extract dissolved in ethyl acetate and cyclohexane solvents and, hence, the photostability test could not be conducted.

Figure 4.19 shows the photostability of avobenzone mixed with the Cancer Bush ethanol-water extract and dissolved in methanol. A maximum absorbance of 1.29 is seen at a λ_{\max} of 358 nm before irradiation and this increased to 1.35 after 30 minutes of irradiation. The absorbance remained higher than the initial 1.29 before irradiation until 90 minutes of irradiation and decreased to 1.16 after the total six-hour irradiation period. Although an increase in absorbance is seen at the *keto*-range of 260 nm, there is no evidence of a correlation taking place. The increase in absorbance at 245 nm starts with 0.64 before irradiation and decreases to 0.62 after six hours of irradiation. This phenomenon is confirmed in Figure 4.20 and suggests that the Cancer Bush ethanol-water extract was successful in photostabilising avobenzone by preventing phototautomerisation upon irradiation.

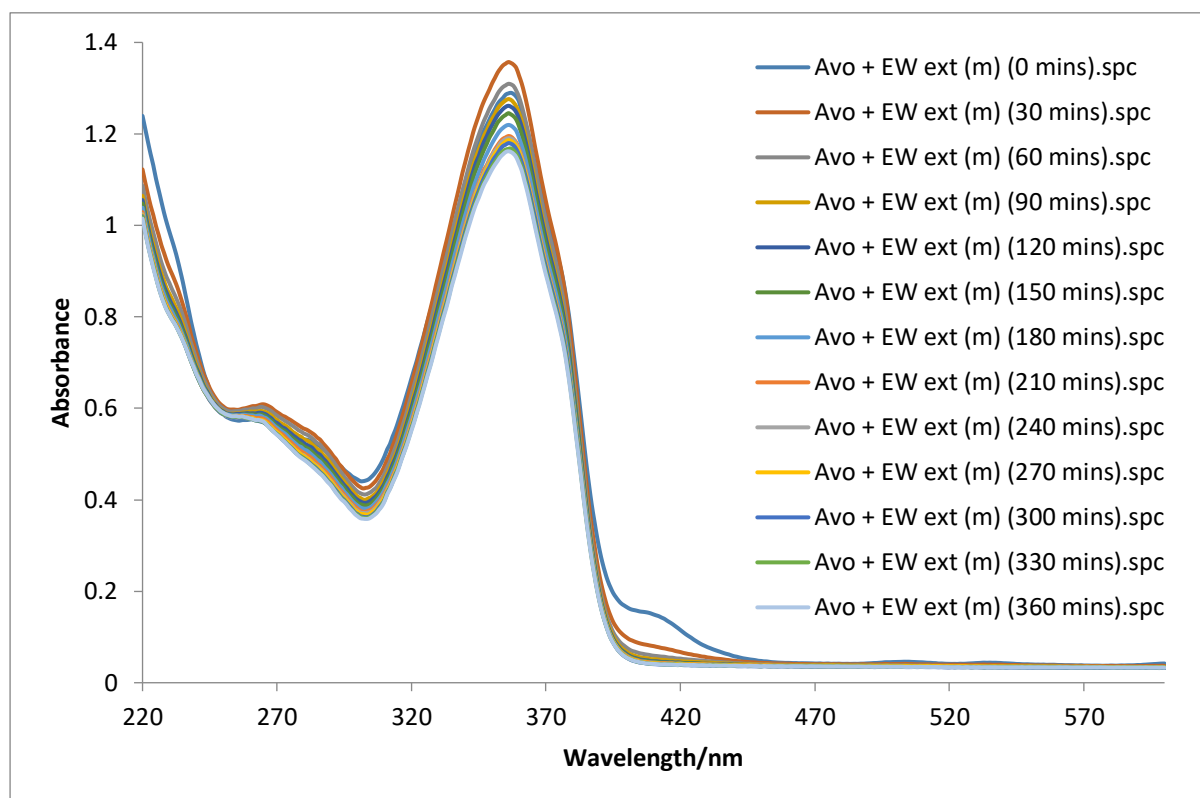


Figure 4.19: Photostability of avobenzone mixed with the Cancer Bush ethanol-water extract dissolved in methanol. The spectra were recorded every 30 minutes for a total period of six hours, and were acquired in a 1 cm pathlength quartz cuvette against air as the reference.

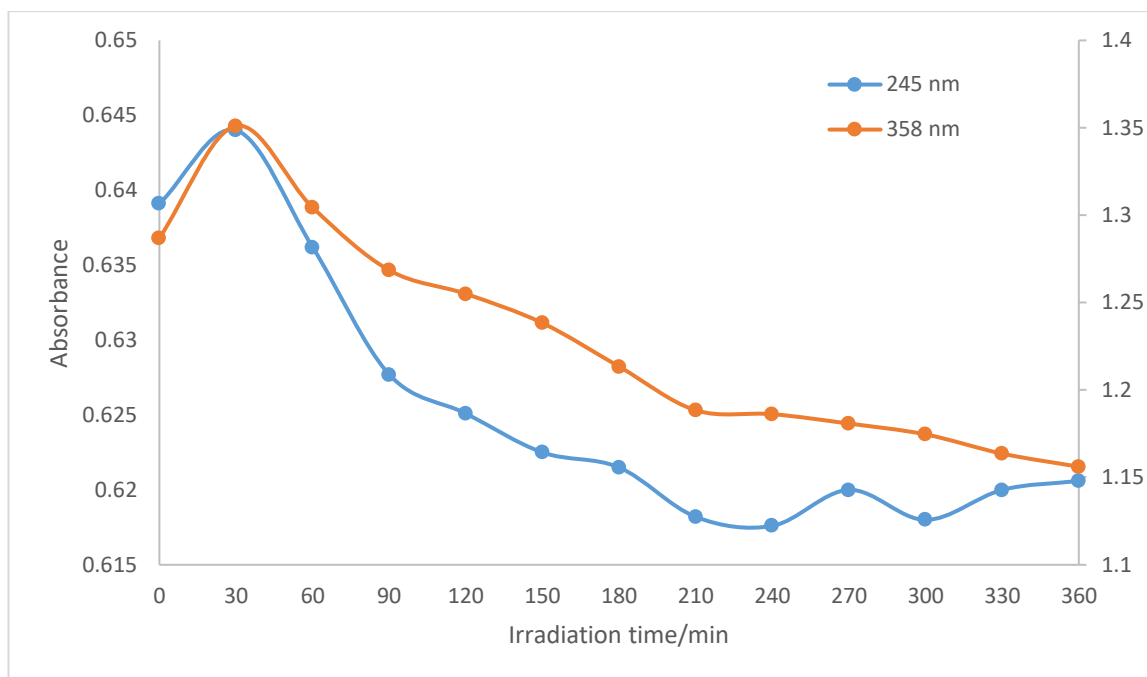


Figure 4.20: Absorbance of avobenzene mixed with the Cancer Bush ethanol-water extract dissolved in methanol at 245 and 356 nm after 30 minute irradiation intervals confirming that phototautomerization was prevented.

Avobenzene was mixed with the Cancer Bush ethanol-water extract and dissolved in ethyl acetate and the UV spectra obtained after six hours of irradiation are shown in Figure 4.21. A maximum absorbance of 1.58 is seen at a λ_{\max} of 356 nm, a higher absorbance than for avobenzene dissolved in ethyl acetate alone, and this decreases significantly to 1.24 after 30 minutes of irradiation. A decrease in absorbance is observed until 270 minutes is reached, and absorbance is maintained thereafter. An increase in absorbance after each irradiation interval is seen in the *keto*-form region of 270 nm and this phenomenon confirms that phototautomerisation took place.

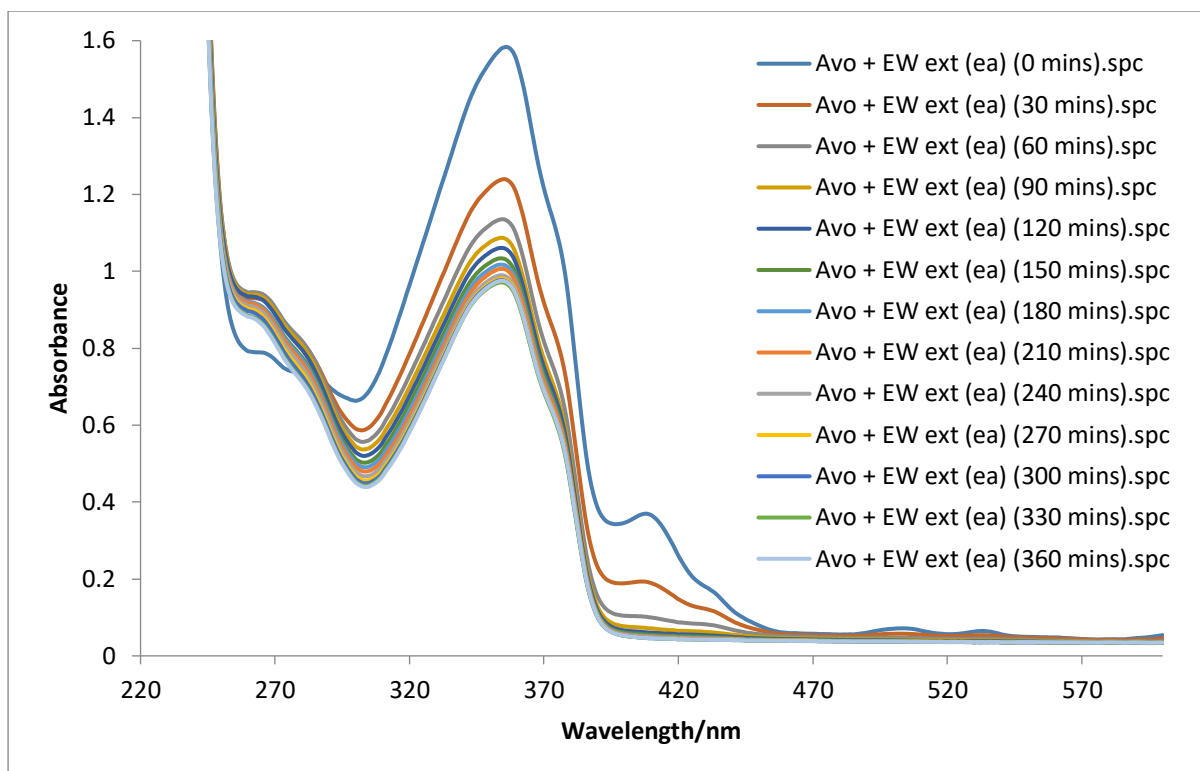


Figure 4.21: Photostability of avobenzone mixed with the Cancer Bush ethanol-water extract dissolved in ethyl acetate. The spectra were recorded every 30 minutes for a total period of six hours, and were acquired in a 1 cm pathlength quartz cuvette against air as the reference.

The UV spectra obtained for avobenzone mixed with the Cancer Bush ethanol-water extract dissolved in cyclohexane, shown in Figure 4.22, are almost identical to the UV spectra obtained for avobenzone dissolved in cyclohexane alone with the exception of the higher absorbance values obtained. A substantial amount of photodegradation is observed due to the non-polar solvent used.

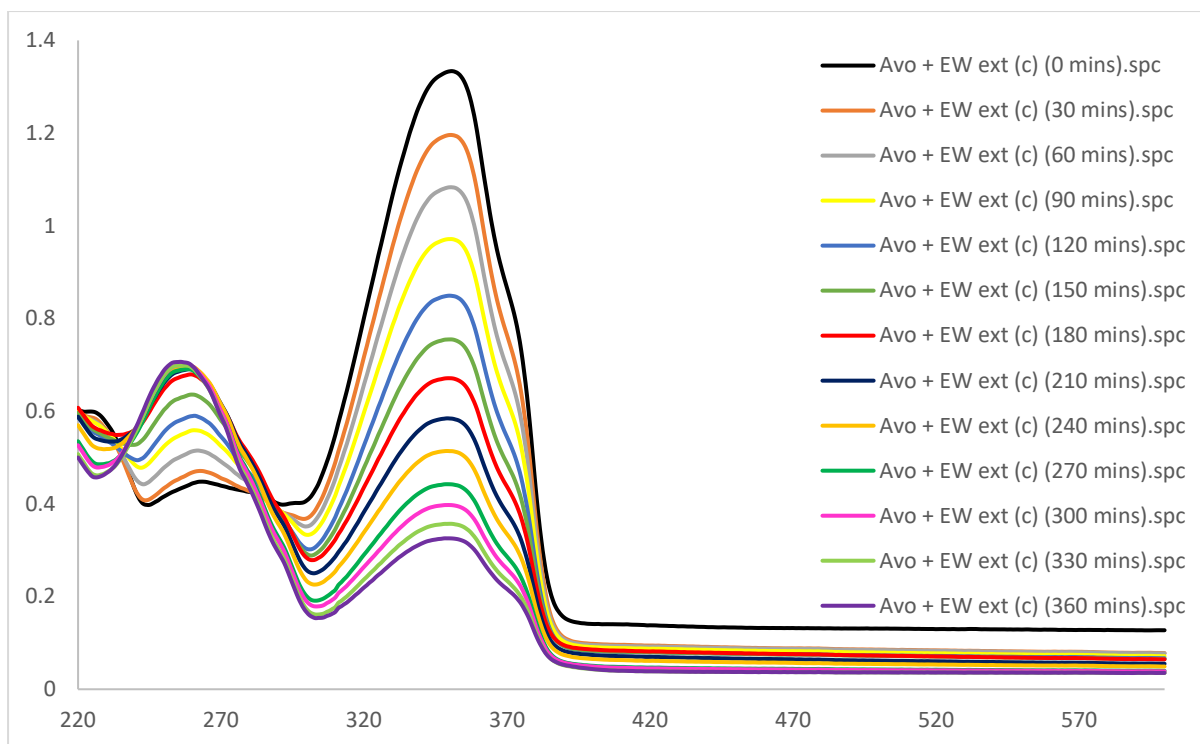


Figure 4.22: Photostability of avobenzone mixed with the Cancer Bush ethanol-water extract dissolved in cyclohexane. The spectra were recorded every 30 minutes for a total period of six hours, and were acquired in a 1 cm pathlength quartz cuvette against air as the reference.

A maximum absorbance of 1.33 is seen at a λ_{\max} of 351 nm and this decreased significantly to 0.33 after the six-hour irradiation time interval. An isosbestic point is seen at 263 nm after 180 minutes and confirms the phototautomerisation reaction. The phototautomerisation experienced by irradiation and the correlation between the two forms of avobenzone is also shown in Figure 4.23.

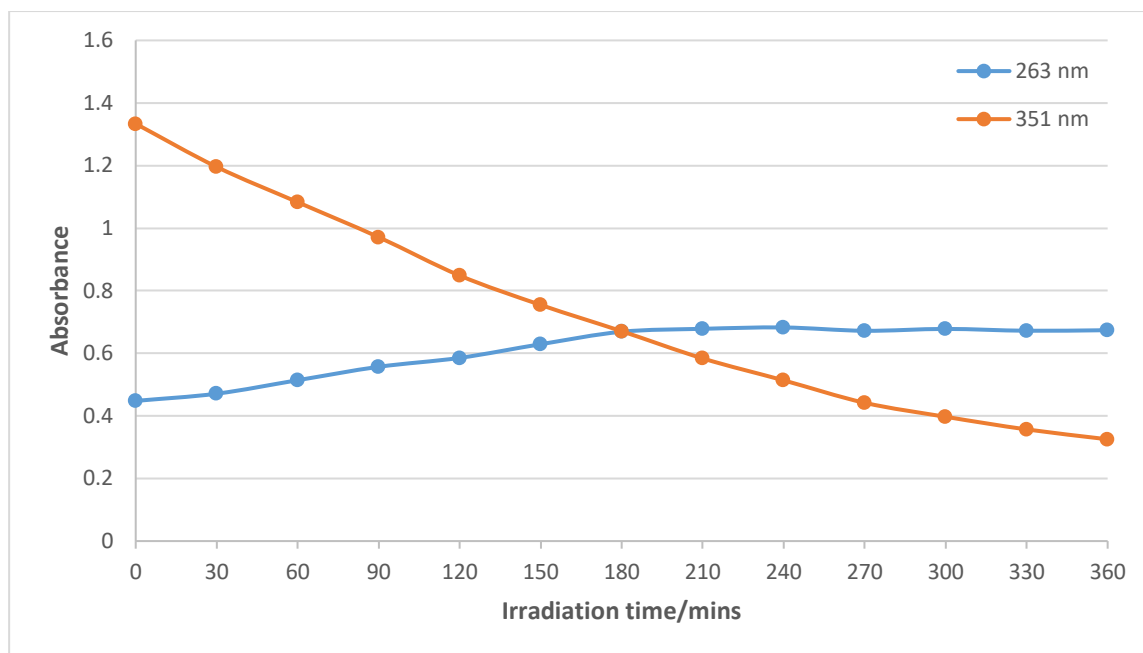


Figure 4.23: Absorbance of avobenzene mixed with the Cancer Bush ethanol-water extract and dissolved in cyclohexane monitored at 351 nm and at 261 nm after 30-minute irradiation intervals indicating the loss of the *enol*-form (at 351 nm) and the formation of the *keto*-form (at 263 nm).

The Cancer Bush ethanol-water extract was only successful in photostabilising avobenzene in methanol. The extract merely provided avobenzene with higher absorbance values but did not prevent photodegradation when dissolved in ethyl acetate or cyclohexane. Since avobenzene showed photodegradation at a faster rate in cyclohexane than for methanol, the photostability of the UV filter remained dependent on the polarity of the solvent. Overall, both types of Cancer Bush extracts were unable to influence the photostability of avobenzene and were unable to provide the structural adjustments required to favour stabilisation of the *enol*-form.

4.1.3.3 4-Methylbenzylidene camphor and Cancer Bush extract

4-Methylbenzylidene camphor was not miscible with the boiling water Cancer Bush extract and, hence, photostability was not studied with this extract.

The spectra obtained for the ethanol-water extract dissolved in methanol are shown in Figure 4.24. The absorbance values obtained were higher than those for MBC in methanol alone. The irradiated solution showed the largest decrease in absorbance after the first 30 minutes, greater than for the absorbance of MBC in methanol alone, i.e.: from 1.41 to 1.33 at the maximum absorbance of 300 nm. The total degradation of absorbance seen at λ_{\max} after the six hours of irradiation was $(1.41 - 1.16) 0.25$. There was no isosbestic point observed with this mixture.

The increase in absorbance seen at a wavelength of 245 nm confirms photoisomerisation. The absence of the isosbestic point with subsequent irradiations showing further degradation at 245 and 300 nm could be attributed to the photodegradation of the ethanol-water extract. The ethanol extract mixed with MBC in methanol allowed for higher absorbances to be obtained but the extract did not photostabilise MBC in methanol.

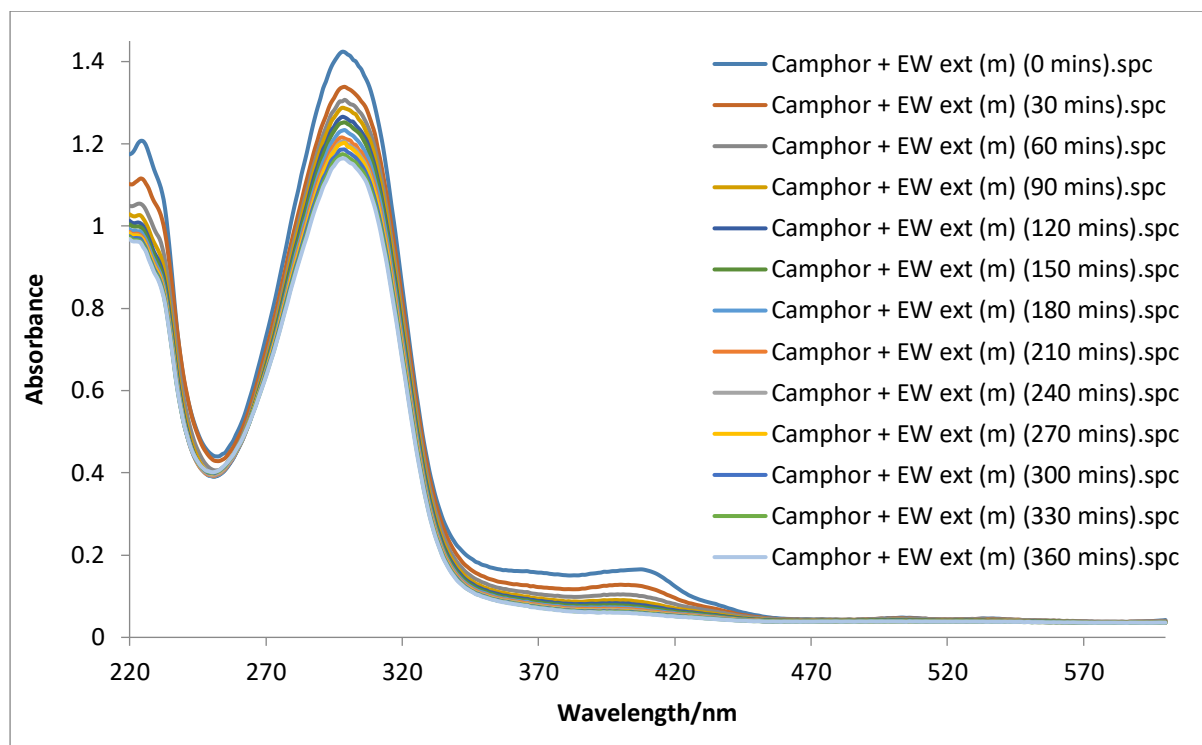


Figure 4.24: Photostability of MBC mixed with the Cancer Bush ethanol-water extract dissolved in methanol. The spectra were recorded every 30 minutes for a total period of six hours, and were acquired in a 1 cm pathlength quartz cuvette against air as the reference.

The photo-instability of MBC with the ethanol-water extract dissolved in ethyl acetate is shown in Figure 4.25. The results are similar to the spectra of MBC in ethyl acetate alone, with the exception of the absorbance seen at 410 nm which degrades after 30 minutes of irradiation. The total loss of absorbance seen at the maximum absorbance after the six hours of irradiation was $(1.27 - 1.09) 0.18$. Once again, higher absorbance values are obtained with the ethanol-water extract, a large decrease in absorbance is seen at 300 nm after the 30 minutes of irradiation (1.42 to 1.34) and photoisomerisation could not be confirmed due to the solvent absorption at wavelengths shorter than 235 nm.

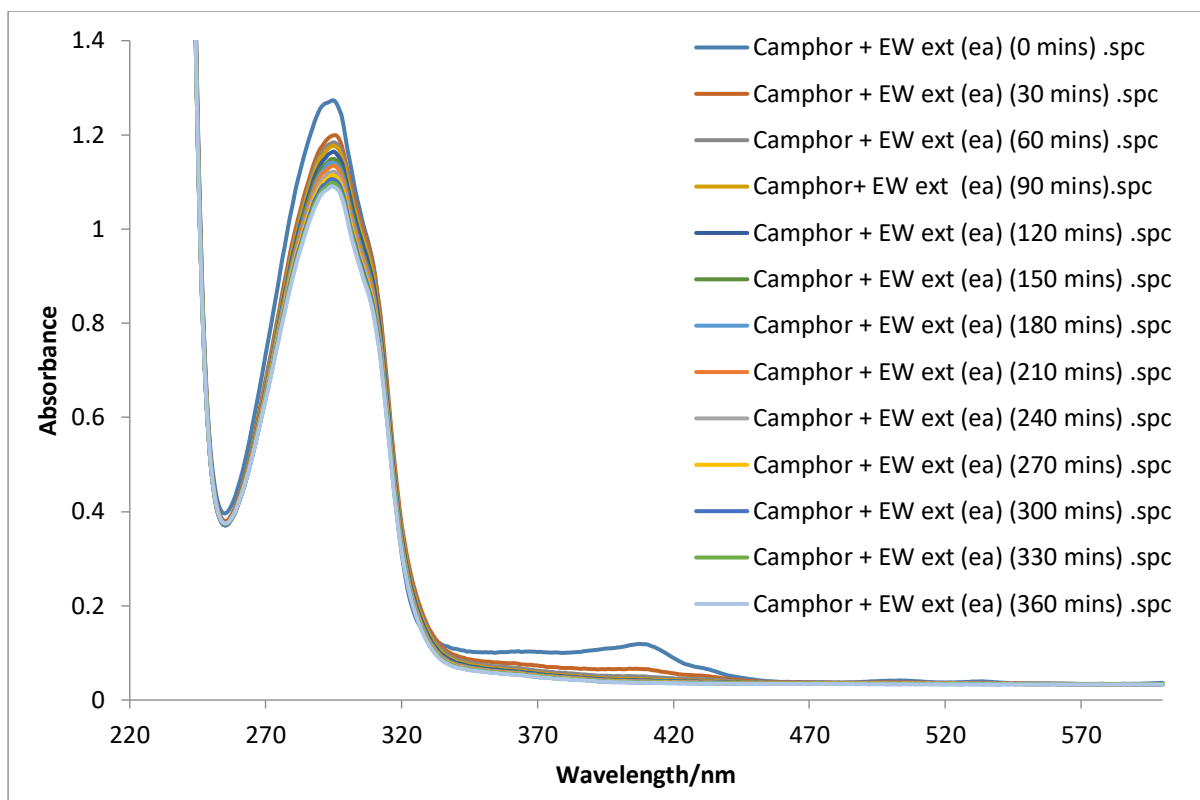


Figure 4.25: Photostability of MBC mixed with the Cancer Bush ethanol-water extract dissolved in ethyl acetate. The spectra were recorded every 30 minutes for a total period of six hours, and were acquired in a 1 cm pathlength quartz cuvette against air as the reference.

The UV spectra obtained for MBC with the ethanol-water extract in cyclohexane are shown in Figure 4.26. The spectra are identical to MBC in cyclohexane alone with the exception of a very slight increase in absorbance. A maximum absorbance of 1.23 is seen at 293 nm. The total loss of absorbance seen at λ_{max} after the six hours of irradiation was $(1.23 - 1.10)$ 0.13. The presence of an isosbestic point at 260 nm confirms that photoisomerisation took place, however, this was not evident in the previous two solvents. The confirmation of the photoisomerisation and the almost identical spectra obtained suggests that the ethanol-water extract mixed with MBC had no effect when dissolved in cyclohexane or perhaps the solvent did not dissolve the extract well.

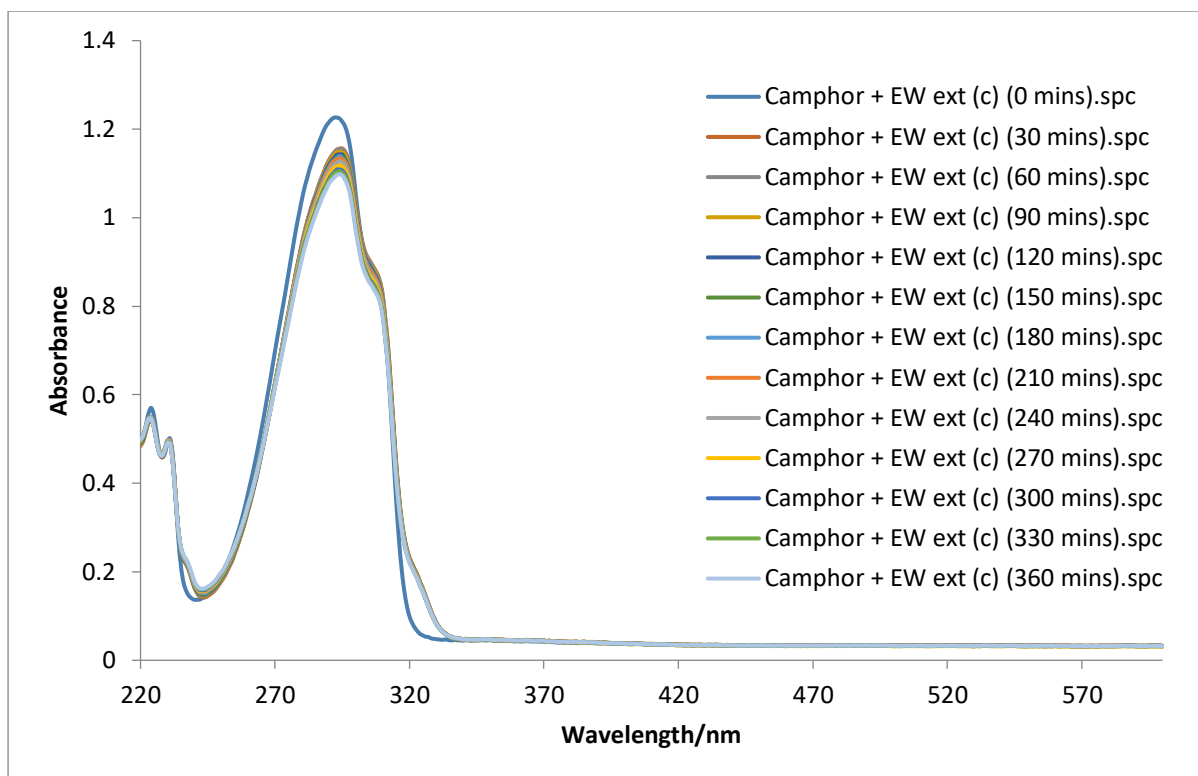


Figure 4.26: Photostability of MBC mixed with the Cancer Bush ethanol-water extract dissolved in cyclohexane. The spectra were recorded every 30 minutes for a total period of six hours, and were acquired in a 1 cm pathlength quartz cuvette against air as the reference.

Overall, the ethanol-water extract mixed with MBC in the three solvents merely provided an increase in absorbance but did not prevent photoisomerisation. This extract was unsuccessful in photostabilising MBC.

4.1.3.4 2-Ethylhexyl-*p*-methoxycinnamate and Cancer Bush extract

EHMC is the most commonly used UVB absorber as it absorbs maximally in the UVB region. The filter undergoes photoisomerisation upon irradiation and loses some of its absorbing ability through *trans-cis* isomerisation.^{101, 102} This is due to the smaller molar absorption coefficient of the *cis*-isomer and that the *cis*-isomer absorbs at shorter wavelengths. Attempts to photostabilise EHMC with the Cancer Bush extracts were conducted. The cinnamate was not miscible in the boiling water extract and, therefore, UV analysis was only conducted for the ethanol-water extract. Panday²⁷⁰ showed that EHMC is photolabile in methanol. The ethanol-water extract was mixed thoroughly with EHMC in methanol. The spectra are shown in Figure 4.27. Photostabilisation of EHMC was not achieved when irradiated for the same intervals as EHMC in methanol alone, although a higher absorbance was seen. The photodegradation pattern observed was also similar. At 310 nm a rapid decrease in absorbance was seen from

1.65 to 1.15 in the first 30 minutes of irradiation and it continued to decrease with further irradiation. However, the spectra showed that a photostationary state was not achieved, and further loss of absorbance was observed upon irradiation. EHMC did not photoisomerise in the same manner as for EHMC in methanol alone. This implies that the extract allowed for a longer absorption time before the *trans*-isomer could be converted to the *cis*-isomer.

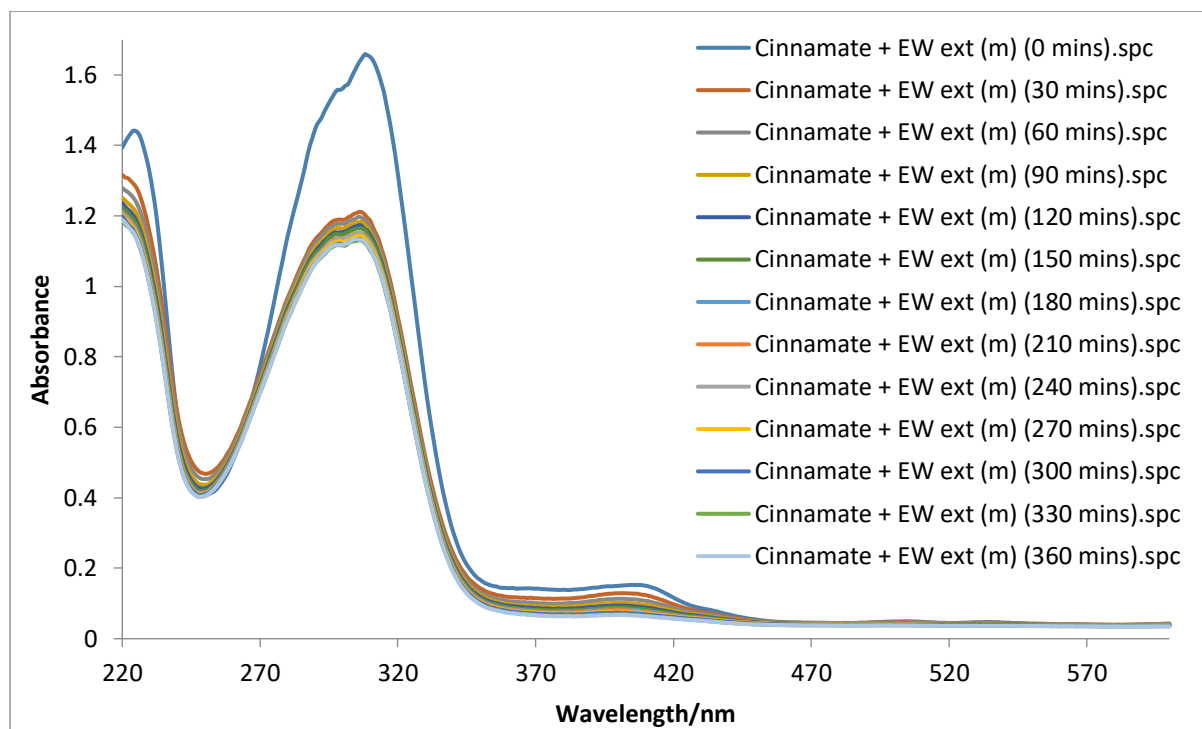


Figure 4.27: Photostability of EHMC mixed with the Cancer Bush ethanol-water extract dissolved in methanol. The spectra were recorded every 30 minutes for a total period of six hours, and were acquired in a 1 cm pathlength quartz cuvette against air as the reference.

The photostability of EHMC mixed with the Cancer Bush ethanol-water extract dissolved in ethyl acetate is shown in Figure 4.28. The spectra are similar to those for EHMC in ethyl acetate alone, but with a higher shift of absorbance values. An absorbance of 1.40 is seen at 308 nm with a shoulder at around 300 nm and a rapid drop in absorbance of 0.28 is seen after 30 minutes of irradiation. An isosbestic point is observed at 270 nm thereby confirming photoisomerisation took place. A photostationary state was reached thereafter as the absorbance remained stable. The addition of the Cancer Bush ethanol-water extract was unable to photostabilise EHMC and merely provided higher absorbance values.

Figure 4.29 shows the spectra for EHMC mixed with the Cancer Bush ethanol-water extract dissolved in cyclohexane and they are similar to those for EHMC in cyclohexane alone. A maximum absorption of 1.46 is seen at 290 nm with a right shoulder at 300 nm with an

absorbance of 1.36. A rapid drop of 0.20 is seen in absorbance after 30 minutes of irradiation. Thereafter, a photostationary state is reached. The ethanol-water extract was unsuccessful in photostabilising EHMC in cyclohexane.

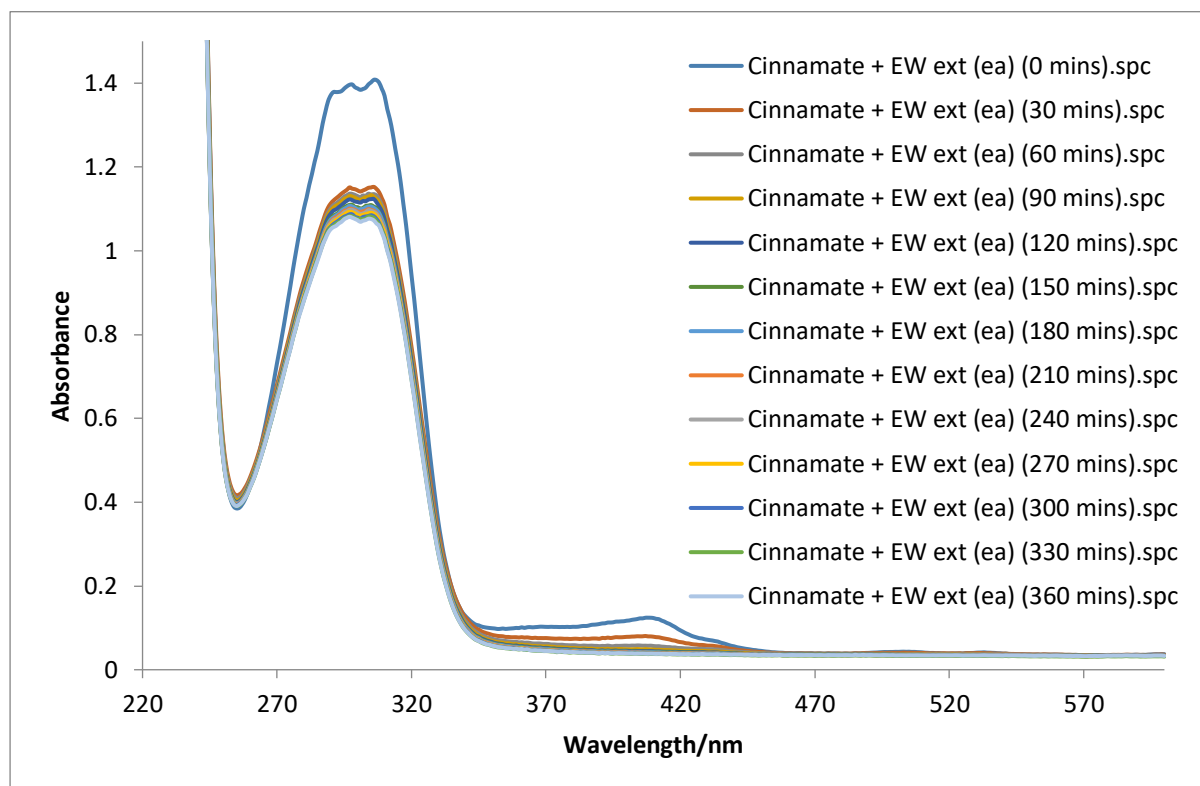


Figure 4.28: Photostability of EHMC mixed with the Cancer Bush ethanol-water extract dissolved in ethyl acetate. The spectra were recorded every 30 minutes for a total period of six hours, and were acquired in a 1 cm pathlength quartz cuvette against air as the reference.

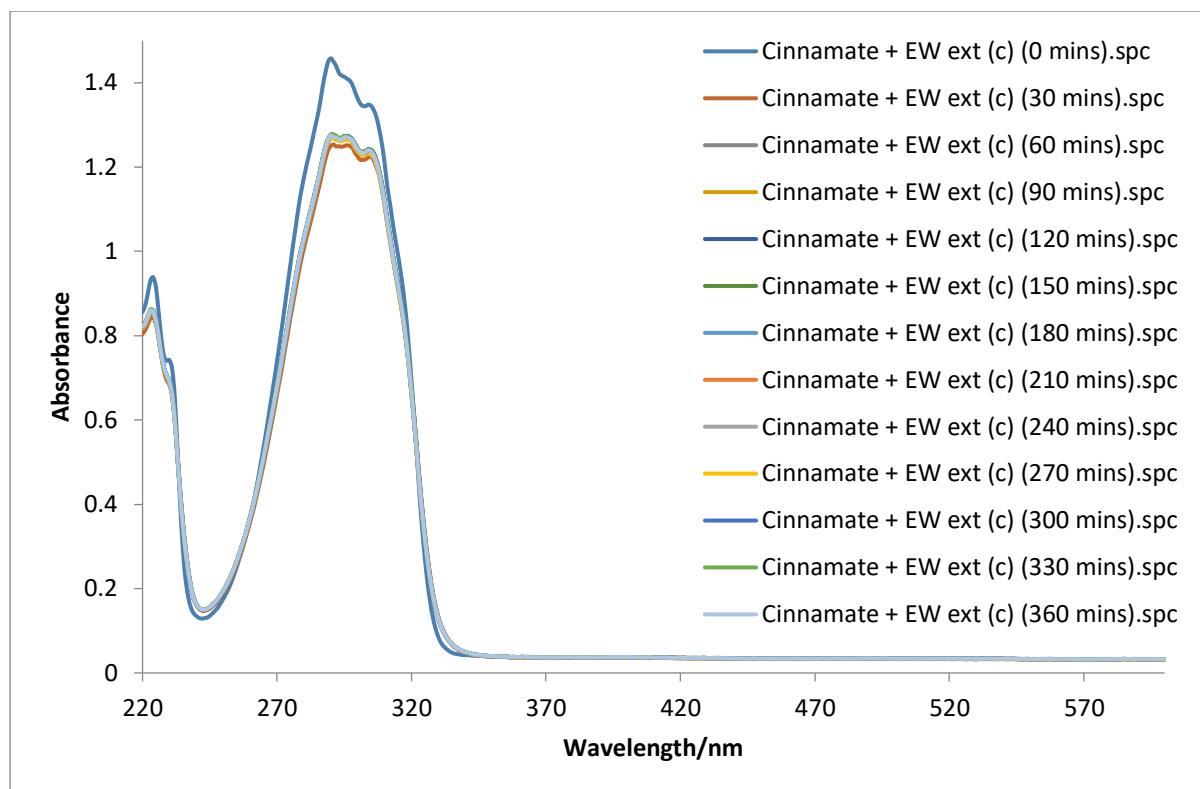


Figure 4.29: Photostability of EPMC mixed with the Cancer Bush ethanol-water extract dissolved in cyclohexane. The spectra were recorded every 30 minutes for a total period of six hours, and were acquired in a 1 cm pathlength quartz cuvette against air as the reference.

In summary, the addition of Cancer Bush extracts in small amounts gave higher absorbance values than did the UV filters on their own, but they were not successful in photostabilising the UV filters. From these results, we can see that although the extracts were successful in obtaining a higher absorbance, there was no definite improvement seen.

4.1.4 Flavonoid extracts from the Cancer Bush plant

Flavonoids found in plants can be triggered by excessive exposure to UV radiation to produce non-photosynthetic pigments. Flavonoids provide many beneficial effects to various cell layers of the skin. These benefits include antioxidant activity and anti-inflammatory effects. Flavonoids contain a high reactivity at the hydroxyl substituents, with a number of hydroxyl groups on the β -ring.^{279, 280} These substituents correlate with the ROS scavenging capability attributing to the antioxidant capacity and are responsible for blocking UV radiation.²⁸⁰ To date, no correlation between SPF and flavonoid content has been established.

Two extraction techniques were adopted, along with a simple colour identification test, to determine the content of flavonoids extracted. The solubility of the UV filters mixed with the extracts in the three solvents are shown in Table 4.4.

Table 4.4: Solubility of flavonoid extracts and UV filters in solvents of different polarity

	methanol	cyclohexane	ethyl acetate
Water-ethanol	S	NS	
+ benzophenone-9	S		
+ avobenzone	S		
+ 4-methylbenzylidene camphor	S		
+ 2-ethylhexyl- <i>p</i> -methoxycinnamate	S		
Ethyl acetate-ethanol	S	ND	ND
Ether	ND	ND	ND

S – Soluble, NS – Not soluble, ND – Not determined

The first extraction utilising the water-ethanol solvent system gave a light red colour in the flavonoid test signifying that a medium amount of flavonoids was extracted. The second solvent system, ethyl acetate-ethanol, indicated a low presence of flavonoids. The Soxhlet extraction method, conducted in triplicate, resulted in no change of colour indicating that no flavonoids were present. No further tests were conducted on the Soxhlet extracts.

4.1.4.1 Water-ethanol extract

A light red colour was observed after conducting the flavonoid identification test. This indicated that the extract contained a medium content of flavonoids. The water-ethanol extract had to be filtered before running the UV analysis. The UV spectrum, shown in Figure 4.30, is similar to the boiling water extraction method (see Figure 4.13) but achieved a higher

absorbance. The spectra also exhibited a maximum at 265 nm with an absorbance of 1.07. After the six-hour irradiation period, the absorbance decreased to 0.95. The spectrum and results were similar to the boiling water extraction method conducted in Section 4.1.2.1. A similar decrease in absorbance was seen after 30 minutes of irradiation. This indicates that the boiling water extraction method only extracted flavonoids and it is highly likely that photostability studies conducted with the water-ethanol extract and UV filters will be similar. The water-ethanol extract was not soluble in ethyl acetate and cyclohexane.

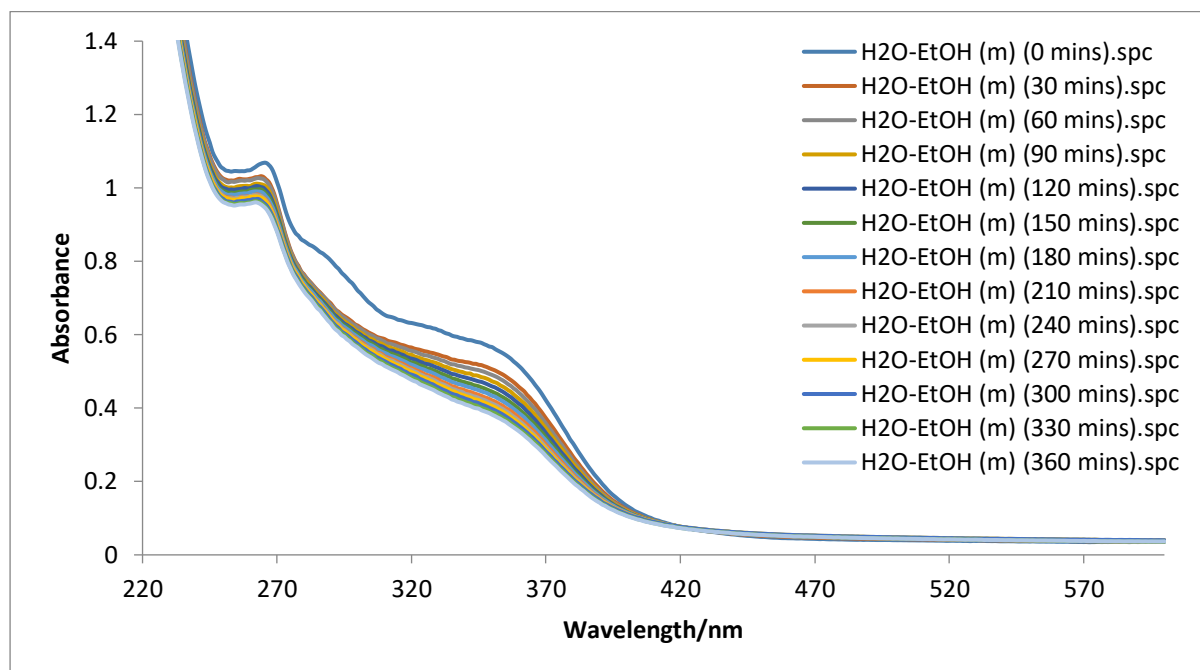


Figure 4.30: Photostability of water-ethanol flavonoid extract from the Cancer Bush dissolved in methanol. The spectra were recorded every 30 minutes for a total period of six hours, and were acquired in a 1 cm pathlength quartz cuvette against air as the reference.

Benzophenone-9

Figure 4.31 shows the UV spectra for the Cancer Bush water-ethanol flavonoid extract mixed with benzophenone-9 and dissolved in methanol. The spectrum was similar to the spectrum achieved for benzophenone-9 mixed with the boiling water extract (see Figure 4.15) and dissolved in methanol. Although, the mixture achieved higher absorbances, it revealed a similar degradation pattern indicating a possible problem with this extract since benzophenone-9 was shown to be photostable in methanol alone (see Figure 4.1). The two maxima exhibited at 281 nm and 332 nm decreased in absorbance from 1.76 to 1.69, and 1.47 to 1.38, respectively. Therefore, the flavonoid extract was deemed unsuccessful in providing benzophenone-9 with positive attributes.

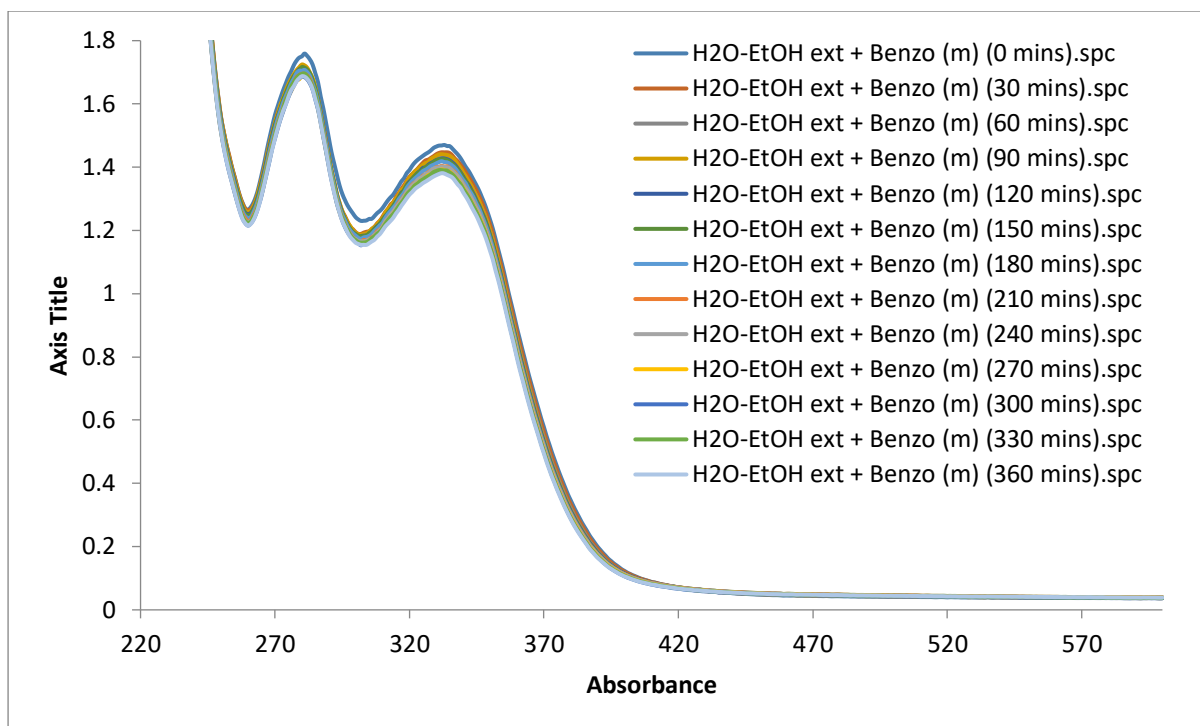


Figure 4.31: Photostability of Cancer Bush water-ethanol extract mixed with benzophenone-9 and dissolved in methanol. The spectra were recorded every 30 minutes for a total period of six hours, and were acquired in a 1 cm pathlength quartz cuvette against air as the reference.

Avobenzone

The UV spectra obtained for avobenzone when mixed with the Cancer Bush water-ethanol flavonoid extract and dissolved in methanol are shown in Figure 4.32. The spectra are comparable to those obtained when avobenzone was mixed with the boiling water Cancer Bush extract and show similar characteristics. This extract was unsuccessful in photostabilising avobenzone and the tendency of the filter to phototautomerise in a polar protic environment was favoured. The maximum absorption of 1.48 seen at λ_{max} of 358 nm decreased to 0.99 after the six-hour irradiation period. The correlation that exists between the loss of absorption at 358 nm and the increase in absorbance at 245 nm, shown in Figure 4.33, confirms that the phototautomerisation reaction took place. The only positive attribute obtained with this flavonoid extract was that the absorbance of the avobenzone peak was higher than the original value after irradiation for three hours.

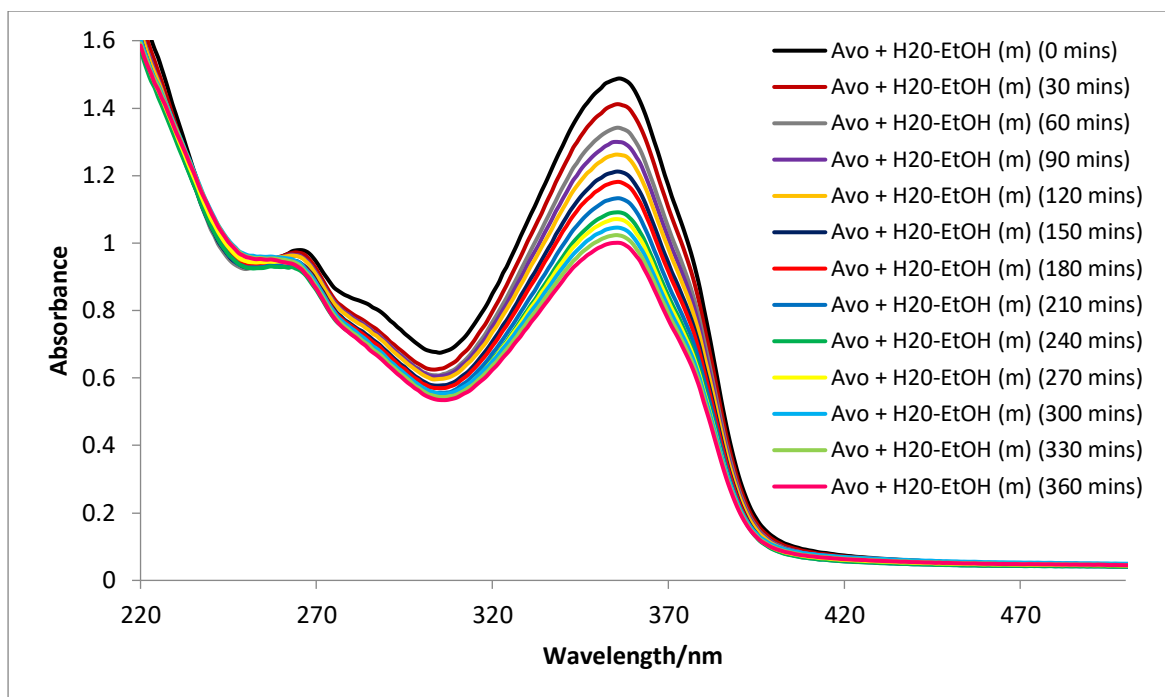


Figure 4.32: Photostability of Cancer Bush water-ethanol flavonoid extract mixed with avobenzone and dissolved in methanol. The spectra were recorded every 30 minutes for a total period of six hours, and were acquired in a 1 cm pathlength quartz cuvette against air as the reference.

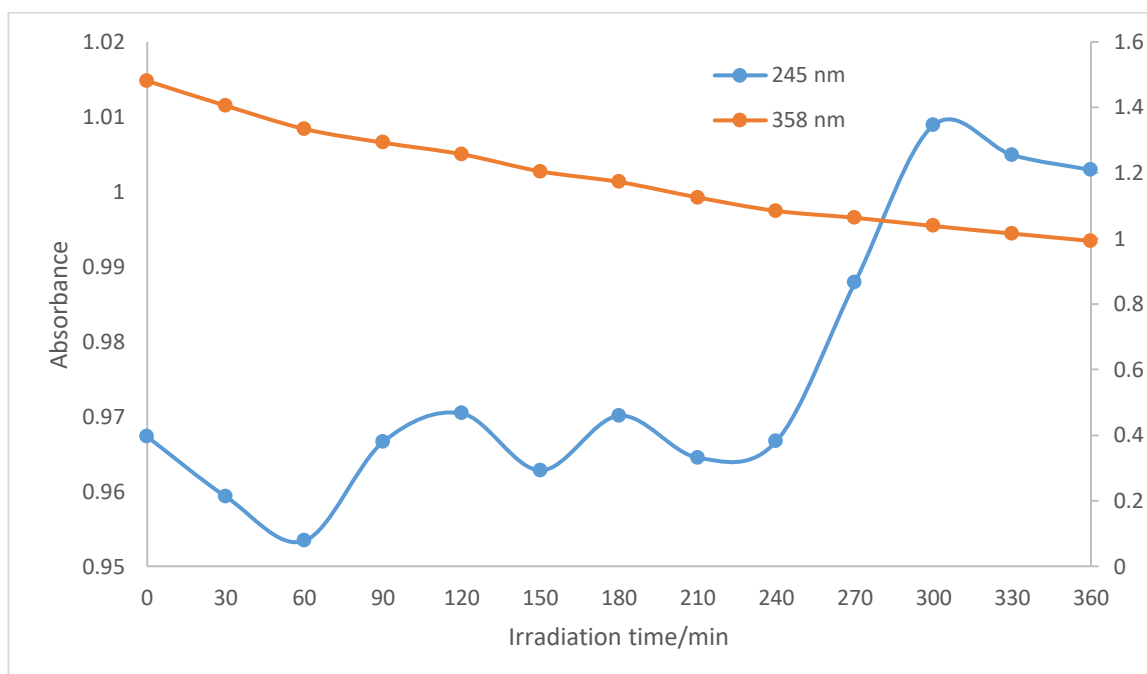


Figure 4.33: Absorbance of avobenzone mixed with the Cancer Bush water-ethanol flavonoid extract dissolved in methanol at 245 nm and 356 nm after 30-minute irradiation intervals indicating the loss of the *enol*-form and the formation of the *keto*-form.

4-Methylbenzylidene camphor

Figure 4.34 shows the spectra obtained for MBC mixed with the Cancer Bush water-ethanol flavonoid extract in methanol. The absorbance values obtained are higher than for MBC in methanol alone (see Figure 4.7) and when mixed with the Cancer Bush ethanol-water extract (see Figure 4.24). Photodegradation still occurred at the maximum absorbance of 300 nm, whereby the total loss of absorbance seen at λ_{\max} was 0.2 (1.59 – 1.39). However, no isosbestic point was observed at 265 nm as previously seen with MBC in methanol alone and photoisomerisation appears to have been prevented. MBC is an effective UVB filter, however, the UV filter mixed with the water-ethanol extract provided an absorbance of 0.33 in the UVA region. This confirms that there is a potential to broaden the amount of UV protection achieved through the use of flavonoids found in the Cancer Bush extract. MBC was not miscible in the boiling water Cancer Bush extract and, hence, that could not be compared with the flavonoid water-ethanol extract.

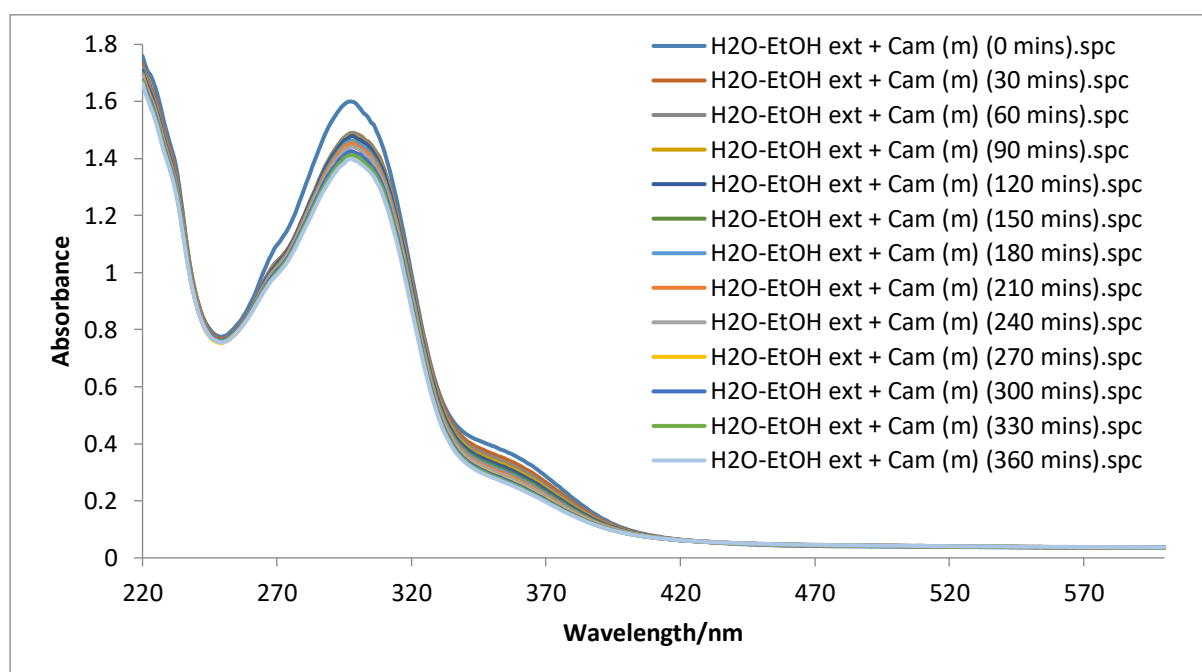


Figure 4.34: Photostability of the Cancer Bush water-ethanol extract mixed with MBC dissolved in methanol. The spectra were recorded every 30 minutes for a total period of six hours, and were acquired in a 1 cm pathlength quartz cuvette against air as the reference.

2-Ethylhexyl-*p*-methoxycinnamate

The spectra for EHMC mixed with the Cancer Bush water-ethanol flavonoid extract in methanol are shown in Figure 4.35. The absorbance values obtained are similar to those for EHMC mixed with the Cancer Bush ethanol-water extract dissolved in methanol (see Figure

4.27) and higher than with EHMC dissolved in methanol alone (see Figure 4.10). Photodegradation still occurred at the maximum absorbance. The total loss of absorbance seen at maximum absorption was 0.44 (1.58 – 1.14). No isosbestic points were observed at 240 nm and 270 nm indicating that photoisomerisation did not take place. An average absorbance of 0.35 was observed in the UVA region between 340 to 360 nm. This confirms that there is a potential to broaden the amount of UV protection through the use of flavonoids.

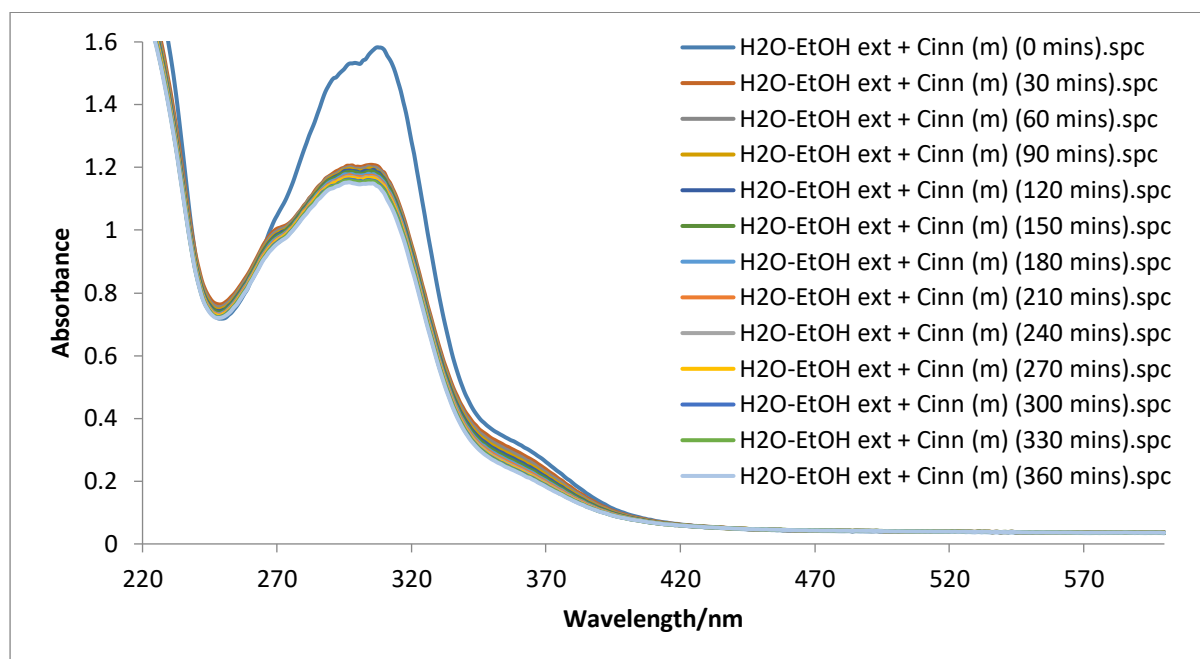


Figure 4.35: Photostability of the Cancer Bush water-ethanol flavonoid extract mixed with EHMC and dissolved in methanol. The spectra were recorded every 30 minutes for a total period of six hours, and were acquired in a 1 cm pathlength quartz cuvette against air as the reference.

In summary, the results achieved for the water-ethanol flavonoid extraction method were identical to those for the boiling water extraction method observed for benzophenone-9 and avobenzone. This indicates that both the extraction methods were able to extract flavonoids, but were unsuccessful in photostabilising the UV filters. However, the flavonoid extraction techniques were successful in preventing photoisomerisation in both MBC and EHMC, as well as, provided some UVA protection. Further investigation is required to confirm the effectiveness of flavonoids on MBC and EHMC, and the prevention of photoisomerisation needs to be confirmed chromatographically.

4.1.4.2 Ethyl acetate-ethanol extract

A second solvent system, namely, ethyl acetate-ethanol, required to extract flavonoids was investigated. The method quantities were halved for the maceration technique. Five grams of the Cancer Bush powder was dissolved in 25 ml of solvent (20 ml ethyl acetate and 5 ml ethanol) and stirred for 3 days. The colour observed after conducting the flavonoid identification test was light orange, which indicated a very low presence of flavonoid compounds. UV analysis was conducted and the spectra shown in Figure 4.36 illustrate that the sample degraded very rapidly upon irradiation and was unable to maintain absorbance.

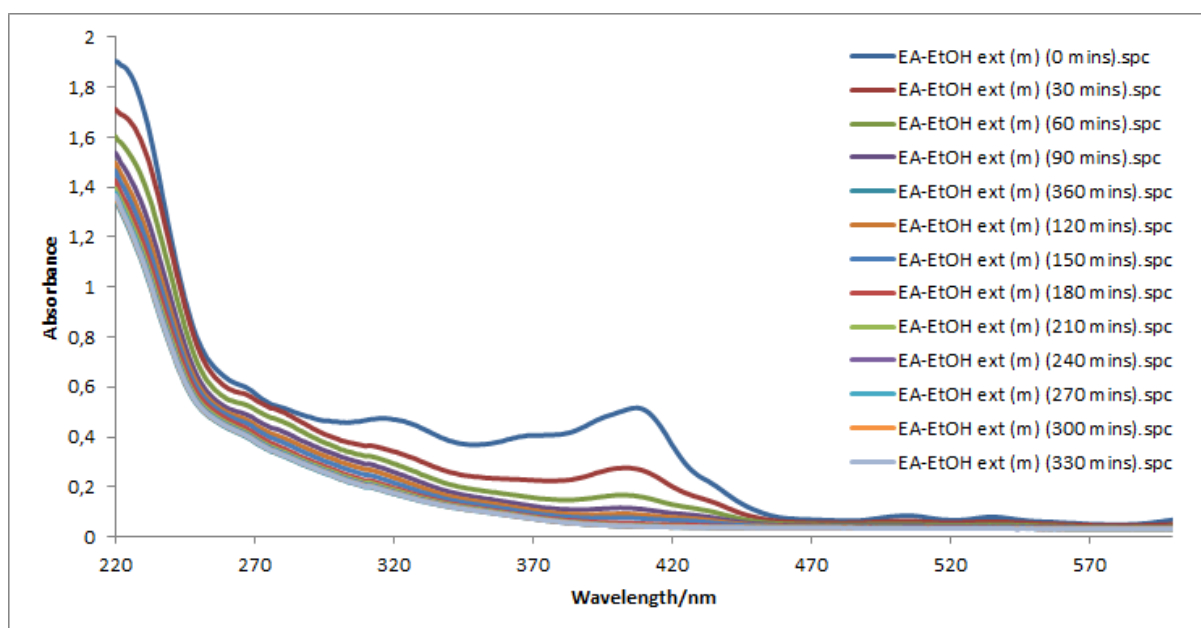


Figure 4.36: Photostability of Cancer Bush ethyl acetate-ethanol flavonoid extract dissolved in methanol. The spectra were recorded every 30 minutes for a total period of six hours, and were acquired in a 1 cm pathlength quartz cuvette against air as the reference.

Figure 4.37 shows the UV spectra obtained for avobenzone mixed with the Cancer Bush ethyl acetate-ethanol flavonoid extract and dissolved in methanol. The maximum absorption of 1.18 seen at λ_{\max} of 358 nm decreased to 0.63 after the six-hour irradiation period.

Results indicated that the second flavonoid solvent extraction method was ineffective in maintaining photostability. Further photostability testing was not conducted using this extract due to the flavonoid colour test indicating a low presence of flavonoids and the rapid degradation observed upon irradiation of the extract dissolved in methanol alone and when mixed with avobenzone.

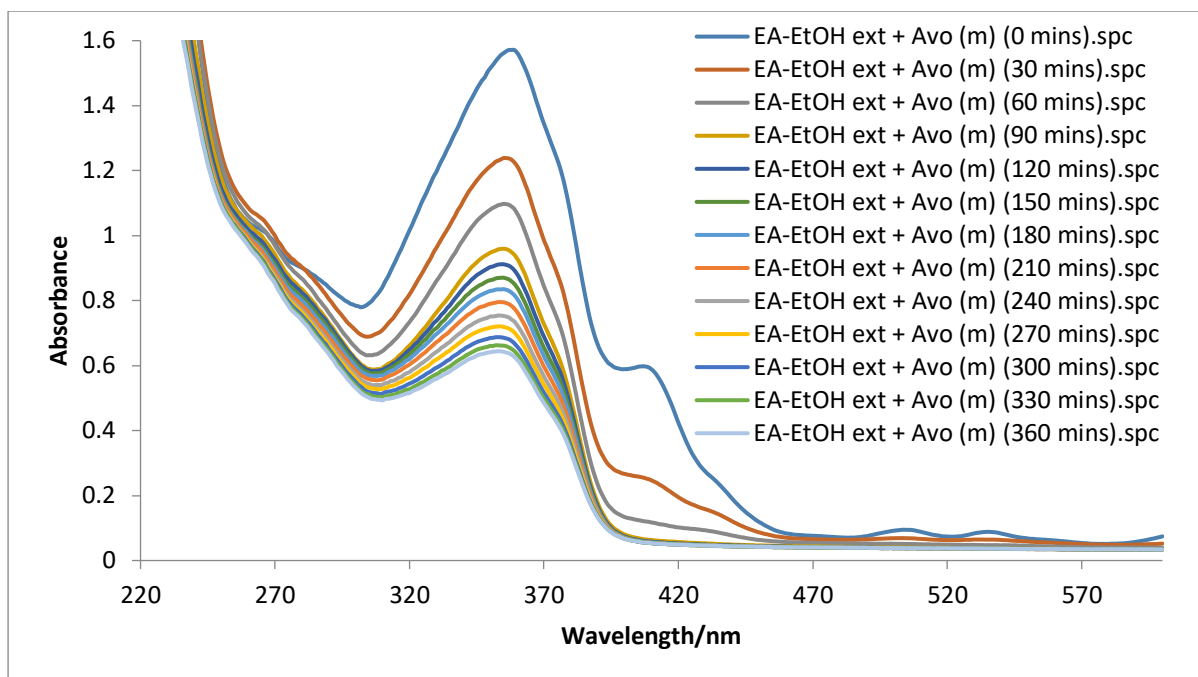


Figure 4.37: Photostability of the Cancer Bush ethyl acetate-ethanol flavonoid extract mixed with avobenzone and dissolved in methanol. The spectra were recorded every 30 minutes for a total period of six hours, and were acquired in a 1 cm pathlength quartz cuvette against air as the reference.

4.1.4.3 Ether extract using Soxhlet extraction

Soxhlet extraction was conducted according to Section 3.2.4.1 and there was no colour change after the flavonoid colour test was performed, indicating that no flavonoid content was successfully extracted. Hence, further studies were not carried out.

4.1.5 Phenolic acids extracted from the Cancer Bush plant

Medicinal plant extracts contain bioactive compounds such as phenolic compounds. Phenolic compounds demonstrate a diverse range of pharmacological properties such as providing mechanical strength, response to stress, and defence against pathogens.^{281, 282} Due to these positive attributes, plant phenolic compounds have gained relevance as therapeutic compounds in both modern and traditional medicine. Environmental factors, cultivation, genetic factors, degree of maturation, and the variety of the plant, determines the content of phenolic compounds and phytochemicals present in a medicinal plant.²⁸³

Phenolic compounds are secondary plant metabolites. Metabolites are an intermediate or end-product of metabolism in small molecules.²⁸⁴ The function of metabolites include fuel, structure, signalling, stimulatory and inhibiting effects on enzymes, among others.²⁸⁴ There

are two types of metabolites: primary and secondary. A primary metabolite is directly involved in normal growth, development and reproduction, and the secondary metabolite has important ecological functions. The secondary metabolite is not directly involved in the process. Secondary plant metabolites, such as phenolic compounds, determine the sensorial and nutritional quality of plants, fruits and vegetables.^{285, 286} Secondary metabolites are used in most cosmetics and pharmaceuticals.²⁸⁷

Shaik *et al.*²⁵³ conducted a study on the Cancer Bush plant and found that the phenolic content was higher in leaf extracts (*in vitro* and the leaves) when compared with the seed extract. The shoots and leaves were also reported to contain a high amount of phenolic content when compared with other parts of the plant.²⁸⁸ The reason for the variation in phenolic content in the plant is due to the endogenous degradation of the phenolic compounds that occurs after air, light and temperature exposure during sampling.²⁸⁹ Simple phenolics contain at least one hydroxyl group attached to an aromatic ring. Polyphenolics contain two or more hydroxyl groups attached to an aromatic ring. Phenolic acids are strong antioxidants and powerful scavengers of almost all oxidant molecules.²⁹⁰ Phenolic acid compounds can scavenge one or two oxidant molecules such as free radicals.²⁹¹ The scavenging ability of phenolic acids is due to their highly hydroxylated molecular properties.²⁹¹ The radical scavenging ability of polyphenolics is beneficial in cosmetic products as these properties are known to protect and restore the skin from UVB and UVA radiation, aging, wrinkling, hyperpigmentation and inflammation. The use of natural products, such as phenolic acids, has been on the rise in the cosmetic industry.

Phenolic acids were extracted from the Cancer Bush plant by using the methods described in Section 3.2.4. The percentage yield of the content extracted from the crude phenolic extract was calculated from Equation 5 based on dry weight. Table 4.5 shows the masses of Cancer Bush powder used for the extraction methods and the yields of extracts obtained for both the Soxhlet and ultrasonication methods. The extracts obtained were further refined by liquid-liquid extraction with either diethyl ether or ethyl acetate. UV spectroscopy and HPLC techniques were conducted to characterise the polyphenolic extracts and assess their photostabilising potential.

$$\% \text{ yield} = \frac{\text{mass of dry extract}}{\text{mass taken for extraction}} \times 100 \quad (5)$$

Table 4.5: Yield of crude extract and purified extract obtained for each phenolic acid extraction method

	Soxhlet	Ultrasonication
Mass of dried Cancer Bush plant powder/g	9.7804	9.5765
Mass of crude extract/g	3.6859	3.7852
% yield of crude extract/%	37.69	39.53
Diethyl ether layer		
Mass of crude extract/g	1.8078	1.1267
Mass of purified extract/g	0.1677	0.1621
% yield	9.2764	14.3871
Ethyl acetate layer		
Mass of crude extract/g	1.7081	1.6542
Mass of purified extract/g	0.1525	0.1862
% yield	8.9280	11.2561

4.1.5.1 Test for phenols

Each extract obtained was tested for phenolic compounds by using colour indication. Extracts for both the Soxhlet and ultrasonication extraction techniques showed an olive-green colour. The green colouring confirms the presence of phenolic material.

4.1.5.2 Comparison of Soxhlet and ultrasonication methods

Both the diethyl ether layer and the ethyl acetate layer obtained from the Soxhlet and ultrasonication extraction methods was made up in a 1:1 ratio with methanol, and UV analysis was performed to determine which extract displayed a higher absorbance value. The UV spectra are shown in Figure 4.38.

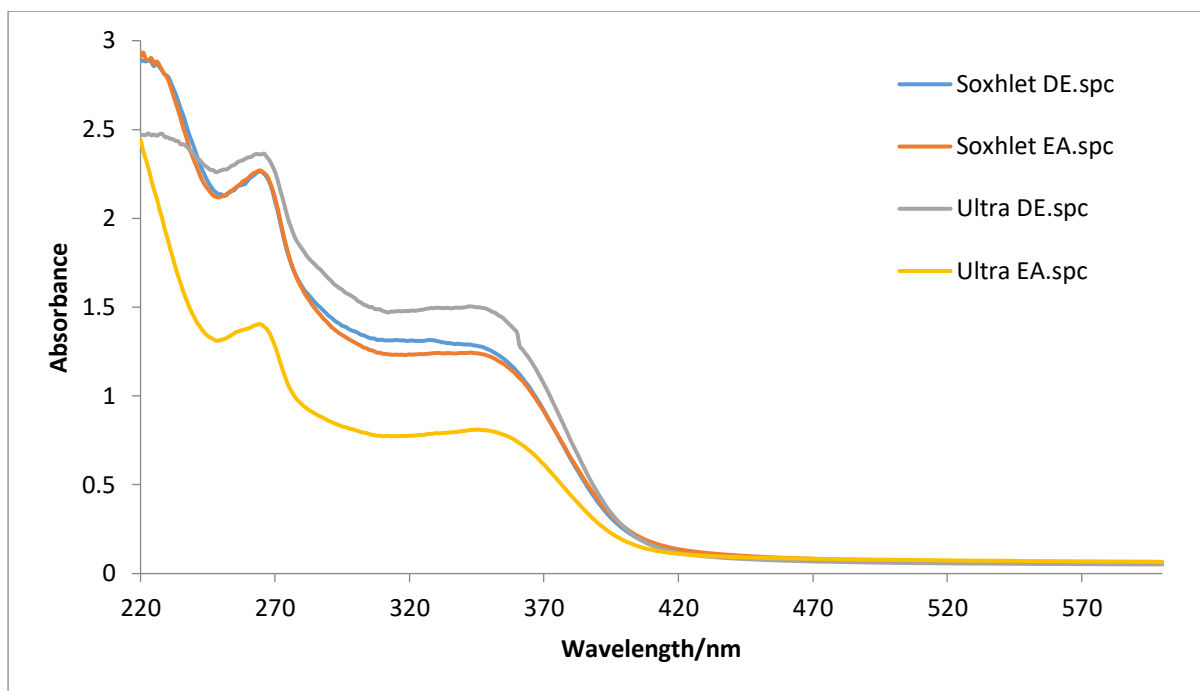


Figure 4.38: Comparison of the diethyl ether and ethyl acetate layers obtained after Soxhlet and ultrasonic-assisted extraction of phenolic acids from the Cancer Bush. The spectra were acquired in a 1 cm pathlength quartz cuvette against air as the reference.

From the results, the diethyl ether layer from the ultrasonication extraction technique exhibited the highest absorbance of the four. Therefore, ultrasonic-assisted extractions were selected for further photostability analysis.

4.1.5.3 Ultrasonic-assisted extracts

The diethyl ether and ethyl acetate extracted layers were diluted with methanol until an absorbance of 1.2 nm was obtained to obey Beers Law. The UV spectra for the diethyl ether layer, shown in Figure 4.39, showed two peaks at 264 and 345 nm. After the six-hour irradiation period, the loss of absorbance observed for the peak in the UVB range was 0.08, and 0.14 for the peak in the UVA range. The ethyl acetate layer, shown in Figure 4.40, also displayed two peaks at 264 and 345 nm. After the six-hour irradiation period, the loss of absorbance observed for the peak in the UVB range was 0.08, and 0.14 for the peak in the UVA range. The absorbance values obtained for both solvents used in the liquid-liquid extraction were almost identical and the amount of degradation was the same. This showed that either solvent was able to extract almost identical phenolic compounds.

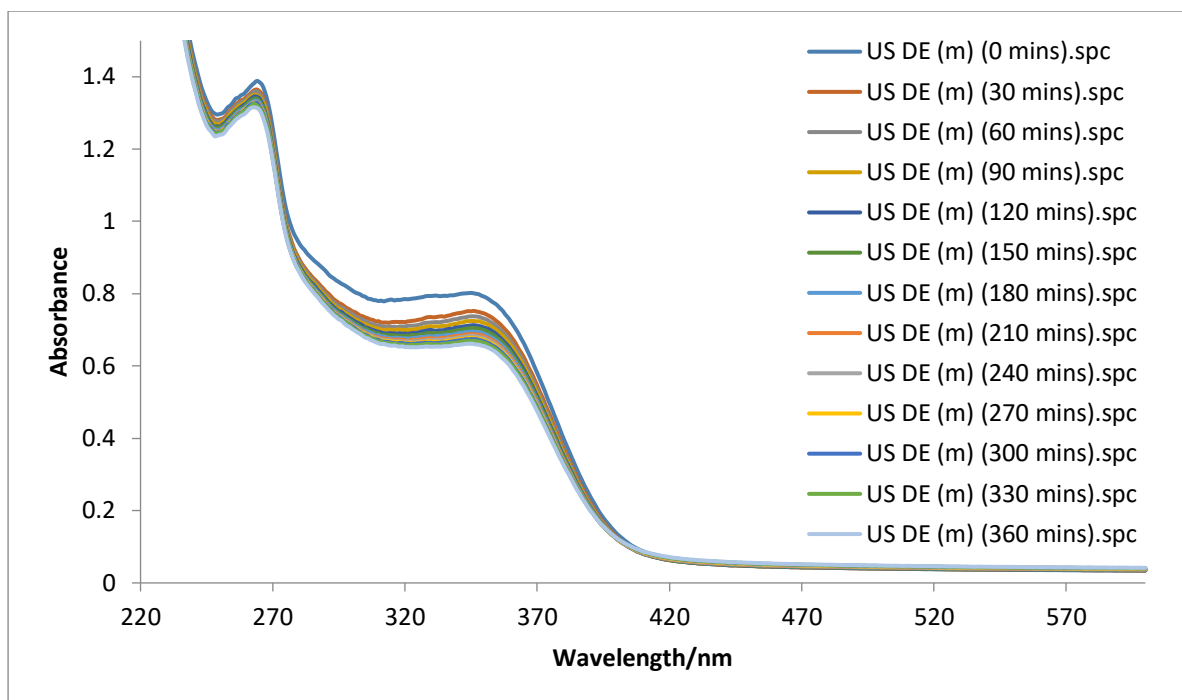


Figure 4.39: Photostability of the diethyl ethyl layer from the ultrasonic-assisted phenolic acid extraction of the Cancer Bush dissolved in methanol. The spectra were recorded every 30 minutes for a total period of six hours, and were acquired in a 1 cm pathlength quartz cuvette against air as the reference.

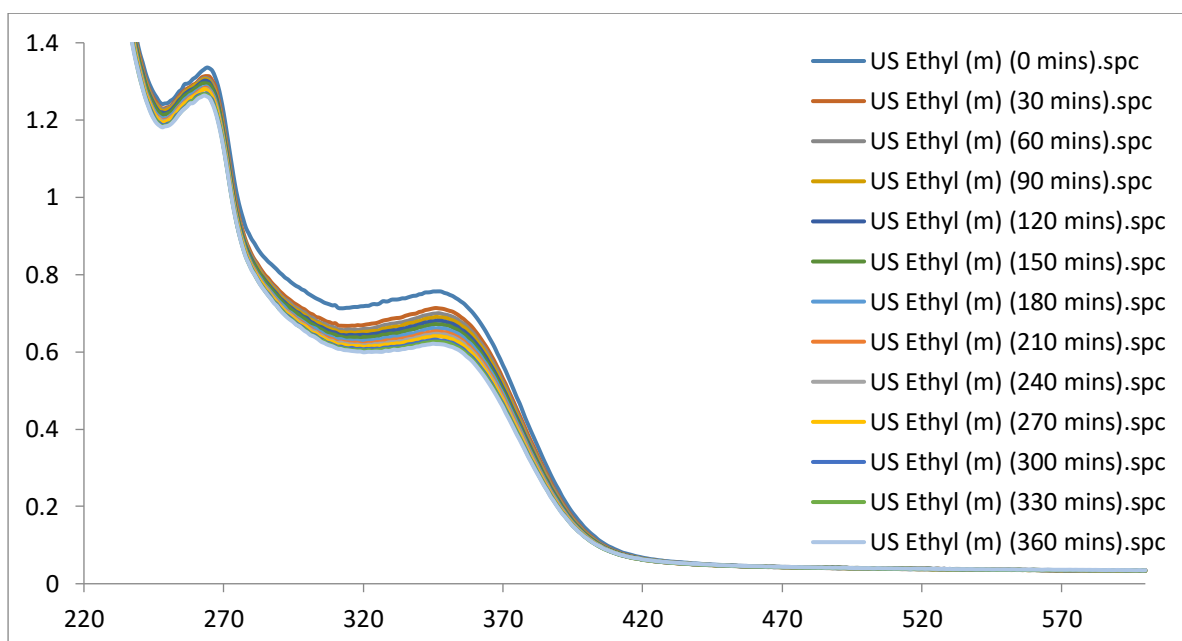


Figure 4.40: Photostability of the ethyl acetate layer from the ultrasonic-assisted phenolic acid extraction of the Cancer Bush dissolved in methanol. The spectra were recorded every 30 minutes for a total period of six hours, and were acquired in a 1 cm pathlength quartz cuvette against air as the reference.

Benzophenone-9

Figure 4.41 shows the UV spectra of 0.032 g of the diethyl ether phenolic acid layer extract mixed with 0.01 g benzophenone-9 dissolved in methanol. The blue line shows the UV filter benzophenone-9 dissolved in methanol alone. Benzophenone-9 dissolved in methanol exhibits two maxima at 281 and 332 nm (see Figure 4.1). The maximum at 281 nm moved to 266 nm when the solution was mixed with the diethyl ether layer extract. The absorbance at 266 nm decreased from 1.80 to 1.72 after six hours of irradiation. The second maximum at 332 nm also showed some degradation, with an absorbance value of 1.22 decreasing to 1.08 after six hours of irradiation. The phenolic acid addition to the UV filter still provides both UVB and short wavelength UVA protection achieving higher absorbance values, however, this mixture is susceptible to photodegradation. Therefore, the use of phenolic acids with benzophenone-9 is ineffective, since benzophenone-9 is photostable.

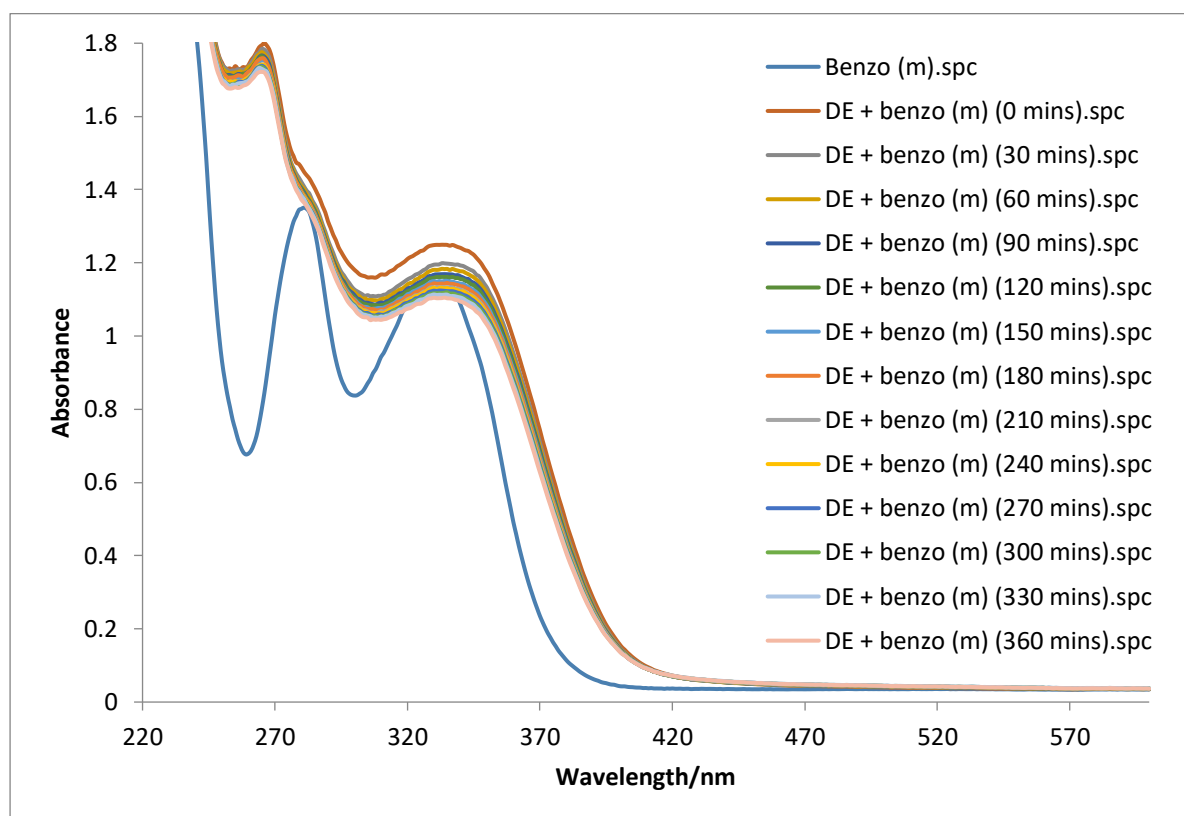


Figure 4.41: Photostability of the diethyl ether phenolic acid layer from ultrasonic-assisted extraction of the Cancer Bush mixed with benzophenone-9 and dissolved in methanol. The spectra were recorded every 30 minutes for a total period of six hours, and were acquired in a 1 cm pathlength quartz cuvette against air as the reference.

The UV spectra obtained for the ethyl acetate phenolic acid layer mixed with benzophenone-9 are similar to those obtained for benzophenone-9 mixed with the diethyl ether phenolic acid layer and are shown in Figure 4.42. The spectra also exhibit two maxima at 265 and 333 nm with absorbances of 1.87 and 1.29 respectively. The absorbances at the two maxima decreased to 1.81 and 1.16 respectively after six hours of irradiation. Again, although higher absorbances were obtained, the use of phenolic acids with benzophenone-9 is deemed ineffective as its photoprotective power was reduced. This could suggest that the phenolic acids will possibly have a negative impact on the other UV filters.

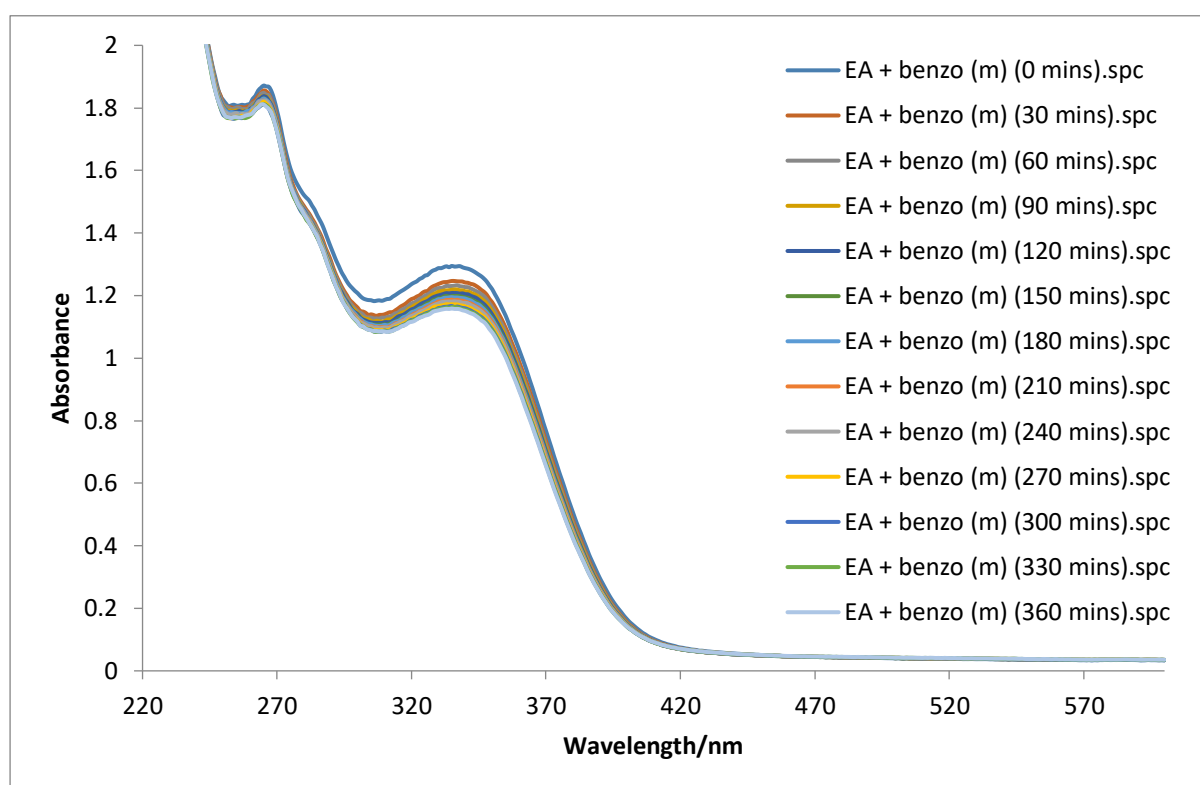


Figure 4.42: Photostability of the ethyl acetate phenolic acid layer from ultrasonic-assisted extraction of the Cancer Bush mixed with benzophenone-9 and dissolved in methanol. The spectra were recorded every 30 minutes for a total period of six hours, and were acquired in a 1 cm pathlength quartz cuvette against air as the reference.

Avobenzone

Mturi¹⁷ suggested that polyphenols found in the Cancer Bush plant contain considerable UV absorption capabilities and can be used alone or as additives to enhance the absorption capabilities of UV filters in sunscreen formulations. Avobenzone absorbs in the UVA range between 340 to 360 nm with a maximum absorption at 358 nm when dissolved in methanol. Avobenzone was mixed with the diethyl ether layer and dissolved in methanol. This solution

was irradiated at 30-minute intervals for a total period of six hours and the photostability is shown in Figure 4.43. Avobenzone dissolved in methanol alone and the diethyl ether phenolic acid layer dissolved in methanol, are also shown in Figure 4.43. The spectra showed that the mixture was additive giving a higher absorbance with a maximum absorbance of 1.27 now shown at 350 nm. The absorbance decreased to 1.04 after six hours of irradiation. Although the spectrum shows a slight decrease in absorbance at λ_{\max} after each irradiation interval there is no evidence of a correlation taking place at the *keto*-range below 270 nm. This is confirmed in Figure 4.44 whereby the initial absorbance of 1.71 at 245 nm decreased to 1.67 after six hours of irradiation. Here, the *enol*-form of avobenzone showed no conversion to the *keto*-form upon irradiation. The lack of a correlation confirms that phototautomerisation did not take place and the addition of the diethyl ether phenolic acid extract was successful in photostabilising avobenzone.

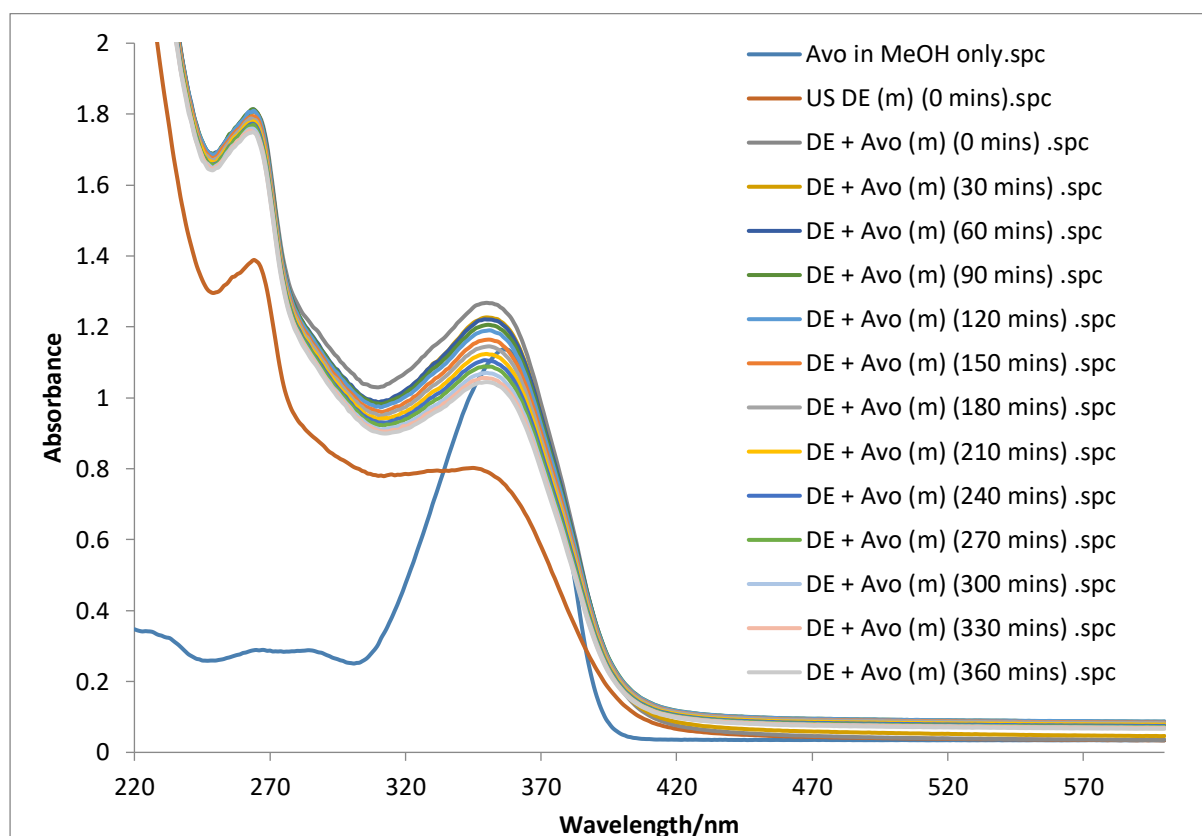


Figure 4.43: Photostability of the diethyl ether phenolic acid layer from ultrasonic-assisted extraction of the Cancer Bush mixed with avobenzone and dissolved in methanol. The spectra were recorded every 30 minutes for a total period of six hours, and were acquired in a 1 cm pathlength quartz cuvette against air as the reference.

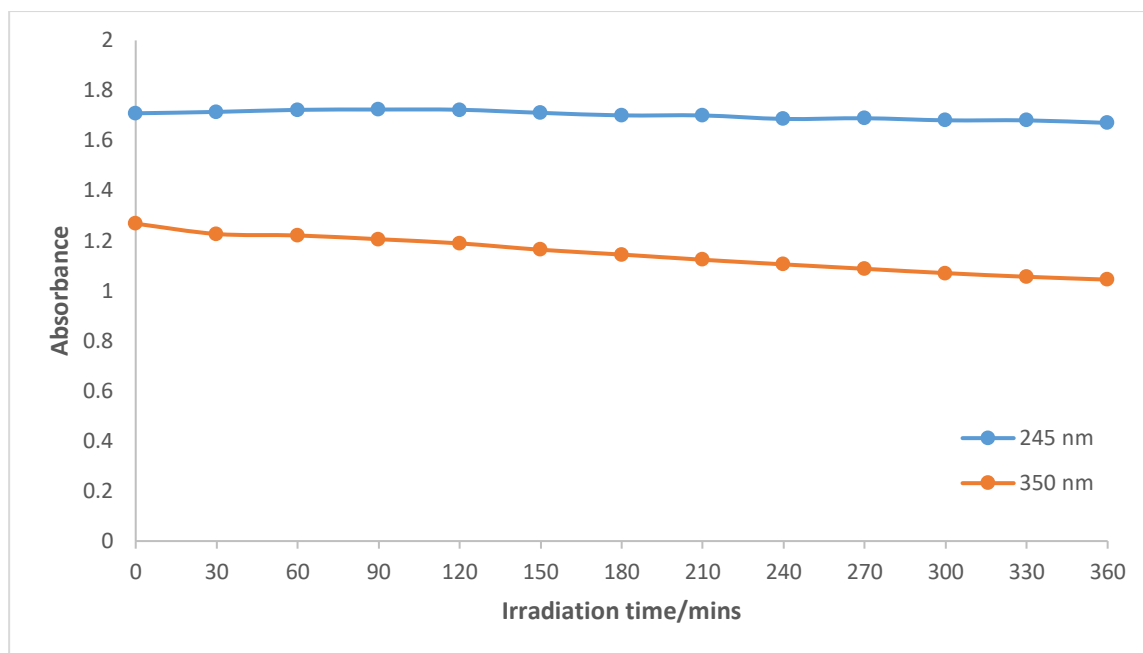


Figure 4.44: Absorbance of the diethyl ether phenolic acid layer from ultrasonic-assisted extraction of the Cancer Bush mixed with avobenzone dissolved in methanol at 245 and 358 nm after 30-minute irradiation intervals indicating little change in the *enol*- and *keto*-forms of avobenzone.

The UV spectra of avobenzone mixed with the ethyl acetate phenolic acid layer and dissolved in methanol are shown in Figure 4.45. The spectra show similar results to those obtained with the diethyl layer phenolic acid extract shown in Figure 4.43. The maximum absorbance seen at 358 nm was 1.13, slightly lower than that of avobenzone dissolved in methanol alone. After six hours of irradiation, the absorbance decreased to 0.90. There is no correlation observed at the *keto*-range of 245 nm. This is confirmed in Figure 4.46 where the initial absorbance of 1.48 decreased to 1.47 after the six-hour irradiation period. Therefore, the ethyl acetate phenolic acid extract was also successful in photostabilising avobenzone.

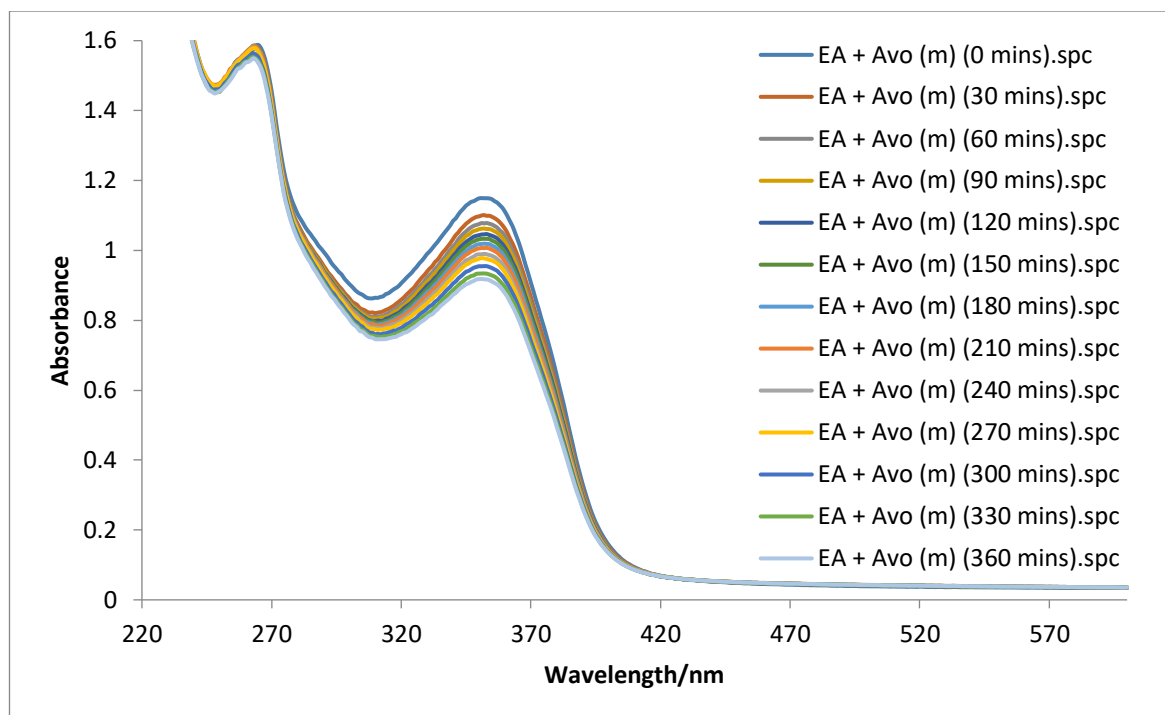


Figure 4.45: Photostability of the ethyl acetate phenolic acid extract from ultrasonic-assisted extraction of the Cancer Bush mixed with avobenzone and dissolved in methanol. The spectra were recorded every 30 minutes for a total period of six hours, and were acquired in a 1 cm pathlength quartz cuvette against air as the reference.

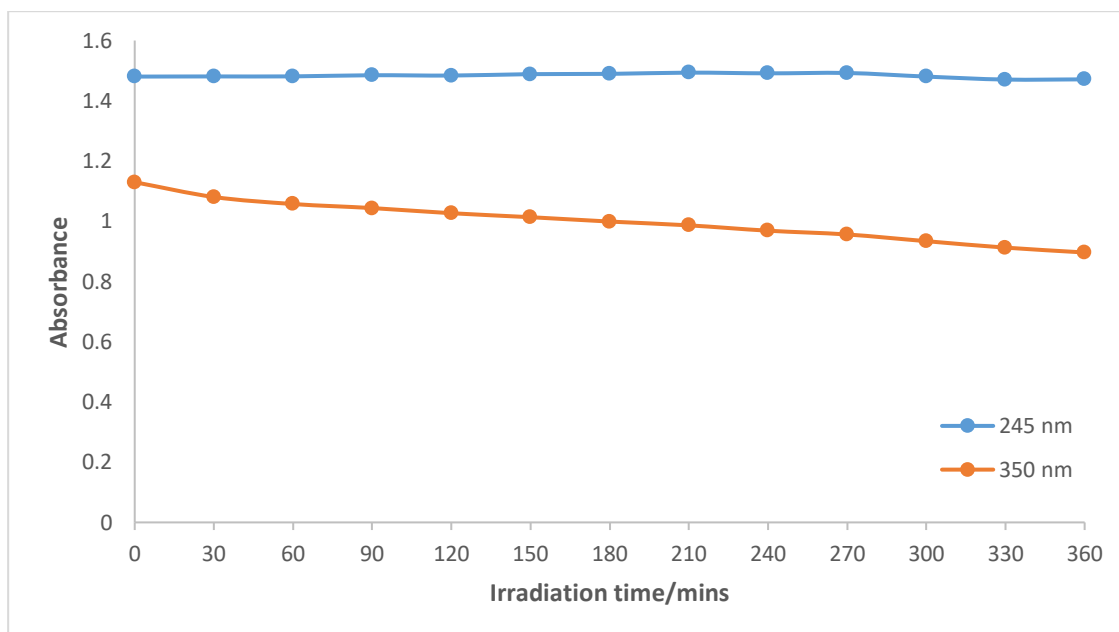


Figure 4.46: Absorbance of the ethyl acetate phenolic acid extract from ultrasonic-assisted extraction of the Cancer Bush mixed with avobenzone dissolved in methanol at 245 and 358 nm after 30-minute irradiation intervals indicating little change in the *enol*- and *keto*-forms of avobenzone

Mturi *et al.*¹³³ showed that the photostability of avobenzone is dependent on the polarity and proticity of the solvent. In a polar protic environment, avobenzone undergoes *keto-enol* phototautomerisation whereby a carbonyl hydrogen abstraction reaction takes place. This reaction occurs with the polar solvent or other hydrogen donors in the environment. Schwack and Rudolph¹²⁹ showed that avobenzone photodegrades by reactive radical formation of benzoyl and phenacyl radicals in a non-polar environment. This reaction yields photoproducts with reduced efficacy. Due to the improved photostability of avobenzone mixed with the phenolic acids dissolved in the polar protic solvent, we can conclude that phenolic acid extracts create a favourable polar protic environment to enhance the *enol*-form of avobenzone and prevent phototautomerisation from taking place.

4-Methylbenzylidene camphor

The UV spectra obtained for the solution of MBC mixed with the diethyl ether layer prepared in methanol are shown in Figure 4.47. The spectra display absorbances in both the UVB (280 to 315 nm) and UVA (315 to 400 nm) ranges confirming a positive interaction between the UV filter and the phenolic acid extract. At the maximum wavelength the total loss of absorbance seen was 0.19 (from 1.50 to 1.31). The absence of an isosbestic point confirms that photoisomerisation did not take place. A distinct absorbance feature is observed in the UVA region. This feature was not observed in previous MBC spectra. The total loss in absorbance seen between 340 to 370 nm was 0.07. This implies that the diethyl ether layer interacts positively with the UV filter in order to prevent photoisomerisation as well as provide broad spectrum UV protection.

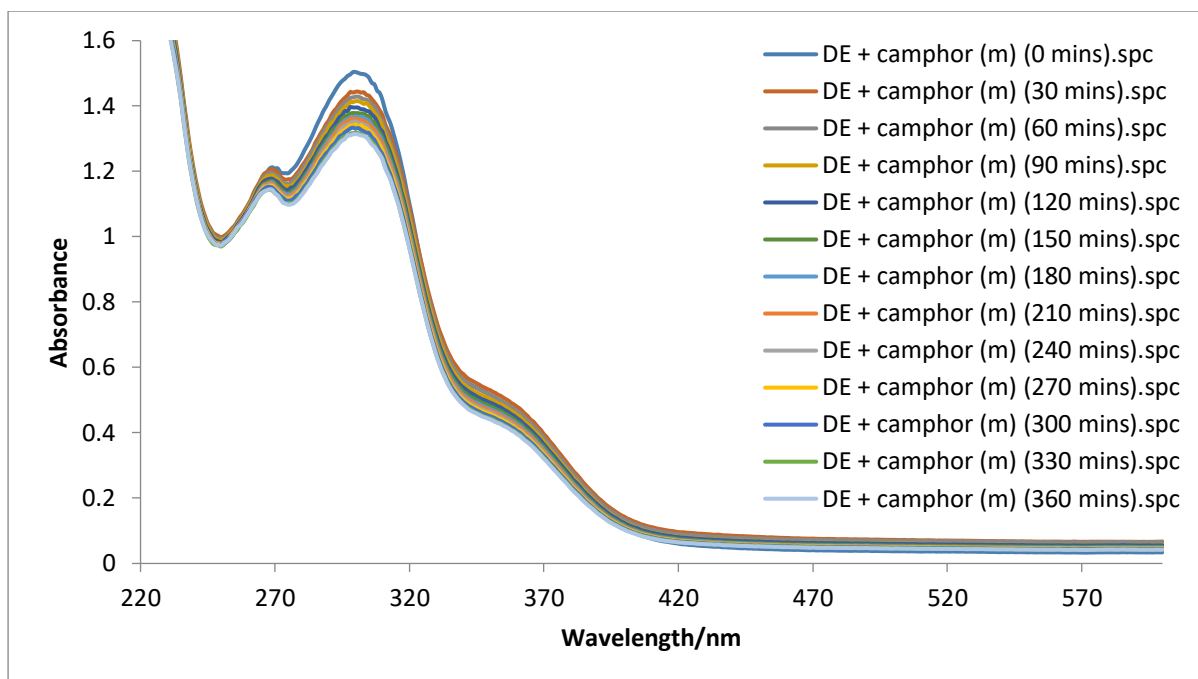


Figure 4.47: Photostability of MBC mixed with the diethyl ether extract from ultrasonic-assisted extraction of the Cancer Bush and dissolved in methanol. The spectra were recorded every 30 minutes for a total period of six hours, and were acquired in a 1 cm pathlength quartz cuvette against air as the reference.

Figure 4.48 shows the UV spectra obtained for the solution of MBC mixed with the ethyl acetate layer prepared in methanol. The spectra also display absorbances in both the UVB and UVA range. The total loss of absorbance in the UVB after six hours of irradiation was 0.17 (from 1.54 to 1.27) at maximum absorbance. No isosbestic point was observed, thereby confirming the lack of photoisomerisation. The absorbance observed in the UVA region between 340 to 360 nm showed a total loss of 0.10. The ethyl acetate layer extract was successful in preventing photoisomerisation and has the potential to provide UV protection in the UVA range when mixed with MBC.

The diethyl ether layer and the ethyl acetate layer extracts were not soluble in ethyl acetate or cyclohexane and, therefore, studies were not conducted in those solvents. A solubility test was conducted to determine if the extracts were soluble in any other solvents. This test showed that the phenolic acid extracts were only soluble in methanol.

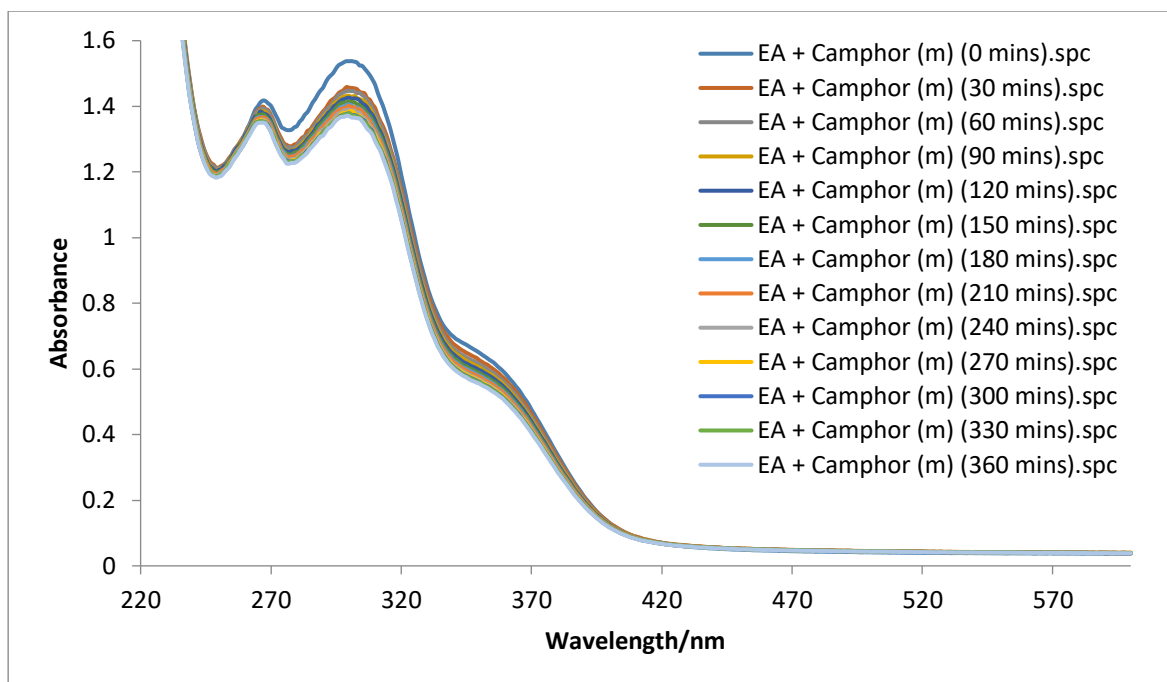


Figure 4.48: Photostability of MBC mixed with the ethyl acetate phenolic acid extract from ultrasonic-assisted extraction of the Cancer Bush and dissolved in methanol. The spectra were recorded every 30 minutes for a total period of six hours, and were acquired in a 1 cm pathlength quartz cuvette against air as the reference.

2-Ethylhexyl-*p*-methoxycinnamate

The UV spectra obtained for the solution of EHMC mixed with the diethyl ether layer prepared in methanol are shown in Figure 4.49. Absorbances are observed in the UVB and UVA regions. The loss of absorbance seen at the maximum wavelength in the UVB range was 0.50 (from 1.75 to 1.25). This is attributed to photoisomerisation. Thereafter, a shoulder is observed where a photostationary state is reached. The UVA absorbance is seen below 390 nm indicating a positive interaction between the UV filter and the extract, since EHMC does not absorb at wavelengths greater than approximately 350 nm when dissolved in methanol.

Figure 4.50 shows the photostability of EHMC mixed with the ethyl acetate layer extract dissolved in methanol. Similar absorbance values were observed as with EHMC and the diethyl ether layer (see Figure 4.49). The loss of absorbance seen at the maximum wavelength in the UVB was also 0.50 (from 1.60 to 1.10). A similar shoulder and photostationary state is seen as with the diethyl ether layer. This implies that both flavonoid extracts behaved in the same manner and provided similar results. The lack of isosbestic points seen for both flavonoid extracts mixed with EHMC indicate that the flavonoid has a beneficial effect by preventing photoisomerisation.

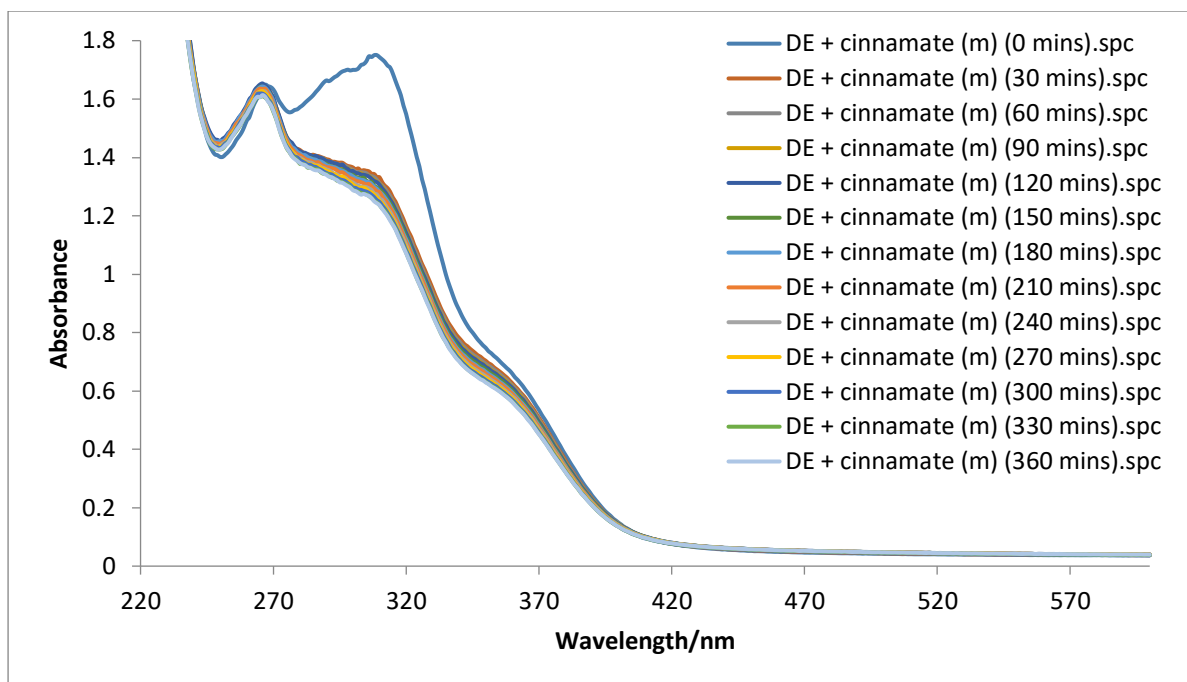


Figure 4.49: Photostability of EHMC the mixed with diethyl ether phenolic acid extract from ultrasonic-assisted extraction of the Cancer Bush and dissolved in methanol. The spectra were recorded every 30 minutes for a total period of six hours, and were acquired in a 1 cm pathlength quartz cuvette against air as the reference.

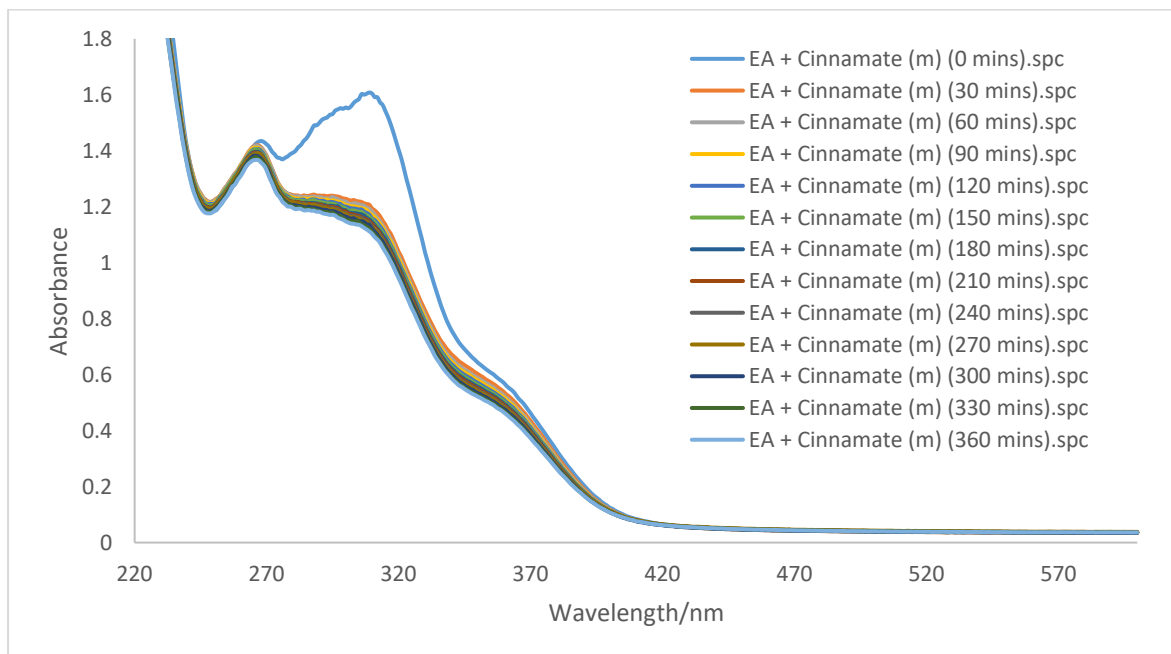


Figure 4.50: Photostability of EHMC mixed with the ethyl acetate phenolic acid extract from ultrasonic-assisted extraction of the Cancer Bush and dissolved in methanol. The spectra were recorded every 30 minutes for a total period of six hours, and were acquired in a 1 cm pathlength quartz cuvette against air as the reference.

The diethyl ether layer and the ethyl acetate layer extracts were not soluble in ethyl acetate or cyclohexane and, therefore, studies were not conducted in those solvents. A solubility test was conducted to determine if the extracts were soluble in any other solvents. This test showed that the phenolic acid extracts were only soluble in methanol.

In summary, phenolic acids are able to absorb at wavelengths similar to photolabile UV absorbers. The use of extracts containing these compounds allowed for successful photostabilisation of the chemical absorbers. Therefore, it is assumed that if this technology is introduced into a sunscreen formulation, there is a potential to photostabilise chemical UV absorbers and scavenge free radicals. The efficacy of the formulation will increase and the potential for adverse reactions would decrease.

4.1.6 Phenolic acids extracted from tea leaves

Natural compounds have grown in interest as potential agents for sunscreen formulations due to their powerful antioxidant potential and photoprotective capabilities.¹⁴⁵ Natural compounds contain high amounts of polyphenols that have been shown to have an abundance of health benefits. Studies have shown that naturally occurring polyphenols are able to neutralise free radicals, aid in inhibiting damage caused by free radicals, and prevent various oxidative stress.^{226, 245, 246} Commonly used UV filters formulated in sunscreens are not effective against ROS.²²⁶ Therefore, sunscreen formulations must include polyphenols to neutralise ROS through their antioxidant benefits.

Tea is obtained from the plant *Camellia sinensis*. Tea extracts are a natural source of polyphenolic compounds and are well known for their antioxidant capabilities. Tea polyphenolics have been shown to contain photoprotective properties and have exhibited the ability to quench singlet oxygen, and superoxide and hydroxyl radicals.²³⁸ Tea can be found in abundance and is relatively inexpensive.

Two types of teas: Rooibos and green tea, obtained from a local South African market were investigated for their phenolic content. The ethanol-water extraction method described in Section 3.3 was used to extract phenolic acids from Rooibos tea and green tea. The solid extracts obtained were dissolved in ethyl acetate and diluted in methanol for UV analysis. A Cancer Bush extract obtained by the same procedure was assessed against the tea extracts to compare the polyphenolic extraction efficiency. The photostability studies were also compared. Table 4.6 reveals the yields of green and Rooibos teas, and Cancer Bush extracts obtained.

Table 4.6: Amounts of materials used to extract phenolic acids from teas and the Cancer Bush, and the yields of extracts obtained

	Green tea	Rooibos tea	Cancer Bush plant
Mass of leaves/g	5.0018	5.0008	5.0208
Mass of extract/g	0.6787	0.072	0.3717
Yield/%	19.99	1.44	7.40

4.1.6.1 Green tea

Green tea extracts are receiving increased attention worldwide as a cosmetic component. This is due to their powerful antioxidant activity, low photoinstability, free radical scavenging ability and disease-preventing properties.²⁹²⁻²⁹⁴ There is a need to enhance the efficacy of current sunscreens and natural products containing polyphenols are being investigated for that purpose. Green tea polyphenols are able to safeguard against oxidative stress and possess anti-inflammatory benefits.²⁹⁵

A study conducted by Garbossa *et al.*²⁹³ showed that green tea extracts contain a higher polyphenolic content than other tea extracts. A high phenolic content is associated with a high UV absorption capability and this is seen in the UV spectrum shown in Figure 4.51. The UV spectrum shows that green tea absorbs in the UVC range, with the tail end of the peak absorbing in the UVB range, exhibiting maximum absorbance of 0.96 at 275 nm. At this λ_{max} , an increase in absorbance was seen after 30-minutes irradiation until 270 minutes, thereafter, the absorbance values decreased. The increase in absorption seen after irradiation shows that photodegradation does not take place. However, a conversion is seen at around 260 nm wavelength. This conversion increases after each irradiation period. Hence, irradiation causes interaction between the components of the green tea extract that improve its UV absorption ability.

The disadvantage with green tea polyphenols, as seen in the UV spectrum, are that they do not provide sufficient protection against the UVB and UVA radiation. This implies that green tea polyphenols need to be combined with other UV filters in sunscreen formulations. The combination may have synergistic or additive photoprotective capabilities when compared with either agent alone. Green tea polyphenols cannot be used as a good alternative for conventional

sunscreens as they do not absorb in the required UV region. However, they can be included for their effective chemopreventative and anti-inflammatory properties, as well as alleviate allergic reactions to persons who react to conventional sunscreens.⁷⁸ Green tea is also known to contain antioxidants which can help to delay the signs of ageing. Green tea is considered safe (GRAS status),²⁹⁶ but a thorough safety and toxicity study is essential.

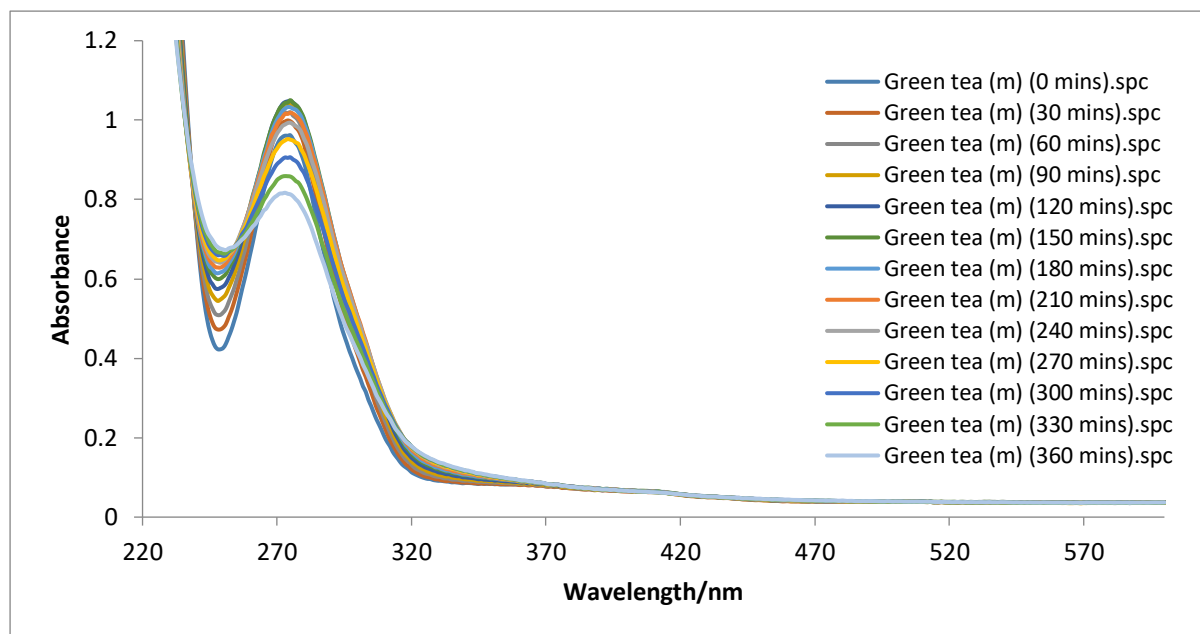


Figure 4.51: Photostability of an ethanol-water green tea extract dissolved in methanol. The spectra were recorded every 30 minutes for a total period of six hours, and were acquired in a 1 cm pathlength quartz cuvette against air as the reference.

4.1.6.2 Rooibos tea

Aspalathus linearis, commonly known as Rooibos, is an indigenous leguminous shrub found in the native region of the Cedarberg mountains in South Africa.²⁹⁷ Rooibos tea is known to possess various health-giving properties due to its rich source of phenolic acids and flavonoids.^{242, 298} The leaves and stems are used to produce unfermented and fermented Rooibos tea and the phenolic composition of the tea extract is dependent on the processing. Unfermented Rooibos contains high levels of flavonoids when compared with fermented rooibos.²⁹⁹ Fermented Rooibos tea has been shown to contain various biological properties. These include the calming of various stomach issues, relieving allergies, reducing nervous tension, and topical treatment of dermatological diseases such as photosensitive dermatitis.^{300,}

Bramati *et al.*²⁹⁹ and McKay *et al.*³⁰² showed that the antioxidant activity found in unfermented Rooibos was due to the presence of polyphenolic fractions. The polyphenolics determined were aspalathin, isoorientin, orientin, rutin, isovitexin, isoquercitrin, hyperoside, quercetin, luteolin and chrysoeryol.²⁹⁹ Bramati *et al.*²⁹⁹ also found that copious amounts of polyphenols were found in unfermented Rooibos than in fermented Rooibos. This occurrence is due to the fermentation process which causes the degradation of aspalathin.³⁰³ During the fermentation process, aspalathin is oxidised and undergoes cyclisation to form the flavanones, dihydro-orientin and dihydro-iso-orientin.^{303, 304} Joubert³⁰³ and Dziedzic *et al.*³⁰⁵ showed that the flavanones are less effective than dihydrochalcones from unfermented Rooibos as the fermentation process decreases the hydrogen donating ability in fermented Rooibos.

The UV spectra obtained for the Rooibos extract dissolved in methanol is shown in Figure 4.52. Absorbance was seen from ~252 to 434 nm wavelengths. The absorbance range displays that Rooibos is able to provide broad spectrum protection against UV radiation. However, degradation is seen during irradiation, although no conversion was observed. Therefore, the combination of Rooibos with other agents may have synergistic or additive photoprotective capabilities.

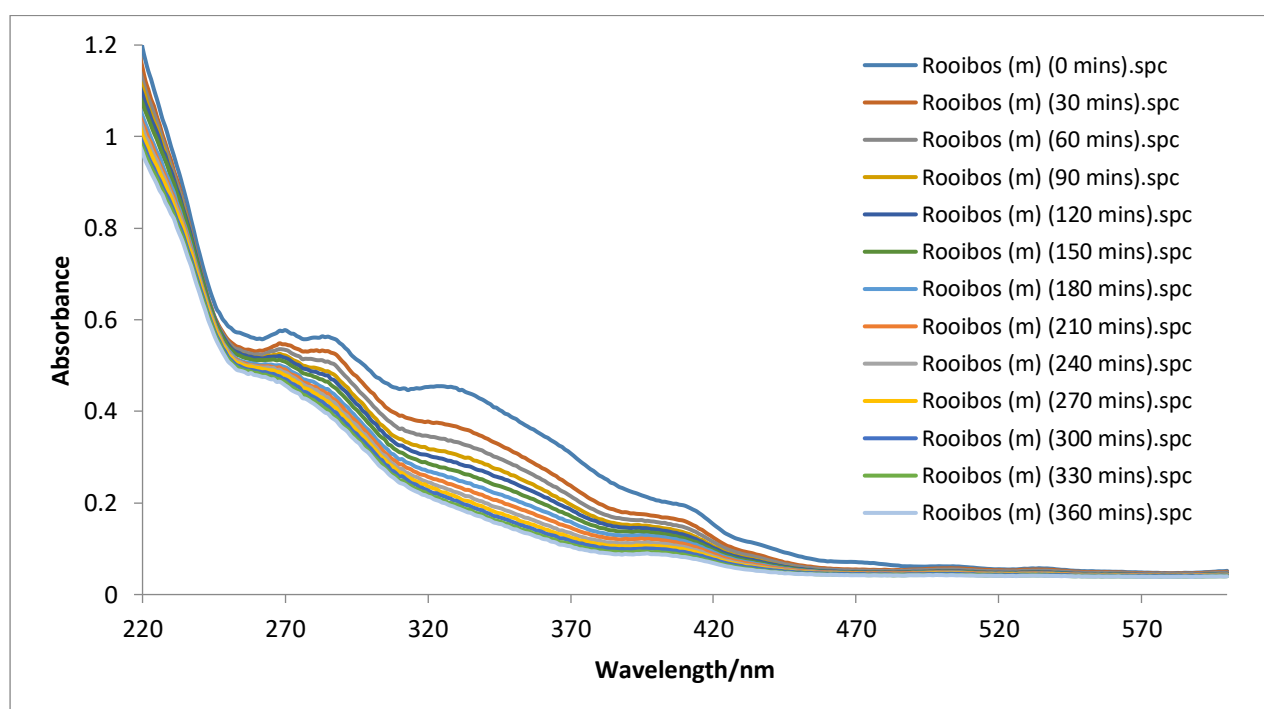


Figure 4.52: Photostability of an ethanol-water Rooibos tea extract dissolved in methanol. The spectra were recorded every 30 minutes for a total period of six hours, and were acquired in a 1 cm pathlength quartz cuvette against air as the reference.

4.1.6.3 Cancer Bush

For comparison, the phenolic acid extraction method used for tea leaves was repeated with the Cancer Bush powder. The UV spectra obtained for the Cancer Bush plant using the tea extraction method, shown in Figure 4.53, were almost exact replicas of those achieved for the ethanol-water extraction process shown in Section 4.1.2.2. The absorption achieved in both the UVB and UVA regions was slightly lower than that achieved for the ethanol-water extraction process. An arbitrary wavelength chosen at 295 nm showed an initial absorbance of 0.39. The arbitrary wavelength chosen for the UVA region was 350 nm, which showed an initial absorbance of 0.27. After the first 30 minutes of irradiation, the absorption decreased to 0.27 and 0.11, respectively. The absorbance continued to decrease after each irradiation period.

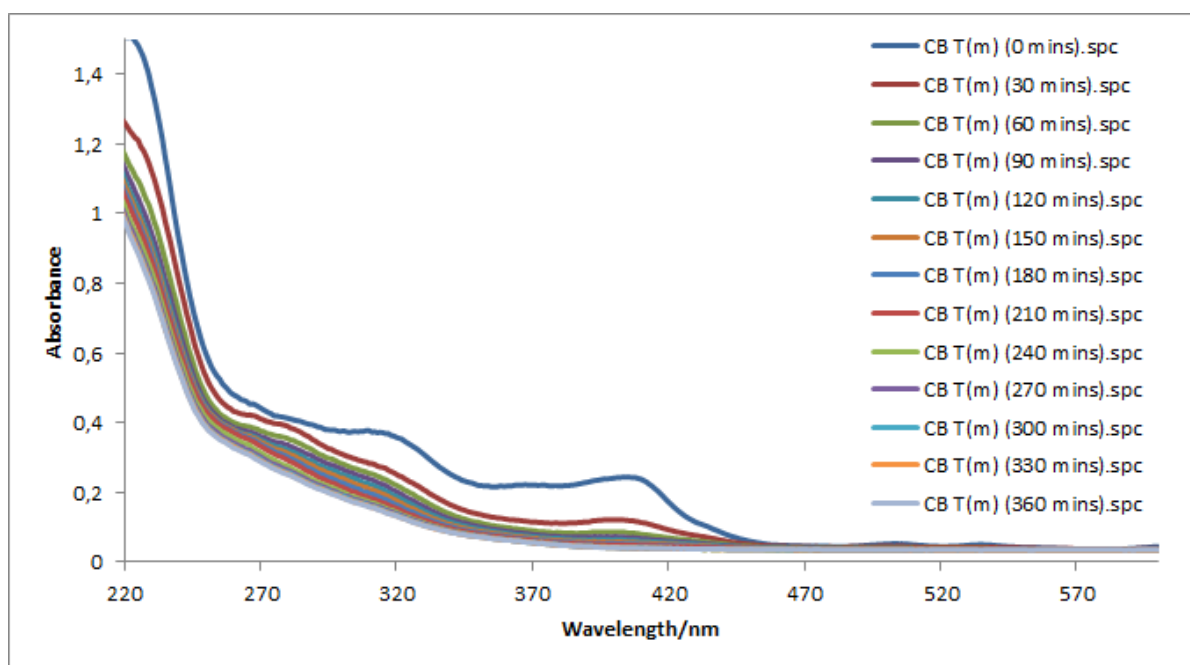


Figure 4.53: Photostability of an ethanol-water Cancer Bush extract dissolved in methanol. The spectra were recorded every 30 minutes for a total period of six hours, and were acquired in a 1 cm pathlength quartz cuvette against air as the reference.

4.1.6.4 Mixture of green tea, rooibos tea and Cancer Bush plant extracts

The green tea, Rooibos tea and Cancer Bush plant extracts were combined and dissolved in methanol to determine if synergistic or additive photoprotection could be achieved. The UV spectra obtained for this mixture are shown in Figure 4.54. A significant amount of absorbance was observed in the UVB region with poor absorbance seen in the UVA region. A maximum absorbance of 0.96 was seen at 280 nm. After six hours of irradiation, the absorbance seen at 280 nm decreased to 0.61. At 350 nm the absorbance decreased from 0.32 to 0.18 after six

hours of irradiation. Therefore, the blend of the tea extracts with the Cancer Bush plant was not as effective in providing UVB protection as seen with green tea, and UVA protection as seen with Rooibos tea alone.

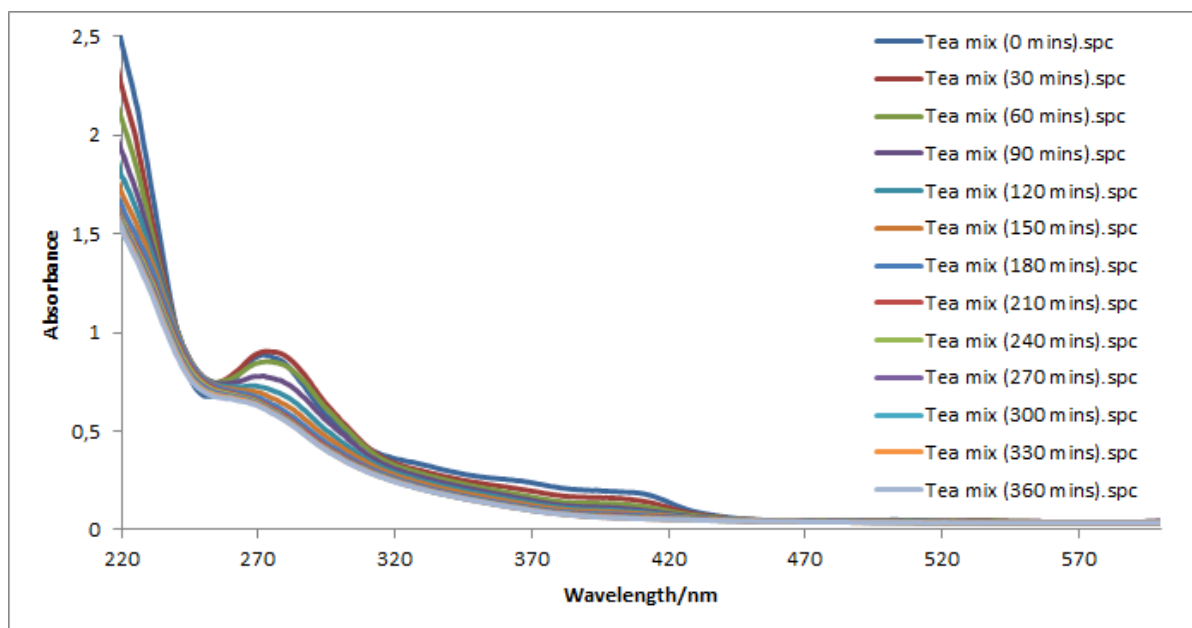


Figure 4.54: Photostability of green and Rooibos tea extracts, with the Cancer Bush plant extract dissolved in methanol. The spectra were recorded every 30 minutes for a total period of six hours, and were acquired in a 1 cm pathlength quartz cuvette against air as the reference.

In summary, the results obtained may be related to the quality and quantity of phenolic content, as well as the interaction with other components in solution. Phenolic compounds are known to be susceptible to solar radiation as a result of chemical structure.³⁰⁶ However, due to the variation observed in the UV spectra of the tea extractions, it can be said that the photostability of phenolics greatly depends on the variety of compounds available in the extract, as well as the type of structure.

4.2 HPLC analysis

Phenolic acids found in plant material consist of a complex matrix. The structural diversity of phenolic acids influences their polarity and acidity.³⁰⁷ The sample preparation, extraction and purification of phenolic acids are critical steps for HPLC in order to quantify the plant material. Staliskas³⁰⁷ and Waksmundzka-Hajnos³⁰⁸ have extensively reviewed the methods required for the preparation and determination of phenolic acids.

Air-drying or freeze-drying of the solid matrices is the first step required for sample preparation. This step is then followed by grinding, milling and homogenisation.³⁰⁷ Step two involves the extraction of phenolic acids. This is further divided into two steps: crude extraction and a purification technique. Crude extraction is achieved by liquid-solid extraction (LSE) using either methanol, ethanol, acetone, diethyl ether, or ethyl acetate as the solvent system.^{307, 308} The techniques required for LSE can include ultrasound-assisted extraction, Soxhlet extraction, supercritical fluid extraction, pressurised solvent extraction, or microwave-assisted solvent extraction. Waksmundzka-Hajnos³⁰⁸ studied the effects of LSE extraction techniques on phenolic acids and found that the yield achieved depended predominantly on the plant material used. For example, Soxhlet extraction was found to be the most effective when extracting phenolic acids from flowers.³⁰⁸ Zadernowski *et al.*³⁰⁹ found that extraction methods for plants are influenced by the free or bound forms of the phenolic acids. Both the free or bound types can be directly extracted by LSE. Bound phenolic acids are linked by ester, ether or acetal bonds, and the LSE method requires an acid or base hydrolysis step to separate the bond.^{307, 309}

A purification step can be conducted before analysis if the crude extract cannot be analysed directly after filtration. This depends on the type of sample or analytical method used. The purification can be accomplished using LLE or solid-phase extraction using either ethyl acetate or diethyl ether as the solvent system.³⁰⁸ The purification step can also be used to remove lipophilic substances from the extract, as described in Section 3.2.4.3, by using non-polar solvents such as petroleum ether or hexane. Lipophilic substances are removed from plant extracts in order to remove interferences from HPLC analysis.

4.2.1 Phenolic acids

Reversed-phase (RP) HPLC with a C18 column is frequently used for the separation and determination of phenolic acids in plant extracts.³⁰⁷ This method is suitable for the separation of phenolic acids as they differ in polarity. The elution of the phenolic acids can be optimised by varying the composition of the mobile phase. Tarnawski *et al.*¹⁵¹ developed a procedure to successfully separate phenolic acids from concentrated peak extracts. However, in this work, the method had to be modified due to a different C18 column used.

The separation of the six phenolic acid standards was achieved by RP-HPLC. The standards were prepared according to the method described in Section 3.7.3.4. Stock solutions of the six phenolic acids were prepared by dissolving one gram of each acid to a total volume of 100 ml

of methanol. The mass and concentration of each stock solution is shown in Table 4.7. A Zorbax C18 column was used with isocratic elution of a 12% MeOH and 1% acetic acid in Millipore water mobile phase. The injection volume was 10 μl and the flow rate was set at 1.000 ml min^{-1} . An aliquot of 10 μl of each phenolic acid stock solution was injected separately into the HPLC. Each phenolic acid injection allowed for the identification of the retention time and UV/visible wavelength of maximum absorption (λ_{max}). The peak profiles in each of the UV/visible spectra were used to identify a distinct λ_{max} for each phenolic acid. The retention times and maximum absorption, λ_{max} , for the six phenolic acids were identified and are shown in Table 4.8.

Table 4.7: Preparation of standard phenolic acid solutions made up to a total volume of 100 ml in MeOH

Phenolic acid standard	Mass/g	Actual conc./mg ml⁻¹
gallic acid	1.0012	10.012
<i>p</i> -hydroxybenzoic acid	1.0000	10.000
vanillic acid	1.0043	10.043
caffeic acid	1.0004	10.004
syringic acid	1.0004	10.004
<i>p</i> -coumaric acid	1.0000	10.000

The UV spectra recorded by the PDA detector for each of the six phenolic acids are shown in Figure 4.55. A PDA detector is able to monitor multiple wavelengths simultaneously and is suitable for the analysis of phenolic acids due to their conjugation and aromatic bonds absorbing in the UV range between 200 and 360 nm.³⁰⁷ Benzoic acid derivatives show maximum absorption between 200 and 290 nm. Cinnamic acid derivatives show absorbance between 270 to 360 nm.³⁰⁷ The PDA detector used in this analysis was set to scan the eluates from 190 to 500 nm. The detection wavelengths for the chromatograms collected were set for each of the six λ_{max} values indicated in bold in Table 4.8.

Table 4.8: Retention times and λ_{\max} values for each phenolic acid standard

Phenolic acid	RT/min	λ_{\max}/nm
gallic acid	3.048	214/ 271 /230/376
<i>p</i> -hydroxybenzoic acid	11.095	215/ 255 /466
vanillic acid	17.524	213/228/ 260 /292/424
caffeic acid	19.164	214/ 323 /431
syringic acid	26.109	212/ 274 /230/431/476
<i>p</i> -coumaric acid	38.787	213/233/ 309 /431/481

Multi-standard solutions with concentrations of 10, 20, 40, 80 and 100 mg ml⁻¹ were prepared by diluting each standard stock solution respectively. The multi-standard solutions were prepared three times and analysed in triplicate by injecting into the chromatograph. Table 4.9 shows the actual concentrations of each multi-standard solution. Figure 4.56 shows the chromatogram of a 10 mg ml⁻¹ multi-standard solution monitored at 254 nm. All peaks were well resolved at the baseline. The run time for the standards was fixed at 42 minutes because the retention time observed for *p*-coumaric acid was 38 minutes.

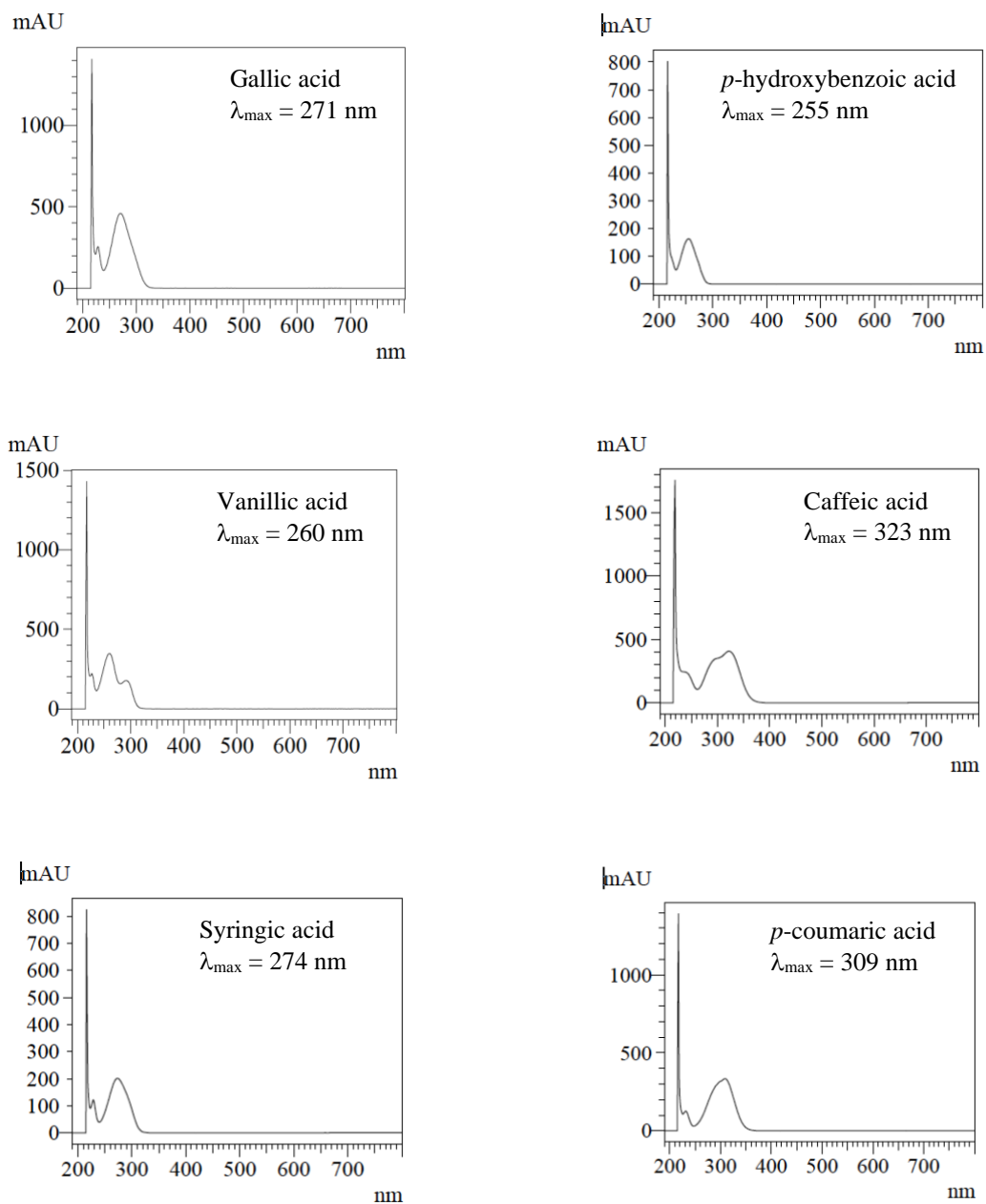


Figure 4.55: UV spectra of the six phenolic acid standards recorded by the PDA detector

Table 4.9: Concentration of each phenolic acid used for calibration

	Concentration of multi-standard solutions/mg ml⁻¹				
Nominal concentration	10	20	40	80	100
gallic acid	10.012	20.024	40.048	80.096	100.120
<i>p</i> -hydroxybenzoic acid	10.000	20.000	40.000	80.000	100.000
vanillic acid	10.043	20.086	40.172	80.344	100.430
caffeic acid	10.004	20.008	40.016	80.032	100.040
syringic acid	10.004	20.008	40.016	80.032	100.040
<i>p</i> -coumaric acid	10.000	20.000	40.000	80.000	100.000

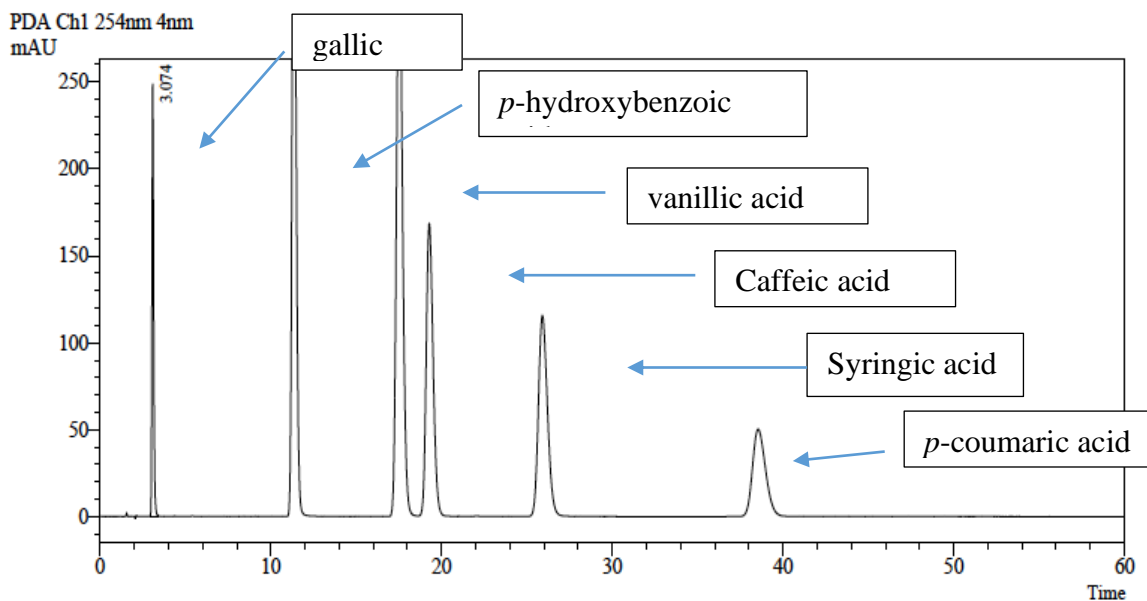
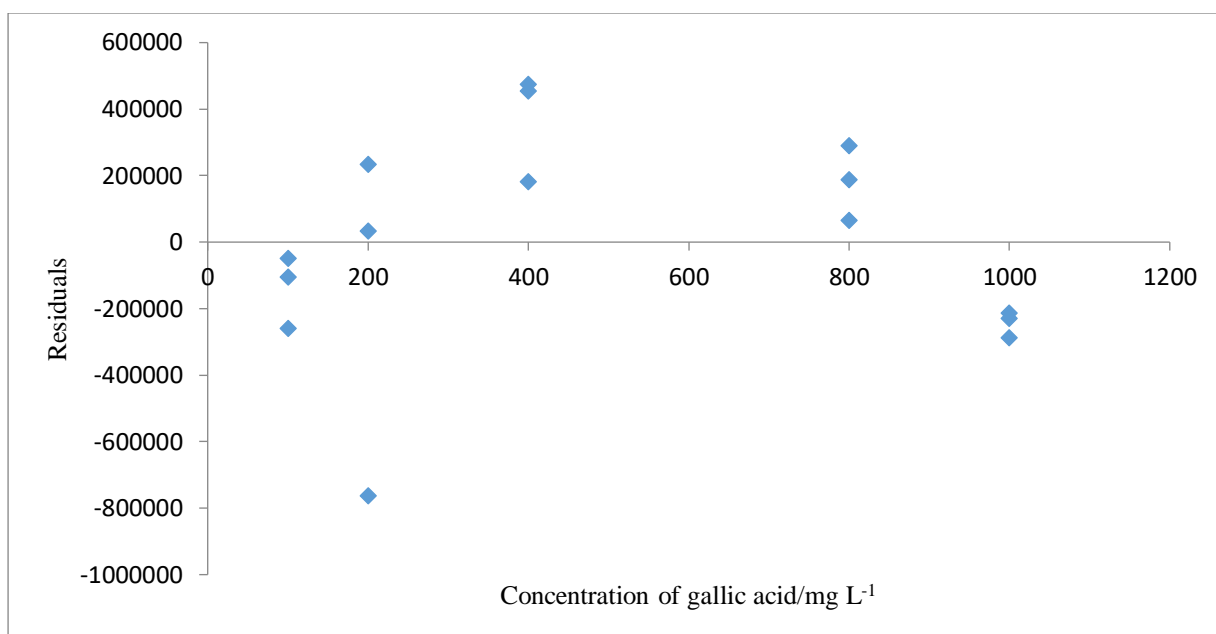
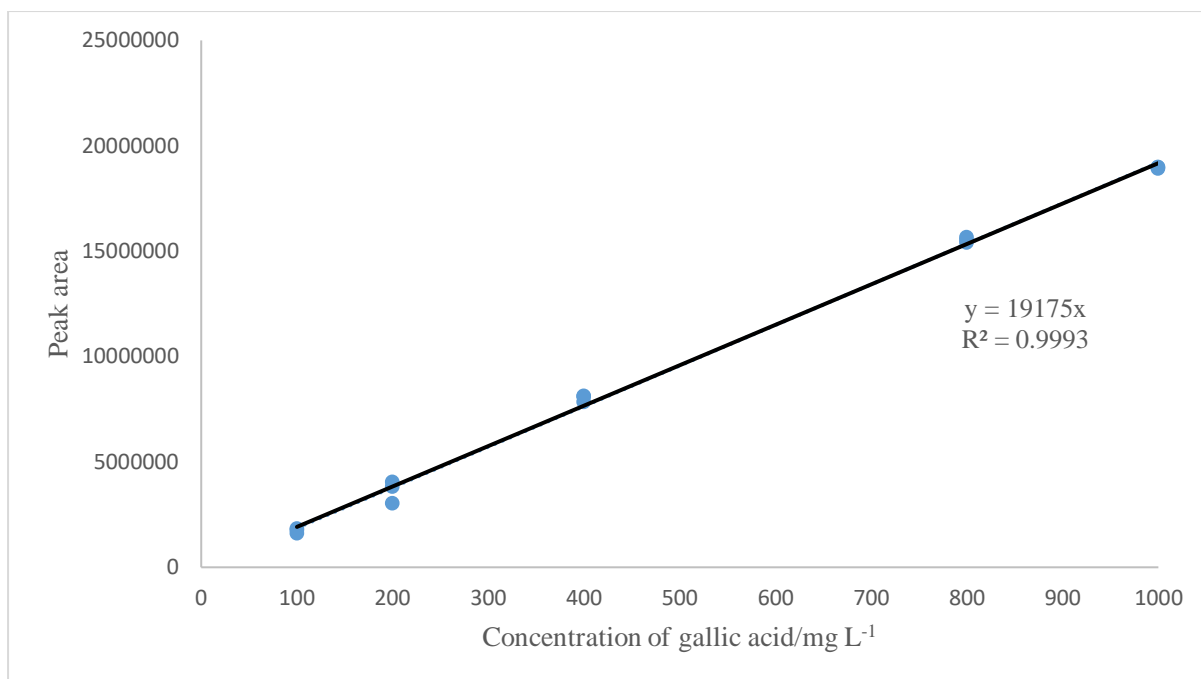
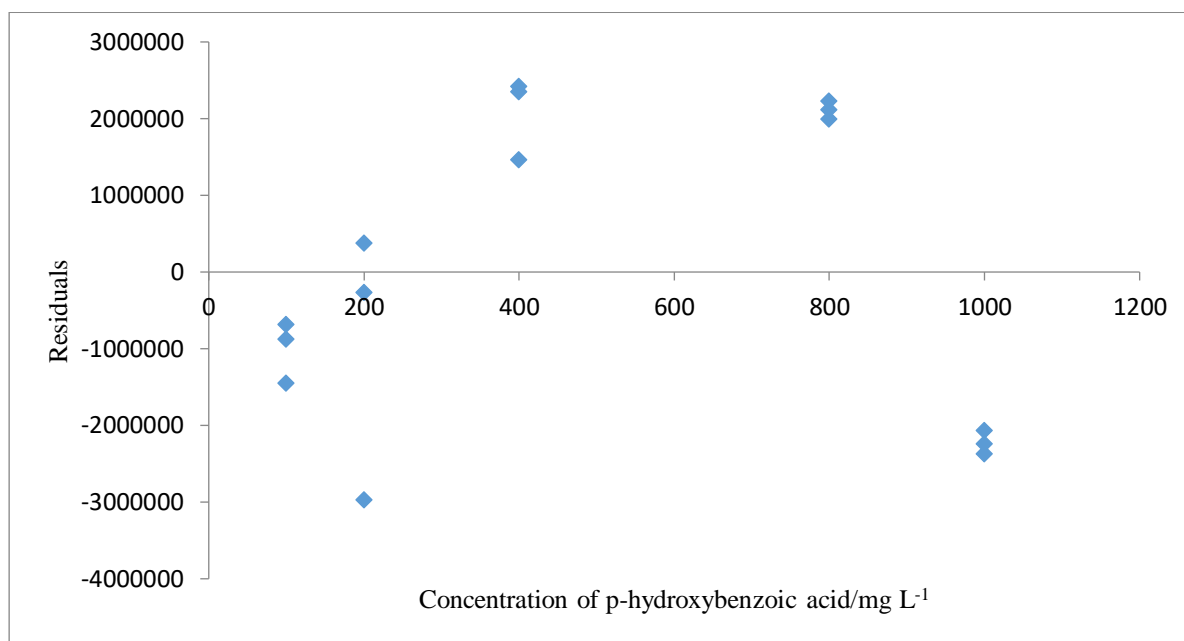
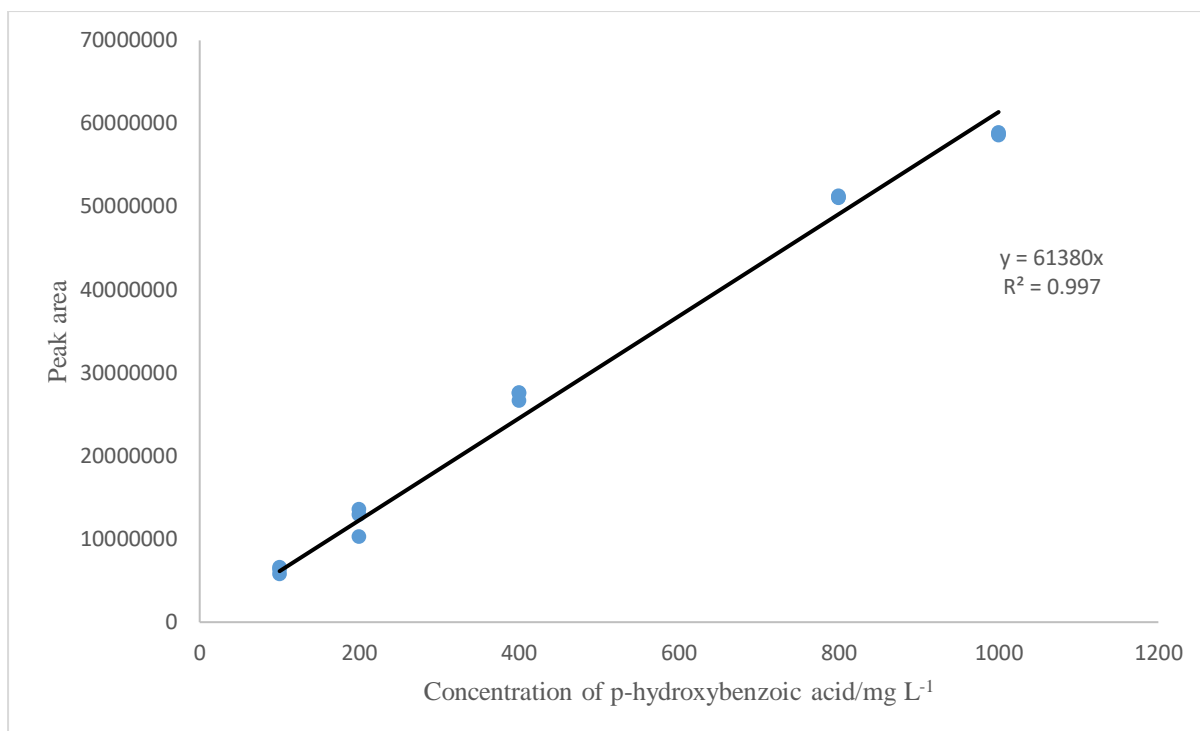


Figure 4.56: HPLC chromatogram of the 10 mg ml^{-1} multi-standard phenolic acid solution obtained at 254 nm with the mobile phase composition of 12% MeOH and 1% acetic acid in Millipore water. The column was a Zorbax Eclipse XDB C18, the flow rate was 1.00 ml min^{-1} , and the injection volume was $10 \text{ }\mu\text{l}$.

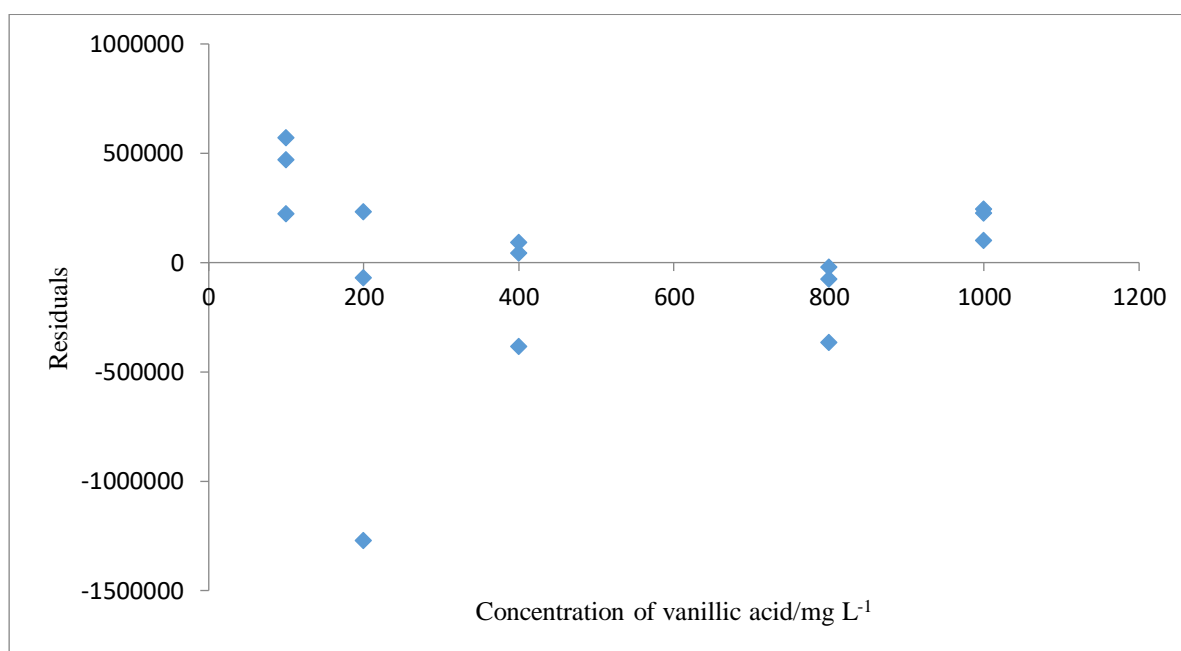
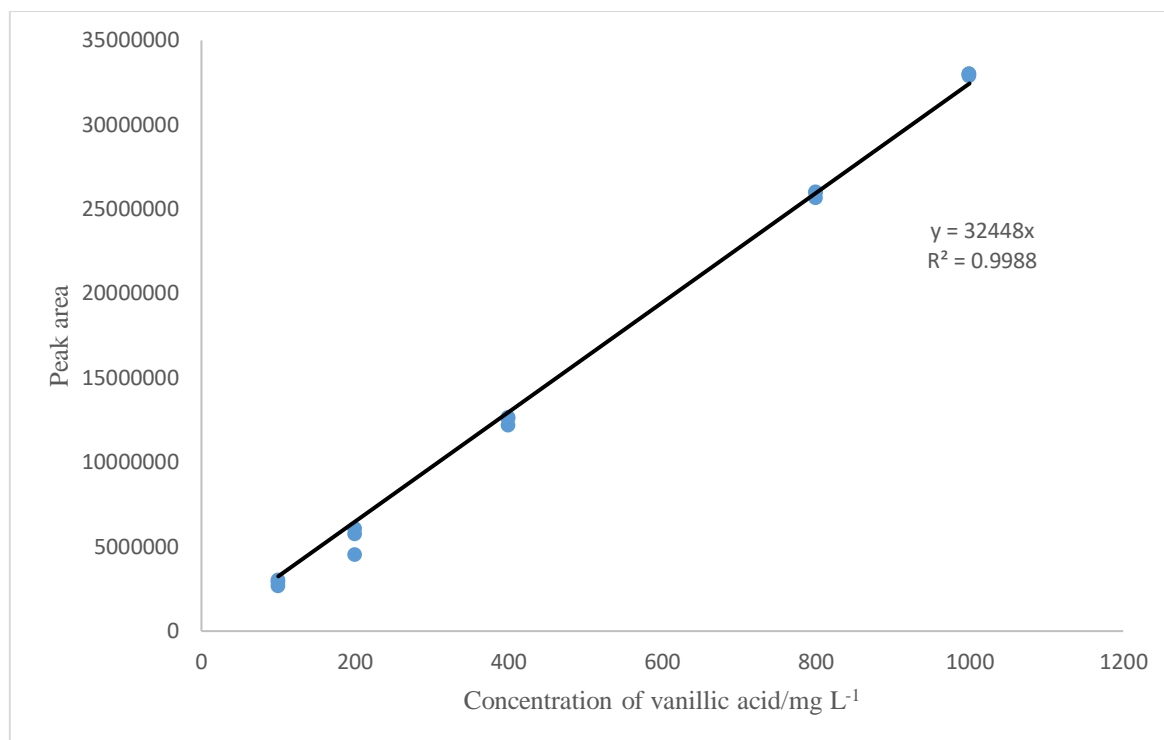
The order of elution was gallic acid (3.05 min), *p*-hydroxybenzoic acid (11.10 min), vanillic acid (17.52 min), caffeic acid (19.16 min), syringic acid (26.11 min), and *p*-coumaric acid (38.79 min). Calibration curves of peak areas obtained at 254 nm were plotted against the concentration of each standard by making use of the linear regression method from Microsoft Excel[®] Analysis ToolPak. The calibration curves and the residual plots obtained for the six phenolic acids are shown in Figure 4.57 (A-F). The calibration curves show that the concentrations used allowed for the instrument to respond linearly. The residual plots show a good distribution and no bias was detected.



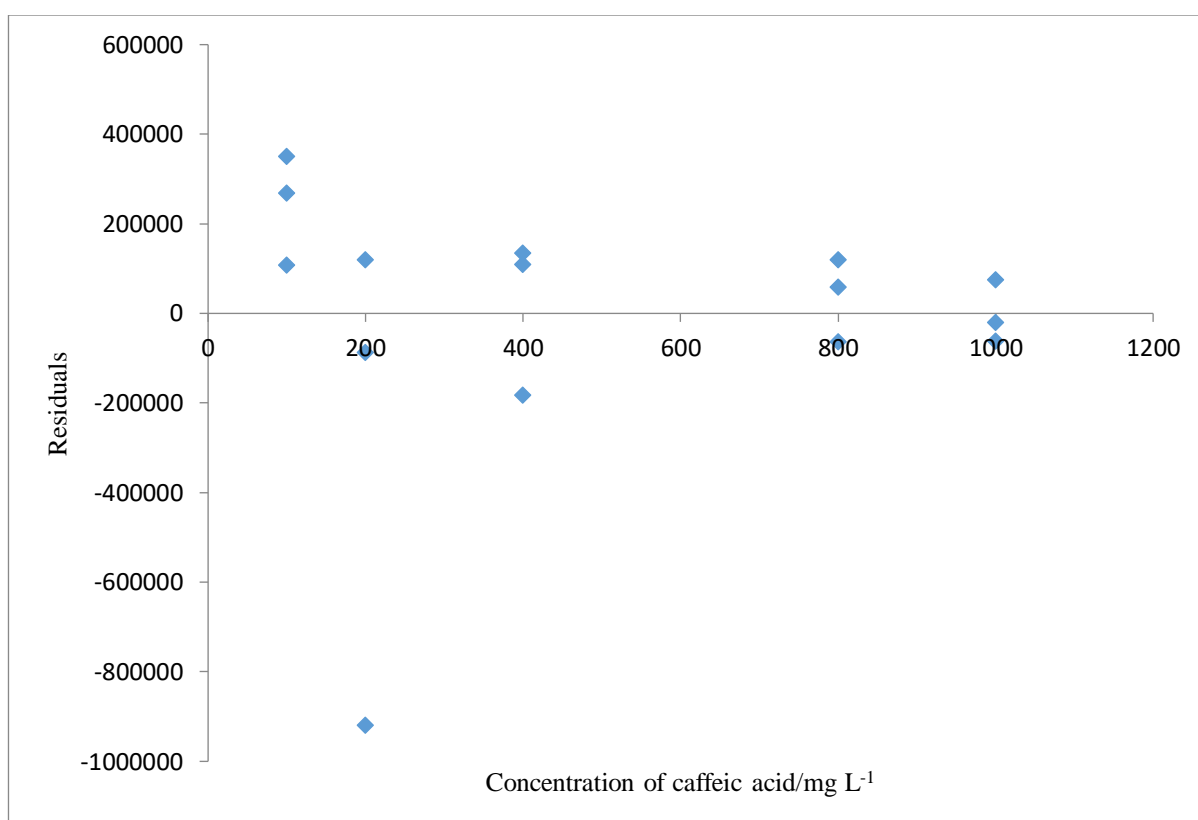
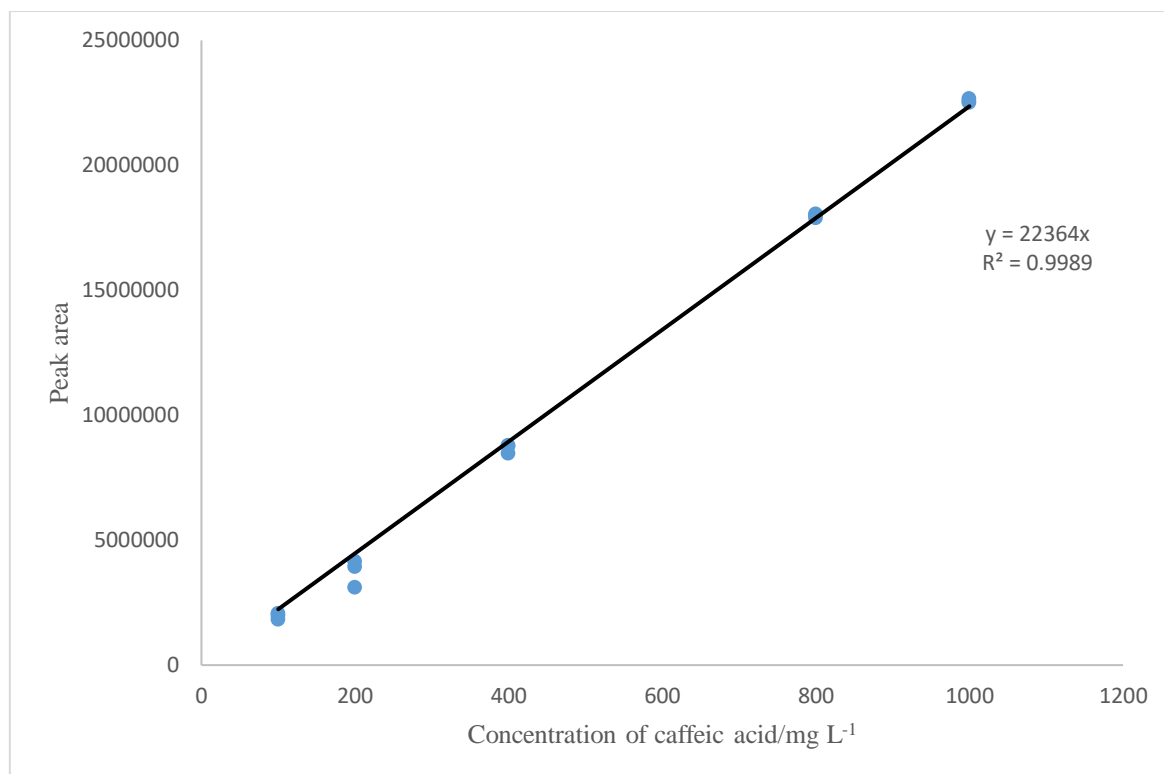
(A)



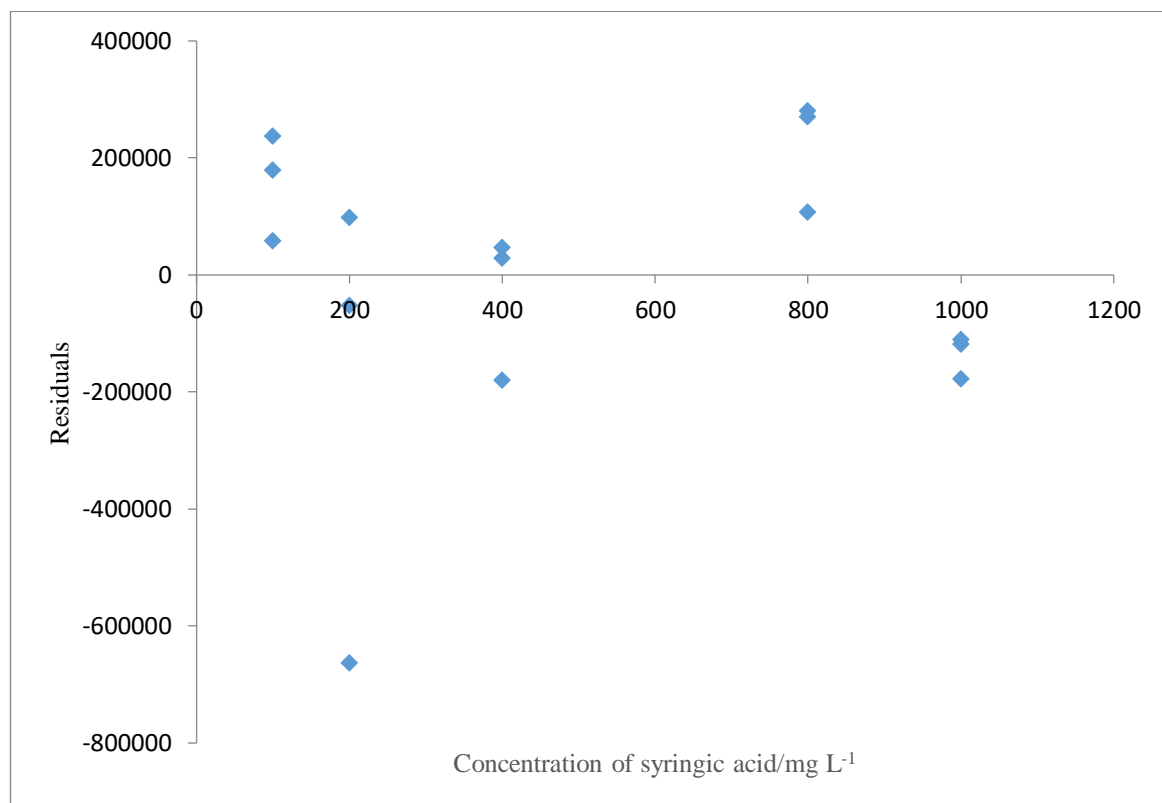
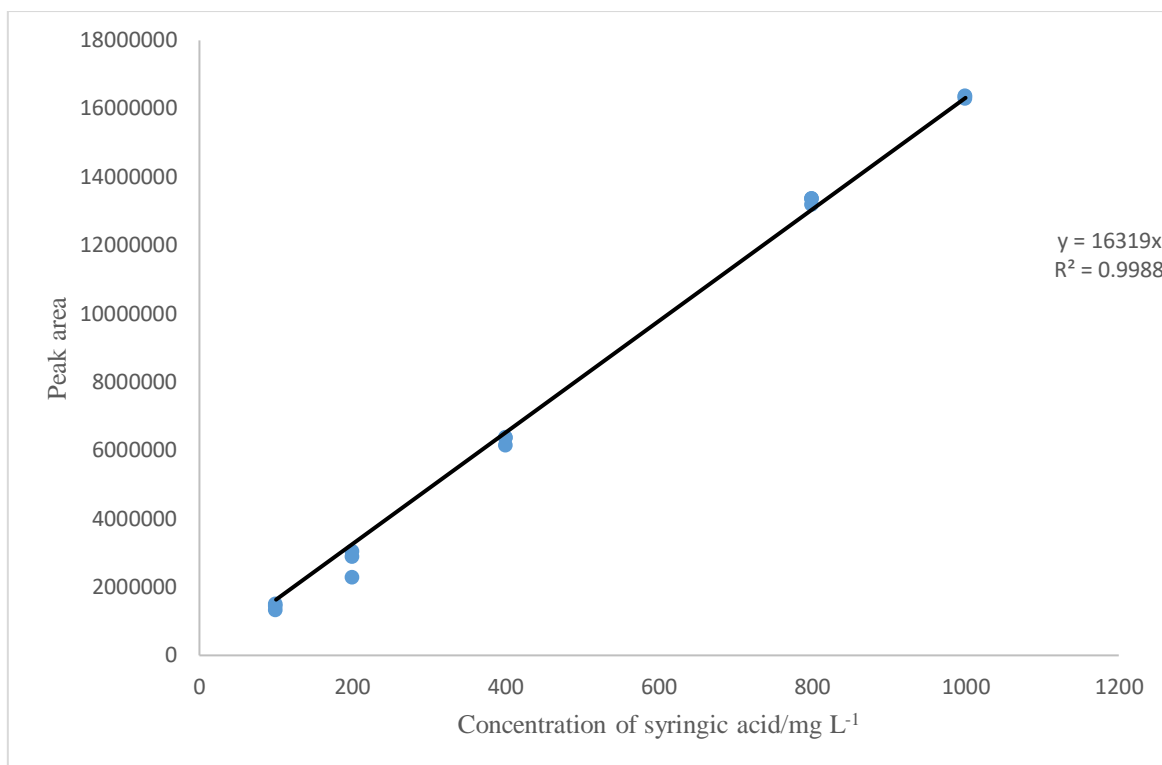
(B)



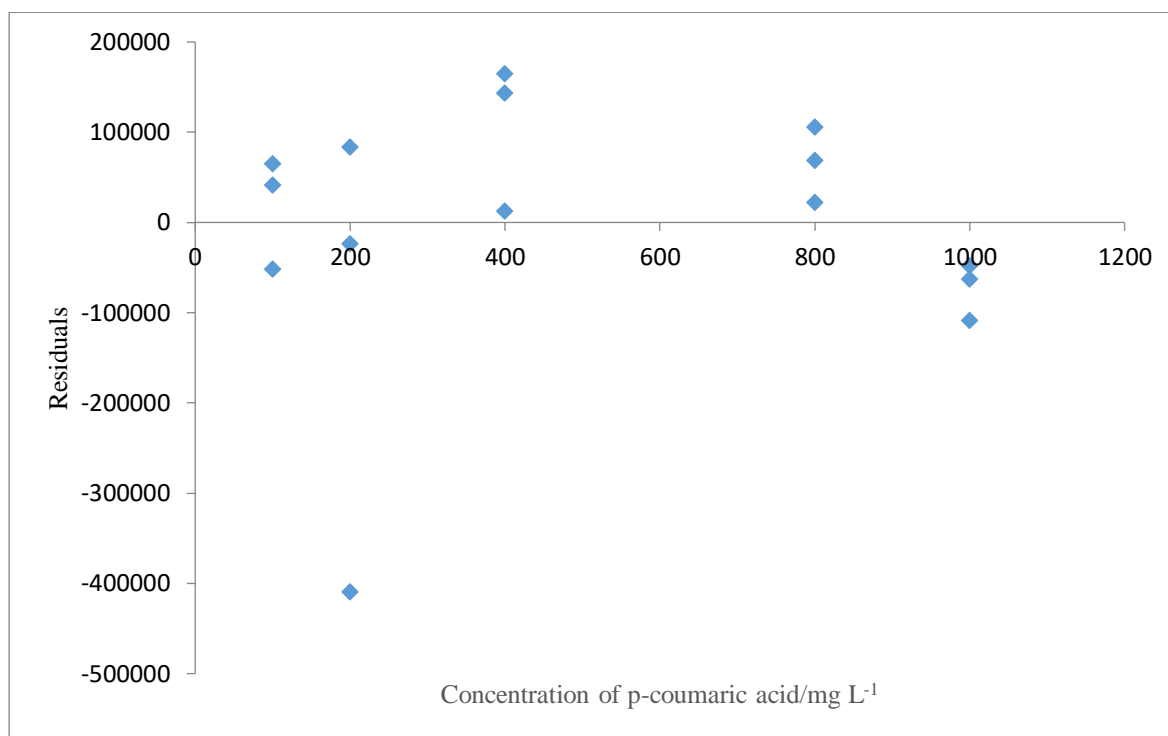
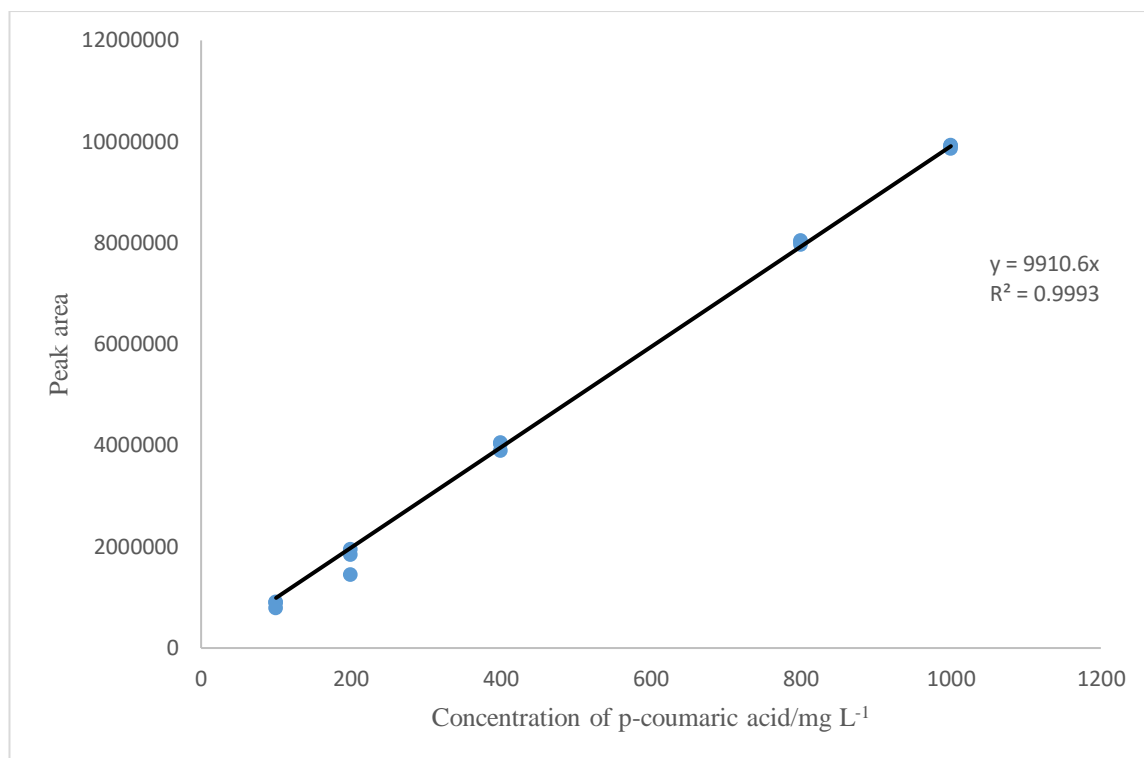
(C)



(D)



(E)



(F)

Figure 4.57: Calibration curves and residual plots for the determination of (A) gallic acid, (B) *p*-hydroxybenzoic acid, (C) vanillic acid, (D) caffeic acid, (E) syringic acid and (F) *p*-coumaric acid obtained at 254 nm.

The limits of detection (LOD) and limits of quantification (LOQ) of each phenolic acid were calculated from the slope and standard error of the slope of the calibration lines according to the method used by Bunhu.⁴⁷ Equation 7 shows the LOD and Equation 8 shows the LOQ.

$$\text{LOD} = 3 \frac{S_{y/x}}{m} \quad (7),$$

where y is the peak area, x is the concentration of the analyte, $S_{y/x}$ is the standard error of the slope of the calibration line, and m is the slope of the calibration curve.

$$\text{LOQ} = 3.33 S_{y/x} \quad (8)$$

Table 4.10 shows the LOD, LOQ, and R^2 values, and the calibration range for each phenolic acid. The R^2 values obtained for the six calibration curves are greater than 0.997 showing that good linearity was achieved for the calibration ranges. *p*-Hydroxybenzoic acid had the highest LOD, whilst *p*-coumaric acid had the lowest.

The equations of the straight lines obtained from the six calibration curves have the form $y = mx$, where y is the peak area, m is the slope, and x is the concentration of the analyte. These equations were used to calculate the concentrations of the phenolic acids identified in the Cancer Bush and tea extracts.

Table 4.10: Quality control parameters for the determination of phenolic acids

Acid	Calibration range/mg l ⁻¹	Slope (m)/10 ⁴ ml mg ⁻¹	Standard error of slope ($S_{y/x}$)/10 ²	R^2	LOD/10 ⁻² ml mg ⁻¹	LOQ/10 ² ml mg ⁻¹
gallic	10.012 – 100.120	1.92	2.52	0.9993	3.95	8,39
<i>p</i> -hydroxybenzoic	10.000 – 100.000	6.14	15.22	0.9916	23.8	50.70
vanillic	10.043 – 100.430	3.25	3.39	0.9987	5.31	11.30

caffeic	10.004 – 100.040	2.24	2.23	0.9988	3.50	7.44
syringic	10.004 – 100.040	1.71	1.84	0.9984	2.89	6.16
<i>p</i> -coumaric	10.000 – 100.000	1.63	1.06	0.9986	1.67	3.55

4.2.2 Cancer Bush plant

The Cancer Bush ethanol-water extract and the Cancer Bush extract from the tea extraction method were analysed by HPLC according to methods described in Section 3.7.3.7. The run time was set for 60 minutes. Impurity peaks were observed between 0.50 and 7.12 minutes which were confirmed to be solvent peaks as these were observed during the blank injections. Figures 4.58 and 4.60 show the chromatograms obtained for the Cancer Bush ethanol-water extract and the Cancer Bush extract obtained by the tea extraction technique respectively. The chromatograms were monitored at 254 and 309 nm. The results show that there were slight deviations in the retention times when compared with the retention times of the phenolic acid standards. The differences could be ascribed to the column temperature, polarity of the mobile phase, or the lengthy time difference between the runs of the standards and the extracts. Therefore, peaks were assigned to values closest to the retention times of the standards and peak areas were assessed.

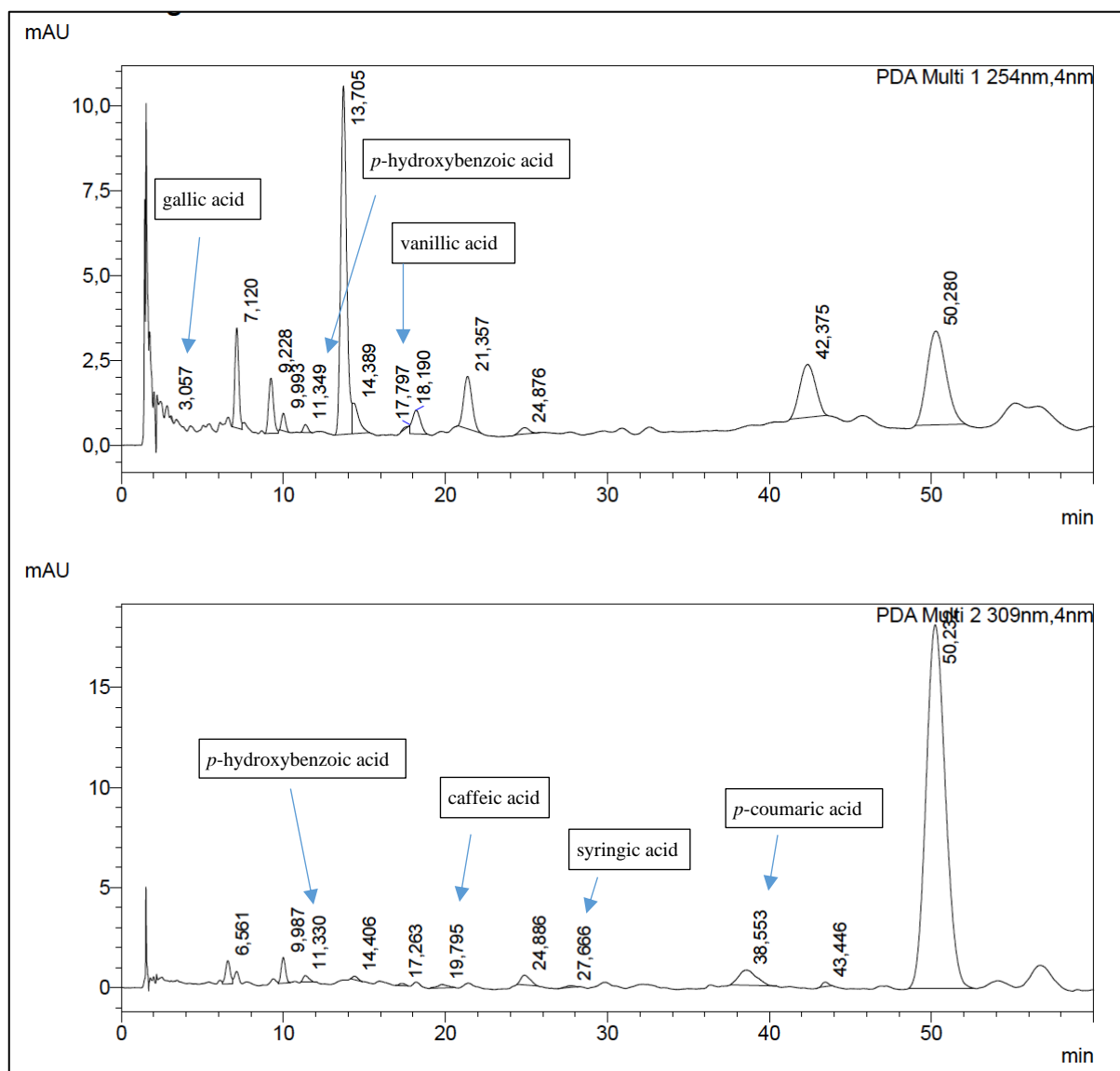


Figure 4.58: HPLC chromatograms of the Cancer Bush ethanol-water extract obtained at 254 and 309 nm with the mobile phase composition of 12% MeOH and 1% acetic acid in Millipore water. The column was a Zorbax Eclipse XDB C18, and the flow rate was 1.00 ml min^{-1} . The injected volume was 10 μl .

All six of the phenolic acids were identified in the extract by matching the retention time and UV spectra for the Cancer Bush ethanol-water extract. Three of the phenolic acids were seen at 254 nm with the order of elution as gallic acid (3.057 min), *p*-hydroxybenzoic acid (11.349 min), and vanillic acid (17.797 min). Four of the phenolic acids were observed at 309 nm, and the order of elution was *p*-hydroxybenzoic acid (11.330 min), caffeic acid (19.795 min), syringic acid (27.666 min), and *p*-coumaric acid (38.553 min). There were also predominant unidentified peaks at 7.120, 13.705, 42.375 and 50.280 mins.

The UV spectra obtained during the HPLC analysis were used to confirm the presence of each phenolic acid. An example is shown in Figure 4.59 where the UV spectra for vanillic acid (acquired for the chromatogram detected at 254 nm) and *p*-hydroxybenzoic acid (acquired for the chromatogram detected at 309 nm) are shown respectively. It is important to note that the wavelengths observed in Figure 4.59 will never be an identical match to those observed for the individual phenolic acid standards in Table 4.8. This is due to the analyte variations found in the extracts.

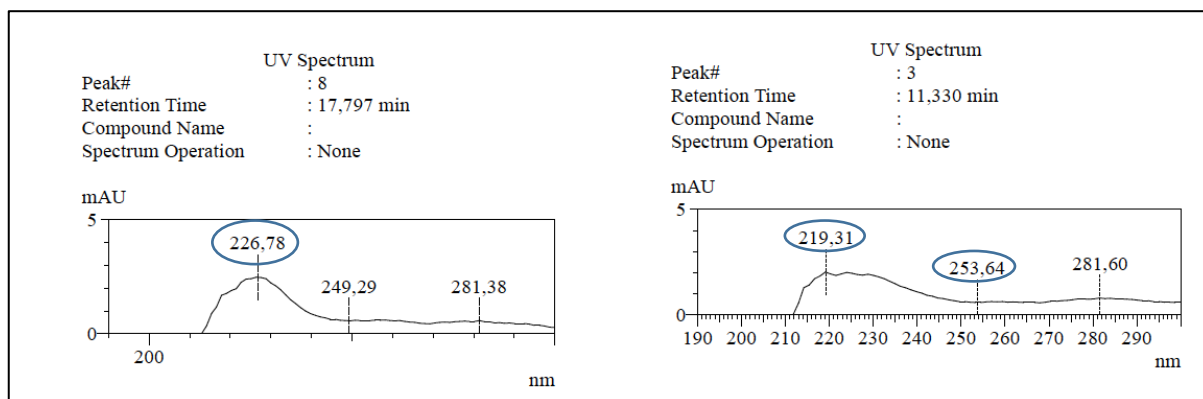


Figure 4.59: UV spectra observed for vanillic acid and *p*-hydroxybenzoic acid respectively.

The chromatogram obtained for the Cancer Bush extract using the tea extraction method, shown in Figure 4.60, shows that only five of the six phenolic acids were identified. The order of elution observed at 254 nm was gallic acid (3.075 min) and vanillic acid (17.990 min). At 309 nm the order of elution was vanillic acid (18.006 min), caffeic acid (19.438 min) and *p*-coumaric acid (37.677 min).

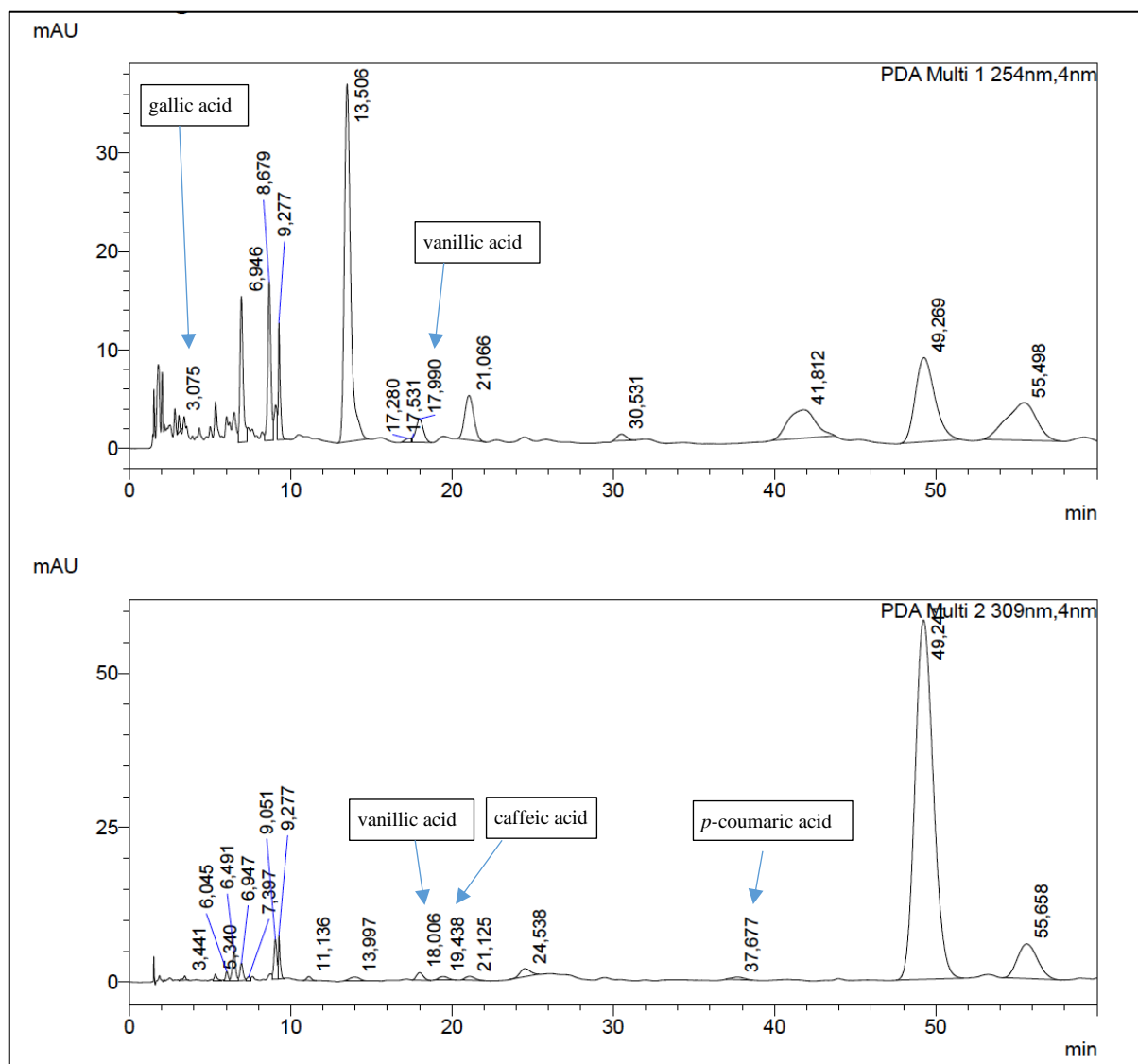


Figure 4.60: HPLC chromatograms of the Cancer Bush extract (tea extraction method) obtained at 254 and 309 nm with the mobile phase composition of 12% MeOH and 1% acetic acid in Millipore water. The column was a Zorbax Eclipse XDB C18, the flow rate was 1.00 ml min⁻¹. The injected volume was 10 μ l.

4.2.3 Tea extracts

Both the green tea extract and the Rooibos tea extract were analysed by means of HPLC to determine if any of the selected six phenolic acids could be identified. The green tea extract HPLC chromatogram is shown in Figure 4.61. Only three of the phenolic acids were successfully identified by matching the retention times and UV spectra. The order of elution at 254 nm was *p*-hydroxybenzoic acid (11.004 min) and *p*-coumaric acid (40.892 min). Syringic acid (27.798 min) was identified at 309 nm. Four of the six phenolic acids were identified in the Rooibos tea extract and the chromatograms are shown in Figure 4.62. The

order of elution at 254 nm was *p*-hydroxybenzoic acid (10.611 min), caffeic acid (21.087 min), and syringic acid (27.396 min). At 309 nm, syringic acid (27.479 min) was observed again, and *p*-coumaric acid (37.814 min).

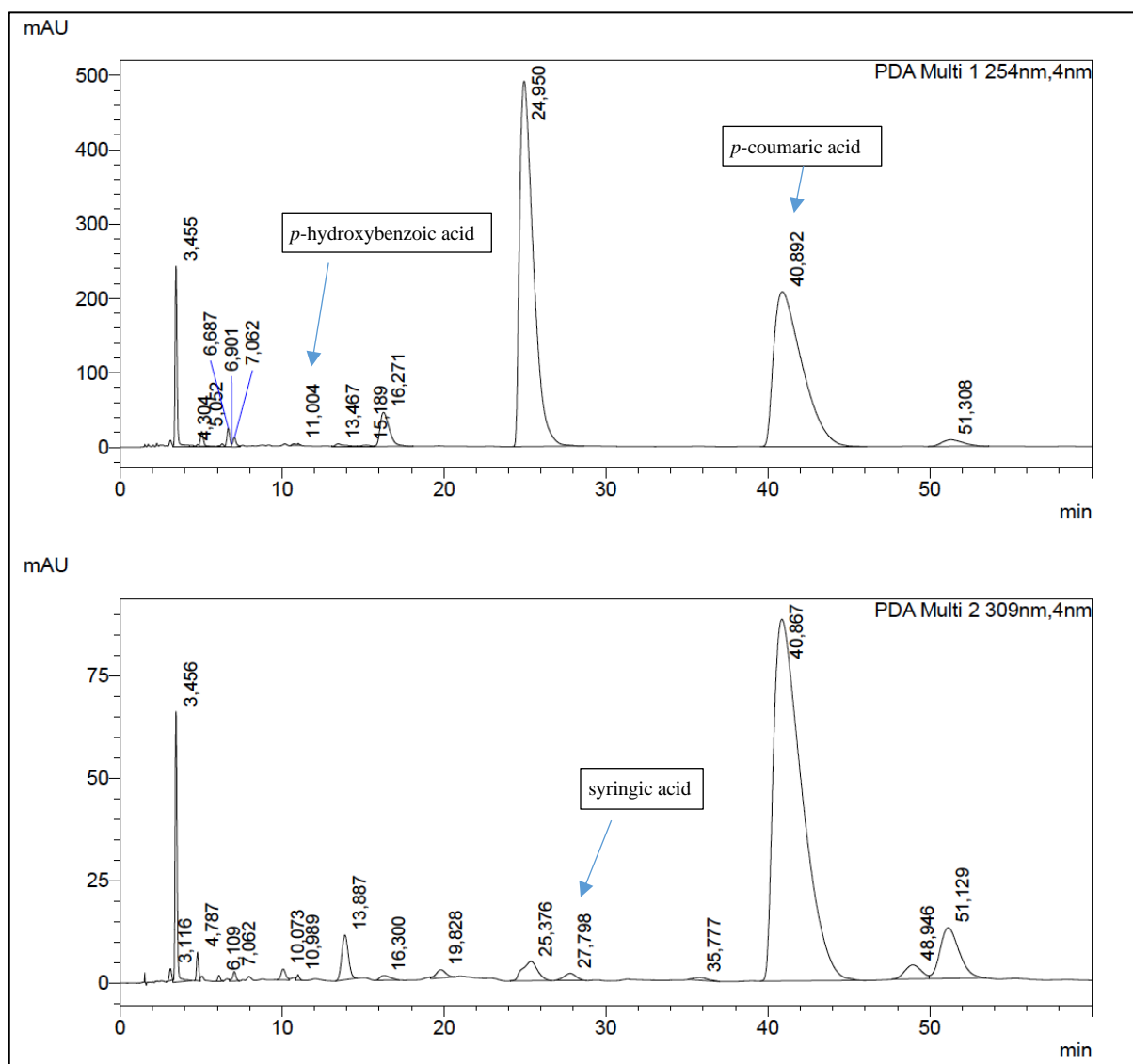


Figure 4.61: HPLC chromatograms of the green tea extract obtained at 254 and 309 nm with the mobile phase composition of 12% MeOH and 1% acetic acid in Millipore water. The column was a Zorbax Eclipse XDB C18, the flow rate was 1.00 ml min⁻¹. The injected volume was 10 μ l.

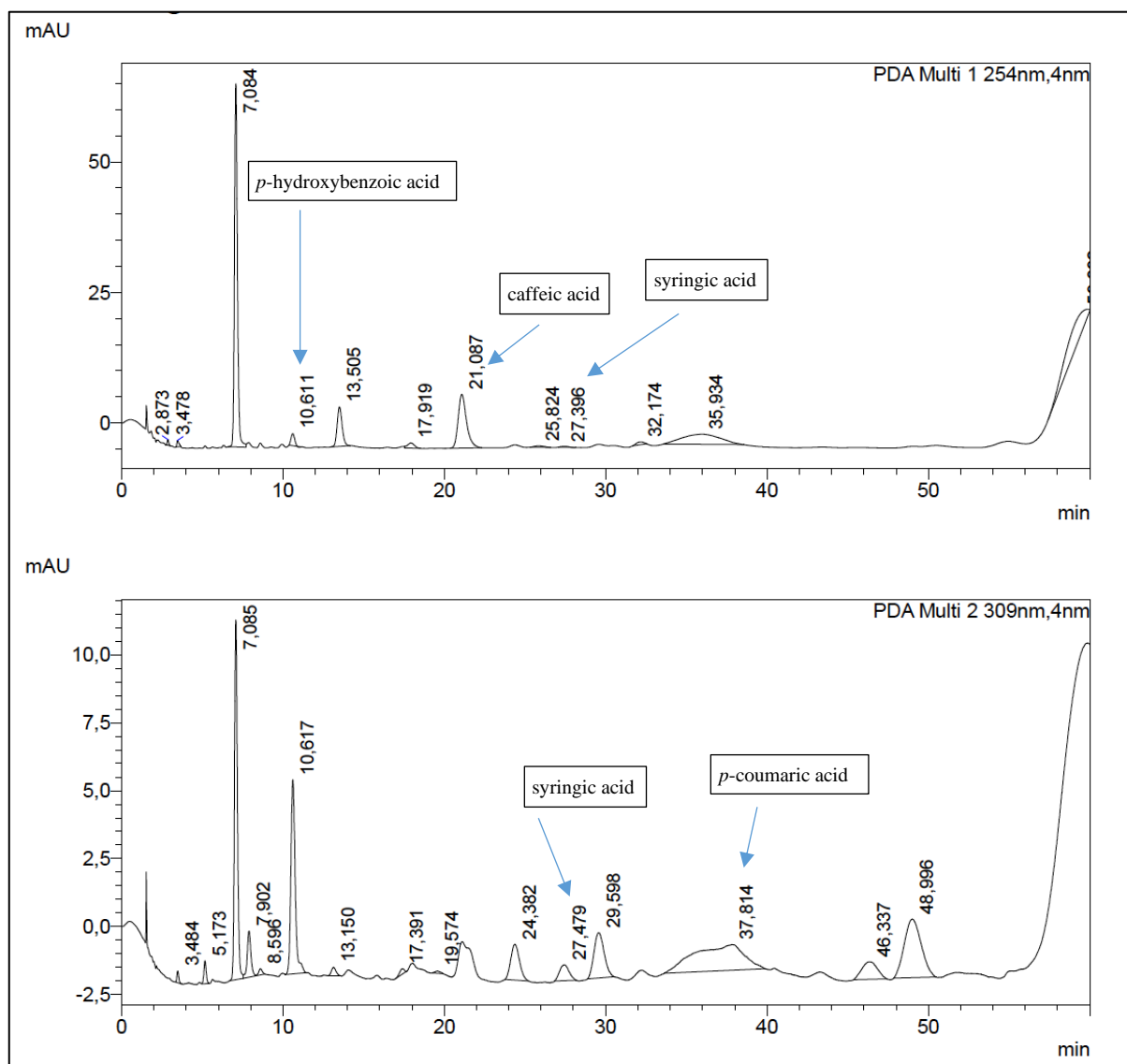


Figure 4.62: HPLC chromatograms of the Rooibos tea extract obtained at 254 and 309 nm with mobile phase composition of 12% MeOH and 1% acetic acid in Millipore water. The column was a Zorbax Eclipse XDB C18, the flow rate was 1.00 ml min⁻¹. The injected volume was 10 µl.

4.2.4 Concentrations of phenolic acids in plant extracts

The equations of the calibration curves for the phenolic acids (shown in Figure 4.57) were used to determine the concentrations of the identified phenolic acids in each extract. The results for the Cancer Bush and tea extracts are shown in Table 4.11.

For example, from the calibration curve of gallic acid, $y = 19175x$

$$\text{Therefore, } x = \frac{y}{m} = \frac{\text{peak area}}{\text{slope}} = \text{mg l}^{-1}$$

$$x = \frac{520}{19175} = 0.027 \text{ mg l}^{-1}$$

Table 4.11: Concentration (mg l⁻¹) of phenolic acids found in plant extracts

Phenolic acids	Straight line equation	Cancer Bush ethanol-water extract	Cancer Bush tea extraction method	Green tea extract	Rooibos tea extract
gallic acid	$y = 19175x$	0.027	0.438	ND	ND
<i>p</i> -hydroxybenzoic acid	$y = 61380x$	0.075	ND	0.860	0.556
vanillic acid	$y = 32448x$	0.035	2.389	ND	ND
caffeic acid	$y = 22364x$	0.368	1.008	ND	16.54
syringic acid	$y = 16319x$	0.204	ND	5.552	1.481
<i>p</i> -coumaric acid	$y = 9910.6x$	5.848	2.151	2552.074	20.840

ND – not determined

A comparison of the phenolic acid content of the Cancer Bush extracts showed that the concentration of *p*-coumaric acid was the highest. The Cancer Bush tea extraction method did not show the presence of *p*-hydroxybenzoic and syringic acids. The concentration of gallic acid was the lowest when compared with the other five phenolic acids. Only three phenolic acids were identified in the green tea extract, and four in the Rooibos tea extract.

The concentration of *p*-coumaric acid was the highest in the green tea and Rooibos tea extracts. Kaeswurm *et al.*³¹⁰ determined the absorption coefficients of selected phenolic acid structures in three different solvent systems. The coefficients were used to determine accurate concentrations of phenolic acids. According to Beer's law, a substance's light absorption is proportional to its concentration. The larger the molar absorption coefficient, the larger the absorption capabilities. Their work showed that *p*-coumaric, for example, obtained a molar

absorption coefficient of $18279 \pm 1237 \text{ L mol}^{-1} \text{ cm}^{-1}$ at 309 nm in a methanol-water solvent and $17867 \pm 301 \text{ L mol}^{-1} \text{ cm}^{-1}$ in water. Therefore, at the same concentration, *p*-coumaric is a better absorber and since it was found predominantly in the extracts, there will be a better coverage in the UVB region where it has its wavelength of maximum absorption.

The HPLC analysis was successful in identifying phenolic acids in the extracts by matching the retention times and UV spectra to those of authentic samples. Not all of the six phenolic acids tested were successfully identified in each of the six extracts.

4.3 Sunscreens

The sun is a key player in sustaining life on planet Earth and is responsible for the production of a wide range of electromagnetic radiation. Visible light is the only form of electromagnetic radiation that can be seen by the human eye. Infrared radiation is responsible for heating of the planet, and UV radiation is responsible for sunburn, sun tan and the risk of skin cancer. UV radiation is divided into three ranges: UVA, UVB and UVC. UVC is the radiation in the 100 to 280 nm range and is absorbed completely by the Earth's ozone layer. Some of the UVB (280 to 315 nm) is absorbed by the ozone layer, and all of the UVA (315 to 400 nm) radiation is transmitted through the ozone layer. For a long time, UVB was blamed for UV damage to the skin but recent studies have shown that UVA is also responsible.^{54, 67}

A first-degree radiation burn is considered mild sunburn and produces reddening of the skin with accompanying pain. As the skin repairs itself, the outer layers of the epidermis will peel within a week with persistent reddening and itching. A second-degree burn is a result of prolonged exposure to UV radiation. This is characterised by blistering of the skin and more severe pain. A third degree sunburn is rare. The production of a pigment known as melanin is one of the human body's natural defences against UV radiation. The production of melanin causes the skin to darken. Melanin production and how an individual responds to UV radiation greatly depends on the colour of the skin and genetic factors. However, even if an individual has dark skin or the ability to produce melanin rapidly when exposed, overexposure can also result in sunburn.

Sunscreen products are cosmetic formulations that include UV filter substances that are designed to protect human skin from erythema. These products include chemical UV-absorbing compounds and physical blockers that allow UV light to be reflected, scattered, or absorbed. However, UV filters are susceptible to photodegradation over time, their degradation

products can be phototoxic, and they provide protection only over a limited wavelength region. This becomes problematic for sunscreen products as their efficacy is reduced.

Sunscreen products come with the instruction of being most effective when reapplied every three to four hours. This rule applies when using general sunscreens at the beach, for example. The reason for this rule is that the UV filters used in these sunscreen products tend to degrade over time which is proportional to the amount of exposure received. They also rub off with wear and towelling, and disperse while swimming. In the cosmetic industry, UV filters are added to everyday products, such as lipsticks and everyday foundations. A woman on the go, she is only likely to apply her foundation in the morning, and is out about her day leaving no time for reapplication. As a cosmetic scientist, it is necessary to ensure that these products have a level of protection from the sun as this adds to the appeal of the product, thereby increasing sales. Sun protection is one of the major concerns in the cosmetic industry and the need to increase the efficacy of the formulation is necessary.

This section discusses the results obtained for the experimental procedure described in Section 3.9.

4.3.1 UV analysis of sunscreen formulations

An example formulation obtained from the formulation guideline by a supplier chemical company, Elementis (S22011-02), was selected as a standard. This formulation was selected based on the incorporation of ethanol at 5%. The alcohol is needed for the dissolution of the plant extracts. The formulation selected was an SPF 15 which gave room for an increase in SPF with the addition of the plant extract. The standard formulation as per guideline, SPF 1.1, was prepared and UV analysis was performed. The absorbance values obtained were well above 1.2 and did not obey Beer's Law. The percentage of UV filters was then halved and the percentage volume was made up with water. This formulation was labelled SPF 1.2.

All photostability studies of the sunscreen formulations were conducted on sunny days. The surface application density of the sunscreen product was $\sim 1.0 \text{ mg cm}^{-2}$ for adults.⁹⁵ However, for aesthetic reasons, consumers typically apply much less than the recommended value. The prepared sunscreen formulations were applied on a quartz plate by using a smearing technique with a gloved finger. The product was spotted in a circular fashion to achieve a uniform thin film. The quartz plates were weighed on application of the sunscreen, allowed to dry for 30 minutes in a dark place, reweighed, and then exposed to sunlight for a total duration of six hours. The mass variations are reported in Table 4.12.

Table 4.12: Masses obtained for photostability analysis of sunscreen formulations

	SPF 1.2	SPF 1.3	SPF 2.1	SPF 2.2	SPF 2.3
Mass of empty quartz plate/g	5.6872	5.6888	5.6893	5.6872	5.6860
mass of plate + sunscreen/g	5.7880	5.7765	5.7014	5.7114	5.6902
Mass of plate after drying/g	5.6837	5.6843	5.6940	5.6830	5.6892
Mass of sunscreen after drying/g	0.0035	0.0046	0.0047	0.0042	0.0032

4.3.1.1 Example formulation – Elementis Maui Milk SPF 15

Figure 4.63 shows the UV spectra obtained for formulation SPF 1.2 taken every 30 minutes for a total period of six hours. Maximum wavelengths, λ_{\max} , were observed at 236, 306 and 350 nm. After six hours of irradiation, the absorbance decreased from 0.748 to 0.682 (-0.120) at 236 nm and from 0.616 to 0.495 (-0.121) at 306 nm. The peak observed at 306 nm matches the absorption profile of the salicylate derivatives: octisalate (ethylhexyl salicylate) and homosalate (homomenthyl salicylate). The UVB filter, octocrylene, also has a maximum absorbance at 307 nm. Therefore, the peak shown at 306 nm is the sum of the three UVB filters as absorbance is known to be additive. The peak shown at 350 nm is due to the absorbance capabilities of avobenzone which has an absorption profile ranging from 310 to 400 nm. The absorbance at 350 nm decreased from 0.412 to 0.303 (-0.109). This decrease in absorbance is similar to the loss of absorbance seen in avobenzone dissolved in methanol (Figure 4.2). However, there were no isosbestic points noted. Therefore, no photodegradation reactions occur. The decrease in absorbance of 0.12 is negligible for a sunscreen formulation.

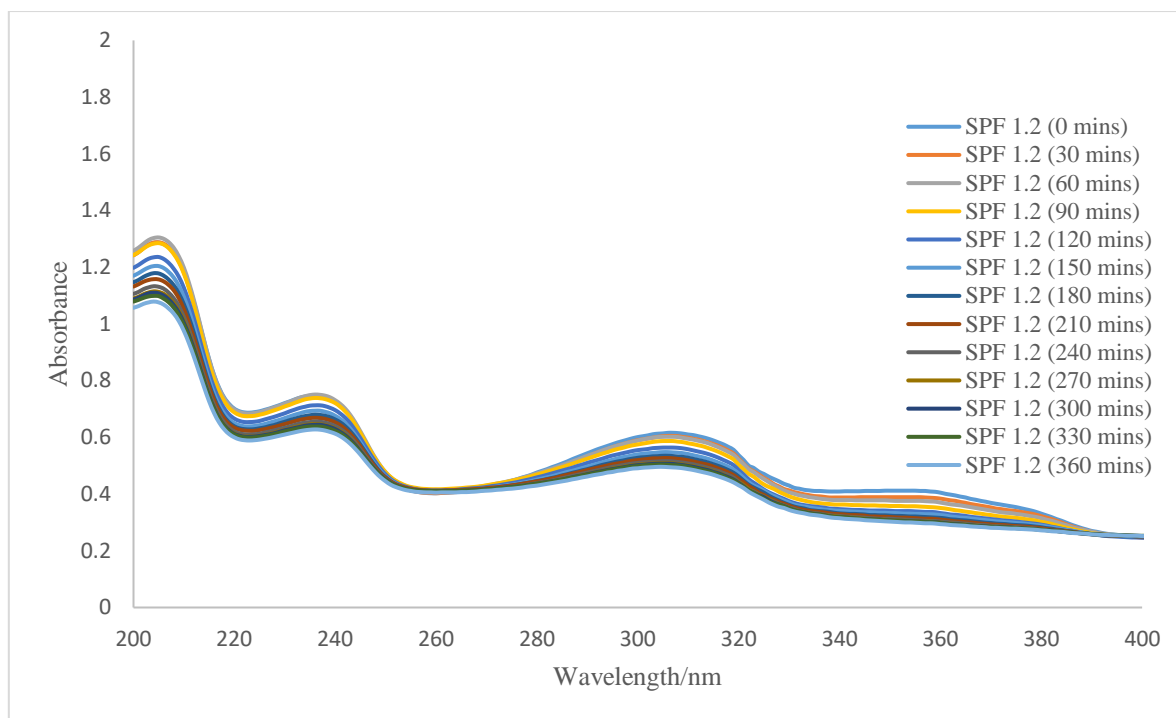


Figure 4.63: SPF 1.2 – Example formulation with reduced concentrations of UV filters. The spectra were recorded every 30 minutes for a total period of six hours, and were acquired on a quartz plate against air as the reference.

Chemical UV filters are used in high concentrations in sunscreen products on the market in order to achieve a high SPF value. Higher concentrations can cause toxicity and allergic reactions. Safer sunscreens are currently being explored which include lower concentrations of chemical UV filters with effective UV protection. Natural compounds, such as phenolic acids, are being considered as safer sunscreen active ingredients because of their ability to attenuate UV radiation, and are harmless and do not cause irritation to the skin.

Formulation SPF 1.3 was prepared with the addition of the Cancer Bush ethanol-water extract dissolved in 5% ethanol. The UV spectrum obtained for SPF 1.3, shown in Figure 4.64, showed a significant increase in absorption. Maximum wavelengths, λ_{\max} , at 236, 306 and 347 nm increased from 0.748 to 1.559, 0.616 to 1.364, and 0.412 to 0.978 respectively with the addition of the Cancer Bush extract. The absorbance values increased from 1.559 to 1.604 (0.045) after six hours of irradiation at 236 nm. The peak observed for the collective absorption of UVB filters: octisalate, homosalate, and octocrylene, at 306 nm decreased from 1.364 to 1.359 (-0.005). This showed that the addition of the Cancer Bush extract improved the stability of the UVB filters. The peak observed for UVA filter, avobenzone, shifted to 347 nm. The absorbance decreased from 0.978 to 0.788 (-0.19). Although, the loss of absorbance was

similar to avobenzone without the plant extract, a higher absorbance was achieved. Therefore, the increase in absorbance seen with the addition of 0.5% Cancer Bush ethanol-water extract shows that the inclusion provides a significant improvement to sunscreen formulations with no photodegradation reactions noted.

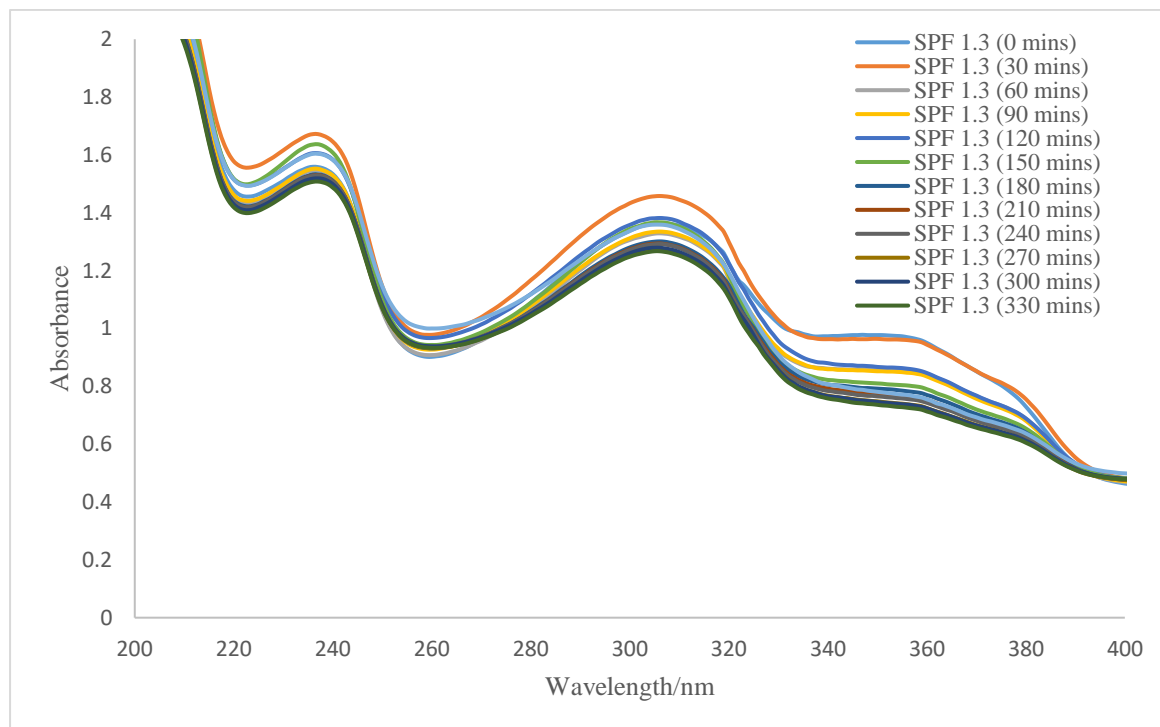


Figure 4.64: SPF 1.3 – Example formulation with reduced concentrations of UV filters and the addition of the Cancer Bush ethanol-water extract. The spectra were recorded every 30 minutes for a total period of six hours, and were acquired on a quartz plate against air as the reference.

4.3.1.2 Adjusted formulation

In order to confirm if the addition of plant polyphenols is beneficial to sunscreen formulations the example formulation UV filters was replaced with the four UV chemical absorbers studied in this dissertation, namely: avobenzone, benzophenone-9, MBC and EHMC. The UV spectrum was first analysed to determine if Beer's Law was obeyed. Absorbance values were below 1.2 and the photostability test was resumed (see Figure 4.65). Maximum wavelengths, λ_{\max} , were observed at 225, 295, 311 and 360 nm. At 225 nm, the absorbance value decreased from 0.994 to 0.817 (-0.177). The peak observed at 295 nm matches the absorption profile of benzophenone-9 and the absorbance decreased from 1.232 to 0.789 (-0.443) at 295 nm. MBC is expected to show peak absorption at 300 nm. The absorption decreased from 1.219 to 0.779 (-0.44). The peak absorption expected for EHMC is 311 nm and this decreased from 1.161 to

0.728 (-0.433). Collectively, the three UV filters showed a large peak between 250 to 340 nm due to the synergistic effect of combining the UV filters. The peak absorption for avobenzone was observed at 360 nm which decreased from 0.456 to 0.307 (-0.149).

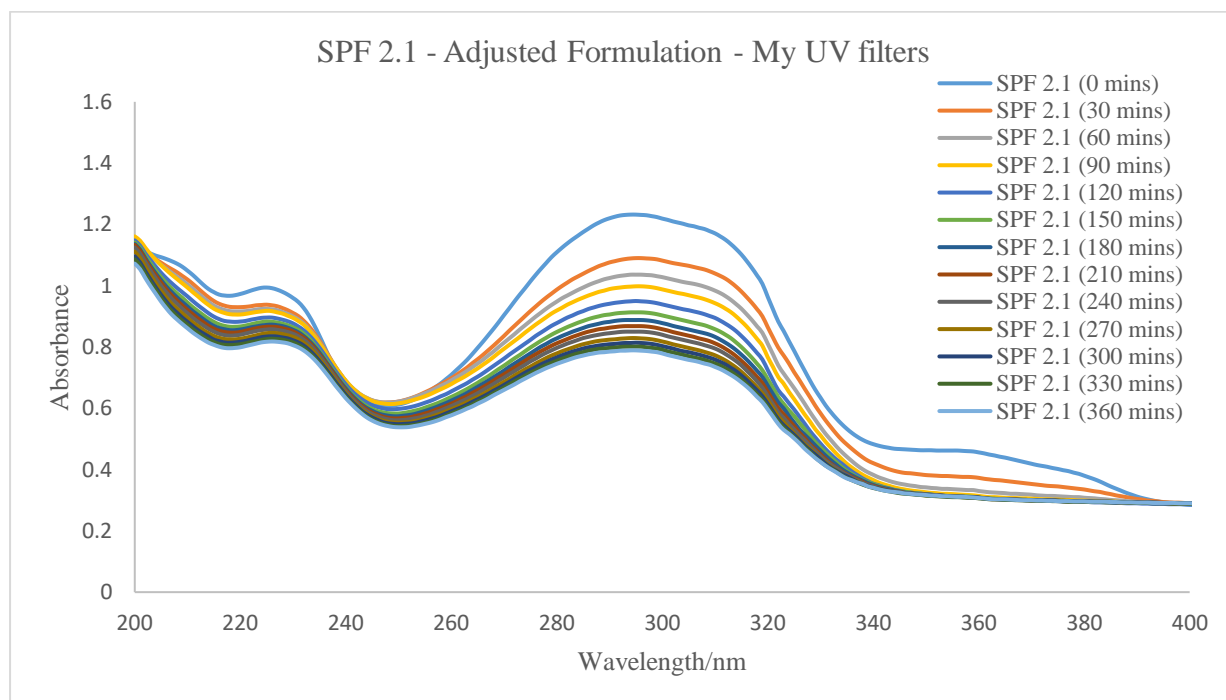


Figure 4.65: SPF 2.1 – Adjusted formulation with avobenzone, benzophenone-9, MBC and EHMC. The spectra were recorded every 30 minutes for a total period of six hours, and were acquired on a quartz plate against air as the reference.

The adjusted formulation was repeated with the inclusion of 5% Cancer Bush ethanol-water extract (SPF 2.2) and 5% green tea extract (SPF 2.3).

The maximum wavelengths, λ_{\max} , for Formulation SPF 2.2 (see Figure 4.66) shifted from 228 nm to 226 nm, the second peak remained between 250 and 340 nm and the third peak remained at 360 nm. At 226 nm, the absorbance decreased from 1.208 to 1.056 (-0.152). The peak observed for benzophenone-9, at 295 nm, decreased from 1.485 to 1.023 (-0.462). At 300 nm, MBC decreased from 1.473 to 1.014 (-0.459) and at 311 nm, EHMC decreased from 1.410 to 0.959 (-0.451). Avobenzone was shown to decrease in absorbance from 0.625 to 0.409 (-0.216). The addition of the Cancer Bush ethanol-water extract showed that although higher absorbances were achieved, the loss of absorbance after each irradiation period was similar. Therefore, the addition of the Cancer Bush ethanol-water extract was only beneficial in achieving higher absorbances.

The UV spectra obtained for Formulation SPF 2.3, shown in Figure 4.67, included the green tea extract. The spectra were identical to the example formulation, SPF 2.1, showing that the green tea extract did not impact photostability. Studies by Elmets *et al.*²⁴⁶, Camouse *et al.*²⁴⁷ and Belo *et al.*²⁴⁸ all confirm that green tea has photoprotective capability to protect the skin from erythema, DNA damage and protection of Langerhans cells. However, the protection was not due to direct UV absorption by the extract but rather its antioxidant potential. The UV absorbance of green tea extract was found to be 270 nm.²⁴⁸ The UV spectrum shown in Figure 4.67 confirms this result and shows that the absorption values were not affected by the addition of the green tea extract. Maximum wavelengths, λ_{\max} , were observed at 225, between 250 to 340, and at 360 nm. At 225 nm, the absorbance value decreased from 0.969 to 0.776 (0.083) after the six-hour irradiation period. The absorbance decreased from 1.240 to 0.700 (0.540) at 295 nm. At 300 and 311 nm, absorbance decreased from 1.226 to 0.690 (-0.536) and 1.167 to 0.647 (-0.520) respectively. The peak observed for avobenzone was shown to decrease from 0.472 to 0.320 (-0.152).

Results from the HPLC analysis in Section 4.2 showed that *p*-coumaric was the major component found in the Cancer Bush and tea extracts. *p*-coumaric was shown to absorb predominantly at 309 nm. This was confirmed by the UV spectra and the retention time obtained from Section 4.2. Therefore, it can be assumed that *p*-coumaric found in the Cancer Bush and green tea extract could play a synergistic role in increasing the absorbance obtained at 309 nm.

The loss of absorbance seen at the respective wavelengths was higher than the loss seen for the sunscreen formulation, SPF 2.1, therefore, the green tea extract was not effective in providing the formulation with improved photostability. The use of green tea extracts in cosmetic products are to solely provide antioxidant benefits.

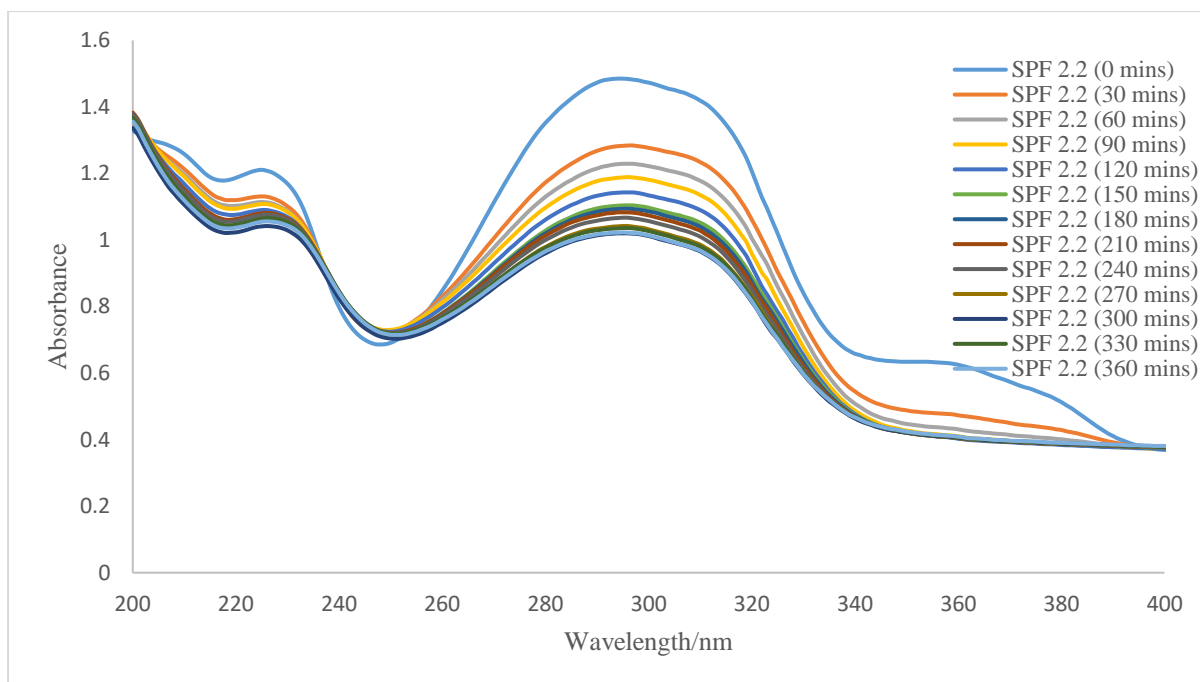


Figure 4.66: SPF 2.2 – Adjusted formulation with avobenzone, benzophenone-9, MBC and EHMC with the addition of the Cancer Bush ethanol-water extract. The spectra were recorded every 30 minutes for a total period of six hours, and were acquired on a quartz plate against air as the reference.

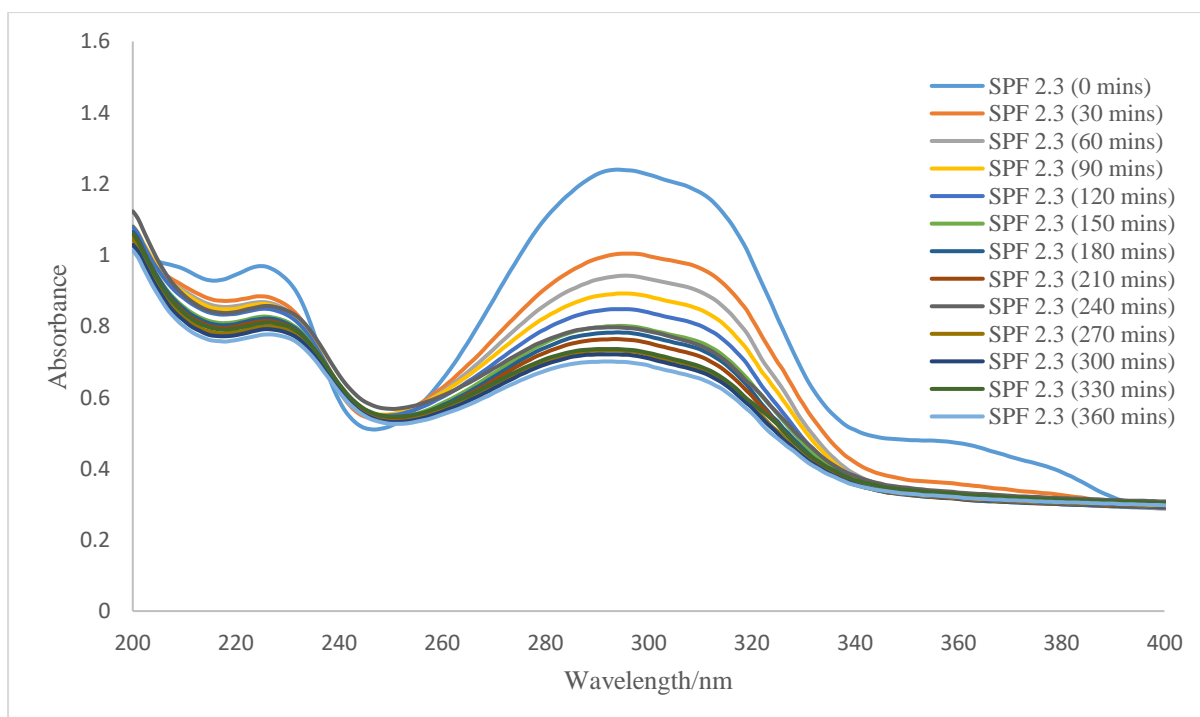


Figure 4.67: SPF 2.3 – Adjusted formulation with avobenzone, benzophenone-9, MBC and EHMC with the addition of green tea extract. The spectra were recorded every 30 minutes for a total period of six hours, and were acquired on a quartz plate against air as the reference.

The sunscreen formulations containing the Cancer Bush extract showed improved photostability when compared with products without plant extracts. This implies that a synergistic contribution was achieved. The lack of isosbestic points in all five formulations showed that the addition of the plant extract did not negatively impact the formulation and was able to enhance the formulation by achieving higher absorbance values.

4.3.2 Stability studies

Preliminary stability studies are used to determine the initial phase of product development. Stability studies use various conditions to accelerate the potential reactions between compounds and demonstrate the most common types of instability processes of emulsion-based products.³¹¹ Instability processes include phase separation, flocculation and creaming. The sunscreen formulations described in Section 3.8 were successfully prepared and initial images were taken after the formulations were allowed to stabilise for 24 hours. The example formulations: SPF 1.1, SPF 1.2 and SPF 1.3, were prepared and are shown in Figure 4.68. Figure 4.69 shows the adjusted formulations: SPF 2.1, SPF 2.2 and SPF 2.3.



Figure 4.68: Images shown in order of left to right respectively, example formulation SPF 1.1 – Elementis Maui Milk SPF 15 – Attempt 1 (standard concentrations), SPF 1.2 – Elementis Maui Milk SPF 15 – Attempt 2 (reduced UV filter concentrations), and SPF 1.3 – Elementis Maui Milk SPF 15 – Attempt 3 (reduced UV filter concentrations with the Cancer Bush extract).



Figure 4.69: Images shown in order of left to right respectively, adjusted formulation SPF 2.1 – Elementis Maui Milk SPF 15 – Attempt 3 (the four UV filters used in this study), SPF 2.2 – Elementis Maui Milk SPF 15 – Attempt 2 (the four UV filters used in this study with Cancer Bush extract), and SPF 2.3 – Elementis Maui Milk SPF 15 – Attempt 3 (the four UV filters used in this study with green tea extract).

It is necessary to perform some stability studies with the addition of the plant and tea extracts to the formulations since the product could either be positively or adversely affected. The organoleptic observations, namely, appearance, colour, and odour, remained the same before and after testing. The formulations were a cream-based texture, white in colour, and had a chemical odour. The use of a fragrance can improve the odour profile. The recommended pH requirement for sunscreen preparations are between 4.0 and 8.0 to be safe for topical application. pH was determined with pH indicator sticks and remained at a pH of 7 before and after testing. The pH determination was unsuccessful when conducted with a Mettler Toledo pH meter. The reason for the instrument error is due to the formulation type being a water-in-oil emulsion and pH electrodes do not function well in non-aqueous media. In this formulation the water is packed in the internal phase and, therefore, is not accessible to the electrode. The initial observations and results after the preliminary stability studies are summarised in Table 4.13.

Table 4.13: Physiochemical parameters of SPF formulations before and after preliminary stability studies

		SPF 1.1	SPF 1.2	SPF 1.3	SPF 2.1	SPF 2.2	SPF 2.2
Appearance	Initial	Emulsion					
	After centrifuge	Emulsion with a small oil layer indicating phase separation and emulsion instability					
	After freeze/thaw cycling	Emulsion, i.e. no phase separation					
Colour	Initial	White					
	After centrifuge	White					
	After freeze/thaw cycling	White					
Odour	Initial	Characteristic					
	After centrifuge	Characteristic					
	After freeze/thaw cycling	Characteristic					
pH	Initial	7.0					
	After centrifuge	7.0					

	After freeze/thaw cycling	7.0					
Viscosity S05/10 rpm Brookfield RV-DVE/ cps	Initial	5800 – 5880	23120 – 23000	24520 – 24000	22600 – 24000	26200 – 25800	27729 – 27400
	After freeze/thaw cycling	5520 – 5600	18880 – 18760	19560 – 19520	17880 – 17280	19080 – 18720	22680 – 22320

Formulation samples were subjected to three cycles of centrifugation and three cycles of freeze/thaw testing. A decrease in viscosity was seen in the six sunscreen samples after three freeze/thaw cycles. There were no changes in the appearance, colour and odour profile. A decrease in viscosity is acceptable in stability studies, provided the samples do not become unstable. Figure 4.70 shows the image of three samples before and after the centrifuge tests. After three centrifugation cycles, all formulations show a very small oil layer. Although, this is an indication of formulation instability, it can be said that even with the addition of the Cancer Bush and the green tea extracts, the formulations reacted in the same manner when compared with the standard. Therefore, the addition of the plant and tea extract did not adversely affect the formulation and, together with their UV spectra, the potential to incorporate such extracts to photostabilise sunscreen formulations is deemed successful.

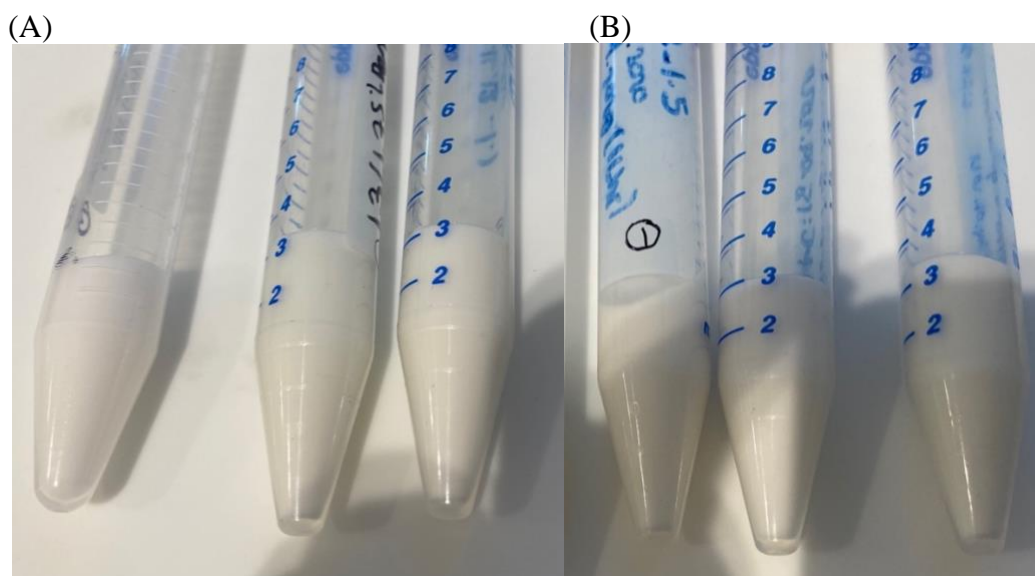


Figure 4.70: Centrifugation before (A) and after (B) three consecutive runs.

4.3.3 In vitro tests

4.3.3.1 SPF

The efficacy of a sunscreen product is expressed by an SPF value and is defined as the UV energy required to produce a minimal erythema dose (MED) on protected skin, divided by the UV energy required to produce a MED on unprotected skin.^{77, 312} A higher SPF implies that the sunscreen product is more effective in UVB protection. The photoprotection achieved by topical sunscreens against UV radiation can be determined by *in vivo* methods which usually involve testing on human volunteers.¹¹ The disadvantages of using such testing includes complex and expensive techniques, as well as lengthy testing times. This led to the development of *in vitro* testing to assess the photostability of sunscreens. *In vitro* methods include either the measurement of absorption or transmission of UV radiation through sunscreen product films on quartz plates or biomembranes, or through methods involving spectrophotometric analysis of dilute solutions.^{264, 265, 313}

Mansur *et al.*²⁶⁴ developed a simple mathematical equation based on an *in vitro* method proposed by Sayre *et al.*²⁶⁵ and involves UV spectrophotometry. The determination of the SPF values of the sunscreen preparations by application of Equation 6 are shown in Table 4.14. The Mansur method requires testing of dilute sunscreen formulations.³¹² The example formulation, Formulation SPF 1.1, obtained an SPF value of 28.80, undiluted. Because SPF 1.1 obtained an initial absorbance above 1.2, Beer's Law was not obeyed and the photostability analysis was not carried out. The UV filters for Formulation SPF 1.2 had to be reduced by 50% in order to obey Beer's Law. Because the UV filters were strategically reduced, the sunscreen preparations were not diluted further as per the Mansur test method. Therefore, the SPF was reduced to 6.02 which is almost half the SPF of the example formulation SPF 1.1 which was stated to be an SPF of 15. This implies that the formulation did not have to be diluted further in order to obtain the correct SPF values. The SPF of Formulation SPF 1.2 decreased by 1.14 to an SPF of 4.88 after six hours of irradiation. This is an acceptable decrease for the recommended sunscreens. The SPF value for Formulation 1.3 was 13.41 before irradiation and decreased to 13.39 after the irradiation period. This implies that the addition of the Cancer Bush extract helped the UV filters to maintain the absorbance values effectively.

Formulations SPF 2.1-2.3 were an adjusted formulation with the four UV filters investigated in this work. The SPF values obtained for SPF 2.1 before and after the six-hour irradiation period were 11.90 and 7.54 respectively. The decrease in SPF shows that the four sunscreens

selected for this formulation do not work effectively in combination. Nevertheless, the addition of the Cancer Bush extract to Formulation SPF 2.2 showed an increase in SPF value before irradiation to 14.42. This confirms that the addition of the Cancer Bush extract acts synergistically with the UV filters, therefore, providing improved photostability. After the six-hour irradiation period the SPF value decreased to 9.87. The decrease of SPF was similar to Formulation SPF 2.1 but the Cancer Bush extract was able to achieve a higher SPF value. The green tea extract added to Formulation SPF 2.3 had no impact on the SPF value; this result was expected.

Table 4.14: SPF values determined for the sunscreen preparations

Formulation	SPF – Before irradiation	SPF – After six hours of irradiation
SPF1.1	28.80	-
SPF1.2	6.02	4.88
SPF1.3	13.41	13.39
SPF2.1	11.90	7.54
SPF2.2	14.42	9.87
SPF2.3	11.95	6.70

It can be concluded that the addition of the Cancer Bush extract, with the correct choice of UV filters, can provide improved photostability. Therefore, the addition of the Cancer Bush extract was successful in providing additional UV protection.

4.3.3.2 Occlusion factor

Sunscreen active ingredients used in cosmetic products are required to protect the skin from UV radiation. However, in order to be effectively used in the cosmetic industry, these products must also contain additional benefits so that they can be used in a wide range of applications. One of the factors considered in the industry is the occlusion level that a skincare product may provide. Occlusive ingredients are moisturising agents that work by forming a protective layer on the surface of the skin and create a barrier to prevent moisture loss.³¹⁴ These ingredients can also repair the skin barrier. The protective layer formed prevents water loss from the skin to the environment, which allows for moisture to be maintained in the stratum corneum.³¹⁵

This section discusses the results obtained for the assessment of the occlusion effects of the sunscreen formulations prepared in Section 3.8. The occlusive property of a sunscreen product

can determine the extent of skin hydration.²³⁶ An occlusion factor of zero indicates that no occlusion was achieved and a value of 100 is the maximum occlusive factor that can be achieved. The occlusion factors found for the sunscreen preparations were between 83.70% to 93.07% and are shown in Table 4.15. Therefore, the sunscreen formulations prepared showed good hydrating effects and these add to the benefits of the product.

Table 4.15: Occlusion factors obtained for the six sunscreen formulations prepared.

Formulation	Initial – mass of beaker + water/g	After 24 hours in 37 °C – mass of beaker + water/g	Mass difference/g	Occlusive factor, F/%
Control	84.337	67.263	17.074	-
SPF 1.1	84.266	81.483	2.783	83.70
SPF 1.2	86.184	84.880	1.304	92.24
SPF 1.3	82.403	81.220	1.183	93.07
SPF 2.1	87.243	85.943	1.300	92.39
SPF 2.2	83.717	81.759	1.958	88.53
SPF 2.3	84.748	83.525	1.223	92.83

Chapter 5: Conclusion and Recommendations for Future Work

The aim of the study was to determine whether polyphenols from the Cancer Bush plant and tea extracts could serve as sunscreen active ingredients either on their own or when used correctly with approved UV filters. Approved UV filters, namely; benzophenone-9, avobenzene, EHMC and MBC were assessed for their photostability capabilities. Benzophenone-9 was not susceptible to photodegradation and was used as the control to determine if the addition of polyphenols would negatively impact photostability. Avobenzene photodegrades due to photochemical reactions, such as, phototautomerisation. The UV filter is also dependent on the polarity and proticity of the solvent. Both the camphor and cinnamate derivatives are photolabile and undergo photoisomerisation. The camphor derivatives are known to be more stable than cinnamates, however, this was not evident in the results obtained where MBC degraded more rapidly than EHMC. In both, benzylidene camphor derivatives and cinnamates, a photostationary state is reached shortly after exposure to UV radiation due to photoisomerisation.

Attempts at photostabilising the selected UV filters were made by using polyphenols, specifically phenolic acids and flavonoids, obtained from the Cancer Bush and tea extracts. Photostability studies were conducted on the extracts alone and when mixed with each of the UV filters. The extracts from both extraction methods used for the Cancer Bush plant showed some absorption up to 400 nm and their photostability was tested in combination with the UV chemical absorbers. The addition of Cancer Bush extracts in small amounts gave higher absorbance values than for the UV filters on their own, but they were not successful in photostabilising the UV filters. Results show that although the extracts were successful in obtaining a higher absorbance, there was no definite improvement seen.

Results showed that the water-ethanol flavonoid extraction method yielded an extract identical to that for the boiling water extraction method as observed with benzophenone-9 and avobenzene. This indicates that both the extraction methods were able to extract flavonoids, but were unsuccessful in photostabilising the UV filters. However, the flavonoid extracts were successful in preventing photoisomerisation in both MBC and EHMC, and provided some UVA protection. Further investigation is required to confirm the effectiveness of flavonoids on MBC and EHMC, and the prevention of photoisomerisation needs to be confirmed chromatographically. The second flavonoid solvent extraction method and the Soxhlet extract were unsuccessful and further studies were not conducted.

The Soxhlet and ultrasonication extraction techniques were successful in extracting phenolic acids. From the results, the diethyl ether layer from the ultrasonication extraction technique exhibited the higher absorbance of the four extracts obtained. Therefore, ultrasonic-assisted extractions were selected for photostability analysis. Phenolic acids were able to absorb at wavelengths similar to photolabile UV absorbers. The use of extracts containing these compounds allowed for successful photostabilisation of the chemical absorbers. Therefore, it is assumed that if this technology is introduced into a sunscreen formulation, there is a potential to photostabilise chemical UV absorbers and scavenge free radicals. The efficacy of the formulation will increase and the potential for adverse reactions would decrease.

The results obtained for green and Rooibos tea may be related to the quality and quantity of phenolic content, as well as the interaction with other components in solution. Phenolic compounds are known to be susceptible to solar radiation as a result of chemical structure.³⁰⁶ Green tea was shown to be ineffective in providing UV protection. Due to the variations observed in the UV spectra of the tea extractions, it can be said that the photostability of phenolics greatly depends on the variety of compounds available in the extract, as well as the type of structure.

HPLC was utilised to identify and quantify the phenolic acid content in the Cancer Bush leaves, green tea leaves and Rooibos tea leaves. The separation of the six phenolic acids in the standard solution and the extracts was achieved on a RP-HPLC C18 column, and isocratic elution with a mobile phase composition of 12% MeOH and 1% acetic acid in Millipore water. The injection volume was 10 μL and the flow rate was set to 1.000 ml min^{-1} . The identified phenolic acids were gallic acid, *p*-hydroxybenzoic acid, vanillic acid, caffeic acid, syringic acid and *p*-coumaric acid. A few phenolic acids were identified in each extract. The UV/Visible spectra obtained for each of the extracts showed that there was a potential to use the extracts to enhance the protection of sunscreen products.

A general sunscreen formulation was employed to assess the possible inclusion of polyphenols in sunscreens. Sunscreens were made with and without plant based UV filters and photostability tests were conducted. The Cancer Bush extract was shown to improve the absorbance and SPF of the sunscreen formulations. The occlusion factor obtained showed that the sunscreens provided a beneficial hydrating property which is an important factor for cosmetic products.

It can be concluded that the addition of the Cancer Bush extract, with the correct choice of UV filters, can provide an improved photostability. Therefore, the addition of the Cancer Bush extract was successful in providing additional UV protection. Future work is required to assess the phototoxicity and safety profile of sunscreen formulations that include plant polyphenols.

The current trend in the cosmetic industry is focused at multifunctional cosmetic formulations that include antioxidants with a reduction of synthetic UV filters. Therefore, improved photostability achieved with the use of antioxidants in sunscreen formulations will result in an improved safety profile and efficacy.

References

1. J. C. Maxwell, *A Treatise on Electricity and Magnetism*, Oxford University Press, London, 1904.
2. G. K. Stillwell, *Therapeutic Electricity and Ultraviolet Radiation*, Williams & Wilkins, Baltimore, 1983.
3. The Electromagnetic Spectrum, Columbia University, www.columbia.edu/~vjd1/electromag_spectrum, (accessed 27 March 2018).
4. C. Stiefel and W. Schwack, Photoprotection in changing times - UV filter efficacy and safety, sensitization processes and regulatory aspects, *International Journal of Cosmetic Science*, 2015, **37**, (1), 2-30.
5. M. Petrazzuoli, Advances in sunscreens, *Current Problems in Dermatology*, 2000, **12**, (6), 287-290.
6. L. R. Koller, *Ultraviolet Radiation*, Wiley, New York, 1965.
7. R. L. McKenzie, P. J. Aucamp, A. F. Bais, L. O. Björn and M. Ilyas, Changes in biologically-active ultraviolet radiation reaching the earth's surface, *Photochemical & Photobiological Sciences*, 2007, **6**, (3), 218-231.
8. E. Dupont, J. Gomez and D. Bilodeau, Beyond UV radiation: A skin under challenge, *International Journal of Cosmetic Science*, 2013, **35**, (3), 224-232.
9. G. T. Wondrak, M. K. Jacobson and E. L. Jacobson, Endogenous UVA-photosensitizers: mediators of skin photodamage and novel targets for skin photoprotection, *Photochemical & Photobiological Sciences*, 2006, **5**, (2), 215-237.
10. M. Ichihashi, H. Ando, M. Yoshida, Y. Niki and M. Matsui, Photoaging of the skin, *Anti-Ageing Medicine*, 2009, **6**, (6), 46-59.
11. F. P. Gasparro, M. Mitchnick and J. F. Nash, A review of sunscreen safety and efficacy, *Photochemistry and Photobiology*, 1998, **68**, (3), 243-256.
12. A. Gurib-Fakim, *Novel Plant Bioresources: Applications in Food, Medicine and Cosmetics*, Wiley, Hoboken, 2014.
13. M. B. Raselabe, Effects of pruning and fertilizer on growth, phytochemistry and biological activity of *Sutherlandia frutescens* (L.) R. Br, Master of Science Dissertation, University of KwaZulu-Natal, 2017.
14. C. A. Smith, E. P. Phillips, E. Van Hoepen, E. P. Phillips and E. Van Hoepen, *Common Names of South African Plants*, Government Printer, Pretoria, 1966.
15. B. A. Stander, S. Maas, T. J. Steynberg, D. Theron, F. Joubert, C. Albrecht and A. Joubert, Influence of *Sutherlandia frutescens* extracts on cell numbers, morphology and gene expression in MCF-7 cells, *Journal of Ethnopharmacology*, 2007, **112**, 312-318.
16. B. E. van Wyk and C. Albrecht, A review of the taxonomy, ethnobotany, chemistry and pharmacology of *Sutherlandia frutescens* (Fabaceae), *Journal of Ethnopharmacology*, 2008, **119**, (3), 620-629.
17. G. J. Mturi, An investigation of the photostabilisation of sunscreen absorbers by plant polyphenols, Master of Science Dissertation, University of KwaZulu-Natal, 2005.
18. C. Smith and K. H. Myburgh, Treatment with *Sutherlandia frutescens* sp. microphylla alters the corticosterone response to chronic intermittent immobilization stress in rats: Research letter, *South African Journal of Science*, 2004, **100**, (3), 229-232.
19. S. Federico, A brief illustrated history on sunscreens and sun protection, *Pure and Applied Chemistry*, 2015, **87**, (9-10), 929-936.
20. R. Wolf, D. Wolf, P. Morganti and V. Ruocco, Sunscreens, *Clinics in Dermatology*, 2001, **19**, (4).

21. K. Holubar and C. Schmidt, Historical, anthropological, and biological aspects of sun and the skin, *Clinics in Dermatology*, 1998, **16**, (1).
22. H. Brodthagen, Stamps commemorating medicine: "Niels Finsen". Physician, photobiologist, nobel laureate, *The Journal of Dermatologic Surgery and Oncology*, 1979, **5**, (8).
23. H. Grünewald, Nobel Lectures. Physiology or medicine 1901-1921. H. Grünewald. Herausgeg. von der Nobel Foundation. Elsevier Publishing Company, Amsterdam-London-New York 1967, *Angewandte Chemie*, 1969, **81**, (4), 159.
24. R. Roelandts, A new light on Niels Finsen, a century after his Nobel Prize, *Photodermatology, Photoimmunology & Photomedicine*, 2005, **21**, (3), 115-117.
25. J. Picardie, *Coco Chanel: The Legend and the Life*, HarperCollins, London, 2011.
26. C. N. Paul, *The Influence of Sunlight in the Production of Cancer of the Skin*, H.K. Lewis & Co., Ltd., London, 1918.
27. K. W. a. V. Hausser, W, Die Abhängigkeit des Lichterytherms und der Pigmentbildung von der Schwingungszahl (Wellenlänge) der erregenden Strahlung, *Strahlentherapie*, 1922, **13**, 41-71.
28. Z. K. Draelos, Cosmeceuticals, <https://www.clinicalkey.com/dura/browse/bookChapter/3-s2.0-C20130097939>, (accessed 19 February, 2019).
29. B. S. Mackie and L. E. Mackie, The PABA story, *Australasian Journal of Dermatology*, 1999, **40**, (1), 51-53.
30. W. N. MacEachern, A practical sunscreen "Red Vet Pet", *Dermatol Archives of Dermatology*, 1964, **89**, (1), 147.
31. N. A. Shaath, *Sunscreens: Regulations and Commercial Development: Third edition*, 2005.
32. K. H. Kaidbey, The photoprotective potential of the new superpotent sunscreens, *Journal of the American Academy of Dermatology*, 1990, **22**, (3), 449-452.
33. N. D. M. Hodges, S. H. Moss and D. J. G. Davies, The sensitizing effect of a sunscreen agent, p-aminobenzoic acid, on near UV induced damage in a repair deficient strain of escherichia coli, *Photochemistry and Photobiology*, 1977, **26**, (5), 493-498.
34. J. C. Sutherland and K. P. Griffin, P-aminobenzoic acid can sensitize the formation of pyrimidine dimers in DNA: direct chemical evidence, *Photochemistry and Photobiology*, 1984, **40**, (3), 391-394.
35. A. A. Shaw, L. A. Wainschel and M. D. Shetlar, Photoaddition of p-aminobenzoic acid to thymine and thymidine, *Photochemistry and Photobiology*, 1992, **55**, (5), 657-663.
36. R. L. Mayer, Experimental sensitization with food dyes and cross-sensitization to paraphenylenediamine, *The Journal of Allergy*, 1949, **20**, (3), 159-166.
37. R. Stokes and B. Diffey, How well are sunscreen users protected?, *Photodermatology, Photoimmunology & Photomedicine*, 1997, **13**, (01).
38. E. N. Marieb, *Essentials of Human Anatomy and Physiology*, Pearson/Benjamin Cummings, San Francisco, 2006.
39. C. B. Clayman, *The Human Body: An Illustrated Guide to its Structure, Function, and Disorders*, Dorling Kindersley Publications., London; New York, 1995.
40. K. A. Holbrook and G. F. Odland, Regional differences in the thickness (cell layers) of the human stratum corneum: an ultrastructural analysis, *The Journal of Investigative Dermatology*, 1974, **62**, (4), 415-422.
41. W. Montagna and P. F. Parakkal, *The Structure and Function of Skin*, Academic Press, New York, 1974.

42. J. J. Thiele, C. Schroeter, S. N. Hsieh, M. Podda and L. Packer, The antioxidant network of the stratum corneum, *Current Problems in Dermatology*, 2001, **29**, 26-42.
43. M. R. Chedekel, Photochemistry and photobiology of epidermal melanins, *Photochemistry and Photobiology*, 1982, **35**, (6), 881-885.
44. H. Adhoute, J. De Rigal, J. P. Marchand and Y. Privat, Influence of age and sun exposure on the biophysical properties of the human skin: An in vivo study, *Photodermatology, Photoimmunology and Photomedicine*, 1992, **9**, (3), 99.
45. D. Bissett, D. Hannonand and T. Orr, An animal model of solar-aged skin: Histological, physical, and visible changes in UV-irradiated hairless mouse skin, *Photochemistry and Photobiology*, 1987, **46**, (3), 367-378.
46. S. González, M. Fernández-Lorente and Y. Gilaberte-Calzada, The latest on skin photoprotection, *Clinics in Dermatology*, 2008, **26**, (6), 614.
47. T. Bunhu, An assessment of the photostability of South African commercial sunscreens, Master of Science Dissertation, University of KwaZulu-Natal, 2006.
48. R. B. Sollitto, K. H. Kraemer and J. J. DiGiovanna, Normal vitamin D levels can be maintained despite rigorous photoprotection: Six years' experience with xeroderma pigmentosum, *Journal of the American Academy Of Dermatology*, 1997, **37**, (6), 942-947.
49. T. Douki, M. Court and J. Cadet, Electrospray-mass spectrometry characterization and measurement of far-UV-induced thymine photoproducts, *Journal of Photochemistry & Photobiology, B: Biology*, 2000, **54**, (2), 145-154.
50. J. Cadet and T. Douki, Formation of UV-induced DNA damage contributing to skin cancer development, *Photochemical & Photobiological Sciences*, 2018, **17**, (12), 1816-1841.
51. J. L. Ravanat, T. Douki and J. Cadet, in *Comprehensive Series in Photosciences*, Chapter 10 - UV Damage to Nucleic Acid Components, ed. P. U. Giacomoni, Elsevier, 2001, vol. 3, pp. 207-230.
52. J.-L. Ravanat, T. Douki and J. Cadet, Direct and indirect effects of UV radiation on DNA and its components, *Journal of Photochemistry and Photobiology, B: Biology*, 2001, **63**, (1), 88-102.
53. J.-S. Taylor, DNA, sunlight, and skin cancer, *Journal of Chemical Education*, 1990, **67**, (10), 835.
54. J. Kockler, M. Oelgemöller, S. Robertson and B. D. Glass, Photostability of sunscreens, *Journal of Photochemistry & Photobiology, C: Photochemistry Reviews*, 2012, **13**, (1), 91-110.
55. F. Greiter and F. Gschnait, Effect of UV light on humans, *Photochemistry and Photobiology*, 1984, **39**, 869-873.
56. Z. Assefa, A. Van Laethem, M. Garmyn and P. Agostinis, Ultraviolet radiation-induced apoptosis in keratinocytes: On the role of cytosolic factors, *Biochimica et Biophysica Acta.*, 2005, **1755**, (2), 90-106.
57. L. L. Hill, A. Ouhtit, S. M. Loughlin, M. L. Kripke, H. N. Ananthaswamy and L. B. Owen-Schaub, Fas ligand: a sensor for DNA damage critical in skin cancer etiology, *Science (New York, N.Y.)*, 1999, **285**, (5429), 898-900.
58. S. Q. Wang, R. Setlow, M. Berwick, D. Polsky, A. A. Marghoob, A. W. Kopf and R. S. Bart, Ultraviolet A and melanoma: A Review, *Journal of the American Academy of Dermatology*, 2001, **44**, (5), 837-846.
59. P.-L. So, *Skin Cancer*, Chelsea House, New York, 2008.
60. American Cancer Society, Skin cancer: basal and squamous cell, <http://www.cancer.org/cancer/skincancer-basalandsquamouscell/detailedguide/skin->

- [cancer-basal-and-squamous-cell-what-is-basal-and-squamous-cell](#), (accessed 05 October, 2017).
61. S. Kaimal and A. Abraham, Sunscreens, *Indian Journal of Dermatology, Venereology and Leprology*, 2011, **77**, (2), 238-243.
 62. C. F. Garland, F. C. Garland and E. D. Gorham, Melanoma incidence in Connecticut, *Cancer, Causes & Control*, 1994, **5**, (6), 581.
 63. C. F. Garland, More on preventing skin cancer: Sun avoidance will increase incidence of cancers overall, *The BMJ*, 2003, **327**, (7425), 1228-a-1228.
 64. R. P. Gallagher, Sunscreens in melanoma and skin cancer prevention, *Canadian Medical Association Journal*, 2005, **173**, (3), 244-245.
 65. D. Moyal, The development of efficient sunscreens, *Indian Journal of Dermatology, Venereology and Leprology*, 2012, **78**, 31-34.
 66. G. A. Grovies, Sunburn and its prevention, *Australasian Journal of Dermatology*, 1980, **21**, (3), 115-141.
 67. D. R. Sambandan and D. Ratner, Sunscreens: An overview and update, *Journal of the American Academy of Dermatology*, 2011, **64**, (4), 748-758.
 68. S. Q. Wang, Y. Balagula and U. Osterwalder, Photoprotection: A review of the current and future technologies, *Dermatologic Therapy*, 2010, **23**, (1), 31-47.
 69. W. Lyambila, A study of photoinduced transformations of sunscreen chemical absorbers, Doctoral Degree (Chemistry), University of KwaZulu-Natal, 2009.
 70. S. Bett, What is the Jablonski diagram?, <http://www.quora.com/What-is-the-Jablonski-diagram>, (accessed 03 May, 2018).
 71. B. Wardle, *Principles and Applications of Photochemistry*, Wiley, Chichester, U.K., 2009.
 72. C. Bonda, Research pathways to photostable sunscreens, *Cosmetics and Toiletries*, 2008, **123**, (2), 49-60.
 73. Roelandts, Shedding light on sunscreens, *Clinical and Experimental Dermatology*, 1998, **23**, (4), 147-157.
 74. M. D. Rik Roelandts, Advances in sunscreen technology: Choosing the sunscreen to suit, *Current Opinion in Dermatology*, 1995, **2**, (1), 173.
 75. R. Schwarzenbach and U. Huber, Optimization of sunscreen efficacy, *SOFW Journal*, 2002, **128**, 20-23.
 76. A. Hunter and M. Trevino, Film formers enhance water resistance and SPF in sun care products, *Cosmetics and Toiletries*, 2004, **119**, (7), 51.
 77. H. W. Lim, H. Hönigsmann and J. L. M. Hawk, Photodermatology, <http://www.crcnetbase.com/isbn/9781420019964>, (accessed 11 September, 2021).
 78. P. Kullavanijaya and H. W. Lim, Photoprotection, *Journal of the American Academy of Dermatology*, 2005, **52**, (6), 937-958.
 79. Z. D. Draelos, Compliance and sunscreens, *Dermatologic Clinics*, 2006, **24**, (1), 101-104.
 80. *COLIPA Guidelines: International Sun Protection Factor (SPF) Test Method*, European Cosmetic, Toiletry and Perfumery Association (COLIPA), Japanese Cosmetic, Toiletry, Fragrance and Industry Association, Brussels, 2006.
 81. S. Lautenschlager, H. C. Wulf and M. R. Pittelkow, Photoprotection, *The Lancet*, 2007, **370**, (9586), 528-537.
 82. Scherschun and Lim, Photoprotection by sunscreens, *American Journal of Clinical Dermatology*, 2001, **2**, (3), 131-134.
 83. D. Moyal, A. Chardon and N. Kollias, Determination of UVA protection factors using the persistent pigment darkening (PPD) as the end point: (Part 1) Calibration of the

- method, *Photodermatology, Photoimmunology & Photomedicine*, 2000, **16**, (6), 245-249.
84. D. Moyal, A. Chardon and N. Kollias, UVA protection efficacy of sunscreens can be determined by the persistent pigment darkening (PPD) method: (Part 2), *Photodermatology, Photoimmunology & Photomedicine*, 2000, **16**, (6), 250-255.
 85. D. Moyal, V. Alard, C. Bertin, F. Boyer, M. W. Brown, L. Kolbe, P. Matts and M. Pissavini, The revised COLIPA in vitro UVA method, *International Journal of Cosmetic Science*, 2013, **35**, (1), 35-40.
 86. P. J. Matts, V. Alard, M. W. Brown, L. Ferrero, H. Gers-Barlag, N. Issachar, D. Moyal and R. Wolber, The COLIPA in vitro UVA method: A standard and reproducible measure of sunscreen UVA protection, *International Journal of Cosmetic Science*, 2010, **32**, (1), 35-46.
 87. European Commission, Commission recommendation of 22 September 2006 on the efficacy of sunscreen products and claims made relating thereto, www.colipa.eu, (accessed 11 October, 2006).
 88. J. Ferguson, M. Brown, D. Alert, S. Bielfeldt, J. Brown, A. Chardon, C. Hourseau, C. Mazilier, J. Cuthbert, K. D'Arcy-Burt, J. Jolley, M. Murdoch, P. Finkel, P. Masson, F. Merot, A. MacLennan, J. Poret and S. Siladgi, Collaborative development of a sun protection factor test method: A proposed European standard. COLIPA task force sun protection measurement, Europe, *International Journal of Cosmetic Science*, 1996, **18**, (5), 203-218.
 89. K. H. Kaidbey and A. Barnes, Determination of UVA protection factors by means of immediate pigment darkening in normal skin, *Journal of the American Academy of Dermatology*, 1991, **25**, (2), 262-266.
 90. C. Cole, Multicenter evaluation of sunscreen UVA protectiveness with the protection factor test method, *Journal of the American Academy of Dermatology*, 1994, **30**, (5), 729-736.
 91. M. Hupel, N. Poupart and E. Ar Gall, Development of a new in vitro method to evaluate the photoprotective sunscreen activity of plant extracts against high UV-B radiation, *Talanta*, 2011, **86**, (1), 362-371.
 92. Method for the in vitro determination of UVA protection provided by sunscreen products, COLIPA Guideline, [http://biblioscreen.helioscreen.fr/Reglementation-Comission/Method for the In Vitro Determination of UVA Protection provided by Sunscreen Products 2007a%20methode%20COLIPA.PDF](http://biblioscreen.helioscreen.fr/Reglementation-Comission/Method%20for%20the%20In%20Vitro%20Determination%20of%20UVA%20Protection%20provided%20by%20Sunscreen%20Products%202007a%20methode%20COLIPA.PDF), (accessed 04 March, 2022).
 93. J. K. Robinson and A. W. Rademaker, Sun protection by families at the beach, *Archives of Pediatrics & Adolescent Medicine*, 1998, **152**, (5), 466-470.
 94. M. A. Pathak and P. Robins, A response to concerns about sunscreens: A report from the Skin Cancer Foundation, *The Journal of Dermatologic Surgery and Oncology*, 1989, **15**, (5), 486-487.
 95. H. Maier, H. Hönigsmann, G. n. Schauburger and K. Brunnhofer, Change of ultraviolet absorbance of sunscreens by exposure to solar-simulated radiation, *Journal of Investigative Dermatology*, 2001, **117**, (2), 256-262.
 96. D. L. Giokas, A. Salvador and A. Chisvert, UV filters: From sunscreens to human body and the environment, *Trends in Analytical Chemistry*, 2007, **26**, (5), 360-374.
 97. E. Chatelain and B. Gabard, Photostabilisation of butyl methoxydibenzoylmethane (Avobenzone) and ethylhexyl methoxycinnamate by bis-ethylhexyloxyphenol methoxyphenyl triazine (Tinosorb S), a new UV broadband filter, *Photochemistry and Photobiology*, 2001, **74**, (3), 401-406.

98. T. Poiger, H.-R. Buser, M. E. Balmer, P.-A. Bergqvist and M. D. Müller, Occurrence of UV filter compounds from sunscreens in surface waters: Regional mass balance in two Swiss lakes, *Chemosphere*, 2004, **55**, (7), 951-963.
99. K. Fent and P. Y. Kunz, Occurrence and effects of hormonally active UV filters in the aquatic environment, *SOFW JOURNAL*, 2009, **135**, (7), 2-13.
100. N. A. Shaath, Ultraviolet filters, *Photochemical and Photobiological Sciences*, 2010, **9**, (4), 464-469.
101. N. Tarras-Wahlberg, G. Stenhagen, O. Larkö, A. Rosén, A. M. Wennberg and O. Wennerström, Changes in ultraviolet absorption of sunscreens after ultraviolet irradiation, *The Journal of Investigative Dermatology*, 1999, **113**, (4), 547-553.
102. K. K. Broadbent, B. S. Martincigh, M. W. Raynor, L. F. Salter, R. Moulder, P. Sjöberg and K. E. Markides, Capillary supercritical fluid chromatography combined with atmospheric pressure chemical ionisation mass spectrometry for the investigation of photoproduct formation in the sunscreen absorber 2-ethylhexyl- p-methoxycinnamate, *Journal of Chromatography A*, 1996, **732**, (1), 101-110.
103. M. Norval and H. C. Wulf, Does chronic sunscreen use reduce vitamin D production to insufficient levels?, *The British Journal of Dermatology*, 2009, **161**, (4), 732-736.
104. M. D. Palm and M. N. O'Donoghue, Update on photoprotection, *Dermatologic Therapy*, 2007, **20**, (5), 360-376.
105. C. S. Cockell and J. Knowland, Ultraviolet radiation screening compounds, *Biological Reviews*, 1999, **74**, (3), 311-345.
106. M. A. Pathak, Sunscreens: Topical and systemic approaches for protection of human skin against harmful effects of solar radiation, *Journal of the American Academy of Dermatology*, 1982, **7**, (3), 285-312.
107. J. Knowland, E. A. McKenzie, P. J. McHugh and N. A. Cridland, Sunlight-induced mutagenicity of a common sunscreen ingredient, *FEBS Letters*, 1993, **324**, (3), 309-313.
108. P. J. McHugh and J. Knowland, Characterization of DNA damage inflicted by free radicals from a mutagenic sunscreen ingredient and its location using an in vitro genetic reversion assay, *Photochemistry and Photobiology*, 1997, **66**, (2), 276-281.
109. A. Deflandre and G. Lang, Photostability assessment of sunscreens: Benzylidene camphor and dibenzoylmethane derivatives, *International Journal of Cosmetic Science*, 1988, **10**, (2), 53-62.
110. B. S. Martincigh, K. Kowlaser and M. W. Raynor, Photoproducts of 2-ethylhexyl-para-methoxycinnamate, *Photochemistry and Photobiology*, 1999, **69**, WAM-D8.
111. S. Pattanaargson, T. Munhapol, P. Hirunsupachot and P. Luangthongaram, Photoisomerisation of octyl methoxycinnamate, *Journal of Photochemistry and Photobiology, A: Chemistry*, 2004, **161**, (2-3), 269-274.
112. S. T. Butt and T. Christensen, Toxicity and phototoxicity of chemical sun filters, *Radiation Protection Dosimetry*, 2000, **91**.
113. D. Dondi, A. Albin and N. Serpone, Interactions between different solar UVB/UVA filters contained in commercial suncreams and consequent loss of UV protection, *Photochemical & Photobiological Sciences*, 2006, **5**, (9), 835-843.
114. A. Kikuchi, N. Oguchi-Fujiyama, K. Miyazawa and M. Yagi, Triplet-triplet energy transfer from a UV-A absorber butylmethoxydibenzoylmethane to UV-B absorbers, *Photochemistry and Photobiology*, 2014, **90**, (3), 511-516.
115. C. Mendrok-Edinger, K. Smith, A. Janssen and J. Vollhardt, The quest for avobenzene stabilizers and sunscreen photostability, *Cosmetics and Toiletries*, 2009, **124**, (2), 47-54.

116. P. Perugini, S. Simeoni, S. Scalia, I. Genta, T. Modena, B. Conti and F. Pavanetto, Effect of nanoparticle encapsulation on the photostability of the sunscreen agent, 2-ethylhexyl- p-methoxycinnamate, *International Journal of Pharmaceutics*, 2002, **246**, (1), 37-45.
117. G. Deepak, K. J. Sunil, K. Y. Awesh and G. P. Agrawal, Microsphere based improved sunscreen formulation of ethylhexyl methoxycinnamate, *Current Drug Delivery*, 2007, **4**, (2), 153-159.
118. C. Stevenson and R. J. Davies, Photosensitization of guanine-specific DNA damage by 2-phenylbenzimidazole and the sunscreen agent 2-phenylbenzimidazole-5-sulfonic acid, *Chemical Research in Toxicology*, 1999, **12**, (1), 38-45.
119. J. F. Nash, Human safety and efficacy of ultraviolet filters and sunscreen products, *Dermatologic Clinics*, 2006, **24**, (1), 35-51.
120. Complife, New restrictions on benzophenone-3 and octocrylene, <https://mailchi.mp/a5f7fb9276dd/complife-pills-1-hand-sanitizing-gel-cosmetics-or-borderline-20170260?e=16af02e4ed>, (accessed 15 July, 2022).
121. A. Beeby and A. E. Jones, The photophysical properties of menthyl anthranilate: A UVA sunscreen, *Photochemistry and Photobiology*, 2000, **72**, (1), 10.
122. V. A. Deleo, Photocontact dermatitis, *Dermatologic Therapy*, 2004, **17**, (4), 279-288.
123. K. U. Schallreuter, J. M. Wood, D. W. Farwell, J. Moore and H. G. Edwards, Oxybenzone oxidation following solar irradiation of skin: photoprotection versus antioxidant inactivation, *The Journal of Investigative Dermatology*, 1996, **106**, (3), 583-586.
124. C. Sundaram, W. Köster and K. U. Schallreuter, The effect of UV radiation and sun blockers on free radical defence in human and guinea pig epidermis, *Archives of Dermatological Research*, 2004, **282**, 526-531.
125. N. R. Janjua, B. Mogensen, A.-M. Andersson, J. H. Petersen, M. Henriksen, N. E. Skakkebæk and H. C. Wulf, Systemic absorption of the sunscreens benzophenone-3, octyl-methoxycinnamate, and 3-(4-methyl-benzylidene) camphor after whole-body topical application and reproductive hormone levels in humans, *Journal of Investigative Dermatology*, 2004, **123**, (1), 57-61.
126. R. Danovaro, L. Bongiorno, C. Corinaldesi, D. Giovannelli, E. Damiani, P. Astolfi, L. Greci and A. Pusceddu, Sunscreens Cause Coral Bleaching by Promoting Viral Infections, *Environmental Health Perspectives*, 2008, **116**, (4), 441-447.
127. C. A. Downs, E. Kramarsky-Winter, R. Segal, J. Fauth, S. Knutson, O. Bronstein, F. R. Ciner, R. Jeger, Y. Lichtenfeld, C. M. Woodley, P. Pennington, K. Cadenas, A. Kushmaro and Y. Loya, Toxicopathological effects of the sunscreen UV filter, oxybenzone (benzophenone-3), on coral planulae and cultured primary cells and its environmental contamination in Hawaii and the U.S. Virgin Islands, *Archives of Environmental Contamination and Toxicology*, 2016, **70**, (2), 265-288.
128. University of Maryland Center for Environmental Science, New study measures UV-filter chemicals in seawater and corals from Hawaii: First study to look at UV-filter concentrations in coral tissues in US, <https://www.sciencedaily.com/releases/2019/04/190401121805.htm>, (accessed 1 September, 2021).
129. W. Schwack and T. Rudolph, Photochemistry of dibenzoyl methane UVA filters Part 1, *Journal of Photochemistry and Photobiology, B: Biology.*, 1995, **28**, (3), 229.
130. M. Dubois, P. Gilard, P. Tiercet, A. Deflandre and M. A. Lefebvre, Photoisomerisation of the sunscreen filter Parsol © 1789, *Journal de Chimie Physique*, 1998, **95**, 388.

131. I. Andrae, A. O. Bringhen, F. B^hm, H. U. Gonzenbach, T. J. Hill, L. Mulroy and T. G. Truscott, A UVA Filter (4-tert-butyl-4'-methoxydibenzoylmethane): Photoprotection reflects photophysical properties, *Journal of Photochemistry and Photobiology B: Biology*, 1997, **37**, 147-150.
132. N. J. Lowe, An overview of ultraviolet radiation, sunscreens, and photo-induced dermatoses, *Dermatologic Clinics*, 2006, **24**, (1), 9-17.
133. G. J. Mturi and B. S. Martincigh, Photostability of the suncreening agent 4-tert-butyl-4'-methoxydibenzoylmethane (avobenzone) in solvents of different polarity and proticity, *Journal of Photochemistry and Photobiology, A: Chemistry*, 2008, **200**, (2-3), 410-420.
134. R. M. Sayre, J. C. Dowdy, A. J. Gerwig, W. J. Shields and R. V. Lloyd, Unexpected photolysis of the sunscreen octinoxate in the presence of the sunscreen avobenzone, *Photochemistry and Photobiology*, 2005, **81**, (2).
135. C. Bonda and P. Marinelli, The photochemistry of sunscreen photostability, *Agro Food Industry Hi Tech*, 2000, **11**, (Part 1), 29-32.
136. L. R. Gaspar and P. M. B. G. Maia Campos, Evaluation of the photostability of different UV filter combinations in a sunscreen, *International Journal of Pharmaceutics*, 2006, **307**, (2), 123-128.
137. R. Bissonnette, Update on sunscreens, *Skin Therapy Letter*, 2008, **13**, (6).
138. R. K. Chaudhuri, M. A. Ollengo, P. Singh and B. S. Martincigh, 3-(3,4,5-Trimethoxybenzylidene)-2,4-pentanedione: Design of a novel photostabiliser with in vivo SPF boosting properties and its use in developing broad-spectrum sunscreen formulations, *International Journal of Cosmetic Science*, 2017, **39**, (1), 25-35.
139. D. L. Damian, G. M. Halliday and R. S. Barnetson, Broad-spectrum sunscreens provide greater protection against ultraviolet-radiation-induced suppression of contact hypersensitivity to a recall antigen in humans, *Journal of Investigative Dermatology*, 1997, **109**, (2), 146-151.
140. H. Maier, G. Schauburger, B. S. Martincigh, K. Brunnhofer and H. Hönigsmann, Ultraviolet protective performance of photoprotective lipsticks: Change of spectral transmittance because of ultraviolet exposure, *Photodermatology, Photoimmunology & Photomedicine*, 2005, **21**, (2), 84-92.
141. S. Séite, D. Moyal, S. Richard, J. d. Rigal, J. L. Lévêque, C. Hourseau and A. Fourtanier, Mexoryl® SX: A broad absorption UVA filter protects human skin from the effects of repeated suberythemal doses of UVA, *Journal of Photochemistry & Photobiology, B: Biology*, 1998, **44**, (1), 69-76.
142. D. Moyal, Prevention of ultraviolet-induced skin pigmentation, *Photodermatology, Photoimmunology & Photomedicine*, 2004, **20**, (5), 243-247.
143. S. Seité, A. Colige, P. Piquemal-Vivenot, C. Montastier, A. Fourtanier, C. Lapière and B. Nussgens, A full-UV spectrum absorbing daily use cream protects human skin against biological changes occurring in photoaging, *Photodermatology, Photoimmunology & Photomedicine*, 2000, **16**, (4), 147-155.
144. F. Hollósy, Effects of ultraviolet radiation on plant cells, *Micron*, 2002, **33**, (2), 179-197.
145. F. Bonina, M. Lanza, L. Montenegro, C. Puglisi, A. Tomaino, D. Trombetta, F. Castelli and A. Saija, Flavonoids as potential protective agents against photo-oxidative skin damage, *International Journal of Pharmaceutics.*, 1997, **145**, (1-2), 87.
146. A. Solovchenko and M. Merzlyak, Screening of visible and UV radiation as a photoprotective mechanism in plants, *Russian Journal of Plant Physiology*, 2008, **55**, (6), 719-737.
147. Z. D. Draelos, Botanicals as topical agents, *Clinics in Dermatology*, 2001, **19**, (4).

148. A. Kligman, The future of cosmeceuticals: An interview with Albert Kligman, MD, PhD. Interview by Zoe Diana Draelos, *Dermatologic Surgery: Official Publication for American Society for Dermatologic Surgery*, 2005, **31**, (7), 890-891.
149. I. B. Allemann and L. Baumann, Botanicals in skin care products, *International Journal of Dermatology*, 2009, **48**, (9), 923-934.
150. S. F'Guyer, F. Afaq and H. Mukhtar, Photochemoprevention of skin cancer by botanical agents, *Photodermatology, Photoimmunology & Photomedicine*, 2003, **19**, (2), 56-72.
151. M. Tarnawski, K. Depta, D. Grejciun and B. Szelepin, HPLC determination of phenolic acids and antioxidant activity in concentrated peat extract—a natural immunomodulator, *Journal of Pharmaceutical and Biomedical Analysis*, 2006, **41**, (1), 182-188.
152. E. Yordi, E. Molina Pérez, M. J. Matos and E. Uriarte, Antioxidant and Pro-Oxidant Effects of Polyphenolic Compounds and Structure-Activity Relationship Evidence, 2012, DOI: 10.5772/29471.
153. F. Shahidi and M. Naczk, *Food phenolics: Sources, Chemistry, Effects, Applications*, Technomic Publishing Company Incorporated, Lancaster, Pa., 1995.
154. A. Jarzycka, A. Lewinska, R. Gancarz and K. A. Wilk, Assessment of extracts of *Helichrysum arenarium*, *Crataegus monogyna*, *Sambucus nigra* in photoprotective UVA and UVB; photostability in cosmetic emulsions, *Journal of Photochemistry and Photobiology. B, Biology*, 2013, **128**, 50-57.
155. F. Giampieri, J. M. Alvarez-Suarez, S. Tulipani, A. M. Gonzàles-Paramàs, C. Santos-Buelga, S. Bompadre, J. L. Quiles, B. Mezzetti and M. Battino, Photoprotective potential of strawberry (*Fragaria × ananassa*) extract against UV-A irradiation damage on human fibroblasts, *Journal of Agricultural and Food Chemistry*, 2012, **60**, (9), 2322-2327.
156. F. Fischer, E. Zufferey, J.-M. Bourgeois, J. Héritier and F. Micaux, UV-ABC screens of luteolin derivatives compared to edelweiss extract, *Journal of Photochemistry & Photobiology, B: Biology*, 2011, **103**, (1), 8-15.
157. L. C. Cefali, J. A. Ataide, P. Moriel, M. A. Foglio and P. G. Mazzola, Plant-based active photoprotectants for sunscreens, *International Journal of Cosmetic Science*, 2016, **38**, (4), 346-353.
158. M. A. Ollengo, The photochemistry and photostabilisation potential of plant extracts on sunscreen absorbers, Doctoral Degree (Chemistry), University of KwaZulu-Natal, 2014.
159. N. Lall and N. Kishore, Are plants used for skin care in South Africa fully explored?, *Journal of Ethnopharmacology*, 2014, **153**, (1), 61-84.
160. O. A. Wintola and A. J. Afolayan, Phytochemical constituents and antioxidant activities of the whole leaf extract of *Aloe ferox* Mill, *Pharmacognosy Magazine*, 2011, **7**, (28), 325-333.
161. D. T. Loots, F. H. van der Westhuizen and L. Botes, *Aloe ferox* leaf gel phytochemical content, antioxidant capacity, and possible health benefits, *Journal of Agricultural and Food Chemistry*, 2007, **55**, (17), 6891.
162. B.-E. Van Wyk, B. Van Oudtshoorn and N. Gericke, *Medicinal Plants of South Africa*, Briza Publications, Pretoria, 1997.
163. W. Chen, B.-E. Van Wyk, I. Vermaak and A. M. Viljoen, Cape aloes—A review of the phytochemistry, pharmacology and commercialisation of *Aloe ferox*, *Phytochemistry Letters*, 2012, **5**, (1), 1-12.
164. D. J. Newton and H. Vaughan, *South Africa's Aloe Ferox Plant: Parts and Derivatives Industry*, Traffic East/Southern Africa, Johannesburg, 1996.

165. A. Melin, A bitter pill to swallow: A case study of the trade and harvest of *Aloe ferox* in the Eastern Cape, South Africa, Master of Science Dissertation, Imperial College, London, 2009.
166. L. J. Haynes, D. K. Holdsworth and R. Russell, C-Glycosyl compounds. Part VI. Aloesin, a C-glucosylchromone from *Aloe* sp, *Journal of the Chemical Society C: Organic*, 1970, DOI: 10.1039/J39700002581, (18), 2581-2586.
167. A. Yagi and S. Takeo, Anti-inflammatory constituents, aloesin and aloemannan in aloe species and effects of tanshinon VI in *Salvia miltiorrhiza* on heart, *Yakugaku Zasshi Yakugaku Zasshi*, 2003, **123**, (7), 517-532.
168. K. Jones, J. Hughes, M. Hong, Q. Jia and S. Orndorff, Modulation of melanogenesis by Aloesin: A competitive inhibitor of tyrosinase, *Pigment Cell Research*, 2002, **15**, (5), 335-340.
169. S. Choi, S. K. Lee, J. E. Kim, M. H. Chung and Y. I. Park, Aloesin inhibits hyperpigmentation induced by UV radiation, *Clinical and Experimental Dermatology*, 2002, **27**, (6), 513-515.
170. L. H. Steenkamp, Mitra, R.K., Heggie, S.J., Pehane, V.N, Method for converting aloeresin A to aloesin, *US Patent 2008/0280348*, 2008.
171. L. G. Grollier JF, Gratien S, Forestier S, Rosenbaum G., *Cosmetic composition containing Aloesin as an agent for protection against sunlight and its use for skin and hair protection.*, US Patent 4,656,029, 1987.
172. W. Stahl, U. Heinrich, O. Aust, H. Tronnier and H. Sies, Lycopene-rich products and dietary photoprotection, *Photochemical & Photobiological Sciences*, 2006, **5**, (2), 238-242.
173. N. I. Krinsky, The Antioxidant and Biological Properties of the Carotenoids, *Annals of the New York Academy of Sciences*, 1998, **854**, (1), 443-447.
174. A. J. Young and G. M. Lowe, Antioxidant and prooxidant properties of carotenoids, *Archives of Biochemistry and Biophysics*, 2001, **385**, (1), 20-27.
175. M. M. Mathews-Roth, M. A. Pathak, J. Parrish, T. B. Fitzpatrick, E. H. Kass, K. Toda and W. Clemens, A clinical trial of the effects of oral beta-carotene on the responses of human skin to solar radiation, *The Journal of Investigative Dermatology*, 1972, **59**, (4), 349-353.
176. H. P. M. Gollnick, W. Hopfenmueller, C. Hemmes, S. C. Chun, C. Schmid, K. Sundermeier and H. K. Biesalski, Systemic beta carotene plus topical UV-sunscreen are an optimal protection against harmful effects of natural UV-sunlight: Results of the Berlin-Eilath study, *European Journal of Dermatology*, 1996, **6**, (3), 200-205.
177. M. Garmyn, J. D. Ribaya-Mercado, R. M. Russel, J. Bhawan and B. A. Gilchrest, Effect of beta-carotene supplementation on the human sunburn reaction, *Experimental Dermatology*, 1995, **4**, (2), 104-111.
178. J. Terao, Y. Minami and N. Bando, Singlet molecular oxygen-quenching activity of carotenoids: relevance to protection of the skin from photoaging, *Journal of Clinical Biochemistry and Nutrition*, 2011, **48**, (1), 57-62.
179. J. G. Lovas, G. E. Kaugars and S. Silverman, Jr., Beta-carotene and lung cancer?, *Oral Surgery, Oral Medicine, Oral Pathology, Oral Radiology, and Endodontics*, 1996, **82**, (3), 236-237.
180. K. Woodson, D. Albanes, J. A. Tangrea, M. Rautalahti, J. Virtamo and P. R. Taylor, Association between alcohol and lung cancer in the alpha-tocopherol, beta-carotene cancer prevention study in Finland, *Cancer Causes & Control*, 1999, **10**, (3), 219-226.
181. G. S. Omenn, G. E. Goodman, M. D. Thornquist, J. Balmes, M. R. Cullen, A. Glass, J. P. Keogh, F. L. Meyskens, Jr., B. Valanis, J. H. Williams, Jr., S. Barnhart, M. G. Cherniack, C. A. Brodtkin and S. Hammar, Risk factors for lung cancer and for

- intervention effects in CARET, the Beta-Carotene and Retinol Efficacy Trial, *Journal of the National Cancer Institute*, 1996, **88**, (21), 1550-1559.
182. J. V. Freitas and L. R. Gaspar, In vitro photosafety and efficacy screening of apigenin, chrysin and beta-carotene for UVA and VIS protection, *European Journal of Pharmaceutical Sciences*, 2016, **89**, 146-153.
 183. M. E. Darvin, J. W. Fluhr, M. C. Meinke, L. Zastrow, W. Sterry and J. Lademann, Topical beta-carotene protects against infra-red-light-induced free radicals, *Experimental Dermatology*, 2011, **20**, (2), 125-129.
 184. J. V. Freitas, N. P. Lopes and L. R. Gaspar, Photostability evaluation of five UV-filters, trans-resveratrol and beta-carotene in sunscreens, *European Journal of Pharmaceutical Sciences*, 2015, **78**, 79-89.
 185. O. Eichler, H. Sies and W. Stahl, Divergent optimum levels of lycopene, beta-carotene and lutein protecting against UVB irradiation in human fibroblastst, *Photochemistry and Photobiology*, 2002, **75**, (5), 503-506.
 186. A. Mortensen, Scavenging of benzylperoxyl radicals by carotenoids, *Free Radical Research*, 2002, **36**, (2), 211-216.
 187. F. Fianny Rezka Sjahjadi, Henny Lucida, Formula optimization of a sunscreen cream of tomato's purified extract, *Advances in Health Sciences Research*, 2012, **40**, (2nd International Conference on Contemporary Science and Clinical Pharmacy 2021 (ICCSCP 2021)).
 188. A. J. Ruby, G. Kuttan, K. D. Babu, K. N. Rajasekharan and R. Kuttan, Anti-tumour and antioxidant activity of natural curcuminoids, *Cancer Letters*, 1995, **94**, (1), 79-83.
 189. P. Limtrakul, S. Lipigorngoson, O. Namwong, A. Apisariyakul and F. W. Dunn, Inhibitory effect of dietary curcumin on skin carcinogenesis in mice, *Cancer Letters*, 1997, **116**, (2), 197-203.
 190. M. A. Azuine and S. V. Bhide, Chemopreventive effect of turmeric against stomach and skin tumors induced by chemical carcinogens in Swiss mice, *Nutrition and Cancer*, 1992, **17**, (1), 77-83.
 191. A. H. Conney, T. Lysz, T. Ferraro, T. F. Abidi, P. S. Manchand, J. D. Laskin and M. T. Huang, Inhibitory effect of curcumin and some related dietary compounds on tumor promotion and arachidonic acid metabolism in mouse skin, *Advances in Enzyme Regulation*, 1991, **31**, 385-396.
 192. M. T. Huang, R. C. Smart, C. Q. Wong and A. H. Conney, Inhibitory effect of curcumin, chlorogenic acid, caffeic acid, and ferulic acid on tumor promotion in mouse skin by 12-O-tetradecanoylphorbol-13-acetate, *Cancer Research*, 1988, **48**, (21), 5941-5946.
 193. M. C. Y. Heng, Signaling pathways targeted by curcumin in acute and chronic injury: burns and photo-damaged skin, *International Journal of Dermatology*, 2013, **52**, (5), 531-543.
 194. N. C. Adusumilli, B. Mordorski, J. Nosanchuk, J. M. Friedman and A. J. Friedman, Curcumin nanoparticles as a photoprotective adjuvant, *Experimental Dermatology*, 2021, **30**, (5), 705-709.
 195. M. Rodrigues, J. Fernandes, R. Ruggiero and W. Guerra, Palladium complex containing curcumin as ligand: Thermal and spectral characterization, *American Journal of Chemistry*, 2012, **2**, 157-159.
 196. I. P. Z. Woldemariam, *Sunscreen comprising a curcuma extract*, United States, 2012.
 197. Y. Cao, Q. Chu, Y. Fang and J. Ye, Analysis of flavonoids in Ginkgo biloba L. and its phytopharmaceuticals by capillary electrophoresis with electrochemical detection, *Analytical and Bioanalytical Chemistry*, 2002, **374**, (2), 294-299.

198. V. Exarchou, N. Nenadis, M. Tsimidou, I. P. Gerothanassis, A. Troganis and D. Boskou, Antioxidant activities and phenolic composition of extracts from Greek oregano, Greek sage, and summer savory, *Journal of Agricultural and Food Chemistry*, 2002, **50**, (19), 5294-5299.
199. H. Wei, R. Saladi, Y. Lu, Y. Wang, S. R. Palep, J. Moore, R. Phelps, E. Shyong and M. G. Lebwohl, Isoflavone genistein: photoprotection and clinical implications in dermatology, *The Journal of Nutrition.*, 2003, **133**, (11), 3811.
200. H. Wei, R. Bowen, Q. Cai, S. Barnes and Y. Wang, Antioxidant and antipromotional effects of the soybean isoflavone genistein, *Experimental Biology and Medicine*, 1995, **208**, (1), 124-130.
201. H. Wei, L. Wei, K. Frenkel, R. Bowen and S. Barnes, Inhibition of tumor promoter-induced hydrogen peroxide formation in vitro and in vivo by genistein, *Nutrition and Cancer*, 1993, **20**, (1), 1-12.
202. S. Kang, J. H. Chung, J. H. Lee, G. J. Fisher, Y. S. Wan, E. A. Duell and J. J. Voorhees, Topical n-acetyl cysteine and genistein prevent ultraviolet-light-induced signaling that leads to photoaging in human skin in vivo, *Journal of Investigative Dermatology*, 2003, **120**, (5), 835-841.
203. J. O. Moore, Y. Wang, W. G. Stebbins, D. Gao, X. Zhou, R. Phelps, M. Lebwohl and H. Wei, Photoprotective effect of isoflavone genistein on ultraviolet B-induced pyrimidine dimer formation and PCNA expression in human reconstituted skin and its implications in dermatology and prevention of cutaneous carcinogenesis, *Carcinogenesis*, 2006, **27**, (8), 1627-1635.
204. H. Shi and E. Niki, Stoichiometric and kinetic studies on Ginkgo biloba extract and related antioxidants, *Lipids*, 1998, **33**, (4), 365-370.
205. M. K. Ozkur, M. S. Bozkurt, B. Balabanli, A. Aricioglu, N. Ilter, M. A. Gürer and H. S. Inalöz, The effects of EGb 761 on lipid peroxide levels and superoxide dismutase activity in sunburn, *Photodermatology, Photoimmunology & Photomedicine*, 2002, **18**, (3), 117-120.
206. S. Y. Lin and H. P. Chang, Induction of superoxide dismutase and catalase activity in different rat tissues and protection from UVB irradiation after topical application of Ginkgo biloba extracts, *Methods and Findings in Experimental and Clinical Pharmacology*, 1997, **19**, (6).
207. C.-W. Zhang, M.-F. Li, R. Tao, M.-J. Peng, Z.-H. Wang, Z.-W. Qi, X.-Y. Xue and C.-Z. Wang, Physicochemical property and antibacterial activity of formulation containing polyphenol extracted from Ginkgo biloba leaves, *Industrial Crops and Products*, 2020, **147**, 112213.
208. D. G. Mercurio, T. A. L. Wagemaker, V. M. Alves, C. G. Benevenuto, L. R. Gaspar and P. M. B. G. Maia Campos, In vivo photoprotective effects of cosmetic formulations containing UV filters, vitamins, Ginkgo biloba and red algae extracts, *Journal of Photochemistry and Photobiology B: Biology*, 2015, **153**, 121-126.
209. O. Lanzalunga and M. Bietti, Photo- and radiation chemical induced degradation of lignin model compounds, *Journal of Photochemistry & Photobiology, B: Biology*, 2000, **56**, (2), 85-108.
210. S. Barsberg, T. Elder and C. Felby, LigninQuinone interactions: Implications for optical properties of lignin, *Chemistry of Materials*, 2003, **15**, (3), 649-655.
211. K. V. Sarkanen and C. H. Ludwig, *Lignins: Occurrence, Formation, Structure and Reactions*, Wiley-Interscience, New York, 1971.
212. Y. Qian, X. Qiu and S. Zhu, Lignin: A nature-inspired sun blocker for broad-spectrum sunscreens, *Green Chemistry*, 2015, **17**, (1), 320-324.

213. Y. Qian, X. Qiu and S. Zhu, Sunscreen performance of lignin from different technical resources and their general synergistic effect with synthetic sunscreens, *ACS Sustainable Chemistry & Engineering*, 2016, **4**, (7), 4029-4035.
214. A. Horvath, F. Alvarado, J. Szöcs, Z. N. de Alvarado and G. Padilla, Metabolic effects of calagualine, an antitumoral saponine of *Polypodium leucotomos*, *Nature*, 1967, **214**, (5094), 1256-1258.
215. A. J. Gomes, C. N. Lunardi, S. Gonzalez and A. C. Tedesco, The antioxidant action of *Polypodium leucotomos* extract and kojic acid: reactions with reactive oxygen species, *Brazilian Journal of Medical and Biological Research*, 2001, **34**, (11), 1487-1494.
216. S. Gonzalez, Y. Gilaberte, N. Philips and A. Juarranz, Fernblock, a nutraceutical with photoprotective properties and potential preventive agent for skin photoaging and photoinduced skin cancers, *International Journal of Molecular Sciences*, 2011, **12**, (12), 8466-8475.
217. J. R. Siscovick, T. Zapolanski, C. Magro, K. Carrington, S. Prograis, M. Nussbaum, S. Gonzalez, W. Ding and R. D. Granstein, *Polypodium leucotomos* inhibits ultraviolet B radiation-induced immunosuppression, *Photodermatology, Photoimmunology & Photomedicine*, 2008, **24**, (3), 134-141.
218. M. A. Middelkamp-Hup, M. A. Pathak, C. Parrado, D. Goukassian, F. Rius-Díaz, M. C. Mihm, T. B. Fitzpatrick and S. González, Oral *Polypodium leucotomos* extract decreases ultraviolet-induced damage of human skin, *Journal of the American Academy of Dermatology*, 2004, **51**, (6), 910-918.
219. A. Zamarrón, S. Lorrio, S. González and Á. Juarranz, Fernblock prevents dermal cell damage induced by visible and infrared A radiation, *International Journal of Molecular Sciences*, 2018, **19**, (8).
220. C. Parrado, M. Mascaraque, Y. Gilaberte, A. Juarranz and S. Gonzalez, Fernblock (*Polypodium leucotomos* extract): Molecular mechanisms and pleiotropic effects in light-related skin conditions, photoaging and skin cancers, A Review, *International Journal of Molecular Sciences*, 2016, **17**, (7).
221. K. Subbaramaiah, W. J. Chung, P. Michaluart, N. Telang, T. Tanabe, H. Inoue, M. Jang, J. M. Pezzuto and A. J. Dannenberg, Resveratrol inhibits cyclooxygenase-2 transcription and activity in phorbol ester-treated human mammary epithelial cells, *The Journal of Biological Chemistry*, 1998, **273**, (34), 21875-21882.
222. F. Afaq, V. M. Adhami and N. Ahmad, Prevention of short-term ultraviolet B radiation-mediated damages by resveratrol in SKH-1 hairless mice., *Toxicology and Applied Pharmacology*, 2003, **186**, (1), 28-37.
223. M. Jang, L. Cai, G. O. Udeani, K. V. Slowing, C. F. Thomas, C. W. Beecher, H. H. Fong, N. R. Farnsworth, A. D. Kinghorn, R. G. Mehta, R. C. Moon and J. M. Pezzuto, Cancer chemopreventive activity of resveratrol, a natural product derived from grapes, *Science (New York, N.Y.)*, 1997, **275**, (5297), 218-220.
224. M. Athar, J. H. Back, X. Tang, K. H. Kim, L. Kopelovich, D. R. Bickers and A. L. Kim, Resveratrol: A review of preclinical studies for human cancer prevention, *Toxicology and Applied Pharmacology*, 2007, **224**, (3), 274-283.
225. M. H. Aziz, F. Afaq and N. Ahmad, Prevention of ultraviolet-B radiation damage by resveratrol in mouse skin is mediated via modulation in survivin, *Photochemistry and Photobiology*, 2005, **81**, (1).
226. S. Bhattacharya and A. P. Sherje, Development of resveratrol and green tea sunscreen formulation for combined photoprotective and antioxidant properties, *Journal of Drug Delivery Science and Technology*, 2020, **60**.

227. P. Ody and S. Herb, *The Herb Society's Complete Medicinal Herbal*, Human & Rousseau, Cape Town, 1994.
228. J. A. Duke, *Handbook of Phytochemical Constituents of GRAS Herbs and Other Economic Plants*, CRC Press, Boca Raton, 1992.
229. H. Tabrizi, S. A. Mortazavi and M. Kamalinejad, An in vitro evaluation of various *Rosa damascena* flower extracts as a natural antisolar agent, *International Journal of Cosmetic Science*, 2003, **25**, (6), 259-265.
230. A. Svobodová, J. Psotová and D. Walterová, Natural phenolics in the prevention of UV-induced skin damage. A Review, *Biomedical papers of the Medical Faculty of the University Palacký, Olomouc, Czechoslovakia*, 2003, **147**, (2), 137-145.
231. H. Wagner, P. Diesel and M. Seitz, The chemistry and analysis of silymarin from *Silybum marianum* Gaertn., *Arzneimittel-Forschung*, 1974, **24**, (4), 466-471.
232. A. Comoglio, G. Leonarduzzi, R. Carini, D. Busolin, H. Basaga, E. Albano, A. Tomasi, G. Poli, P. Morazzoni and M. J. Magistretti, Studies on the antioxidant and free radical scavenging properties of Idb 1016 a new flavanolignan complex, *Free Radical Research*, 1990, **11**, (1-3), 109-115.
233. R. P. Singh and R. Agarwal, Flavonoid antioxidant silymarin and skin cancer, *Antioxidants & Redox Signaling*, 2002, **4**, (4), 655-663.
234. J. Rojas, C. Londono and Y. Ciro, The health benefits of natural skin UVA photoprotective compounds found in botanical sources, *International Journal of Pharmacy and Pharmaceutical Sciences*, 2016, **8**, (3), 13-23.
235. A. Rajnochová Svobodová, E. Gabrielová, L. Michaelides, P. Kosina, A. Ryšavá, J. Ulrichová, B. Zálešák and J. Vostálová, UVA-photoprotective potential of silymarin and silybin, *Archives of Dermatological Research*, 2018, **310**, (5), 413-424.
236. G. Netto Mpharm and J. Jose, Development, characterization, and evaluation of sunscreen cream containing solid lipid nanoparticles of silymarin, *Journal of Cosmetic Dermatology*, 2018, **17**, (6), 1073-1083.
237. F. Afaq and H. Mukhtar, Photochemoprevention by botanical antioxidants, *Skin Pharmacology and Applied Skin Physiology*, 2002, **15**, (5), 297-306.
238. S. R. Pinnell, Cutaneous photodamage, oxidative stress, and topical antioxidant protection, *Journal of the American Academy of Dermatology*, 2003, **48**, (1), 1-19.
239. J. Zhao, X. Jin, E. Yaping, Z. S. Zheng, Y. J. Zhang, M. Athar, V. A. DeLeo, H. Mukhtar, D. R. Bickers and Z. Y. Wang, Photoprotective effect of black tea extracts against UVB-induced phototoxicity in skin, *Photochemistry and Photobiology*, 1999, **70**, (4), 637-644.
240. I. Sopyan, R. Permata, D. Gozali and I. Syah, Formulation of lotion from black tea extract (*Camellia sinensis* linnaeus) as sunscreen, *International Journal of Applied Pharmaceutics*, 2019, **11**, 205.
241. M. Turkoglu and N. Cigirgil, Evaluation of black tea gel and its protection potential against UV, *International Journal of Cosmetic Science*, 2007, **29**, (6), 437-442.
242. L. Erickson, Rooibos tea: Research into antioxidant and antimutagenic properties, *HerbalGram: The Journal of the American Botanical Council*, 2003, **59**, 34-45.
243. A. Saija, A. Tomaino, D. Trombetta, A. De Pasquale, N. Uccella, T. Barbuzzi, D. Paolino and F. Bonina, In vitro and in vivo evaluation of caffeic and ferulic acids as topical photoprotective agents, *International Journal of Pharmaceutics*, 2000, **199**, (1), 39-47.
244. E. Joubert and D. de Beer, Rooibos (*Aspalathus linearis*) beyond the farm gate: From herbal tea to potential phytopharmaceutical, *South African Journal of Botany*, 2011, **77**, (4), 869-886.

245. D. Picard, The biochemistry of green tea polyphenols and their potential application in human skin cancer, *Scientific Review of Alternative Medicine*, 1996, **1**, (1), 31-42.
246. C. A. Elmets, D. Singh, K. Tubesing, M. Matsui, S. Katiyar and H. Mukhtar, Cutaneous photoprotection from ultraviolet injury by green tea polyphenols, *Journal of the American Academy of Dermatology*, 2001, **44**, (3), 425-432.
247. M. M. Camouse, D. S. Domingo, F. R. Swain, E. P. Conrad, M. S. Matsui, D. Maes, L. Declercq, K. D. Cooper, S. R. Stevens and E. D. Baron, Topical application of green and white tea extracts provides protection from solar-simulated ultraviolet light in human skin, *Experimental Dermatology*, 2009, **18**, (6), 522-526.
248. S. E. Dal Belo, L. R. Gaspar and P. M. B. G. Maia Campos, Photoprotective effects of topical formulations containing a combination of Ginkgo biloba and green tea extracts, *Phytotherapy Research*, 2011, **25**, (12), 1854-1860.
249. S.-J. Kim, Effect of biflavones of Ginkgo biloba against UVB-induced cytotoxicity *in vitro*, *The Journal of Dermatology*, 2001, **28**, (4), 193-199.
250. V. C. Korb, The effects of Sutherlandia frutescens on normal human lymphocytes in vitro, Master of Science Dissertation, 2009.
251. A. C. Fernandes, A. D. Cromarty, C. Albrecht and C. E. Jansen van Rensburg, The antioxidant potential of Sutherlandia frutescens, *Journal of Ethnopharmacology*, 2004, **95**, (1), 1-5.
252. J. V. Seier, G. Van Der Horst, M. De Kock and K. Chwalisz, The detection and monitoring of early pregnancy in the vervet monkey (*Cercopithecus aethiops*) with the use of ultrasound and correlation with reproductive steroid hormones, *Journal of Medical Primatology*, 2000, **29**, (2), 70-75.
253. S. Shaik, Y. H. Dewir, N. Singh and A. Nicholas, Micropropagation and bioreactor studies of the medicinally important plant *Lessertia* (*Sutherlandia*) *frutescens* L., *South African Journal of Botany*, 2010, **76**, (2), 180-186.
254. S. Tobwala, W. Fan, C. J. Hines, W. R. Folk and N. Ercal, Antioxidant potential of *Sutherlandia frutescens* and its protective effects against oxidative stress in various cell cultures, *BMC Complementary and Alternative Medicine*, 2014, **14**, (1).
255. J. Tai, S. Cheung, E. Chan and D. Hasman, In vitro culture studies of *Sutherlandia frutescens* on human tumor cell lines, *Journal of Ethnopharmacology*, 2004, **93**, (1), 9-19.
256. B. G. Chiari, E. Trovatti, D. Pecoraro, M. A. Corra, R. M. B. Cicarelli, S. J. L. Ribeiro and V. L. B. Isaac, Synergistic effect of green coffee oil and synthetic sunscreen for health care application, *Industrial Crops and Products*, 2014, **52**, (13), 389-393.
257. Y. R. Liang, Z. S. Liu, Y. R. Xu and Y. L. Hu, A study on chemical composition of two special green teas (*Camellia sinensis*), *Journal of the Science of Food and Agriculture*, 1990, **53**, (4), 541-548.
258. UV-Vis Spectroscopy, <https://www2.chemistry.msu.edu/faculty/reusch/virttxtjml/spectrpy/uv-vis/uvspec.htm>, (accessed 13 July, 2019).
259. J. Clark, A Double Beam UV-Visible Absorption Spectrometer, <http://www.chemguide.co.uk/analysis/uvvisible/spectrometer.html>, (accessed 07 February, 2017).
260. S. R. Aliwell, Para-aminobenzoic acid photosensitised dimerisation of thymine, Master of Science Dissertation, University of KwaZulu-Natal, 1991.
261. J. K. Broadbent, Photochemical studies of sunscreen constituents, Master of Science Dissertation, 1994.
262. D. K. K. Showa, Introduction to HPLC, <https://www.shodex.com/en/kouza/a.html>, (accessed 17 July, 2018).

263. International Federation of Societies of Cosmetic Chemists, The Fundamentals of Stability Testing, *IFSCC Monograph, Number 2*, 1992.
264. J. S. B. Mansur, M. N. R.; Mansur, M. C. A.; Azulay, R. D., Determinação do fator de proteção solar por espectrofotometria, *Anais Brasileiros de Dermatologia*, 1986, **61**, 1221-1224.
265. R. M. Sayre, P. P. Agin, G. J. LeVee and E. Marlowe, A comparison of in vivo and in vitro testing of sunscreens formulas, *Photochemistry and Photobiology*, 1979, **29**, (3), 559-566.
266. S. A. Wissing and R. H. Müller, The influence of the crystallinity of lipid nanoparticles on their occlusive properties, *International Journal of Pharmaceutics*, 2002, **242**, (1), 377-379.
267. C. Couteau, S. El-Boury, E. Papis, V. Sébille-Rivain and L. J. Coiffard, In vitro UV-A protection factor (PF-UVA) of organic and inorganic sunscreens, *Pharmaceutical Development and Technology*, 2009, **14**, (4), 369-372.
268. A. Sewlall, DNA cleavage, photoinduced by benzophenone-based sunscreens, Master of Science Dissertation, University of KwaZulu-Natal, 2003.
269. K. Bolton, B. S. Martincigh and L. F. Salter, The potential carcinogenic effect of Uvinul DS49 — a common UV absorber used in cosmetics, *Journal of Photochemistry & Photobiology, A: Chemistry*, 1992, **63**, (2), 241-248.
270. R. Panday, A photochemical investigation of two sunscreen absorbers in a polar and a non-polar medium, Master of Science Dissertation, University of KwaZulu-Natal, 2002.
271. N. M. Roscher, M. K. O. Lindemann, S. Bin Kong, C. G. Cho and P. Jiang, Photodecomposition of several compounds commonly used as sunscreen agents, *Journal of Photochemistry and Photobiology, A: Chemistry*, 1994, **80**, (1), 417-421.
272. L. E. Agrapidis-Paloympis, R. A. Nash and N. A. Shaath, The effect of solvents on the ultraviolet absorbance of sunscreens, *Journal of the Society of Cosmetic Chemists*, 1987, **38**, 209-221.
273. S. Tobita, J. Ohba, K. Nakagawa and H. Shizuka, Recovery mechanism of the reaction intermediate produced by photoinduced cleavage of the intramolecular hydrogen bond of dibenzoylmethane, *Journal of Photochemistry and Photobiology A: Chemistry*, 1995, **92**, (1), 61-67.
274. S. F. Gerard Lang, Alain LaGrange, Claudine Moire, Andre DeFlandre, Saint Gratien, 4952391 Tert-butyl derivatives of benzylidenecamphor, process for preparing them, their use as antioxidant agents and cosmetic and pharmaceutical compositions containing them, France assigned to L'Oreal, *General Pharmacology*, 1991, **22**, (2), iv-iv.
275. F. Rancan, S. Rosan, K. Boehm, E. Fernández, M. E. Hidalgo, W. Quihot, C. Rubio, F. Boehm, H. Piazena and U. Oltmanns, Protection against UVB irradiation by natural filters extracted from lichens, *Journal of Photochemistry & Photobiology, B: Biology*, 2002, **68**, (2), 133-139.
276. A. R. Magee, B.-E. v. Wyk and P. M. Tilney, A taxonomic revision of the woody South African genus *Notobubon* (apiaceae: apioidae), *Systematic Botany*, 2009, **34**, (1), 220-242.
277. B.-E. G. N. Van Wyk, *People's Plants: A Guide to Useful Plants of Southern Africa*, Briza Publications, Pretoria, South Africa, 2000.
278. I. W. Southon, Systemic significance of canavine in the Papilionoideae (Faboideae) *Biochemical Systematics and Ecology* 6, 1994, **201–212**.

279. L. Al Shaal, R. Shegokar and R. H. Müller, Production and characterization of antioxidant apigenin nanocrystals as a novel UV skin protective formulation, *International Journal of Pharmaceutics*, 2011, **420**, (1), 133-140.
280. N. M. Gavin and M. J. Durako, Localization and antioxidant capacity of flavonoids from intertidal and subtidal *Halophila johnsonii* and *Halophila decipiens*, *Aquatic Botany*, 2011, **95**, (3), 242-247.
281. V. Salnikov, N. M. Pogodina, S. B. Chemikosova, E. V. Yablokova, A. Ulanov, M. Ageeva, J. Dam and V. Lozovaya, Composition and distribution of cell wall phenolic compounds in flax (*Linum usitatissimum* L.) stem tissues, *Annals of Botany*, 2000, **85**, (4), 477-486.
282. V. Bilušić Vundać, A. H. Brantner and M. Plazibat, Content of polyphenolic constituents and antioxidant activity of some *Stachys* taxa, *Food Chemistry*, 2007, **104**, (3), 1277-1281.
283. I. Koleva, v. T. A. Beek, J. P. H. Linssen, d. A. Groot and L. N. Evstatieva, Screening of plant extracts for antioxidant activity: A comparative study on three testing methods, *Phytochemical Analysis*, 2002, **13**, (1), 8-17.
284. D. Venes, *Taber's Cyclopedic Medical Dictionary*, F.A. Davis Company, Philadelphia, 2017.
285. B. Lapornik, M. Prošek and A. Golc Wondra, Comparison of extracts prepared from plant by-products using different solvents and extraction time, *Journal of Food Engineering*, 2005, **71**, (2), 214-222.
286. F. A. Tomás-Barberán, I. Martos, F. Ferreres, B. S. Radovic and E. Anklam, HPLC flavonoid profiles as markers for the botanical origin of European unifloral honeys HPLC flavonoid profiles as unifloral honey markers, *Journal of the Science of Food and Agriculture*, 2001, **81**, (5), 485-496.
287. F. Bourgaud, A. Gravot, S. Milesi and E. Gontier, Production of plant secondary metabolites: a historical perspective, *Plant Science*, 2001, **161**, (5), 839-851.
288. A. P. M. Bernardi, J. de Matos Nunes, M. K. Marchioro, L. M. G. Rosa, G. L. von Poser and S. B. Rech, Phenolic compounds profiles during ex vitro acclimatization of micropropagated *Hypericum polyanthemum*, *Plant Physiology Biochemistry*, 2008, **46**, (7), 694-700.
289. P. C. Santos-Gomes, R. M. Seabra, P. B. Andrade and M. Fernandes-Ferreira, Phenolic antioxidant compounds produced by in vitro shoots of sage (*Salvia officinalis* L.), *Plant Science*, 2002, **162**, (6), 981-987.
290. K. Sevgi, B. Tepe and C. Sarikurkcu, Antioxidant and DNA damage protection potentials of selected phenolic acids, *Food and Chemical Toxicology*, 2015, **77**, 12-21.
291. Z. Sroka and W. Cisowski, Hydrogen peroxide scavenging, antioxidant and anti-radical activity of some phenolic acids, *Food and Chemical Toxicology*, 2003, **41**, (6), 753-758.
292. H.-A. H. Abd-ElSalam, M. A. Al-Ghobashy, M. Al-Shorbagy, N. Nassar, H. E. Zaazaa and M. A. Ibrahim, Correlation of in vivo and in vitro assay results for assessment of free radical scavenging activity of green tea nutraceuticals, *Journal of Food Science*, 2016, **81**, (7), 1707-1715.
293. W. A. C. Garbossa and P. M. B. G. Maia Campos, *Euterpe oleracea*, *Matricaria chamomilla*, and *Camellia sinensis* as promising ingredients for development of skin care formulations, *Industrial Crops & Products*, 2016, **83**, 1-10.
294. L. Juneja, M. Kapoor, T. Okubo and T. Rao, *Green Tea Polyphenols: Nutraceuticals of Modern Life*, 2013.

295. M. P. Barnett, J. M. Cooney, Y. E. Dommels, K. Nones, D. T. Brewster, Z. Park, C. A. Butts, W. C. McNabb, W. A. Laing and N. C. Roy, Modulation of colonic inflammation in Mdr1a(-/-) mice by green tea polyphenols and their effects on the colon transcriptome and proteome, *Journal of Nutritional Biochemistry*, 2013, **24**, (10), 1678-1690.
296. D. P. Gaynor, GRAS notice for oil-soluble green tea extract (green tea catechins palmitate, Journal, 2018.
297. C. G. L. Carreira, 2016.
298. Y. Niwa and Y. Miyachi, Antioxidant action of natural health products and Chinese herbs, *Inflammation*, 1986, **10**, (1), 79-91.
299. L. Bramati, F. Aquilano and P. Pietta, Unfermented rooibos tea: quantitative characterization of flavonoids by HPLC-UV and determination of the total antioxidant activity, *Journal of Agricultural and Food Chemistry*, 2003, **51**, (25), 7472-7474.
300. J. F. Morton, Rooibos tea, *Aspalathus linearis*, a caffeineless, low-tannin beverage, *Economic Botany*, 2008, **37**, 164-173.
301. L. Bramati, M. Minoggio, C. Gardana, P. Simonetti, P. Mauri and P. Pietta, Quantitative characterization of flavonoid compounds in Rooibos tea (*Aspalathus linearis*) by LC-UV/DAD, *Journal of Agricultural and Food Chemistry*, 2002, **50**, (20), 5513-5519.
302. D. L. McKay and J. B. Blumberg, A review of the bioactivity of South African herbal teas: rooibos (*Aspalathus linearis*) and honeybush (*Cyclopia intermedia*), *Phytotherapy Research*, 2007, **21**, (1), 1-16.
303. E. Joubert, HPLC quantification of the dihydrochalcones, aspalathin and nothofagin in rooibos tea (*Aspalathus linearis*) as affected by processing, *Food Chemistry*, 1996, **55**, (4), 403-411.
304. B. H. Koeppen and D. G. Roux, C-glycosylflavonoids. The chemistry of aspalathin, *The Biochemical Journal*, 1966, **99**, (3), 604-609.
305. S. Z. Dziedzic, B. J. F. Hudson and G. Barnes, Polyhydroxydihydrochalcones as antioxidants for lard, *Journal of Agricultural and Food Chemistry*, 1985, **33**, (2), 244-246.
306. K. M. Parida and S. Parija, Photocatalytic degradation of phenol under solar radiation using microwave irradiated zinc oxide, *Solar Energy*, 2006, **80**, (8), 1048-1054.
307. C. D. Stalikas, Extraction, separation, and detection methods for phenolic acids and flavonoids, *Journal of Separation Science*, 2007, **30**, (18), 3268-3295.
308. M. Waksmundzka-Hajnos, A. Oniszczyk, K. Szewczyk and D. Wianowska, Effect of sample-preparation methods on the HPLC quantitation of some phenolic acids in plant materials, *Acta Chromatographica.*, 2007.
309. R. Zadernowski, M. Naczka and J. Nesterowicz, Phenolic acid profiles in some small berries, *Journal of Agricultural and Food Chemistry*, 2005, **53**, (6), 2118-2124.
310. J. A. H. Kaeswurm, A. Scharinger, J. Teipel and M. Buchweitz, Absorption coefficients of phenolic structures in different solvents routinely used for experiments, *Molecules*, 2021, **26**, (15), 4656.
311. S. Tcholakova, N. D. Denkov, I. B. Ivanov and B. Campbell, Coalescence stability of emulsions containing globular milk proteins, *Advances in Colloid and Interface Science*, 2006, **123**, 259-293.
312. E. A. O. Dutra, D. A. G. C.; Kedor-Hackmann, E. R.; Santoro, M. I. R. M Determination of sun protection factor (SPF) of sunscreens by ultraviolet spectrophotometry *Revista Brasileira de Ciências Farmacêuticas*, 2004, **40**, (3), 381-385.

313. M. F. Pissavini, L.; Alaro, V.; Heinrich, U.; Tronnier, H.; Kockott, D.; Lutz, D.; Tournier, V.; Zambonin, M.; Meloni, M, Determination of the in vitro SPF, *Cosmetics and Toiletries*, 2003, **118**, 63-72.
314. H. Hamishehkar, S. Same, K. Adibkia, K. Zarza, J. Shokri, M. Taghaee and M. Kouhsoltani, A comparative histological study on the skin occlusion performance of a cream made of solid lipid nanoparticles and Vaseline, *Research in Pharmaceutical Sciences*, 2015, **10**, (5), 378-387.
315. K. P. Wilhelm, A. B. Cua and H. I. Maibach, Skin aging: Effect on transepidermal water loss, stratum corneum hydration, skin surface pH, and casual sebum content, *Archives of Dermatological Research*, 1991, **127**, (12), 1806-1809.

Appendix A

HPLC calibration data

Table A1: Calibration data for the determination of gallic acid

	a	b	c
100	1763940	1610451	1821068
200	3032524	3828368	4028585
400	7825878	8099000	8119262
800	15408919	15634498	15531386
1000	18979486	18904968	18963977

Table A2: Calibration data for the determination of *p*-hydroxybenzoic acid

	a	b	c
100	6356139	5787506	6553709
200	10233771	12931733	13578283
400	26596241	27487183	27555345
800	50995984	51224433	51118390
1000	58863952	58558854	58692541

Table A3: Calibration data for the determination of vanillic acid

	a	b	c
100	2904787	2657651	3006876
200	4534009	5736421	6039368
400	12165438	12591732	12641121
800	25666672	26011595	25958918
1000	33019028	32877648	33002480

Table A4: Calibration data for the determination of caffeic acid

	a	b	c
100	1972955	1810769	2054343
200	3103641	3935755	4143504
400	8479559	8770905	8796163
800	17877020	17998793	18059803
1000	22558329	22517458	22654712

Table A5: Calibration data for the determination of syringic acid

	a	b	c
100	1432703	1312323	1491224
200	2280908	2891886	3042331
400	6146922	6354961	6372815
800	13197251	13370760	13359988
1000	16361787	16294237	16353107

Table A6: Calibration data for the determination of *p*-coumaric acid

	a	b	c
100	885604	792268	908720
200	1448843	1834519	1941479
400	3898649	4029176	4050770
800	7964350	8010545	8047499
1000	9921978	9861315	9907529

Appendix B

Raw data for HPLC analysis

The following tables list the peak areas obtained for the HPLC analysis of the Cancer Bush and tea extracts.

Table B1: Peak areas obtained for the Cancer Bush ethanol-water extract at 254 nm

Peak #	Retention time	Area	Height
1	3.075	520	73
2	7.120	48483	2938
3	9.228	33818	1629
4	9.993	8892	518
5	11.349	4595	238
6	13.705	260435	10254
7	14.389	23623	885
8	17.797	1134	-8
9	18.190	24523	706
10	21.357	55484	1545
11	24.876	7521	195
12	42.375	106280	1561
13	50.280	226421	2767
Total		802728	23299

Table B2: Peak areas obtained for the Cancer Bush ethanol-water extract at 309 nm

Peak #	Retention time	Area	Height
1	6.561	23252	1156
2	9.987	23446	1282
3	11.330	7524	314

4	14.406	3724	175
5	17.263	2888	113
6	19.795	8238	180
7	24.886	19002	483
8	27.666	3329	94
9	38.553	57953	759
10	43.446	5594	217
11	50.232	1498777	18155
Total		1653796	22929

Table B3: Peak areas obtained for the Cancer Bush tea extraction method at 254 nm

Peak #	Retention time	Area	Height
1	3.075	8403	1720
2	6.946	201026	14816
3	8.679	2212654	16132
4	9.277	93236	11878
5	13.506	983469	36354
6	17.280	10541	386
7	17.531	849	443
8	17.990	77506	2384
9	21.066	1764223	4535
19	30.531	25462	660
11	41.812	343677	2891
12	49.269	718960	8561
13	55.498	495051	3834
Total		33472257	104593

Table B4: Peak areas obtained for the Cancer Bush tea extraction method at 309 nm

Peak #	Retention time	Area	Height
1	3.441	8764	690
2	5.340	13118	1039
3	6.045	16155	1514
4	6.491	62511	4725
5	6.947	38447	2794
6	7.397	7633	587
7	9.051	81749	6445
8	9.277	50044	6933
9	11.136	12365	543
10	13.997	25790	602
11	18.006	34569	1191
12	19.438	22548	569
13	21.125	24443	623
14	24.538	59472	1317
15	37.677	21318	420
16	49.241	4574065	58176
17	55.658	483826	5599
Total		5536815	93865

Table B5: Peak areas obtained for the green tea extract at 254 nm

Peak #	Retention time	Area	Height
1	3.455	2315022	243079
2	4.304	235	207
3	5.052	244496	19718
4	6.687	316641	25526
5	6.901	2453	3833

6	7.062	181491	12573
7	11.004	52810	2352
8	13.467	148143	3671
9	15.189	67924	1605
10	16.271	1811589	45816
11	24.950	28939842	491202
12	40.892	25292582	208015
13	51.308	796761	8649
Total		60169989	1066245

Table B6: Peak areas obtained for the green tea extract at 309 nm

Peak #	Retention time	Area	Height
1	3.116	28082	2947
2	3.456	560313	66152
3	4.787	64963	7011
4	6.109	15793	1433
5	7.062	32233	2304
6	10.073	52321	2660
7	10.989	15748	1359
8	13.887	309393	10902
9	16.300	47930	1096
10	19.828	82138	1985
11	25.376	305846	4733
12	27.798	90600	1725
13	35.777	39421	681
14	40.867	10735772	88316
15	48.946	243179	3431

16	51.129	1020151	12412
Total		13643883	209146

Table B7: Peak areas obtained for the Rooibos tea extract at 254 nm

Peak #	Retention time	Area	Height
1	2.873	6896	1119
2	3.478	11110	1285
3	7.084	885125	69594
4	10.611	34133	2300
5	13.505	162162	7564
6	17.919	28238	963
7	21.087	369927	10284
8	25.824	11222	271
9	27.396	5871	178
10	32.174	18835	574
11	35.934	319271	1935
12	59.892	437107	1054
Total		2289897	97121

Table B8: Peak areas obtained for the Rooibos tea extract at 309 nm

Peak #	Retention time	Area	Height
1	3,484	3484	434
2	5,173	8223	840
3	7,085	166985	13236
4	7,902	26956	1699
5	8,596	3690	234
6	10,617	132408	7145
7	13.150	6053	314
8	17.391	3772	197
9	19.574	1969	91
10	24.382	49287	1318
11	27.479	24163	588
12	29.598	73129	1671
13	37.814	206532	945
14	46.337	42824	641
15	48.996	157071	2156
Total		906545	31509

Appendix C

Data for the determination of SPF using Mansur equation

SPF 1.1	Before irradiation		
wavelength	EE × I	A	EE × I × A
290	0.015	2.4226	0.03639
295	0.0817	2.661	0.217404
300	0.2874	2.836	0.815066
305	0.3278	2.949	0.966682
310	0.1864	2.966	0.552862
315	0.0839	2.898	0.243142
320	0.018	2.678	0.048204
Sum			2.879751
SPF (sum x CF)			28.79751

SPF1.2	Before irradiation		
wavelength	EE x I	A	EE x I x A
290	0.015	0.544	0.00816
295	0.0817	0.576	0.047059
300	0.2874	0.601	0.172727
305	0.3278	0.614	0.201269
310	0.1864	0.61	0.113704
315	0.0839	0.589	0.049417
320	0.018	0.537	0.009666
Sum			0.602003
SPF (sum x CF)			6.020029

SPF1.2	After six hours of irradiation		
wavelength	EE x I	A	EE x I x A
290	0.015	0.462	0.00693
295	0.0817	0.478	0.039053
300	0.2874	0.491	0.141113
305	0.3278	0.496	0.162589
310	0.1864	0.488	0.090963
315	0.0839	0.468	0.039265
320	0.018	0.431	0.007758
Sum			0.487671
SPF (sum x CF)			4.876712

SPF1.3	Before irradiation		
wavelength	EE x I	A	EE x I x A
290	0.015	1.219	0.018285
295	0.0817	1.293	0.105638

SPF1.3	After six hours of irradiation		
wavelength	EE x I	A	EE x I x A
290	0.015	1.237	0.018555
295	0.0817	1.293	0.105638

300	0.2874	1.338	0.38454 1
305	0.3278	1.363	0.44679 1
310	0.1864	1.356	0.25275 8
315	0.0839	1.319	0.11066 4
320	0.018	1.226	0.02206 8
Sum			1.34074 6
SPF (sum x CF)			13.4074 6

300	0.287 4	1.33 7	0.384254
305	0.327 8	1.35 9	0.44548
310	0.186 4	1.35 6	0.252758
315	0.083 9	1.31 9	0.110664
320	0.018	1.22 6	0.022068
Sum			1.339418
SPF (sum x CF)			13.39418

SPF2.1 Before irradiation

wavelength	EE x I	A	EE x I x A
290	0.015	1.22	0.0183
295	0.0817	1.232	0.10065 4
300	0.2874	1.219	0.35034 1
305	0.3278	1.197	0.39237 7
310	0.1864	1.171	0.21827 4
315	0.0839	1.102	0.09245 8
320	0.018	0.964	0.01735 2
Sum			1.18975 6
SPF (sum x CF)			11.8975 6

SPF2.1 After six hours of irradiation

wavelength	EE x I	A	EE x I x A
290	0.015	0.78 5	0.011775
295	0.081 7	0.78 9	0.064461
300	0.287 4	0.77 9	0.223885
305	0.327 8	0.75 8	0.248472
310	0.186 4	0.73 5	0.137004
315	0.083 9	0.68 5	0.057472
320	0.018	0.59 7	0.010746
Sum			0.753815
SPF (sum x CF)			7.538148

SPF2.2 Before irradiation

wavelength	EE x I	A-A2	EE x I x A
290	0.015	1.473	0.02209 5
295	0.0817	1.485	0.12132 5
300	0.2874	1.473	0.42334

SPF2.2 After six hours of irradiation

wavelength	EE x I	A-A2	EE x I x A
290	0.015	1.01 7	0.015255
295	0.081 7	1.02 3	0.083579
300	0.287 4	1.01 4	0.291424

305	0.3278	1.451	0.47563 8
310	0.1864	1.419	0.26450 2
315	0.0839	1.347	0.11301 3
320	0.018	1.207	0.02172 6
Sum			1.44163 8
SPF (sum x CF)			14.4163 8

305	0.327 8	0.99 3	0.325505
310	0.186 4	0.96 8	0.180435
315	0.083 9	0.91 2	0.076517
320	0.018	0.81 6	0.014688
Sum			0.987403
SPF (sum x CF)			9.874031

SPF2.3 Before irradiation

wavelength	EE x I	A-A2	EE x I x A
290	0.015	1.227	0.01840 5
295	0.0817	1.239	0.10122 6
300	0.2874	1.226	0.35235 2
305	0.3278	1.204	0.39467 1
310	0.1864	1.176	0.21920 6
315	0.0839	1.108	0.09296 1
320	0.018	0.952	0.01713 6
Sum			1.19595 9
SPF (sum x CF)			11.9595 9

SPF2.3 After six hours of irradiation

wavelength	EE x I	A-A2	EE x I x A
290	0.015	0.7	0.0105
295	0.081 7	0.7	0.05719
300	0.287 4	0.69	0.198306
305	0.327 8	0.67 2	0.220282
310	0.186 4	0.65 3	0.121719
315	0.083 9	0.61 6	0.051682
320	0.018	0.55 6	0.010008
Sum			0.669687
SPF (sum x CF)			6.696872